# The Role of p97 cofactors SPRTN and FAF1 in DNA replication

DPhil Thesis
Supervised by Prof Kristijan Ramadan

Swagata Halder




Cancer Research UK/MRC Oxford Institute For Radiation Oncology
Department Of Oncology, University Of Oxford

Linacre College

7th October 2016

# Acknowledgement

First of all, I would like to express my sincere gratitude to my supervisor Prof. Kristijan Ramadan for giving me the opportunity to work in his laboratory and especially on the SPRTN/DVC1 project. I thank him for his continuing guidance, encouragement and support, without which many findings in this thesis would not have been possible. I would be ever grateful to him for his mentoring, for always being open to new ideas, and for inculcating in the laboratory the spirit of smart thinking, positive energy and focused work.

I would like to thank my lab mates Abhay, Ignacio, Marta and Bruno for helping me with my thesis with their expertise; John, Judith, Divya, Domenic, Katy, and Henry for all their support. I also thank Regina and Zuzana from our previous lab for their support. Thanks to Selva, Giulia, Sovan, Sally for helping me many times with reagents.

I would also like to thank our external collaborators Ivan Dikic, Davor Lessel, Melanie Philipp, Raimundo Freire, Andre Franz, Thorsten Hoppe, Martin Gill, Jutta Zimmer, Madalena Tarsounas for the opportunity to work and collaborate with them.

I thank my wife Indrani for supporting and motivating me during these extremely stressful DPhil years. She has happily sacrificed countless weekends due to my work at the lab. I also thank my mother for being a constant source of motivation. Their love and support kept me going during this difficult and challenging journey.

Finally, I would like to dedicate this thesis to my father, who passed away in 2011. I thank him for teaching me the value of perseverance and hard work. I did not get the chance to thank him in person, but I wish my words will find their way to him.

# Abstract

It is well known that cancer cells are loaded with excess proteins. To survive this proteotoxic crisis cancer cells rely heavily on the ubiquitin proteasome system (UPS). Valosin containing protein (VCP) or p97 has recently emerged as a central player of UPS. Moreover, p97 inhibitors were shown to possess potent anti-cancer properties. Owing to the essential function of p97, it can be assumed that general p97 inhibition will be equally toxic to surrounding normal tissues. Interestingly, p97 employs diverse sets of cofactors to govern distinct biological pathways. Thus understanding the p97-cofactor interaction in specific pathways may give us the ultimate edge by allowing us to abolish those cancer specific p97-cofactor interactions in our fight against cancer. This thesis explains novel function of two bonafide p97 cofactors SPRTN and FAF1 in DNA replication.

Our discovery of a new human syndrome followed by its characterisation that monogenic and biallelic mutations in SPRTN leads to premature aging and juvenile hepatocellular carcinoma, have led us to identify the critical function of SPRTN in DNA replication. Our follow up work further revealed that SPRTN is a novel protease in humans and has the essential function in covalent DNA-protein crosslinks (DPCs) repair. To this end, we have found that SPRTN proteolytically removes CHK1 from chromatin, which is evolutionary conserved and vital for replication fork progression to preserve genomic integrity.

Additionally, this thesis also explains a novel mechanism through which FAF1 downregulation in cancer cells might promote genomic instability. Our data supports a model where the $p97^{-FAF1}$ complex binds to ubiquitinated CDT1 and degrades it via the proteasome after CDT1 mediated replication initiation, to prevent re-replication and genomic instability.

The notion that high replication stress in some cancers can be utilised as an Achilles heel, led to the search for novel factors involved in DNA replication owing to its high therapeutic potential. Replication factors with enzymatic activities are especially appealing due to the relative ease of targeting them by small molecule inhibitors. This thesis thus highlights the great potential of the p97 systems in our battle against cancer.

***Contents***


**1 Introduction ..... 13**
*1.1 Ubiquitin ..... 15*
1.1.1 Ubiquitin conjugating and de-ubiquitinating enzymes ..... 16
*1.2 Proteasome ..... 18*
*1.3 Targeting the UPS for anti-cancer therapy ..... 20*
*1.4 AAA ATPase p97 ..... 24*
*1.5 Cell cycle ..... 28*
1.5.1 The p97 system in the cell cycle ..... 29
1.5.2 G1/S transition ..... 30
1.5.3 S phase ..... 30
1.5.3.1 DNA replication ..... 30
1.5.3.1.1 Replication Initiation ..... 31
1.5.3.1.1.1 p97 system in replication initiation ..... 32
1.5.3.1.2 Elongation ..... 32
1.5.3.1.3 Termination ..... 33
1.5.3.1.3.1 p97 in replication termination ..... 33
1.5.4 Mitosis ..... 34
1.5.4.1 p97 in mitosis ..... 34
*1.6 DNA damage response ..... 35*
1.6.1 NHEJ ..... 37
1.6.2 HR ..... 38
1.6.2.1 p97 system in the DNA damage response ..... 40
1.6.3 Replication stress response and activation of the ATR-CHK1 signalling cascade ..... 41
1.6.4 Diverse function of CHK1 in S phase ..... 46
1.6.4.1 Cell cycle arrest ..... 46
1.6.4.2 Dormant origin firing ..... 47
1.6.4.3 Replication Fork Stability ..... 48
1.6.4.4 Apoptosis ..... 49
1.6.5 Translesion DNA synthesis ..... 50
1.6.6 Fanconi anemia (FA) pathway ..... 51
1.6.6.1 p97$^{-SPRTN}$ complex in ICL repair ..... 53
1.6.7 DNA-Protein Crosslink (DPC) repair pathway ..... 53
1.6.7.1 CDC48$^{-WSS1-DOA1}$ or p97$^{-SPRTN}$ complex in DPC repair ..... 55

**2 Materials and Methods ..... 58**
*2.1 Tissue culture ..... 59*
2.1.1 Revival of frozen cell lines ..... 59
2.1.2 Maintenance of cell lines ..... 59
2.1.3 Cryopreservation of cell lines ..... 60
2.1.4 Cell lines ..... 60
2.1.5 Generation of stable cell lines by Flp-In ..... 61
2.1.6 Primer sequences ..... 61
2.1.7 Generation of CRISPR-Cas9 cell lines ..... 62
*2.2 Cloning and site directed mutagenesis ..... 62*
*2.3 Bacterial transformation ..... 65*
*2.4 Plasmid purification ..... 65*
*2.5 Plasmid Transfection ..... 66*
*2.6 Gene silencing ..... 66*
*2.7 Cell fractionation assay ..... 67*
*2.8 Co-Immunoprecipitation assay ..... 68*
*2.9 Protein detection by Western blotting ..... 69*
*2.10 Isolation of Proteins On Nascent DNA (iPOND) ..... 70*
*2.11 Double Thymidine Block ..... 71*

*2.12 Antibodies used in this thesis for Western blot experiments* ... *71*
*2.13 DNA fiber assay* ... *72*
*2.14 Metaphase spread* ... *74*
*2.15 Immunofluorescence* ... *74*
2.15.1 Detection of ssDNA foci ... 75
*2.16 DPC assay* ... *77*
2.16.1 DNA-protein crosslinks isolation ... 77
2.16.2 DNA-protein crosslinks detection ... 77
*2.17 In vitro cleavage assay* ... *78*
2.17.1 Protein purification ... 78
*2.18 Zebrafish study* ... *79*

**3 Results** ... **80**
*3.1 Establishing the role of SPRTN in general DNA replication* ... *81*
3.1.1 Introduction ... 82
3.1.2 AIM: To characterise SPRTN function in normal DNA replication ... 85
3.1.3 Results ... 85
3.1.3.1 Identification and characterisation of SPRTN mutated patients ... 85
3.1.3.2 Patient cells are hypersensitive to replication interfering drugs ... 88
3.1.3.3 Patient cells show characteristic features of DNA replication stress ... 90
3.1.3.4 DNA replication defect is the cause of SPRTN syndrome ... 92
3.1.3.5 Complete SPRTN depletion leads to pronounced replication defect ... 95
3.1.3.6 Characterisation of patient mutations ... 97
3.1.3.7 Pol-η codepletion cannot rescue replication defect in SPRTN mutated patient LCLs or in endogenously depleted U2OS cells ... 99
3.1.4 Discussion ... 101
*3.2 Characterisation of the ATR-CHK1 signalling defect in SPRTN depleted cells* ... *104*
3.2.1 Introduction ... 105
3.2.2 AIM: To investigate the ATR-CHK1 signalling cascade in the context of DNA replication in SPRTN-depleted cells ... 108
3.2.3 Results ... 108
3.2.3.1 Characterisation of the ATR-CHK1 signalling cascade in SPRTN depleted cells 108
3.2.3.2 SPRTN forms a physical complex with DNA replication and DDR associated factors 111
3.2.3.3 NSC663284, a potent CDC25 inhibitor rescues DNA replication fork speed in SPRTN depleted cells ... 117
3.2.3.4 Roscovitine, a potent CDK inhibitor rescues DNA replication fork speed in SPRTN depleted cells ... 120
3.2.3.5 Sub-optimal CHK1 phosphorylation in SPRTN depleted cells is rescued by the PP2A inhibitor okadaic acid ... 122
3.2.3.6 PP2A regulatory subunit B55α links PP2A to CHK1 ... 128
3.2.3.7 Ectopic expression of CHK1-WT enables SPRTN depleted cells to efficiently restart stalled replication forks ... 132
3.2.3.8 CHK1 protects stalled replication forks from MRE11 dependent resection ... 135
3.2.4 Discussion ... 139
*3.3 SPRTN proteolytically removes CHK1 from chromatin* ... *144*
3.3.1 Introduction ... 145
3.3.2 AIM: To characterise SPRTN function in proteolytic CHK1 activation ... 147
3.3.3 Results ... 147
3.3.3.1 Formaldehyde induced replication stress, similar to SPRTN depletion, failed to evoke CHK1 phosphorylation ... 147
3.3.3.2 Bulky DPCs bocks helicase-polymerase uncoupling ... 151
3.3.3.3 SPRTN is a constitutive member of the DNA replication fork ... 156
3.3.3.4 SPRTN proteolytically removes DPCs ... 160
3.3.3.5 SPRTN facilitates chromatin release of CHK1 ... 163
3.3.3.6 SPRTN mediated CHK1 activation is evolutionarily conserved ... 167

3.3.4 Discussion ..... 170
*3.4 Characterisation of FAF1, a bonafide p97 cofactor, in DNA replication ..... 173*
3.4.1 Introduction ..... 174
3.4.2 AIM: To characterise the role of FAF in DNA replication ..... 177
3.4.3 Results ..... 177
3.4.3.1 FAF1 depletion in U2OS cells causes severe replication stress ..... 177
3.4.3.2 Co-depletion of CDT1 rescues DNA replication stress in FAF1 depleted cells 180
3.4.3.3 FAF1 depletion causes severe DNA replication stress in HEK293 cells ..... 184
3.4.3.4 FAF1 depletion causes severe DNA replication defect in T24 cells ..... 187
3.4.3.5 Depletion of FAF1 activates the DNA damage signalling cascade ..... 189
3.4.3.6 p97-FAF1 regulates CDT1 turnover ..... 189
3.4.4 Discussion ..... 193
**4 General Discussion ..... 196**
**5 Reference ..... 210**
**6 Appendix ..... 235**

**List of figures**

**Figure 1** Overview of the UPS.. .....20

**Figure 2** Overview of p97 structure, domain organisation and its cofactors.. .....25

**Figure 3** p97 and its adapters in diverse cellular function.. .....27

**Figure 4** Overview of the different DNA repair pathways inside the cell .....37

**Figure 5** Simplified overview of two major DSB repair pathways, HR and NHEJ ...40

**Figure 6** Cartoon showing diverse function of p97 in genomic instability.....57

**Figure 7** Discovery of patients and identification of SPRTN mutations .....86

**Figure 8** Patient cells are hypersensitive to replication interfering drugs.....89

**Figure 9** Patient cells show characteristic features of DNA replication stress. .....91

**Figure 10** A DNA replication defect is the cause of SPRTN syndrome.....94

**Figure 11** Complete SPRTN depletion leads to pronounced replication defect .....96

**Figure 12** Characterisation of patient mutations a. Depiction of constructs.....98

**Figure 13** Pol-η codepletion cannot rescue replication defect in SPRTN mutated patient LCLs or in endogenously depleted U2OS cells. .....100

**Figure 14** Characterisation of the ATR-CHK1 signalling cascade in SPRTN depleted cells. .....110

**Figure 15** SPRTN forms a physical complex with DNA replication and DDR associated factors. .....115

**Figure 16** NSC663284, a potent CDC25 inhibitor, rescues DNA replication fork speed in SPRTN depleted cells.. .....119

**Figure 17** Roscovitine, a potent CDK inhibitor, rescues DNA replication fork speed in SPRTN depleted cells. .....121

**Figure 18** Sub-optimal CHK1 phosphorylation in SPRTN depleted cells is rescued by the PP2A inhibitor okadaic acid. .....126

**Figure 19** PP2A regulatory subunit B55α links PP2A to CHK1.....130

**Figure 20** Ectopic expression of WT CHK1 enables SPRTN depleted cells to efficiently restart stalled replication forks.. .....134

**Figure 21** CHK1 protects stalled replication forks from MRE11 dependent resection. .....138

**Figure 22** Formaldehyde induced replication fork slowing, similar to SPRTN depletion, failed to evoke CHK1 phosphorylation .....149

**Figure 23** Bulky DPCs bock helicase-polymerase uncoupling.....154

**Figure 24** SPRTN is a constitutive member of the DNA replication fork.....158

**Figure 25** SPRTN proteolytically removes DPCs.....162

**Figure 26** SPRTN facilitates chromatin release of CHK1. .....165

**Figure 27** SPRTN mediated CHK1 activation is evolutionary conserved.....168

**Figure 28** FAF1 depletion in U2OS cells causes severe replication stress.....178

**Figure 29** Codepletion of CDT1 rescues DNA replication stress in FAF1 depleted cells.. .....182

**Figure 30** FAF1 depletion causes severe DNA replication stress in HEK293 cells. 185

**Figure 31** FAF1 depletion causes severe replication defect in T24 cells.....188

**Figure 32** Depletion of FAF1 activates the DNA damage signalling cascade.....191

**Figure 33** 1. General mechanism for CHK1 activation 2. Model explaining why CHK1 cannot be fully activated in SPRTN deficient cells 3. Our proposed model of SPRTN dependent non-canonical CHK1 activation .....204

**List of abbreviations**

| | |
|---|---|
| ATP | Adenosine Triphosphate |
| UPS | Ubiquitin Proteasome System |
| DDR | DNA Damage Response |
| DUB | Deubiquitinating enzyme |
| UCH | Ubiquitin C-terminal Hydrolases |
| USP | Ubiquitin-Specific Proteases |
| OUT | Ovarian Tumour Proteases |
| JAMM | Jab1/Mov34/Mpr1 Pad1 N-terminal+ (MPN+) domain proteases |
| UBD | Ubiquitin Binding Domain |
| MDa | Mega Dalton |
| PAC | Proteasome Assembling Chaperone |
| ER | Endoplasmic Reticulum |
| UMP | Uridine Monophosphate Synthetase |
| Rpn | Regulatory particle non-ATPase |
| UCH | Ubiquitin C-terminal Hydrolases |
| CNVs | Copy Number Variations |
| MM | Multiple Myeloma |
| NF-κB | Nuclear Factor kappa B |
| IκB | Inhibitor of kappa B |
| MDM2 | Murine Double Minute 2 |
| IAP | Inhibitor of Apoptosis |
| BIR | Baculovirus Inhibitor of apoptosis protein Repeat |
| VCP | Valosin Containing Protein |
| CDC | Cell Division Cycle |

| | |
|---|---|
| TER94 | Transitional Endoplasmic Reticulum ATPase TER94 |
| VAT | VCP-like ATPase from Thermoplasma acidophilum |
| UFD1 | Ubiquitin Fusion Degradation 1 |
| NPL4 | Nuclear Protein Localization 4 |
| UBX | Ubiquitin Regulatory X |
| UBD | Ubiquitin D |
| PUB | PNGase (peptide N-glycosidase)/ubiquitin associated |
| SHP | Suppressor of High copy Protein |
| VIP | VCP Interacting Protein |
| VIM | VCP Interacting Motif |
| VBM | VCP Binding Motif |
| RNA | Ribonucleic Acid |
| DNA | Deoxyribonucleic Acid |
| CDK | Cyclin Dependent Kinase |
| ORC | Origin Recognition Complex |
| MCM | Minichromosome Maintenance |
| RING | Really Interesting New Gene |
| SCF | Skp, Cullin, F-box containing complex |
| CRL | Cullin-RING-based-E3-ubiquitin ligases |
| FAF1 | FAS Associated Factor 1 |
| RPA | Replication Protein A |
| PCNA | Proliferating Cell Nuclear Antigen |
| RFC | Replication Factor C |
| FEN-1 | Flap Endonuclease-1 |
| CMG | CDC45, MCM2-7 and GINS (Go, Ichi, Nii, San; five, one, two, and |

| | |
|---|---|
| | three in Japanese) |
| PTMs | Post Translational Modifications |
| XAMP | Xenopus Microtubule Associated Protein |
| TPX | Thiol peroxidase |
| PLX | Polo-like Kinase in Xenopus |
| DSB | Double Stranded Break |
| NHEJ | Non-Homologous End Joining |
| HR | Homologous Recombination |
| PIKK | Phosphatidylinositol-3-OH-Kinase-like Kinase |
| ATM | Ataxia-Telangiectasia Mutated |
| ATR | ATM and Rad3-related |
| DNA-PK | DNA-dependent Protein Kinase |
| MDC1 | Mediator of DNA damage Checkpoint protein 1 |
| RNF | Ring Finger |
| 53BP1 | p53-Binding Protein 1 |
| BRCA | Breast Cancer |
| CtIP | CtBP-Interacting Protein |
| MRE11 | Meiotic Recombination 11 |
| XRCC4 | X-ray Cross Complementing protein 4 |
| XLF | XRCC4-Like Factor |
| APLF | Aprataxin-and-PNK-Like Factor |
| PALB2 | Partner And Localiser Of BRCA2 |
| KEAP1 | Kelch-like ECH-Associated Protein 1 |
| RIF1 | Replication Timing Regulatory Factor 1 |
| PTIP | The Pax Transactivation domain-Interacting Protein |

| | |
|---|---|
| BLM | Bloom syndrome helicase |
| Rad | Radiation |
| L3MBTL1 | Lethal (3) Malignant Brain Tumor-Like protein 1 |
| JMJD2 | Jumonji Domain 2 |
| dNTP | Deoxynucleotide |
| HU | Hydroxyurea |
| CPT | Camptothesin |
| APH | Aphidicolin |
| MMC | Mitomycin C |
| UV | Ultra Violet |
| ssDNA | single stranded DNA |
| ATRIP | ATR Interacting Protein |
| TopBP1 | DNA Topoisomerase 2-Binding Protein 1 |
| 9-1-1 | RAD9-RAD1-HUS1 |
| PARP1 | Poly (ADP ribose) Polymerase 1 |
| PIN1 | Peptidyl-prolyl cis-trans Isomerase NIMA-interacting 1 |
| DAPK1 | Death-Associated Protein Kinase 1 |
| BID | BH3 Interacting-domain Death agonist |
| BAX | Bcl2-Associated X protein |
| TLS | Translesion Synthesis |
| FA | Fanconi Anemia |
| AML | Acute Myelogenous Leukemia |
| PIAS | Protein Inhibitor of Activated STAT |
| SENP6 | SUMO1/Sentrin Specific Peptidase 6 |
| ICL | Intra strand Crosslink |

| | |
|---|---|
| DPC | DNA Protein Crosslink |
| WSS1 | Weak Suppressor of SMT3 |
| SUMO | Small Ubiquitin-related Modifier |
| MIU | Motif Interacting with Ubiquitin |
| PIP | PCNA-Interacting Protein |
| SIM | SUMO-Interacting Motif |
| DMSO | Dimethyl Sulfoxide |

# 1 Introduction

ATP utilisation for the degradation of proteins had been considered a wrong hypothesis for a long period of time, however, at that time, it was known that intra cellular proteolysis required ATP[1]. Since then, we have come a long way, as in 2004 the Nobel Prize in chemistry was awarded to Aron Ciechanover, Avram Hershko and Irwin Rose, for their discovery of Ubiquitin Proteasome System (UPS) for protein degradation that requires ATP. It also recognised the functional importance of UPS in diverse cellular processes. Discoveries originating from theirs and other labs, we became aware that cells have a complex and robust protein degradation system, which needs the conjugation of ubiquitin molecules, through the cascade of enzymatic reactions, to a client protein and finally its degradation by proteasome[2,3]. Since this initial discovery, the UPS have emerged as the central player for protein degradation in the cytoplasm and the nucleus of the eukaryotic cells and thus for the maintenance of cellular homeostasis. Inactivation of the UPS or a mutation in key genes associated with UPS, leads to proteotoxic stress, which triggers cell death. Robust functioning of the UPS is absolutely necessary for normal cell physiology. Ironically, cancer cells utilise this essential pathway for their own survival as they have much higher protein loads comparing to normal cells. These findings have given rise to the possibility of inhibiting proteasome activity for cancer cell therapy[4]. Owing to these observations, enormous effort has been made to make novel inhibitors against the proteasome or against different component of the UPS. I thus take this opportunity to briefly introduce the different component of the UPS and their involvement in normal cellular processes and disease aetiology before I start describing specific part of UPS the concerning this thesis.

## 1.1 Ubiquitin

The UPS machinery is composed of three major components; ubiquitin, the proteasome and an array of enzymes responsible for catalyzing ubiquitination reaction on their client proteins. Ubiquitin, unique to eukaryotes, is a highly conserved protein differing only in 3 out of 76 amino acids from yeast to humans. This remarkable feature of conservation is rare and indicates the evolutionary selection pressure on ubiquitin due to its important function[5]. Ubiquitin (Ub) with its C-terminal glycine form an isopeptide bond with a lysine residue in the target protein. As ubiquitin has seven internal lysines (K6, K11, K27, K29, K33, K48, K63), functional diversity in the ubiquitin signalling pathway is achieved through different linkages in ubiquitin chain over these seven lysines or its N-terminal methionine. Thus ubiquitin forms different signals on the substrates; from a substrate monoubiquitination to substrates' polyubiquitination by different ubiquitin chains. Polyubiquitin chains can either be linear or branched, which brings further diversity in the ubiquitin signalling pathways. For example, protein monoubiquitination governs the DNA damage response (DDR) and gene expression, whereas a liner polyubiquitination chain through K48-Ub linkages is generally associated with proteasome mediated degradation[6]. Linear poly-ubiquitination of substrate proteins through K63-Ub linkages facilitates protein localisation to different sub-cellular location, is responsible for the DDR, involves in kinase activation and also involves in endocytosis[78]. Although branched ubiquitin chain can be synthesised *in vitro* by combination of defined enzymes, functional relevance of branched ubiquitin chain remained elusive for a long period of time until a recent report suggesting branched ubiquitin chain of K48 and K11 linkages leads to efficient protein degradation[9] . Further work is necessary to understand the full functional significance of such branched ubiquitin chain. A recent report also

suggested that it is the total number of ubiquitins, rather the configuration of the ubiquitin chain that determines the binding of the proteasome to the substrate. Chain configuration becomes important when the substrate is passed through the translocation channel of the proteasome core to be degraded[10].

### 1.1.1 Ubiquitin conjugating and de-ubiquitinating enzymes

Conjugation of ubiquitin molecule to the substrate protein is well understood and requires three classes of hierarchical enzymes namely E1-Ub activating, E2-Ub conjugating and E3-Ub ligase. The first step involves activating ubiquitin molecule by ubiquitin activating enzyme ($E1_{SH}$) which catalyses the formation of a ternary complex consists of a covalently linked enzyme-ubiquitin complex between active site cysteine of E1 and C-terminal glycine of ubiquitin and a non-covalently linked ubiquitin-AMP to E1 (Figure 1). This ternary complex is then transferred to another member of structurally similar enzyme called ubiquitin-conjugating enzyme E2, which resulted in conjugation of ubiquitin through a thiolester bond to E2 ($E2_s$-Ub). The final step in this enzyme catalysis reaction is accomplished when an E3 ubiquitin-ligase catalyses the formation of an iso-peptide bond between the ubiquitin and a lysine residue of a substrate protein by aminolytic cleavage of E2-ubiquitin thiolester with the subsequent release of E2[5]. The complexity of the ubiquitin signalling pathway is achieved by the fact that there are only two E1-ubiquitin activating enzymes, at least 30 E2-conjugating enzyme and an estimated 600-1000 E3-ubiquitin ligases present in humans[11–13]. Based on sequence homology, E3-ligases can be sub-divided into two major classes, the HECT (homologous to E6-AP C terminus) family ligases and RING (really interesting new genes) family ligases. Mechanistically they are also different in their respective ubiquitination processes. HECT ligases form

transient covalent linkage between their conversed cysteine and ubiquitin, before actual substrate ubiquitination[14]. RING ligases, on the other hand, mediate direct transfer of ubiquitin from E2 to substrate by acting as a scaffold[15]. Presence of such a large number of E3-ubiquitin ligases ensures substrate specificity and also indicates the diversity of the ubiquitin signalling pathway. A ubiquitinated protein is generally recognised by ubiquitin receptors containing specific ubiquitin binding domains (UBDs). The diversity of UBDs determines their specificity towards different ubiquitin chain structure, which further influences the specificity and complexity of the ubiquitin dependent signalling pathways and protein-protein interactions in a cell[16]. Ubiquitination is a reversible reaction. There are specific de-ubiquitinating enzymes (DUBs) that remove ubiquitin from client proteins preventing their degradation or abolishing protein-protein interaction, which also helps in ubiquitin recycling. The human genome contains nearly 100 DUBs. However ubiquitin specificity is found in only five DUB families, for example the UCH, USP, OTU, Josephin and JAMM families. The first four of the DUB families mentioned here are cysteine proteases while the fifth is a metalloprotease. DUBs also interact with their client proteins through their various UBDs thus bringing further specificity and diversity to ubiquitin signalling pathways. Furthermore, since DUBs are proteases, cells have evolved distinct mechanisms to control their activity. Active site rearrangements upon substrates binding and associated conformational changes often determine the fate of DUB catalytic reaction. To this end, scaffold or adapter binding can further influence DUB activity. Post-translational modifications such as phosphorylation and ubiquitination have also been shown to regulate DUB activity [17,18].

## 1.2 Proteasome

Once a targeted protein is marked with a ubiquitin signal for degradation, it is recognised by the 26S proteasome, a large multisubunit 2.6 MDa protein complex. 26S proteasome consists of two main components, a 20S core particle where protein degradation takes place and two 19S regulatory particle, which is involved in substrate recognition and unfolding. The assembly of the 26S proteasome is a highly complex, multistep process and require assistance of proteasome specific chaperones and maturation factors [19]. In general the 20S core particle consist of two sets of α and β rings. Each α and β ring is an assembly of a hetero-heptamer consisting of α1-α7 subunits and β1-β7 subunits, respectively. Once the assembly of α ring is completed, it acts as a base for the assembly of the β ring. PAC1-PAC2 and PAC3-PAC4 are proteasome specific chaperones necessary for proper assembly and prevent premature docking of other proteins. After the assembly of half of the proteasome, consisting of a sandwich of heptamers of corresponding α and β rings, it is then localised to the endoplasmic reticulum (ER) membrane by UMP1, another specialised chaperone, for the final assembly of 20S core particle. Maturation of the 20S core particle involves another such sandwich of heptamers of α and β rings, facing each other in a α-β-β-α orientation. The assembly of base and lid sub-complexes of the 19S proteasome is still not very well understood. This process requires the assistance of specific chaperones (only base specific chaperones have been identified so far) and involves multiple steps. Once the base and lid sub-complexes are assembled, each subunit of the 19S proteasome finally attaches to the 20S core from both sides completing 26S proteasome assembly (19S-20S-19S). There are various ubiquitin receptors such as Rpn13 (present at the lid), Rpn1 (present at the base) and Rpn10 (present at the base)

that recognise a client protein with a very specific ubiquitin signature (K48 linear ubiquitin chain or K48, K11 branched chain) and offer it to the proteasome by acting as shuttle proteins[20]. In addition, these ubiquitin receptors also bind and activate various DUBs, which trim ubiquitin moieties on a client protein, and make it structurally more favorable to pass through the proteasome as a result bringing further complexity and diversity in UPS system. Furthermore, there are also three distinct DUBs: RPN11, UCH37 and USP14, which are associated with the regulatory particle of the proteasome. UCH37 and USP14 recognise inadequately ubiquitinated proteins and by further removing their ubiquitin, prevent their binding to proteasome and ultimately rescue them from premature degradation. RPN11, in contrast, was shown to be associated with substrate degradation [21]. Ubiquitin is generally recycled due to the action of DUBs before the protein is degraded by the 20S core particle and is released as small peptides. There are also various post-translational modifications (phosphorylation, ubiquitination, acetylation) that either increase or decrease the overall activity of the proteasome by modulating different component of this giant machinery. Although the proteasome is considered to be very stable, different components of the proteasome are shown to be Caspase-3 substrates as a result of apoptosis. Lysosomal degradation of the entire 26S proteasome has also been reported and is suggested to be an evolutionarily conserved process[22,23].

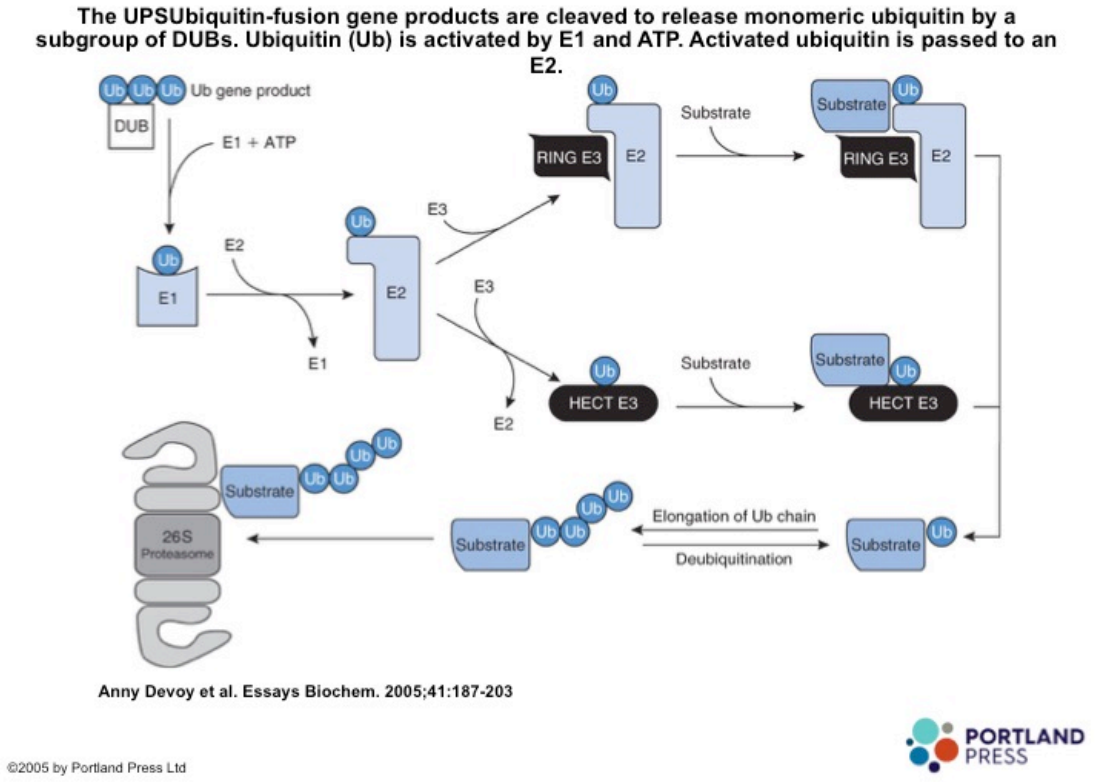



**Figure 1 Overview of the UPS**. Ubiquitin (Ub) is activated by E1 and ATP. Activated ubiquitin is passed to an E2. There are two major classes of E3s: HECT ligases, which directly conjugate ubiquitin before ligating it to the targeted substrate, and RING ligases, which chaperone the Ub-bound E2 to, and facilitate the ubiquitination of the, targeted substrate. Polyubiquitin chains can be assembled by further rounds of ubiquitination, or disassembled by DUBs (Modified from Devoy et al. Essays Biochem.2005;41:187-203.

## 1.3 Targeting the UPS for anti-cancer therapy

The UPS is of the utmost importance for cellular homeostasis. Several lines of evidence suggest a progressive decline in the overall function of the UPS is synonymous with ageing and various age related diseases[24,25]. Cancer cells, on the contrary, have been found to be heavily dependent on the UPS. Owing to whole genome sequencing, we are now able to detect all the genomic alterations present in cancer cells. It is well known that cancer cells have various point mutations in the coding regions of several genes along with large duplications, translocations,

deletions and copy number variations (CNVs). These alterations are albeit beneficial for cancer cells aggressiveness and overall survival, however, having them has its own challenges. Proteins translated from these altered genomic sequences continue to present a challenge to the protein folding machinery and as a result, cancer cells are littered with these unfolded proteins. Furthermore, complete hijacking of various transcription factors and the presence of CNVs associated with various coding regions leads to the voluminous expression of large amount of proteins. These excessive, structurally altered and unwanted proteins lead to protein stress and if not dealt with will initiate apoptosis. Thus, cancer cells rely heavily on various protein degradation pathways and the UPS is one of them. Therefore, it makes every sense to target the UPS in cancer[4,26,27].

Bortezomib (Velcade, Millennium Pharmaceuticals), a boronic-acid derivative, was approved by the US food and drug administration (USFDA) in 2003 for the treatment of multiple myeloma (MM). Bortezomib inhibits the 20S peptidase activity of proteasome. It has been successful in treating patients with MM and mantle cell lymphoma (MCL). Extensive preclinical research has shown that Bortezomib kills both hematological and solid tumors by the induction of apoptosis[4]. It is well known that proteasome activation leads to the degradation of IκB, an inhibitor of the transcription factor NF-κB, which among its various function also inhibits apoptosis. Inhibition of the proteasome will thus induce apoptosis through this mechanism especially in MM cells, which have high NF-κB activity. If this is the sole mechanism of action of Bortezomib for killing hematological and solid tumors, then it cannot explain why PS-1145, a specific inhibitor of IκB, which inhibits NF-κB to the same extent as Bortezomib, is not as effective as bortezomib in killing these cancer cells. It

also suggest proteasome inhibition through Bortezomib has additional effect against these cancers which remains to be explored[28].

Due to proteotoxic stress in cancer cells, the inhibition of the UPS still remained an attractive anti-cancer strategy. Therefore, researchers have also started looking at various other equally important components of the UPS to find out novel therapeutic strategies against cancer. One such avenue is targeting various E3-ligases due to their specific interaction with their substrates[26]. Abolishing such interactions either by inhibiting the E3s active site or by inhibiting its substrate binding ability, will abolish specific interaction in cancer cells and will be minimally toxic in normal cells. Furthermore, strategies like this are specifically interesting in those cancer cells where a particular tumor suppressor is proetosomally degraded by the UPS due to the action of a specific ligase, thus giving cancer cells an unprecedented advantage. For example, targeting the E3-ubiquitin ligase Mdm2 in order to restore p53 activity in cancer cells offers one such example. Mdm2 (Murine double minute 2) is responsible for p53 ubiquitination and degradation. Targeting Mdm2 will thus activate p53 mediated cell cycle arrest and apoptosis. Anti-cancer strategies include inhibiting Mdm2 expression, inhibiting its ligase activity and abolishing the Mdm2-p53 interaction. Treatment of cancer cells with small molecule inhibitors such as nutlins[29], benzodiazepinediones[30], MI-219[31], RITA[32] or synthetic peptide SAH-p53s[33], have shown promising effect *in vivo* but their low potency and off-target effects have prevented them from being fully available for clinics. Multiple clinical trials are underway to understand their long-term efficacy against cancer treatment[34,35].

Targeting other components of the UPS is also underway and one such notable example includes the identification of the inhibitors of apoptosis (IAPs). IAPs contain BIR domain, which have anti-apoptotic activity[36]. IAPs bind to various caspases with

their BIR domain and inhibit their proteolytic activity. A vast number of the IAPs family of protein also posses E3-ligase activity and target various signalling and apoptotic factors for proteasomal degradation[37]. Various small molecule inhibitors targeting IAPs are undergoing clinical trials[36].

Another UPS mediated anticancer strategy includes targeting DUBs. Tremendous effort is underway to understand specific biological function of various DUBs to generate an effective therapeutic strategy. The role of various DUBs such as USP1[38], USP7[39], and USP28 [40] are very well understood in a DNA repair context and can prove fruitful in clinics, either as a mono-therapy or in combination with radiation therapy.

Thus research on targeting UPS components must continue to win this battle against cancer. To this end, Valosin-containing protein (VCP) or p97 (also known as Cdc48 in lower eukaryotes), a central component of the UPS, qualifies as an attractive anti cancer target. p97 has recently emerged as a druggable target for cancer therapy. Intense research is underway to define the biological function p97's at the substrate level along with understanding its interaction with various ligases, DUBs and most importantly at the level of its unique hierarchical sets of adapters[41–45].

## 1.4 AAA ATPase p97

Although the proteasome is present in all cellular compartments, it needs the assistance of p97 when a substrate is tightly bound to another protein or DNA or is misfolded or is heavily aggregated. p97 is an AAA ATPase that acts as a molecular chaperone, which binds to ubiquitinated and sumoylated proteins and unfolds or segregates them from their sub-cellular locations, and in majority of cases deliver them to proteasome for their subsequent degradation[46]. p97 is also known as VCP in vertebrates, Cdc48 in *S.cerevisiae*, Cdc-48 in *C.elegans*, TER94 in *Drosophila* and VAT in archaebacteria. p97 is highly conserved and is one of most abundant proteins inside the cell (1% of total cellular proteins). It belongs to the class II member of ATPases associated with diverse cellular activities (AAA). p97 is a homohexamer and has a barrel like structure. Like all other AAA-ATPases, it also has two ATPase domains on its C-terminal part, namely D1 and D2, with the D2 domain being solely involved in generating the molecular force to remodel their substrates after ATP hydrolysis[47]. A catalytically inactivating mutation in D2 domain leads to a substrate trapping phenotype of p97 (Figure 2). The N-terminal globular domain of p97, on the other hand, associates with majority of p97 cofactors and subsequently to p97 substrates. Once p97 is bound to the substrates, with the help of its cofactors through its N-terminal domain, the C-terminal D2 domain utilises the energy from ATP hydrolysis and stimulates a major conformational changes in p97 structure, which ultimately resonate at the flexible N-terminal domain. This is the molecular mechanism that enables p97 to rescue its substrate from diverse cellular locations (segregase activity) or various protein sub-complexes. In addition, this peculiar mode

of action also helps p97 to unfold highly folded soluble proteins (unfoldase action) and deliver them to proteasome[17,48–51].

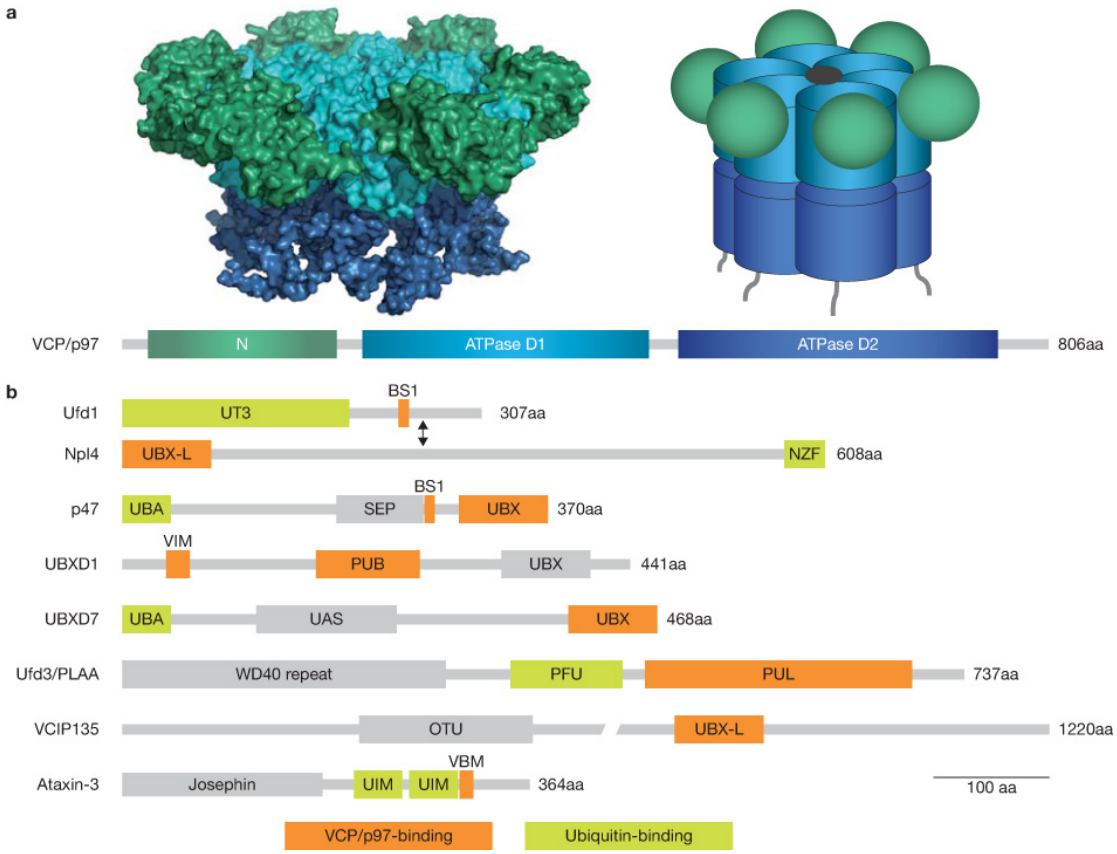



**Figure 2 Overview of p97 structure, domain organisation and its cofactors**. (a) Structure of VCP/p97. Each subunit consists of a globular N-terminal domain (green), the two AAA ATPase domains D1 (cyan) and D2 (blue), and a C-terminal tail (grey) D1 and D2 form two stacked hexameric rings. The N-terminal globular domain is positioned at the periphery of the D1 ring. (b) Domain structure of selected cofactors. (Modified from Meyer et al, NATURE CELL BIOLOGY VOLUME 14 | NUMBER 2 | FEBRUARY 2012) © 2012 Macmillan Publishers Limited. All rights reserved.

Ubiquitin is the main conductor of p97 function. It serves as a signal on the substrates, that bridges p97 and its cofactors along with the substrates. p97 interacts with its ubiquitinated substrates via its diverse sets of hierarchical cofactors. There are about 30 known p97 cofactors that in various combinations form different p97 sub-complexes, which govern the function of p97 in diverse cellular processes. Among

these, there are so far three sets of core cofactors namely p97$^{-Ufd1-Npl4}$, p97$^{-p47}$, p97$^{-UBXD1}$, which are well documented (Figure 3). These cofactors are mutually exclusive for p97 binding[50]. In general, p97 cofactors are those proteins that have p97 interacting domains or motifs. There are seven known p97 interacting domains and motifs: UBX (ubiquitin regulatory X) domain, UBD (ubiquitin D) domain, PUB {PNGase(peptide *N*-glycosidase)/ubiquitin associated} domain, SHP motif, VIP (VCP interacting protein) motif, VIM (VCP interacting motif) or VBM (VCP-binding motif). The majority of the p97 cofactors have a UBX domain, which is also structurally similar to ubiquitin, but lacks sequence homology. The core cofactors when bound to p97 with their distinct p97 interacting domain/motif, can influence p97 activity in distinct biological pathways[52]. For example, the p97$^{-Ufd1-Npl4}$ complex is mostly associated with K48-Ub linked proteasomal degradation in the endoplasmic reticulum, ribosome or chromatin[53–55]. p97$^{-p47}$ and p97$^{-UBXD1}$ core complexes, on the contrary, are involved in ubiquitin-dependent proteasome-independent membrane fusion and vesicular trafficking processes. The specificity of the p97 system is further achieved by several sets of secondary hierarchical cofactors. p97, with its specific set of core cofactors and with different secondary cofactors, can influence different substrates involved in different pathways within the same cellular structures. This is best understood in terms of the p97$^{-Ufd1-Npl4}$ complex. This core complex with the help of secondary cofactors UBX4 and UBX5, can extract RNA pol II from stalled transcription[53]. Alternatively, the secondary cofactor DVC1/SPRTN can extract DNA pol-$\eta$ [55]or negatively regulate DNA pol-$\delta$[56,57] form/at stalled replication forks. Furthermore, the p97$^{-Ufd1-Npl4}$ core complex can also bind to soluble hypoxia inducible factor 1$\alpha$ by UBXD7 secondary adapter[52].

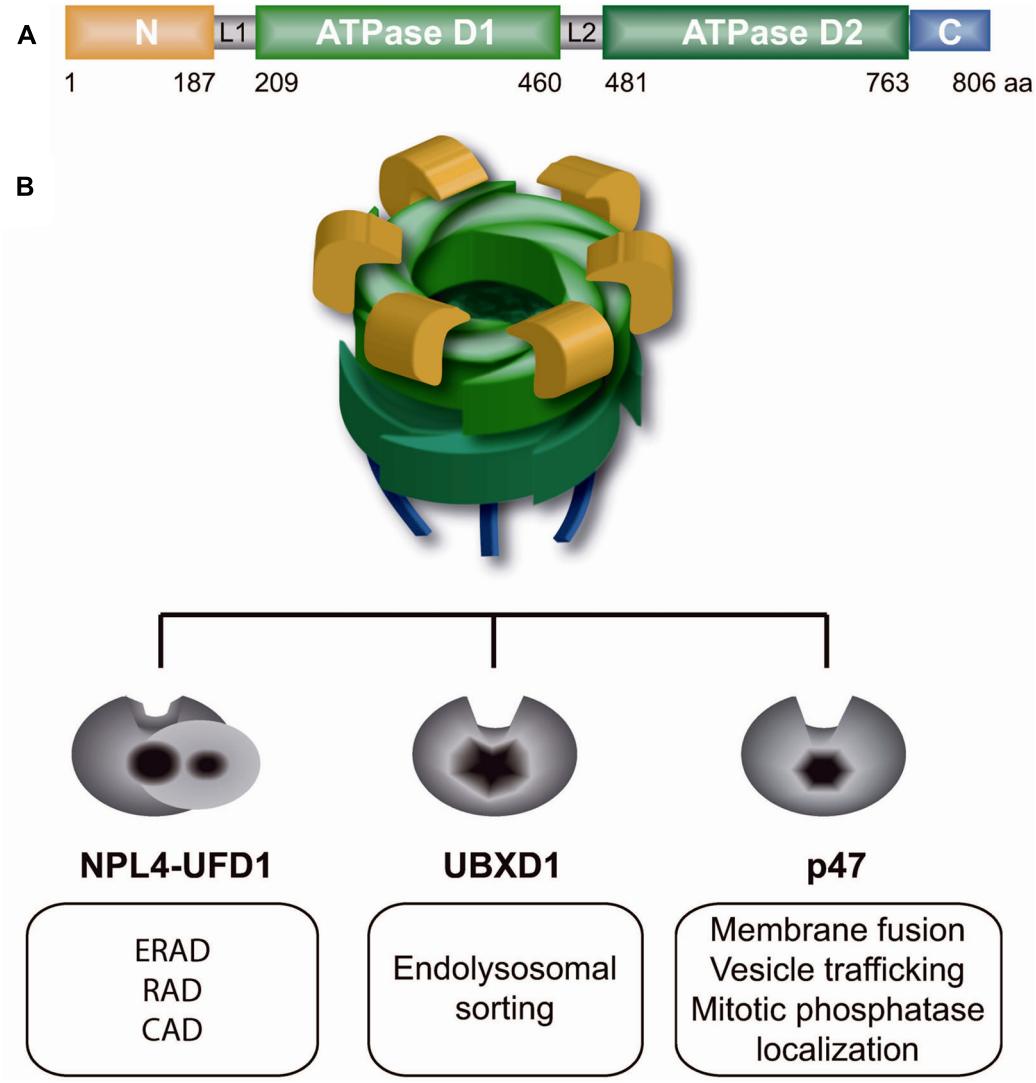



**Figure 3 p97 and its adapters in diverse cellular function**. (Modified from Vaz B, Halder S and Ramadan K (2013) Role of p97/VCP (Cdc48) in genome stability. Front. Genet. 4:60).

All of these interactions ultimately result in proteasomal degradation of specific substrates. It is hypothesised that p97, with its specific core cofactors and diverse sets of secondary cofactors makes specific sub-complexes with its equally broad range of substrates. Identification of those sub-complexes or novel cofactors of p97 will ultimately result in a complete understanding of the p97 system in cellular

homeostasis. Additionally there is also a growing body of evidence highlighting the role of p97 role in other equally important cellular processes such as autophagy[58] and endosomal trafficking[59]. Furthermore, identifying novel cofactors or characterising specific sub-complexes will extend our understanding of p97 biology interior milieu and in diseases aetiology, which will help us to deduce novel therapeutic strategy. Keeping that in mind, and owing to the general lab interest in the p97 system in DNA damage response (DDR), the rest of the introduction will focus on diverse function of p97 in cell cycle, replication and in DDR.

## 1.5 Cell cycle

The cell cycle is a highly regulated process that requires the coordinated and spatiotemporal action of many different proteins. Cyclin-CDK (cyclin dependent kinases) complexes are the major force for cell cycle progression. The cell cycle can be explained in four major stages: G1 (gap1) phase acts as a preparatory stage for upcoming replication, S (synthesis) phase is involved in DNA replication, G2 (gap2) phase makes sure DNA replication is complete and also prepares for the upcoming cell division stage, and finally M (mitosis) phase, where duplicated DNA is segregated into two daughter cells. Among these four major cell cycle stages, much of the late G1 overlaps with early S phase and much of late S phase overlaps with G2 phase. This overlapping function of distinct cell cycle stages ensures checks and balances, before being fully committed to the next phase of the cell cycle. Precisely, three interphase CDKs (CDK2, CDK4 and CDK6) along with mitotic CDK1 and ten cyclins are responsible for cell cycle progression. Together they are arranged in four subclasses, namely cyclin A, B, D and E. Cyclins acts as regulatory subunits for

CDKs, thus transiently stimulating CDKs kinase activity during cell cycle progression. In addition to the transient expression of cyclins, further control is achieved by the expression of INK4 and Cip/Kip family of proteins, which inhibit CDK's kinase activity and are active throughout cell cycle. After exit from mitosis, D type cyclins are expressed, which in complex with CDK4 and CDK6, induce the expression of cyclin E at G1. Formation of the CyclinE-CDK2 complex then drives cell cycle through the G1/S transition, followed by degradation of cyclin E at the onset of S-phase. The CDK4-CyclinD complex also hyper-phosphorylate pRb and releases it from growth suppressive mode. Hyper-phosphorylation of pRb leads to release of the transcription factor E2F along with the induction of many genes, including cyclin E and A that abolish G1/S restriction and allow S-phase progression. Activated E2F also stimulates the transcription of many S-phase specific genes. Cyclin A then further drives the cells cycle through S and G2 phase by stimulating CDK2 activity. At the onset of mitosis, cyclin A is degraded and formation of the cyclin B-CDK1 complex further promotes the cell cycle until the end of mitosis. Evolutionarily conserved cell cycle checkpoints also play equally important roles, especially in the context of the DNA damage response to ensure proper replication and chromosomal segregation[60–62].

### 1.5.1 The p97 system in the cell cycle

Mutation in the *Cdc48 gene* delays G1/S transition and G2/M checkpoint arrest in yeast[63]. In *C.elegans* embryos, depletion of Cdc-48 or one of its cofactors, Ufd-1 or Npl-4 causes intra-S phase checkpoint activation[64]. Inactivation of p97 or its cofactors Ufd-1 or Npl-4 delays progression through anaphase and also exit from mitosis in

*Xenopus* egg[65] extracts or in human cell lines[66]. Collectively, all these evidence suggest that p97 plays important roles in cell cycle progression.

### 1.5.2 G1/S transition

As mentioned earlier, mutations in the *Cdc48* gene cause delays in G1/S transition in budding yeast. Cdc48 interacts with Far1 protein and facilitates its degradation through the proteasome. Far1p acts as an inhibitor of the G1 Cdc28/Cln complex and degradation of Far1p is essential for Cdc28/Cln dependent G1/S transition[63].Such a precise p97 dependent G1/S transition event has not yet been reported in mammalian cells. However, given the sequential degradation of various cyclins, which are the regulators of CDKs at the onset of G1/S transition, it is highly possible that similar mechanism exists in higher eukaryotes.

### 1.5.3 S phase

#### 1.5.3.1 DNA replication

Mammalian DNA replication is a process by which genomic DNA is faithfully copied into two identical DNA molecules during the S-phase of the cell cycle. It is estimated that the haploid human genome contains 3.2 billion base pairs and is approximately 1.8 meter long. During each cell cycle, DNA replication machinery undertakes the mammoth task of replicating the genome.

#### 1.5.3.1.1 Replication Initiation

In mammals, DNA replication is initiated at the multiple locations at the same time. It starts during S-phase but the preparation begins at G1 with the assembly of a multi-subunit origin recognition complex (ORC1-ORC6) as a part of pre-replicative complexes (Pre-RCs). Binding of ORCs at replication origins acts as a launch pad for the other proteins of the pre-RC to assemble and finally form the active pre-RC complex. After ORC binds the origin of replication, two licensing factors, cell division cycle 6 (CDC6) and Cdt1 are recruited to ORC binding sites, this further promotes the assembly of minichromosome maintenance protein (MCM) complex MCM2-7 onto the origin[67]. This is then followed by cyclin E-CDK2 and DDK (Dbf4/Drf1-dependent CDC7 kinase) dependent phosphorylation of pre-RC components leading to association of CDC45 and GINS, which altogether forms a large and active helicase complex called the CMG helicase (CDC45/MCM2-7/GINS)[68].

It is important to mention that only a handful of licensed origins are actually utilised to complete DNA replication. In most of the cases, the extra licensed origins remain dormant and are passively replicated by the incoming replisome from the opposite direction. This gives rise to the question why cells needed such a high number of pre-licensed origins when it requires only few of them to complete DNA replication. It is known that licensing of all potential origins occur only once at late G1 by Cdt1 and after the onset of S phase, the replication licensing factor Cdt1 is rapidly degraded by p97 system; this is important to prevent re-replication.

#### 1.5.3.1.1.1 p97 system in replication initiation

Data obtained from *C.elegans*, *Xenopus* egg extracts and mammalian cells suggest that p97 has a profound effect in controlling DNA replication initiation. It is well known that at the onset of S phase CDT1 is ubiquitinated by two cullin-RING-based-E3-ubiquitin ligases (CRL): $SCF^{-Skp2}$ and $CRL4^{-DDB1-Cdt2}$, which results in the proteosomal degradation of Cdt1[69–72]. It was recently shown that p97 along with its cofactor Ufd1-Npl4 ($p97^{-Ufd1-Npl4}$) immediately identify ubiquitinated Cdt1 and facilitate its proteosomal degradation[73,74]. This thesis will also discuss the role of another cofactor of p97, FAF1, in the recognition and proteasomal degradation of ubiquitinated Cdt1 and its functional consequences in DNA replication in a separate result chapter.

#### 1.5.3.1.2 Elongation

Elongation of DNA replication forks start with CMG helicase mediated unwinding of double stranded DNA into single stranded DNA (ssDNA)[75]. ssDNA serves as a template for DNA polymerases and is coated with replication protein A (RPA). Binding of RPA to ssDNA offers protection from various recombination events thus providing fork stability[76]. MCM10 is required for the stabilisation of the DNA polymerase alpha-primase complex that synthesises the short RNA-DNA primer critical for DNA polymerase dependent chain elongation[77]. Replication factor C then loads PCNA onto the primary template junction, which serves as a processivity factor by tethering the DNA polymerases to the DNA to promote high speed DNA replication. DNA polymerase α acts as a primase, as the replicative DNA polymerases can only elongate a fork but cannot start it. The leading strand DNA synthesis is

carried out by replicative DNA polymerase ε and the lagging strand are by DNA polymerase δ[78]. Switching of polymerase α-primase to the replicative polymerases is achieve by the action of PCNA and RFC, which also loads FEN-1 (flap endonuclease-1) and DNA ligase I to process and seal Okazaki fragments in the lagging strand[79,80]. The role of p97 or any of its cofactors in DNA replication fork elongation was not reported previously in the literature. Our chracterisation of SPRTN and FAF1, both p97 cofactors, sheds light in that regard, which will be discussed in the result section.

#### 1.5.3.1.3 Termination

DNA replication is terminated when two forks from opposite direction approaches each other. This process involves disassembly of the replisome. Sequential assembly of various pre-RC complexes followed by their firing and fork elongation is well understood, however the precise molecular mechanism by which replication forks terminate and how the disassembly of various replisome components occurs, which are generally tightly bound to the chromatin, is not well understood.

##### 1.5.3.1.3.1 p97 in replication termination

Recently, two independent reports have described p97 involvement in replication fork termination. Experiments conducted in budding yeast show that the MCM7 subunit of the CMG helicase is modified with K48-linked polyubiquitin chains by the E3 ubiquitin ligase SCF-Dia2. MCM7 ubiquitination is late S phase specific, which also indicates its functionality with DNA replication fork termination. Indeed, they further showed that disassembly of the CMG helicase is strongly associated with p97/Cdc48 dependent identification of MCM7 ubiquitination followed by removal of whole

CMG complex. They did not find any involvement of the proteasome, a notion that can be attributed to the multiple recycling events associated with these complexes. Inactivation of p97 leads to chromatin accumulation of ubiquitinated MCM7 along with whole CMG complex[81]. Similar results were obtained in *Xenopus* egg extracts, however they could not identify the specific E3 ligase that ubiquitinates MCM7 in higher eukaryotes[82]. Furthermore, both reports, although elegant, did not provide any information regarding p97 cofactors required for this process. In conclusion, they unraveled another very important function of p97 at the termination of DNA replication.

### 1.5.4 Mitosis

Mitosis is a process where already duplicated genomic DNA is faithfully segregated into two daughter cells. This complex process require spatiotemporal requirement of multiple proteins and PTMs, dictating each step of this multistep process.

#### 1.5.4.1 p97 in mitosis

Aurora B, one of the main mitotic kinases, was identified as the first p97 substrate on chromatin, and thus opened a new p97 field of chromatin associated degradation. p97/Cdc-48-$^{Ufd1\text{-}Npl4}$ binds to ubiquitinated Aurora B and extracts it from chromatin, which allows chromatin decondensation and nuclear envelope reformation in *Xenopus* egg extract [65]and *C.elegans*[83]. A similar mechanism was reported in human cervical cancer HeLa cell lines, however it becomes operational at a much earlier stage of mitosis[66]. Inactivation of the p97 cofactor Ufd-1 or Npl-4 leads to sustained activity of Aurora B on late mitotic chromatin, which results in missegregated chromosome

and multi-lobed nuclei. These observations thus provide direct evidence of p97 dependent negative regulation of aurora B kinase activity during mitosis.

Another elegant but completely different mechanism of counteracting Aurora B kinase activity by the p97 system was shown in yeast. The $Cdc48^{-Shp1}$ ($p97^{-p47}$ complex) complex recruits Glc7 {yeast ortholog of protein phosphatase 1(PP1)}, which counterbalances Aurora B kinase activity. Inactivation of this system leads to spindle assembly checkpoint activation[84].

The p97 complex was also shown to interact with the spindle assembly factor XMAP215, TPX2, Plx1 and relocate them to the cytoplasm thus helping in proper spindle disassembly. Inactivation of p97 leads to activation of the spindle assembly checkpoint and mitotic arrest. Thus, it is evident that p97 is involved at different stages of mitosis and guide cells through this complex process[85,86].

## 1.6 DNA damage response

Our DNA is continuously challenged by various endogenous and exogenous sources, which, as a result, cause considerable alterations in the DNA structure, which can be collectively defined as DNA damage. Spontaneous hydrolysis reactions, due to the structure of DNA itself, can produce various abasic sites and depurinations events in the aqueous cellular environment. Various reactive aldehydes, reactive oxygen and nitrogen species produced due to endogenous metabolic bi-products also damage DNA to a great extent. Exposure to sunlight also considerably damages DNA. All of these DNA damaging stimuli constantly producing spontaneous DNA lesions such as abasic sites, depurinations, DNA adducts and single strand breaks, which threaten the

integrity of the DNA. Chemically, these DNA structure altering modifications are mutagenic in nature and are capable of promoting genomic instability. To cope up with this, cells have evolved very robust and evolutionarily conserved DNA damage response pathways. Depending on the type of DNA modifications cells employ precise DNA damage response pathways[87] (Figure 4). In addition, these DNA altering modifications must be resolved in a timely manner as they can be converted to more serious and highly cytotoxic DNA double stranded breaks (DSBs) in a transcription or replication dependent manner. From a cell's perspective even a single DSB can be lethal. An unrepaired DSB can cause chromosomal rearrangements, large deletions, which can ultimately cause genomic instability and cancer. It is estimated that approximately 1% of all cellular single stranded breaks are converted to DSB in a replication dependent manner giving rise to around 50 DSBs per cell cycle[88]. DSB repair pathways are equally complex and require spatio-temporal assembly of multiple proteins. Thus, it is important at this point to discuss two major DSB repair pathways, namely non-homologous end joining (NHEJ) and homologous recombination (HR).

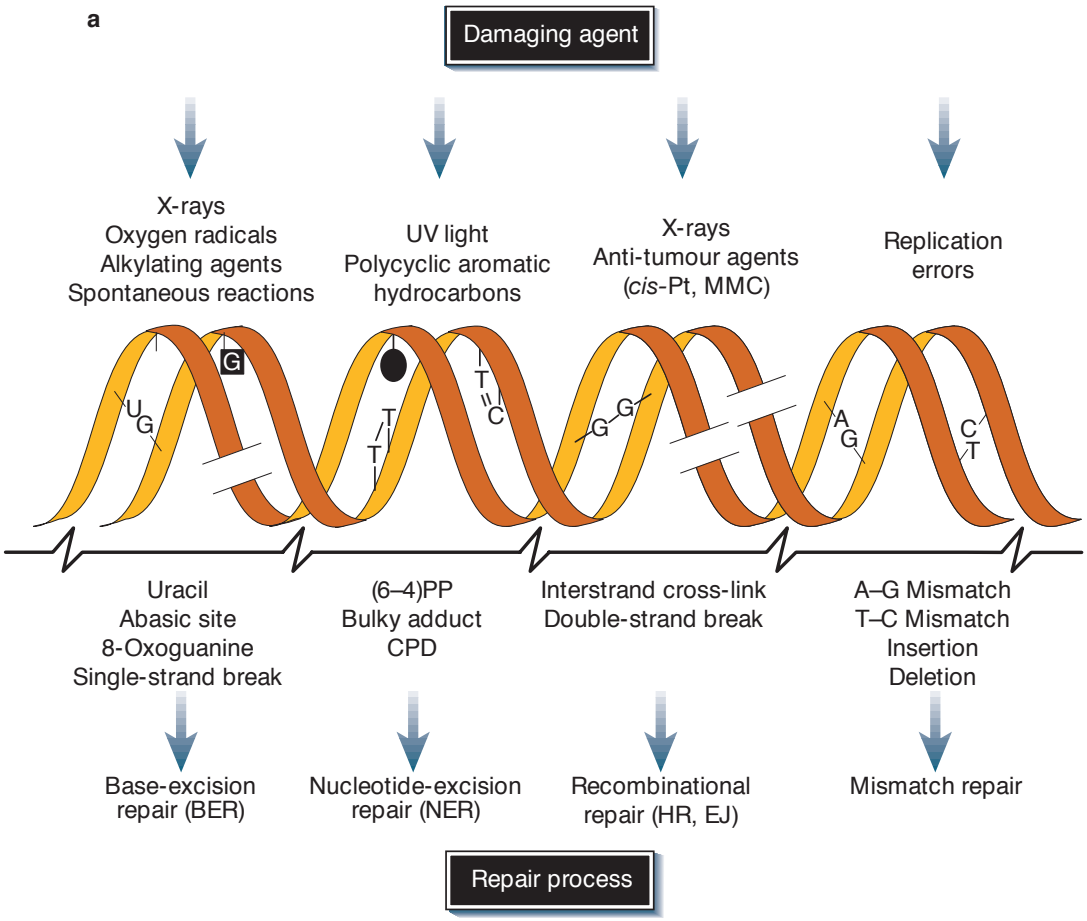



**Figure 4 Overview of the different DNA repair pathways inside the cell** (Modified from Hoeijmakers Nature 411, 366-374 (17 May 2001))

### 1.6.1 NHEJ

NHEJ pathway relies on the simple principle of re-ligating two broken DNA ends after limited resection (with the loss of genetic information) and is operational throughout cell cycle, and therefore it is error prone. DSB repair responses are also intricately aligned with various signal transduction pathways induced by phosphatidylinositol-3-OH-kinase-like kinases (PIKKs), mainly ATM (ataxia-telangiectasia mutated), ATR (ATM and Rad3-related) and DNA-dependent protein kinase (DNA-PK). These kinases along with their adaptors and signal transducers initiate the DNA repair process. In the literature, distinct functions of each kinase have been reported in NHEJ and HR, however they also overlap significantly. Upon

DSB induction, histone variant H2A.X is rapidly phosphorylated at Ser139 (γ-H2AX) by ATM, ATR and DNA-PK[89]. It is followed by recognition of γ-H2AX by Nibrin (Nijmegen breakage syndrome 1 or NBS1)[90] and MDC1 (mediator of DNA damage checkpoint protein 1)[91,92], which helps in signal amplification by stimulating ATM dependent phosphorylation of γ-H2AX[93]. γ-H2AX then helps in the localised recruitment and accumulation of other repair factors such as RNF8, RNF168, 53BP1, BRCA1, CtIP, MRE11, RAD50, RAD51, Ku70/Ku80 dimer[94]. NHEJ is initiated by recognition of the DNA ends by the Ku70/Ku80 dimer, which acts as a scaffold to recruit other NHEJ factors and also protects DNA ends from nonspecific processing. It then recruits additional DNA-PK molecules along with X-ray cross complementing protein 4 (XRCC4)[95], XRCC4-like factor (XLF), DNA Ligase IV, Aprataxin-and-PNK-like factor (APLF) to DSBs. After aligning the two broken DNA ends, they are processed by the XLF-XRCC4 complex and DNA ends are ligated by DNA ligase IV, followed by dissociation of the DNA-repair factors[96] (Figure 5).

### 1.6.2 HR

The HR pathway, on the other hand, is functional only in S/G2 phase of the cell cycle and depends on the availability of the sister chromatid. It is considered to be error-free. A recent report elegantly showed that the BRCA1 interaction site on the PALB2-BRCA2 complex is masked with ubiquitination added by the E3 ligase CRL3-KEAP1, which inactivates BRCA2 to initiate HR in G1. When cells enter S phase, the masked ubiquitination site is subjected to USP11 (USP11 expression is S phase specific) mediated deubiquitination allowing the re-establishment of the BRCA1-PALB2-BRCA2 complex, which then become free to initiate HR. Inactivation of this

specific pathway leads to Rad51 loading and unscheduled DNA synthesis in G1 phase of the cell cycle, thus offering a precise molecular mechanism of HR suppression in G1[97]. Similarly, there must be other pathways that promotes HR in S/G2 phase of the cell cycle. The confusion arises from the fact that upon recognition of a DSB, all the available resources are employed. It is still difficult to imagine, how cells make the decision to select the right pathway and how it orchestrates such intricate process. One could argue that the availability of the sister chromatid alone is sufficient to induce HR, however it still needs the exclusion of those NHEJ factors that might be inhibitory to HR. 53BP1 along with its effector proteins RIF1 and PTIP, is one such example[98–101]. At this point, much of the decision-making is orchestrated by ATM. ATR on the other hand, through CHK1 and other downstream factors prevents secondary consequences to global replication due to DSB formation. ATM then orchestrates the recruitment of BRCA1 and CtIP along with MRE11, to initiate DNA end resection, which ultimately displaces 53BP1 and initiate HR[101]. However, recent report suggested that 53BP1 is not completely excluded and that the presence of 53BP1 will prevent hyper-resection and RAD51 exhaustion[102]. Nevertheless, DSBs are resected in a 5' → 3' direction by the combined action of Mre11[103], CtIP[104] and EXD2[105], creating a 3' overhang. Long-range resection is carried out by EXO1 or DNA2 in conjunction with Bloom syndrome helicase (BLM), thus creating long stretches of single stranded DNA (ssDNA). This ssDNA is then bound by replication protein A (RPA), which is subsequently replaced by RAD51 in a BRCA2 dependent manner. The ssDNA–RAD51 nucleoprotein filaments are then involved in a homology search with a sister chromatid, which leads to strand invasion, D-loop formation, DNA synthesis followed by resolution and repair[106] (Figure 5).

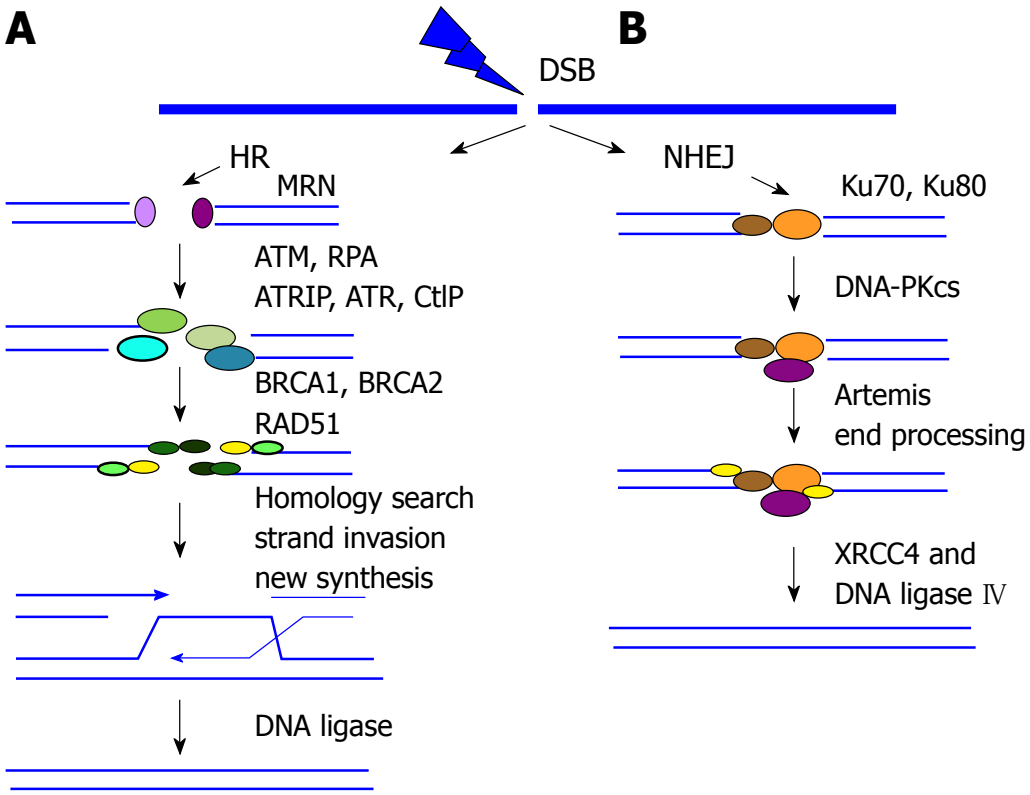



**Figure 5 Simplified overview of two major DSB repair pathways, HR and NHEJ** (modified from Guang Peng, Shiaw-Yih Lin; World J Clin Oncol 2011 February 10; 2(2): 73-79)

### 1.6.2.1 p97 system in the DNA damage response

The p97 system has recently emerged as a major player in both pathways of DSB repair. The $p97^{-Ufd1-Npl4}$ complex is recruited to chromatin immediately after DSB formation, which requires E3 ubiquitin ligase RNF-8 dependent K48-Ub chain formation. Depletion of p97 or expression of the ATPase catalytic mutant of p97 (p97-EQ) leads to hyper accumulation of K48 ubiquitin chain at DSB sites. p97 dependent extraction of K48-Ub linked polyubiquitinated substrates is essential for the recruitment of DSB repair factors such as 53BP1, BRCA1 and Rad51, followed by repair through NHEJ and HR[107]. Discovery of p97 dependent extraction of K48 linked polyubiquitinated L3MBTL1 explained why 53BP1 recruitment to the site of

DSB is severely compromised in p97-EQ cells[108]. In undamaged chromatin, H4K20me2 methylation marks are masked by the binding of L3MBTL1, JMJD2A and JMLD2B through their high affinity tandem Tudor domains, thus making it unavailable to the Tudor domains of 53BP1[109]. p97 dependent L3MBTL1 extraction from damaged chromatin thus clears the platform for 53BP1 recruitment. p97 substrates for other factors at the site of DSB (BRCA1,Rad51) have not been identified yet. Interestingly, JMJD2A and JMJD2B are also ubiquitinated by both RNF8 and RNF168 and degraded by the proteasome, however the involvement of p97 system has not been reported. In conclusion, it is evident the p97 system plays a crucial role in DSB repair. However, the exact role of p97 in DSB repair is far from being understood[48].

### 1.6.3 Replication stress response and activation of the ATR-CHK1 signalling cascade

Various obstacles such as DNA secondary structures, DNA-protein complexes or repetitive DNA elements, constantly challenge the progression of the DNA replication machinery. This phenomenon is most evident when DNA replication approaches heterochromatic regions or when it meets the transcription machinery. In addition, various DNA damages that alter DNA base structure such as depurination or thymidine dimers, DNA intrastrand cross-links or limiting pool of nucleotides also constantly challenge the replication machinery. In the literature, a global slowdown of replication fork speed, followed by aberrant fork stalling and activation of dormant origins is collectively defined as replication stress (RS)[110]. Before the advent of sophisticated techniques such as DNA fiber assay or molecular combing which enabled researchers to measure the precise nature of DNA replication defect in a

given condition, most of the DNA damage repair field relied on the biochemical parameters such as the activation of the ATR-CHK1 pathway, phosphorylation of the RPA32 and γH2AX or the BrdU incorporation assay either by immunofluorescence or by FACS analysis to indirectly measure the health of the DNA replication. Therefore, in consensus with these previous reports and in order to claim the global replication defective phenotype in any given condition as replication stress (RS), it has to qualify all these abovementioned parameters (activation of the ATR-CHK1 pathway, Phosphorylation of RPA and γH2AX). However, this simple rule does not apply to those conditions when the global replication defect is originating due to formation of bulky DNA-Protein crosslinks, which this thesis explores and provides all the possible experiments with proper controls. Moreover, with the use of the most precise technique such as DNA fiber assay, this thesis reproducibly and in multiple different conditions demonstrates that either SPRTN inactivation or low doses of formaldehyde treatment to mammalian cells leads to pronounce replication fork progression defect followed by aberrant fork stalling and as a back up mechanism activates dormant origins to complete replication, which in general must be considered as a marker for DNA replication stress.

Due to the critical nature of DNA replication, followed by the spatio-temporal requirement of multiple specialised proteins makes the replication fork very bulky and vulnerable to RS promoting factors. As a result, DNA replication fork stalling is frequent. Fork stalling leads to the appearance of RPA coated ssDNA due to uncoupling of CMG helicase from replicative DNA polymerases[111]. This is best studied with the use of many different replication interfering agents. For example; Hydroxyurea (HU) inhibits dNTP synthesis by reversible inhibition of ribonucleotide

reductase (RNR), Aphidicolin (APH) binds the active site of DNA polymerase-α and inhibits it, Camptothecin forms covalent protein-DNA crosslinks by trapping Topoisomerase I (Topo I) on the DNA and therefore forming Topo I cleavage complexes (TopoI-cc), Etoposide forms Topo II CCs by trapping Topoisomerase II on the DNA, Mitomycin C (MMC) causes intrastrand crosslinks, methyl methanesulfonate (MMS): alkylates DNA and UV light produces pyrimidine dimers. Furthermore, endogenously produced metabolic bi-products create equally diverse modifications such as abasic sites, depurination, protein-DNA adducts, and ssDNA that present a great challenge to the replication fork progression[112]. The CMG helicases moves ahead of the DNA polymerases to create a template for DNA synthesis by unwinding the double stranded DNA. The ring like structure of the (MCM complex) of CMG helicase has a 2.5 nm internal groove at its end, followed by more wider diameter in the middle, which can accommodate most of the obstacles described above, ahead of the DNA replication fork[113,114]. Thus, upon approaching obstacles, the CMG complex can easily bypass them. On the contrary, replicating DNA polymerases stall at the sites of obstacles. Continuous helicase mediated unwinding of the double stranded DNA ahead of DNA replication fork coupled with polymerase stalling at the back, leads to formation of long stretches of ssDNA[111]. At this point, it is important to control the length of ssDNA as very long stretches of ssDNA can be recognised as a substrate for various nucleases (MUS81, MRE11), which would trigger DSBs formation and unwanted recombination. Formation of DNA breaks and unwanted recombination is also prevented on newly synthesised nascent DNA by the ATR-CHK1 pathway and also by the loading of protective Rad51, which will be discussed below. Nevertheless, it is important to locally regulate helicase activity after initial fork stalling and this is achieved by uncoupling of

CDC45 from the helicase complex. CDC45 has much higher affinity towards ssDNA and the presence of ssDNA will allow CDC45 to leave the CMG complex and bind to ssDNA. Detachment of CDC45 from CMG complex will result in the inhibition of helicase activity and DNA unwinding[115].

Polymerase-Helicase uncoupling followed by the presence of ssDNA triggers a major genome surveillance pathway by activating ATR. The trimeric ssDNA-binding protein complex RPA immediately coats ssDNA. RPA coated ssDNA then recruits ATR and ATR interacting protein (ATRIP). ATR recruitment to the stalled forks offers stability and prevents stalled forks to collapse. The ATR-ATRIP complex then phosphorylates its downstream effector kinase CHK1[116]. Robust CHK1 activation also depends on the action of two mediator proteins, TopBP1[117] and Claspin[118–120]. TopBP1 is recruited to ssDNA-RPA via PCNA like RAD9-RAD1-HUS1 (9-1-1 complex) checkpoint clamp. Claspin, on the contrary, travels with the fork and is an active component of replisome. Upon fork stalling, Claspin is phosphorylated by ATR, which binds to CHK1 and further stimulate ATR mediated CHK1 phosphorylation and also provides CHK1 stability[121]. Timeless and Tipin (Timeless interacting protein) are two additional factors that are also reported to be involved in ATR mediated CHK1 activation[122,123].

CHK1 has multiple SQ/TQ motifs at its C-terminal regulatory domain, which acts as a direct target of ATR kinase activity, as a result CHK1 gets phosphorylated at multiple sites, the most notable being Ser317 and Ser345. A recent report suggested that PARP1 {Poly (ADP ribose) polymerase 1} induced PAR formation is also essential for ATR activation. Phosphorylation of CHK1 at Ser317 and Ser345 is also intricately related with its biological activity as expression of kinase dead versions of CHK1, $CHK1^{345Ala}$ and $CHK1^{317Ala}$ severely impair multiple function of CHK1.

CHK1 also auto-phosphorylate itself at Ser296 upon ATR mediated activation. ATR mediated CHK1 activation stimulates its kinase activity by releasing it from its auto regulatory closed conformation to kinase active open conformation, which leads to release of CHK1 from the replication fork [124]. It is still unknown whether there is an additional mechanism that promotes CHK1 release from chromatin.

### 1.6.4 Diverse function of CHK1 in S phase

#### 1.6.4.1 Cell cycle arrest

Kinase active CHK1 has a plethora of functions. One of the most important functions of CHK1 is to stop cell cycle progression by inhibiting CDKs. This mechanism is responsible for both intra S-phase and G2/M checkpoint arrest. Phosphorylation and activation CHK1 by ATR, immediately releases CHK1 from chromatin[125]. Once free, CHK1 stops the cell cycle by inhibiting CDKs through regulation of CDC25A and CDC25C phosphatases and WEE1 kinase. CDKs are maintained in an inactive state by phosphorylation at Thr14 and Tyr15 by the member of Wee1/Mik1/Myt1 protein kinase family. CDKs are activated by the dual specificity CDC25 phosphatases, in a rate-limiting step, by the removal of these phosphate residues. CDC25A regulates CDK2/Cyclin E during G1 and S phase. CDC25A, CDC25B and CDC25C regulate CDK1/ Cyclin B during G2 and M phase of the cell cycle. CHK1 controls the rate-limiting step of CDK activation. Kinase active CHK1 leads to phosphorylation at Ser123 of CDC25A and Ser216 of CDC25C, respectively[126]. Phosphorylated CDC25A is immediately ubiquitinated by the βTrCP adapter of the cullin–RING ubiquitin ligase SCF (Skp1-cullin-F-box), which is recognised by p97$^{-Ufd1-Npl4}$ complex and degraded by proteasome[127]. Thus, this mechanism highlights an elegant molecular mechanism of the p97 system in the regulation of CHK1 signalling cascade. Phosphorylated CDC25C is recognised by 14-3-3 proteins and sequestrated to the cytosol. Phosphorylation and sequestration of CDC25B has been shown to occur in a UV light induced manner and is a p38 dependent process. Thus, inactivation of CDC25 phosphatases, either by degradation or sequestration from the nucleus, leads to hyperphosphorylation of CDKs and their inactivation. In addition,

CDC25A and CDC25C phosphorylation is also controlled by the ATM-CHK2 pathway. Upon DNA damage, the combined action of CHK1 and CHK2 regulates cell cycle progression by the eliciting intra-S phase checkpoint response and G2/M checkpoint response[128,129]. It is important to mention that abrogation of the G2/M checkpoint is one of major factors through which cancer cells achieve genomic instability.

### 1.6.4.2 Dormant origin firing

As mentioned earlier, eukaryotic cells activate and license all the potential origins by loading excess amount of the MCM2-7 complexes. Furthermore, origin licensing also occur prior to S phase. This is to ensure, replication occur only once per cell cycle, which is important to maintain genetic stability. As a result, only 10% of the all-the dormant origins are actively utilised to complete DNA replication, the rest of the dormant origins are passively replicated. This is especially important in a transient fork stalling context, which is apparent even during physiological replication[130]. How exactly CHK1 controls and utilises the precise number of origins is still not mechanistically understood. However multiple lines of evidence suggest that under normal condition, owing to the basal activity of the ATR-CHK1 pathway, the fork moves at a constant rate, which makes sure that dormant origins are passively replicated before they can be activated by other mechanisms. This is probably achieved by the basal activity of the ATR-CHK1 pathway that locally regulates the CDC25-CDK-Wee1 cascade. The situation changes dramatically, when global DNA replication is slowed down, which leads to full activation of ATR-CHK1 pathway. Activation of CHK1 immediately stops the cell cycle, which also prevent global dormant origin firing. Please recall, with global replication fork stalling, the speed

with which an active fork approaches those pre-licensed dormant origins within a cluster is severely slowed down, which would generally lead to their activation. Full activation of CHK1 inhibits those dormant origins by inhibiting CDK mediated CDC45 loading, which is essential for the origin firing[131].

Unscheduled and aberrant dormant origins firing is one of the major factors that promote replication stress and as a consequence is responsible in part for the genomic instability in cancer cells. Cancer cells achieve this, either through oncogenic expression of Ras, Cyclin E, Myc or through mutation in key genes associated with different stages of DNA replication[132–134].

#### 1.6.4.3 Replication Fork Stability

Both ATR and CHK1 play a critical role in replication fork stability because the inactivation of either of them leads to collapse replication forks followed by DSBs formation[135]. ATR and CHK1 provide fork stability through diverse mechanism such as: (i) **stabilising replisome components at stalled fork-** it was shown that stalled forks retain polymerase ε and polymerase α for a long period of time in a ATR and CHK1 dependent manner, which is important for the fork to restart [136].

**(ii) inhibition of recombination**- the ATR-CHK1 pathway also plays an active role in the inhibition of HR at stalled forks[137]. Cds1 (CHK2), which is also a target of ATR, has been shown to phosphorylate Mus81 (endonuclease) and promotes its dissociation from the chromatin in in *Sc. pombe*[138].

**(iii) recruitment of specialised helicases-** recent studies suggests that ATR and CHK1 also stabilise DNA replication forks by regulation of two additional DNA helicases, Bloom (BLM) and Werner (WRN). ATR-CHK1 phosphorylates BLM, which stimulates BLM recruitment to stalled DNA replication fork[139,140].

**(iv) through the BRCA2-Rad51-MRE11 axis-** it was recently shown that RAD51 is required for normal DNA replication. Precisely, newly synthesised nascent DNA is devoid of any protective histones, which makes it vulnerable to MRE11 dependent exonuclease activity thus producing various replication intermediates and ssDNA gaps. RAD51 protects this nascent DNA by counterbalancing MRE11 mediated cleavage[141]. Interestingly, BRCA2 was shown to load RAD51 onto stalled replication forks to protect nascent DNA from MRE11 mediated degradation [142]. Moreover, upon DNA damage, it was shown that CDK mediated inhibitory phosphorylation of BRCA2 is abolished, which promotes BRCA2-RAD51 complex formation [143]. It was mentioned earlier that under these conditions, CHK1 promotes cell cycle arrest by inhibiting CDKs through phosphorylation and inactivation of CDC25 phosphatases. CHK1 was also shown to directly interact with RAD51 and phosphorylate it at Thr309 and to be responsible for RAD51 foci formation upon DNA damage[144]. In summary CHK1 can be established as the guardian for DNA replication fork stability.

#### 1.6.4.4 Apoptosis

It is well established that the ATR-CHK1 pathway plays a significant anti-apoptotic role by initiating the DDR and cell cycle arrest. A recent report suggested an elegant mechanism through which ATR promotes an anti-apoptotic response. Under normal physiological condition, prolyl isomerase PIN1 keeps ATR in *trans* conformation (ATR-L). Absence of catalytic active PIN1 renders ATR in *cis* conformation (ATR-H), even in the absence of UV damage. Upon UV light induced DNA damage, PIN1 is phosphorylated by DAPK1 at Ser71 and inhibited. This keeps ATR in a *cis* conformation (ATR-H). Interestingly, only cytoplasmic ATR undergoes a conformation change. The ATR-H then binds with BID and makes it unavailable to

BAX. BAX-BID interaction is prerequisite for cytochrome-c release and initiation of apoptosis [145]. This study thus demonstrated first mechanistic insight into how ATR might orchestrate its anti-apoptotic function upon DNA damage. It also suggests why ATR depletion promotes apoptosis[146]. A similar molecular mechanism for CHK1 has not been reported, however CHK1 has a potent anti-apoptotic role. Depletion of CHK1 makes S phase cells susceptible to apoptotic death upon replication stress, which is independent of CHK2 and p53[147]. In conclusion, both ATR and CHK1 are potent anti-apoptotic factors and thus is the reason why so many ATR and CHK1 inhibitors are under clinical trails at the moment[116].

### 1.6.5 Translesion DNA synthesis

UV light and various reactive oxygen species produced as endogenous metabolic bi-products cause DNA alterations such as thymidine dimers, alkylation, abasic sites, depurination, DNA adduct formation, etc. that constantly challenge the integrity of cellular DNA[148]. Cells have evolved various DNA damage specific response pathways. Unrepaired and altered DNA structures that escape such pathways can pose a serious threat to replisome progression during S phase. Replicative DNA polymerases cannot accommodate these altered structures and as a result the replication fork stalls. Replication fork stalling leads to activation of DNA damage tolerance pathways (DDT), which recruits specialised translesion synthesis DNA polymerases by a mechanism also known as TLS. TLS is initiated by mono-ubiquitination of PCNA in a Rad18-E3 ligase dependent manner. PCNA mono-ubiquitination leads to the recruitment of specialised TLS polymerases at sites of stalled replication forks, which can replicate over the distorted DNA structures [149]. The type of TLS polymerase recruited is also critical as it may lead to relatively error

free (pol-η) or error prone (pol-ζ, Rev1 etc.) lesion bypass[150]. Lesion bypass may also involved template switching with an undamaged sister chromatid. Mono-ubiquitination of PCNA offers direct lesion bypass by pol-η, whereas poly-ubiquitination has been suggested to be associated with template switch. Once the specialised TLS polymerases helps the replication fork to pass over the altered or modified bases, replicative DNA polymerases again resume DNA synthesis, by a mechanism known as DNA polymerases switch[151].

p97 and its cofactor SPRTN have recently been characterised in the TLS pathway, which will be discussed in detail in the result section.

### 1.6.6 Fanconi anemia (FA) pathway

FA is a rare autosomal recessive disorder with incidence rate of 1/200,000 to 1/400,000 in the general population. FA patients suffer from developmental anomalies, bone marrow failure and have a high cancer predisposition such as acute myelogenous leukemia (AML)[152]. FA patients have high level of chromosomal abnormalities and they are susceptible to DNA-interstrand (MMC) and intrastrand (cisplatin, psoralin) crosslinking (ICL) agents. ICL promoting agents lead to covalent crosslinking between two DNA strands and distort the DNA double helix structure. It thus offers a great obstacle in front of a moving replication fork. The inability to repair ICL leads to replication fork stalling, fork collapse and DSB formation, which are the reasons why the defect in the FA pathway are associated with replication stress and chromosomal aberration [153]. Various endogenously produced various reactive aldehydes, lipid peroxidation products, such as malondialdehyde, and metabolites from alcohol, cigarette smoke, dietary fats are the major sources of ICL production [154]. There have so far been 19 genes reported to be associated with the FA

pathway and mutations in these genes account for 95% FA patient. Furthermore, many of the FA pathway genes have a well characterised role in other repair pathways (BRCA1/FANCS, BRCA2/FANCD1) and activation of the FA pathway require participation of other pathways as well such as TLS, NER (nucleotide excision repair) and HR for the complete resolution of ICL lesions. Furthermore, the FA pathway also has a role in the DNA replication stress response, which is induced by non-ICL forming drugs. FA genes are reported with the FANC abbreviation. FANCM is one of the early sensors that get recruited to the ICL after ATR mediated phosphorylation. FANCM then acts as a platform for the subsequent recruitment of the FA core complex, which is composed of 14 different proteins (FANCA, FANCB, FANCC, FANCE, FANCF, FANCG, FANCL, FANCM, FANCT, FAAP100, MHF1, MHF2, FAAP20 and FAAP24). The FA core complex then acts as a large ubiquitin ligase for the subsequent ubiquitination of FANCD2 and FANCI [155]. The Ubiquitinated FANCD2-I complex then recruits the nuclease scaffold SLX4 (FANCP), which leads to further recruitment of other structure specific endo-nucleases, such as the heterodimer ERCC4 (also known as XPF or FANCQ)-ERCC1, MUS81–EME1 and SLX1. By the combined actions of these nucleases, the ICL is then unhooked from one of the two parental strands, in way that also involves a controlled DSB formation. TLS is then carried out to bypass the lesion opposite to the ICL and the DSB is repaired by the HR pathway [152].

#### 1.6.6.1 p97$^{-SPRTN}$ complex in ICL repair

Interestingly, the p97$^{-SPRTN}$ complex was recently shown to be involved in ICL repair. The authors suggested that the FANCD2-I complex is also SUMOylated, alongside being phosphorylated and ubiquitinated. The SUMO E3 ligase PIAS1/PIAS4 is responsible for SUMOylation of the FANCD2-I complex, whereas SENP6 (SUMO protease) antagonise it. The SUMOylated FANCD2-I complex is then polyubiquitinated by RNF4 and extracted by the p97$^{-SPRTN}$ complex from the ICL induced stalled replication forks. The p97$^{-SPRTN}$ complex mediated extraction of the FANCD2-I complex from ICLs thus offers an important counter balancing mechanism for the regulation of nucleolytic cleavage required for ICL resolution. This mechanistic insight into the p97$^{-SPRTN}$ complex in ICL repair, although elegant, raises several questions due to fact that SPRTN depleted cells are not as sensitive to MMC treatment as FANCD2 depleted cells. Furthermore, haploinsufficient mice and SPRTN mutated patients do not have any haematological abnormalities, which is the most frequent symptom associated with FA pathway abnormalities. Thus the role of SPRTN-p97 complex in FA pathway might be indirect [156].

### 1.6.7 DNA-Protein Crosslink (DPC) repair pathway

DNA-protein crosslinks (DPCs) are bulky DNA lesions, which occur due to covalent linking of proteins to the DNA. Like most other types of DNA lesion they also pose obstacles in front of a moving replication fork, which can lead to fork stalling, collapsing and DSB formation. DPCs are thus considered to be highly cytotoxic and mutagenic DNA lesions. Exogenous sources such as UV light from the sun, chemicals such as formaldehyde present in automobile exhaustion, cigarette smoke, and various

dermatological ointments are one of those major factors that can produce DPCs inside the body. Endogenous metabolites such as various reactive oxygen and nitrogen species, lipid peroxidation products (malondialdehyde) along with histone de-methylation induced formaldehyde production can also form aberrant DPCs. Enzymatic DPCs, on the contrary, are produced due to the nature of the reaction itself [157]. Although, we knew for a long period of time that DPCs occur in plethora of physiological and pathological conditions, active research and characterisation of DPC repair pathways have somehow been neglected.

Interestingly, we have gained substantial knowledge about enzymatic DPCs, owing to the discovery of specific drugs that promote such DPC formation followed by their rapid success in cancer treatment. Two such examples include the DNA topoisomerase I and II inhibitors, camptothecin and etoposide, respectively. During DNA replication, the DNA helicase mediated unwinding of the double stranded DNA leads to massive torsional stress in the double helical structure of DNA. DNA topoisomerases, for example, Topo-I and Topo-II, are specialised group of enzymes, which are involved in cutting one (Top I) or both (Topo II) the DNA strands and allowing the nicked DNA to rotate relieving the torsional stress. During this process, topo-I and II remain covalently bound to either one or both the strands of the DNA, respectively, and producing either a 3'- (topoI) or 5'- (topoII) phospho-tyrosyl bond between their active site tyrosine and 3'- or 5'- end of the DNA, producing TopoI or TopoII cleavage complexes (cc). Upon stress relaxation, when the nicked 5'-OH end of the DNA is properly aligned with the 3'-TopoI bound DNA, there is nucleophilic attack from the 5'OH (of the other DNA end), which leads to re-ligation of the two DNA end and release of TopoI. TopoII, although involved in similar catalysis reaction, needs ATP and Mg for subsequent cleavage and re-ligation of the broken

end. For the re-ligation step, it is important that the broken ends are aligned properly, as a result, presence of abasic sites, mismatch bases, protein DNA adducts and pre-existing breaks can permanently trap the enzyme to DNA, which are also frequent in the genome. Trapped DPCs are highly cytotoxic in nature and capable of apoptosis upon DSB induction in a replication dependent manner. Interestingly, this is the principle through which camptothecin, etoposide and their derivatives trap TopoI and TopoII, respectively, on the DNA by binding to the enzyme-DNA interface and preventing the re-ligation step. These drugs are also the frontline anti-cancer strategy today [158,159,159–163].

Owing to the endogenous production of these cleavage complexes, cells have evolved specific enzymes, which can cleave these cleavage complexes. TDP1 and TDP2 are specific enzymes that can cleave TopoI and TopoII-ccs, respectively [164–167]. However, it is known from the literature that TDP1 cannot cleave full-length TopoI and it can only process an already pre-processed peptide of TopoI [168]. Involvement of the proteasome has been suggested for such a reaction, however it is questionable how the proteasome identifies and process such structures, especially when one end of the substrate is covalently attached to DNA.

#### 1.6.7.1 CDC48$^{-WSS1-DOA1}$ or p97$^{-SPRTN}$ complex in DPC repair

Two recent reports shed light in that context. Mutation in the SMT3 gene, which encodes the yeast SUMO protein, leads to improper chromosome segregation and overexpression of WSS1 (weak suppressor of SMT3) partially rescues this phenotype. WSS1 was also known for its function in the DNA damage response and recombination dependent repair processes. Moreover, WSS1 depleted yeast strains are hypersensitive to UV light. Two recent reports suggested that WSS1 removes toxic,

covalently attached TopoI-cc from cells[169,170]. WSS1 depleted cells are hyper sensitive to formaldehyde, which is intriguingly known for its potent crosslinking properties. Yeast cells lacking TDP1 and WSS1 accumulate Topo1-cc. WSS1 enzymatically removes covalently trapped Topo1-cc. Balakirev et al further suggested that WSS1 is a sumo isopeptidase, which possess an intrinsic E-3 SUMO ligase activity. They further identified a novel p97/CDC48 cofactor, DOA1, in this regard. p97/CDC48$^{-WSS1-DOA1}$ is recruited to the SUMOylated substrates on chromatin. After recruitment, WSS1 further SUMOylates its substrate in a manner that stimulates its intrinsic protease activity, which is ultimately responsible for the removal of toxic SUMOylated DNA adducts. A very recent report also suggested that aberrant DPCs are removed in a replication dependent manner in *Xenopus* egg extract, however they were unable to identify the protease involved in this process[171]. In conclusion, data originating from yeast and *Xenopus* egg extracts suggest that p97/CDC48$^{-WSS1-DOA1}$ processes bulky DPCs into small peptides before the onset of the canonical DNA repair pathways [170,172]. It is still not known how the remnant peptides, as a result of the WSS1 mediated proteolysis reaction, are removed from DNA. Owing to the structural similarities in the SprT domain, mammalian SPRTN was suggested to be a homologue of yeast WSS1. Along with the N-terminal SprT domain, both WSS1 and SPRTN have p97-binding domain (SHP and VIM in WSS1, SHP in SPRTN). In addition, SPRTN has two ubiquitin binding domain (N-terminal MIU and C-terminal UBZ) and a PCNA interacting motif (PIP box). In contrast, WSS1 only possesses two SUMO-interacting motif (SIM) on its C-terminal end. To this end, our recent manuscript suggested that SPRTN is a novel metalloprotease that removes DPCs in a replication dependent manner in human cell lines.

Collectively, it is evident that p97 along with its myriad of cofactors plays an essential role in the cell cycle, DNA replication and the DNA damage response (Figure 6). Mechanistic insight into the p97 system in replication initiation and termination have been reported, but involvement of this system in DNA replication fork progression was not previously known. We have shown for the first time that the bonafide p97 cofactors, SPRTN [173] and FAF1 [174] control replication fork progression.

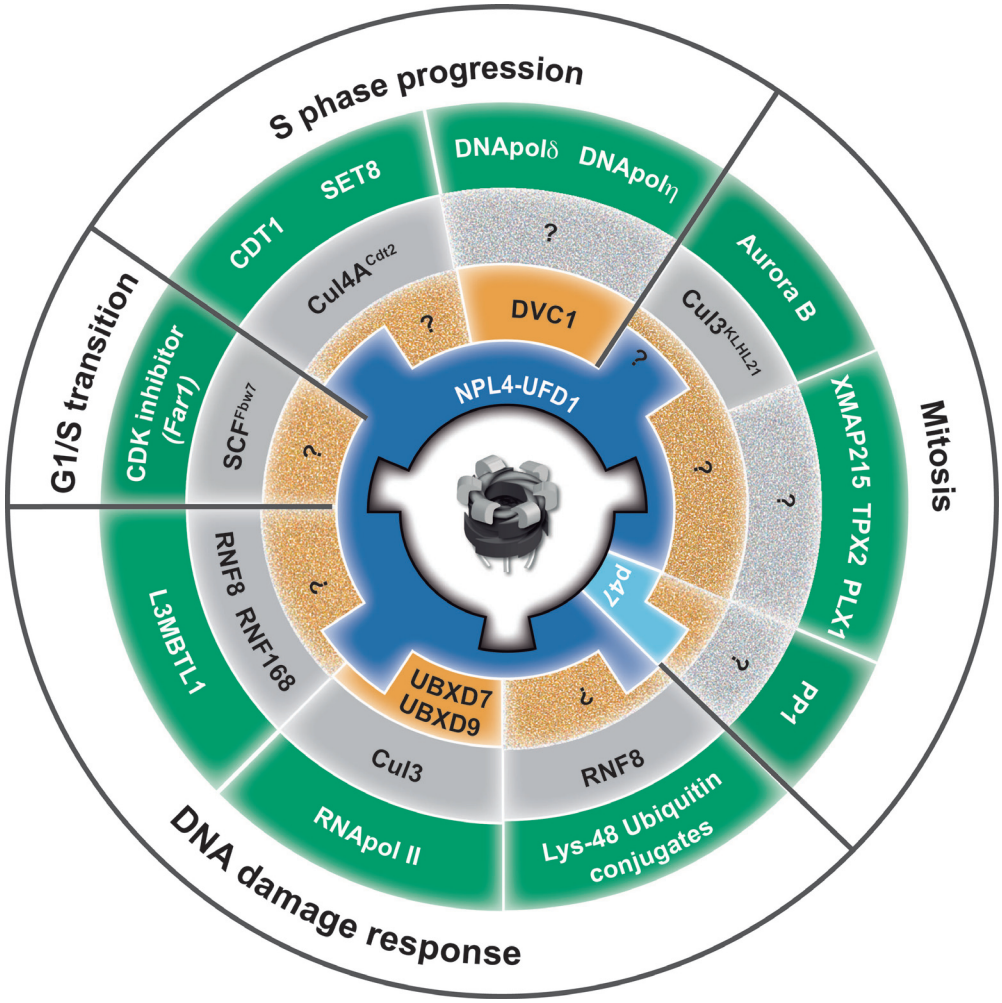



**Figure 6 Cartoon showing diverse function of p97 in genomic instability** (modified from Vaz B, Halder S and Ramadan K (2013) Role of p97/VCP (Cdc48) in genome stability. Front. Genet. 4:60).

# 2 Materials and Methods

# 2.1 Tissue culture

### 2.1.1 Revival of frozen cell lines

Cryovials containing frozen cells were stored in liquid nitrogen and rapidly thawed at 37° C. Cells were then washed with 10 ml of complete media to remove any traces of freezing media containing DMSO by slowly mixing with pipettes and were centrifuged at 600 g for 3 minutes. The supernatant was aspirated and the cell pellet was resuspended in 10 ml of complete media and transferred to a $10cm^2$ tissue culture dish or T25 tissue culture flasks depending on the cell types.

### 2.1.2 Maintenance of cell lines

All cell lines, except lymphoblastoid control and patient cells (LCLs) were maintained in Dulbecco's Modified Eagle's Medium - high glucose (DMEM, Sigma-6429) supplemented with 10% foetal bovine serum (FBS, Gibco-10270), 100U penicillin and 0.1 mg/ml streptomycin (Sigma-P4333). Lymphoblastoid cell lines were maintained in Roswell Park Memorial Institute-1640 (RPMI-1640, Sigma-R8758) supplemented with 15% FBS and 100U penicillin and 0.1 mg/ml streptomycin. All cell lines were grown at 37°C in a humidified incubator with 5% carbon dioxide. Cells were sub-cultured every 3 days by washing them with phosphate buffer saline (PBS) and then incubated with Trypsin-EDTA (Gibco-15400-054) for 5 minutes at 37°C. Trypsinised cells were re-suspended in complete medium and re-plated in 1:10 dilution for further propagation. Lymphoblastoid cells on the other hand were pipetted to gently break cell clumps and re-seeded in 1:10 dilutions.

All cell lines were routinely tested for mycoplasma contamination and found to be negative.

### 2.1.3 Cryopreservation of cell lines

Continuously growing cells were trypsinised as mentioned above. After trypsinisation complete media was added to neutralise the trypsin. Cells were counted and diluted to $1 \times 10^6$ and spun at 600 g. Media was aspirated and 1ml of freezing media containing 10% (v/v) FBS and cell culture grade DMSO (Sigma-D2650) was added. The resuspended cells were transferred to cryovials and frozen at -80° C overnight in a freezing containers which slows down the freezing rate -1° C / minute. For long term storage cells were transferred to liquid nitrogen next day.

### 2.1.4 Cell lines

The cell lines used in this study as follows:

Human osteosarcoma U2OS, human cervical cancer HeLa and human Embryonic Kidney HEK293, human urinary bladder cancer T24 cell lines were obtained from ATCC and cultured as mentioned above. Epstein-Barr virus transformed control and patient cell lines were prepared by collaborators by standard procedure. Prior ethical committee and patient party approval was obtained before any research was undertaken with patient materials.

### 2.1.5 Generation of stable cell lines by Flp-In

HEK293 SPRTN/Flp-InT-REx stable cell lines were prepared according to the manufacturer's protocol for doxycycline inducible constitutive expression of SPRTN-WT and SPRTN-Y117C. SPRTN cDNA was amplified by Polymerase Chain Reaction (PCR) with pW22-SPRTN-BAMH1-forward and pW22-SPRTN-Not1-reverse primers and cloned into the pcDNA5/FRT/TO-cSSH vector (containing Strep, Strep and HA tags at C-terminal) using BamH1 and Not1 restriction sites to generate SPRTN-WT FRT/TO construct. The construct was used as a template to generate SPRTN-Y117C mutants by site directed mutagenesis. The SPRTN-WT and SPRTN-Y117C FRT/TO constructs were transfected along with the pOG44 vector into the Flip-In host cell lines for site-specific integration into genome. The transformed cells were selected under hygromycin B to generate SPRTN Flp-InT-REx stable cell lines. The expression of SPRTN was confirmed by doxycycline induction (1μg/ml) followed by Western blot analysis.

### 2.1.6 Primer sequences

pW22-SPRTN-BAMH1-F:5'-

CAGAGGATCCGCCATGGATGATGACTTGAT GTTGG

pW22-SPRTN-Not1-R:5'-

GTTTGCGGCCGCAAGACTTTCTTCGCTTTTGAC-3'

SPRTN-Y117C-F: 5'-

TGTCGTTATTAGTGACAAATAAACAGGCATGTATCATTTCATGCAGG-3'

SPRTN-Y117C-R: 5'-

TGTCGTTATTAGTGACAAATAAACAGGCATGTATCATTTCATGCAGG-3'

### 2.1.7 Generation of CRISPR-Cas9 cell lines

The CRISPR plasmid was obtained from the Genome Engineering Oxford (GEO) centre, Sir William Dunn School of Pathology, Oxford, UK. The donor plasmid (pX459v2), containing the gRNA, Cas9 and puromycin resistance marker (Ran et al., 2013), was transfected into HeLa cells using FuGENE HD (Promega). 24h after transfection, cells were selected with puromycin for 72h and single-cell colonies were screened and validated by Western blotting and Sanger sequencing. The gRNA sequence (CACGCTCCACTTCACCTCGACGG) targeted the first exon of SPRTN inducing either a 1 bp deletion or 1 bp insertion leading to a frameshift resulting in a premature stop codon. Genomic DNA was purified from 25 HeLa CRISPR clones and PCR primers designed to amplify the guide target regions were used to generate PCR products,which were sub-cloned into TOPO vectors. Out of 25 tested TOPO clones, 17 had frameshift mutation, while the rest remained unchanged. As HeLa cells have 3 copies of chromosome 1,where SPRTN is located, this indicates a partial knockout of SPRTN. CRISPR partial knockout (Δ-SPRTN) was confirmed by Western blot with α- SPRTN antibody. We tried to generate complete SPRTN knockout in HeLa, HEK293 and RPE1 cell lines. However, complete SPRTN knockout was lethal and none of the clones survived selection, thus confirming previously published data that SPRTN knockout is lethal (Maskey et al., 2014).

## 2.2 Cloning and site directed mutagenesis

Full-length SPRTN cDNA (IRATp970E1156D, ImaGenes) was cloned into pcDNA3.1 (containing a Flag tag at the N-terminus) and pCDNA5/FRT/TO-cSSH vectors (containing Strep and HA tags at the C-terminus) for expression in a

mammalian system. For expression in E. coli, SPRTN cDNA clone was cloned into pNIC-ZB vector with N-terminal His and ZB tags (full length SPRTN-WT, and SPRTN-Y117C) or pNIC28-Bsa4 vector with N-terminal His tag. Site-directed mutagenesis using mutagenic primers, designed using the quick-change primer design program from Invitrogen. PCR was performed using the AccuPrime Pfx DNA polymerase (Invitrogen) according to the manufacturer instructions. This was then followed by Dpn1 digestion (Thermo Scientific) and transformation into competent DH5α,as described below. Mutations were then verified by sequencing at Source Biosciences sequencing service, Oxford, UK.

The pCINeo/CMVFlag-CHK1-WT plasmid was a kind gift from Grigory Dianov. CHK1 mutagenesis were designed and performed as above. Two different mutations were created in pCINeo/CMVFlag-CHK1-WT plasmid by changing amino acid serine to alanine at position 317 and 345, respectively, to obtain a phosphor-dead mutant of CHK1.

A similar strategy was taken for cloning CHK1-WT, CHK1-S345A and CHK1-S317A into the PCS2-GFP Zebrafish expression vector, which we received from our collaborator. Forward and reverse primers were generated for CHK1 with EcoR1 and Xba1 restriction sites, respectively. These were then used to amplify the cDNA for CHK1 by PCR. The PCR product was then run on an agarose gel, followed by gel extraction using a gel extraction kit, according to the manufacturers instruction (Qiagen). Both the vector (PCS2) and the insert (EcoR1-CHK1-Xba1) were then double digested with EcoR1 and Xba1, respectively, according to manufacturers instruction (NEB). Digested product were run on an agarose gel again, followed by gel extraction, as mentioned above. The DNA concentration was measured using the

Nanodrop 1000 (Thermo). The ligation reaction was carried out using a 3:1 insert to vector ratio using T4 DNA ligase (NEB) at 37° C for 1 hour followed by transformation into DH5α cells, as described below. The next day, colonies were further propagated in 5 ml of Lysogeny Broth (LB) overnight and plasmids were isolated using a miniprep kit, according to the manufacturers instructions (Qiagen),followed by sequenced to verify the insert as mentioned above. Once the PCS2-CHK1-GFP plasmid was available, the same mutagenic primers that were used to create CHK1-S317A and CHK1-S345A were used for mutagenesis in the PCS2-CHK1-GFP plasmid, as mentioned above. The Dpn1 digested product was then transformed into DH5α cells, as described above. Several colonies from each condition were further propagated in 5ml of LB broth containing ampicillin from which the plasmid was then isolated, followed by confirmation of the mutation by the sequencing, as mentioned earlier .

Primers

CHK1-S345A-F : GTGGGCTGGGCAAAGCTGATCCCTTGTACC

CHK1-S345A-R: GGTACAAGGGATCAGCTTTGCCCAGCCCAC

CHK1-S317A-F: GGGGTTCTGGCTGAGCACTGGAGTACTTCA

CHK1-S317A-R: GTGAAGTACTCCAGTGCTCAGCCAGAACCC

CHK1-ECOR1-F: GGATGAATTCATGGCAGTGCCTTTTGTG

CHK1-XBA1-R: GAGATCTAGATGTGGCAGGAAGCCAA

## 2.3 Bacterial transformation

Chemically competent E.coli DH5α cells (produced in-house) were used for plasmid transformation. Approximately 100 ng of plasmid was added to bacterial cells and mixed gently. The mixture was then incubated on ice for 20 minutes, heat shocked at 42°C for 90 seconds and then left on ice for 5 minutes. Transformed cells were then allowed to recover in 600 µl of LB broth for 1 hour at 37°C with shaking at 250 rpm. 50-100 µl of the mixture was plated onto a plate containg LB agar and ampicillin 100 µg/ml followed by incubation overnight at 37° C.

## 2.4 Plasmid purification

QIAprep spin Miniprep kit (Qiagen) was used for purification of plasmid from bacterial cultures according to manufacturers instruction. In brief, after growing bacterial culture over night at 37° C while shaking at 250 rpm, bacterial cells were harvested by centrifugation at 6800 g for 15 minutes. The pellet was resuspended in 250 µl of buffer P1 (containing RNase A) and transferred to a microcentrifuge tube. Cells were then lysed by adding 250 µl buffer P2,containing NaOH and mixing by inverting the tubes 5-6 times. The lysis buffer was neutralised by the addition of 350 µl of buffer N3 containing potassium acetate and acetic acid. Cell debris and genomic DNA were precipitated from the mixture by centrifugation at 17,900 g for 10 minutes. The supernatant containing the plasmid DNA was transferred to a QIAprep Spin column and centrifuged for 1 minute at 17,900 g. The plasmid DNA, now bound to silica membrane was washed with 0.75 ml of PE buffer to remove all the impurities. The column was centrifuged again in an empty microcentrifuge tube to remove any traces of buffer PE. The plasmid DNA was then eluted with 50 µl of sterilised water.

## 2.5 Plasmid Transfection

Plasmid transfections were performed using FuGene HD reagent (Promega) according to the manufacturer's protocol. In brief either 2 or 5 μg DNA (for $6cm^2$ or $10cm^2$ dish respectively) was mixed with Opti-Mem (Gibco) and FuGene HD (Promega) reagent and left to form complexes for 15 minutes. This cocktail was then slowly added in a drop wise manner to the cells. Fresh media was added after 6 hours. Transient protein expression was carried out for 48 hours unless otherwise indicated.

## 2.6 Gene silencing

Lipofectamine RNAiMAX (Invitrogen) was used to deliver all siRNAs to cells according to manufacturers instruction. After mixing of RNAiMax, siRNA and Opti-MEM, it was incubated at room temperature for 15 minutes to form complexes and then delivered to cells in a drop wise manner. After 6 hours fresh media was added. siRNA mediated gene silencing was carried out for 72 hours before harvesting.

siRNA sequences and working concentrations are as follows:

| Name | Concentration | Sequence/ID | Vendor |
|---|---|---|---|
| siNS | 40 μM | CGUACGCGGAAUACUUCGAtt | Microsynth |
| siSPRTN#1 | 40 μM | GUCAGGAAGUUCUGGUUAA | Microsynth |
| siSPRTN#2 | 40 μM | AGCCAAUAUAACGGUAUACCA | Microsynth |
| siSPRTN#2 | 40 μM | CACGAUGAGGUGGAUGAGUA | Microsynth |
| siPol-η | 40 μM | CUGGUUGUGAGCAUUCGUGUA | Microsynth |
| siB55**α** | 50 μM | #4390824 | Ambion |
| siFAF1#3 | 40 μM | CUGUACUGUUGGAGAGAUUAA | Microsynth |
| siFAF1#5 | 40 μM | AAGGACGAGGAUGAACGUGAA | Microsynth |
| siFAF1#6 | 40 μM | AACAUUGACGAAGCUAUUACA | Microsy |
| siFAF1#7 | 40 μM | ACCAACGUGUUCUGCUCACAA | Microsynth |
| siFAF1-3'UTR#2 | 40 μM | ACACGCUCGUCUCACUCAA | Microsynth |

## 2.7 Cell fractionation assay

For all cell fractionation based experiments approximately $1x10^7$ cells were used as starting material. After siRNA knockdown for 72 hours and treatment with different genotoxic agents (please refer specific figure legends for duration and concentration of specific drug treatment) cells were washed once with ice cold PBS and then gently lifted with a cell scraper in cold PBS. Cells were pelleted by centrifugation at 600 g for 3 minutes at 4° C. one third of the cells were kept separately for whole cell extract preparation. To the other two thirds of the cell pellet 250 µl Buffer-A was added (10 mM HEPES pH 7.4, 10 mM KCl, 1.5 mM $MgCl_2$, 345 mM Sucrose, 10% Glycerol, 1mM DTT, 20 mM NEM, Protease inhibitors containing 1 µg/ml Chymostatin, 1 µg/ml Aprotinin, 1 µg/ml Leupeptin, 1 mM PMSF and Phosphatase inhibitors containing 1 mM $Na_3VO_4.2H_2O$, 1 mM $Na_4P_2O_7$, 20 mM NaF) in ice. After addition of Buffer-A, cells were lysed by gentle flicking and 0.1% TritonX100 was added. The lysis procedure was further enhanced by gently inverting the tubes a few times. After 5 minutes the cell suspension was spun at 500 g for 4 minutes at 4° C. The supernatant was collected as the Cytosolic fraction. The cytosolic fraction was further centrifuged at a higher speed to obtain a clear fraction. The cell pellet after collection of the cytosolic fraction was washed once with Buffer-A without TritonX100 and spun at 500 g for 4 minutes at 4° C. At this step a further assessment test was carried out by taking 10 µl of cell suspension and observed under microscope for clearly visible nuclei. After washing with Buffer-A, Buffer-B (3 mM EDTA, 0.2 mM EGTA, 1 mM DTT, 20 mM NEM, Protease inhibitors, Phosphatase inhibitors) was added. At this point the extract turned very viscous and it was then properly mixed with a cut pipette tip and left for 10 minutes (nuclear burst). To this 150 mM NaCl was added and mixed once again with a cut pipette tip (to remove all the loosely bound proteins

from chromatin). This was left on ice for an additional 5 minutes, followed by rotating on a wheel C at 15 rpm at 4°. The extract was then centrifuged at 10,000 g for 5 minutes at 4° C. The supernatant was considered as the nuclear soluble fraction. The pellet was washed 2 more times with Buffer-B containing 150 mM NaCl followed by rotation on a wheel and centrifugation, as described earlier. Finally Buffer-C (50 mM Tris-HCl pH 7.5, 5 mM EDTA, 1% SDS, 20 mM NEM, protease and phosphatase inhibitors) with 1:1 ratio (volume/volume) was added to the cell pellet. DNA was sheared with a 22-gauge needle 15-20 times followed by sonication with a cycle of 30 seconds ON and 30 seconds OFF for total 20 cycles at 4°C in a Bioruptor Plus sonicator (Diagenode). The lysate was centrifuged at 15,000 g for 5 minutes. The supernatant was considered as the chromatin fraction.

## 2.8 Co-Immunoprecipitation assay

To isolate SPRTN-interacting proteins, lysates were prepared from Flp-In 293 cells upon doxycycline induction of SPRTN-WT-cSSH (Strep Strep HA tag). To compare the capturing efficiency between SPRTN-WT and patient mutation of SPRTN-Y117C, HEK293 cells were transiently transfected with SPRTN-WT-cSSH and SPRTN-Y117-cSSH plasmid respectively. Samples were lysed in 1% Triton, 150 mM NaCl, 50 mM Tris, 1mM EDTA pH 7.4 for 1hour at 4° C with 10 mM NEM and protease (Thermo) and phosphatase inhibitor cocktail (Thermo) and avidin (IBA), followed by centrifugation at 16,000 g for 10 min. The supernatant was kept at 4° C. The pellet was digested with nuclease Benzonase in the Benzonase buffer (Invitrogen) including NEM, protease and phosphatase inhibitor cocktail, overnight at 4° C. Both supernatant and Benzonase digested fractions were pooled and 10% of this pooled

fraction was stored at -20° C for later use as input. The rest of the fraction was diluted 10 times in IP buffer (150 mM NaCl, 50 mM Tris, pH 8, 10 mM NEM and protease phosphatase inhibitors) followed by preclearing of the lysate with blank sepharose (IBA) for 1hour at 4°C on a rotating wheel. Precleared samples were then incubated with Strep-Tactin sepharose (IBA) for 2hour at 4°C, washed 5 times in IP buffer containing 0.05% NP-40 and eluted in 2 x Laemmli for 10 minutes at 95°C.

## 2.9 Protein detection by Western blotting

Cells were collected from plates by gently scrapping them with a sterilised cells scraper in cold PBS. Cell suspension were then centrifuged at 600 g for 3 minutes to obtain a cell pellet. The PBS was aspirated out and lysis buffer (50 mM Tris-HCl pH 7.5, 150 mM NaCl, 6 mM EDTA, 1% NP-40, 20 mM NEM, Phosphatase inhibitors and protease inhibitors) was added. Cells were lysed on ice for 10 minutes by repeated mixing with pipettes. The lysed cells were then briefly sonicated for 15 seconds ON and 15 seconds OF for 5 cycles at 4°C in a Bioruptor Plus sonicator (Diagenode). Protein extracts were then centrifuged at 15,000 g for 10 minutes at 4° C to remove cellular debris. The supernatant was then transferred to a fresh tube and the protein concentration was measured by Lowry protein assay (BioRad). Samples for Western blots were prepared by diluting protein extracts in 1x Laemmli buffer (1% SDS, 10% Glycerol, 60 mM Tris-HCl, 0.001% Bromophenol blue, 10% β-mercaptoethanol) and boiling for 5 minutes at 95° C. Samples were then loaded alongside a molecular weight ladder (Bio-Rad) on homemade SDS-PAGE gels in a Tris-Glycine buffer containing 1% SDS and electrophoresis was carried out at constant voltage of 100 V. Proteins were transferred onto a PVDF membrane (0.45

μm pore size, Bio-Rad) with a Bio-Rad transfer unit in a Tris-Glycine buffer containing 20% methanol and 0.025% SDS for 1 hour at 100 V. After transfer, PVDF membranes were blocked in blocking buffer (5% milk in TBS containing 0.001% Tween20) at room temperature for 1 hour, washed briefly with 1 x TBS-Tween (0.001%) and incubated with primary antibody diluted in 2% BSA in 1 x TBS-Tween (0.001%) overnight at 4° C. Next morning, membranes were washed in 1 x TBS-Tween (0.001%) for 3 times for 15 minutes each with gentle shaking at room temperature. Membranes were then incubated with HRP-conjugated secondary antibody diluted 1:10,000 in 1% milk prepared in 1 x TBS-Tween (0.001%) at room temperature for 1 hour. Membranes were then washed as previously described. Protein bands on the membranes were then visualised using ECL chemiluminescence substrates (Thermo Scientific) according to the manufacturers instruction using the Bio-Rad ChemiDoc MP system.

## 2.10 Isolation of Proteins On Nascent DNA (iPOND)

iPOND was performed as described in Sirbu *et al.*[175] with the following modifications. Newly synthesised DNA in HEK293 or HeLa (WT or HeLa Δ-SPRTN cells) (~2 x $10^8$ cells per condition) was labelled via incubation with 10 μM 5-ethynyl-2'-deoxyuridine (EdU) for 10 and 15 minutes, respectively. Prior to labeling with EdU, HEK293 cells were synchronised by double thymidine block, as described below, and washed thoroughly with 1 x PBS followed by the addition of complete media and released into S-phase for 4 hours before EdU labelling. For experiments in HEK293 cells, the chromatin was fragmented into approximately 50-300 bp fragments by sonication with a Bioruptor Plus sonicator (30 seconds ON, 30 seconds

OFF for 50 cycles). In HeLa cells, chromatin was fragmented into approximately 300-500 bp fragments (30 seconds ON, 30 seconds OFF for 50 cycles). After biotin was conjugated to EdU by click chemistry, as previously described by Sirbu *et al*[175], the proteins on EdU- labelled DNA were isolated by incubation overnight with streptavidin-coupled agarose beads (Merck Millipore). Aliquots of each extract were kept for loading controls.

## 2.11 Double Thymidine Block

Cells were synchronised at the G1/S boundary by treating cells with 2.5 mM thymidine for 17 hours. Following that, the thymidine containing media is aspirated out and fresh media was added for 8 hours, followed by a further treatment with thymidine for 16 hours. Next fresh media was added and cells are allowed to enter S-phase. Four hours after their release, EdU was incorporated to track nascent DNA synthesis [73].

## 2.12 Antibodies used in this thesis for Western blot experiments

Rabbit anti-CDT1 (Bethyl A300-786A, 1:1,000), rabbit anti-FAF1 (Cell Signalling #4932S, 1:1,000), mouse anti-β-actin (Abcam ab6276, 1:10,000), mouse anti-p97 (Abcam ab11433, 1:1,000), mouse anti-ATM (Sigma-Aldrich A1106, 1:2,000), rabbit anti-phospho ATM ser1941 (Abcam Ab81212, 1:5,000), rabbit anti-ATR (Bethyl A300-A137A, 1:1,000), rabbit anti-phospho ATR Ser428 (Millipore ABE389, 1:1,000), mouse anti-CHK1 (Cell Signalling 2360, 1:1,000), mouse anti-CHK1 (Santa Cruz sc8408, 1:1000), rabbit anti-phospho CHK-1 Ser345 (Cell Signalling 2348,

1:1,000), rabbit anti-phospho CHK1 Ser296 (Abcam ab79758, 1:1,000), rabbit anti-phospho CHK1 Ser317 (Cell Signalling #2344, 1:1,000), rabbit anti-CHK2 (Cell Signalling #2662, 1:1,000), rabbit anti-phospho CHK2 Thr68 (Cell Signalling #2661,1:1000), rabbit anti-phospho H2AX Ser139 (Novus Biologicals NB100-2280, 1:1,000), rat anti-HA (Roche, clone 3F10, 1:5,000) and mouse anti-PCNA (Abcam Ab29, 1:1,000), mouse anti-PP2Ac (Milipore 05-421,1:2000), rabbit anti-PP2Aa (Milipore 2514482, 1:1000), mouse anti-PP2aB55α (Santa Cruz sc81606,1:1000), rabbit anti-Polymeraseδ (Abcam ab10362,1:1000), rabbit anti-RPA32 (Bethyl A300-244A, 1:5000), rabbit anti-phospho RPA32 Ser4/8 (Bethyl A300-245A,1:5000), mouse anti-Vinculin (Abcam ab18058,1:1000), mouse anti-Flag (Sigma F7524, 1:1000), mouse anti-CDC25A (Santa Cruz sc7389, clone f-6, 1:1000), rabbit anti-pCDK substrate (Cell Signalling #9477s, 1:1000), rabbit anti-CDK2 (Abcam ab6538,1:1000), rabbit anti-phospho PP1A Thr320 (Abcam ab62334), rabbit anti-PP1A (Abcam ab150782,1:1000), rabbit anti-SPRTN N-terminal and rabbit anti-SPRTN C-terminal antibodies were produced at home (Lessel *et.al*, 2014). Anti-rabbit, anti-mouse horseradish peroxidase (HRP)-conjugated secondary antibodies were purchased from Sigma- Aldrich (A9169 and A9044, respectively, 1:10,000). Anti-rat HRP-conjugated antibodies were purchased from Bio-Rad (5204-2504,1:10,000). Membranes were activated using Thermo Scientific Super Signal West Pico, Dura and Femto substrates and developed according to the manufacturers instructions.

## 2.13 DNA fiber assay

The DNA fiber assay was performed as described previously[173]. Briefly,

asynchronous HEK293, LCLs or HeLa cells were labelled with 30 μM of 5-Chloro-2'-deoxyuridine (CldU, Sigma-C6891) for 30 min, and then labelled with 250 μM of 5-Iodo-2'-deoxyuridine (IdU, Sigma-17125) for an additional 30 min. HeLa cells were washed 3 times with warm PBS after first nucleotide (CldU) incubation. DNA replication was inhibited by treating cells with ice-cold PBS. Cells were lysed in 200 mM Tris-HCl pH 7.4, 50 mM EDTA and 0.5% SDS, DNA fibers were spread onto a positively charged glass slides, fixed with 3:1 methanol and acetic acid (v/v), denatured with 2.5 M HCl, blocked with blocking solution (2% BSA in PBS containing 0.001% Tween20) and stained with anti-rat and anti-mouse 5-bromo-2′-deoxyuridine (BrdU) that specifically recognize either CldU (Abcam- Ab6326, dilution 1:500) or IdU (BD- 347580, dilution 1:100) for one hour at 37° C. After incubation slides are washed 3 times with 1 x PBS containg 0.05% Tween 20 (PBS-T) and briefly blocked again in blocking solution. Anti-rat Cy3 (dilution 1:300, Jackson Immuno Research, 712-116-153) and anti-mouse Alexa-488 (dilution 1:300, Molecular Probes, A11001) were used as the respective secondary antibodies. Slides were washed 3 times with PBS-T, air-dried at room temperature and mounted with ProLong Gold antifade reagent (ThermoFisher P36930). Microscopy was done using a Leica DMRB microscope with a DFC360FX camera. The lengths of the CldU- and IdU-labelled tracts were measured by ImageJ software and converted into micron scale. Statistical analysis was done by GraphPad Prism software using unpaired *t*-test. For the DNA fiber assay under genotoxic stress, the second nucleotide (IdU) was either mock treated or incubated in the presence of different replication interfering drugs (please see specific figure legends for duration and concentration of the drugs).

## 2.14 Metaphase spread

HEK293 cells were either mock depleted or depleted with siRNAs as indicated in the figure legends for 72 hours. Following protein depletion, they were treated with 100ng/ml colcemid for 2 hours. Following this, cells were washed with warm PBS, trypsinised and collected. Cells were then centrifuged in a complete media for 10 minutes at 1000 g. Ninety percent of the media was aspirated out and cell pellet was resuspended in the remaining media. Following this, 3 ml of hypotonic solution containing 0.4% KCl was added to the cell pellet in a drop wise manner and incubated at 37° C for 15 minutes. Next, 2 ml of fixative containing methanol: acetic acid in 3:1 ratio was added to the cells present in the hypotonic solution, followed by centrifugation at 1000 g for 10 minutes. The supernatant was aspirated out and the cell pellet was resuspended in 5 ml of fixative followed by incubation at room temperature for 15 minutes and centrifugation at 1000 g for 10 minutes. The supernatant was aspirated out and cells were resuspended in 1ml of 100% acetic acid and again incubated at room temperature for 10 minutes followed by centrifugation at 1000 g for 10 minutes. The supernatant was completely aspirated out and cells were resuspended in 5ml of 3:1 fixative. Metaphase spreads were prepared by dropping the cell suspension from a height onto pre-wetted slides. The slides were air dried, stained with DAPI and examined under the microscope.

## 2.15 Immunofluorescence

Cells were seeded on circular coverslips in 6 $cm^2$ plates. The next day the gene of interest was silenced using siRNA for 72 hours, followed by treatment with specific genotoxic agents (please see specific figure legends for duration and concentration of

specific drugs). Coverslips were transferred to a new 12 well plate and washed once with PBS. Cells were pre-extracted for 3 minutes on ice with ice-cold pre-extraction buffer (25 mM HEPES pH 7.5, 50 mM NaCl, 1 mM EDTA, 3 mM $MgCl_2$, 300 mM Sucrose, 0.5%TritonX100). After pre-extraction, the buffer was carefully washed off with PBS. Cells were then fixed by the addition of ice-cold methanol followed by incubation at -20° C for 30 minutes. After fixation, the coverslips were washed 3 times with PBS. Cells were then blocked in blocking buffer (3% BSA, 0.5%Tween20, 1 x PBS) for one hour at room temperature. The primary antibody was diluted in blocking solution and the coverslips with fixed cells were incubated with the primary antibody for 90 minutes at room temperature, washed 3 times and incubated with the respective secondary antibody for 45 minutes. After incubation they were washed again and finally each coverslips were incubated with 2 x DAPI for 15 minutes at room temperature and washed once with 1 x PBS. Coverslips were then mounted with mounting media onto clean glass slides and stored at 4° C. Images of immuno-stained cells were taken with an epifluorescent microscope (Olympus BX51) and acquired with a charge-coupled device (CCD) camera (Orca AG), a Zeiss LSM 510 META laser scanning microscope or an SP2 Leica confocal microscope.

The antibodies used are as follows- phosphorylated -H2AX (Ser139) (dilution 1:300, Millipore, 05-636); anti-zebrafish -H2AX (dilution 1:1,000, gift of J. Amatruda); anti-rabbit 53BP1 (dilution 1:200, Santa Cruz, sc-22760); anti–Ki-67 (dilution 1:200, Millipore, MAB 4190);

### 2.15.1 Detection of ssDNA foci

Cells seeding and siRNA transfection were carried out as mentioned in previously. For Single Stranded DNA (ssDNA) detection 10 μM 5-Bromo-2'-deoxyuridine

(BrdU Sigma-B5002) was added 24 hours after siRNA transfection and continued for 48 hours. Cells were then pulse labeled with 100 μM of CldU for 30 minutes before the addition of different replication interfering drugs (see specific figure legends for duration and concentration of drugs). Cells were washed with PBS, pre-extracted, fixed and blocked as mentioned previously. The coverslips were incubated with mouse anti BrdU antibody (BD-347580) at 1:100 dilution for 1 hour. The bromine atom of the BrdU nucleotide analogue is hidden behind the phospho-di-ester bond of the double stranded DNA. Therefore, the anti-BrdU antibody cannot detect BrdU when the DNA is double stranded, and only BrdU coated single stranded DNA, arising as a consequence of replication stress or double stranded break induced end resection, will be detected. The coverslips were then washed 3 times with PBS and incubated with a goat anti mouse alexa 488 secondary antibody at a 1:1000 dilution for 30 minutes. After incubation, the coverslips were washed again. The primary and secondary antibody conjugates were then fixed with 4% formaldehyde in PBS for 15 minutes followed by one more round of washings. DNA was then denatured in 1.5 N HCl for 30 minutes and washed with PBS. Immunodetection of CldU after denaturation (replication foci) was carried out with rat anti-CldU antibody (Abcam ab6326) with a 1:100 dilution for 1 hour. The coverslips were washed again with PBS followed by one more washing with a high salt buffer for 15 minutes (200 mM NaCl, 0.2% Tween20, 0.2% NP-40, prepared in PBS) followed by a final washing with PBS. Goat anti rat cy-3 at 1:2000 dilution was used to detect CldU for 1 hour followed by washing with PBS. Finally coverslips were mounted in mounting medium supplemented with 2 x DAPI. The images were taken with Leica DMRB microscope with a DFC360FX camera.

# 2.16 DPC assay

### 2.16.1 DNA-protein crosslinks isolation

DPCs were detected using a modified rapid approach to DNA adduct recovery (RADAR) assay [176]. In brief, 1.5 to 2 x $10^6$ cells were lysed in 1 ml of M buffer (6 M GTC, 10 mM Tris–HCl pH 6.8, 20 mM EDTA, 4% Triton X100, 1% Sarkosyl and 1% Dithiothreitol). DNA was precipitated by adding 100% ethanol and washed 3 times in wash buffer (20 mM Tris-HCl pH 6.8, 150 mM NaCl and 50% ethanol) and was then solubilised in 1 ml of 8 mM NaOH. A small aliquot of the recovered DNA was digested with proteinase K (Invitrogen) for 3 hours at 50° C and the DNA concentration was quantified using PicoGreen dye (Invitrogen), according to manufacturer instructions. The DNA concentration was further confirmed by slot-blot analysis, followed by immunodetection with an antibody against dsDNA.

### 2.16.2 DNA-protein crosslinks detection

Total DPCs were visualised by silver staining (Sigma) as recommended by the manufacturer after electrophoretic separation on polyacrylamide gels. The DNA was digested with Benzonase (Invitrogen) for 30 minutes at 37° C, followed by proteins precipitation using a standard Trichloroacetic Acid protocol (Cold Spring Harbor Protocols, 2011), followed by resolution via SDS-PAGE. Specific DPCs were detected using a vacuum slot-blot manifold (Bio-Rad) followed by immunodetection. In brief, equal amounts of DNA were diluted in Tris-buffered saline (TBS) and applied to either a polyvinylidene difluoride (PVDF, Millipore) or nitrocellulose (Bio-Rad, Hercules CA) membrane using a vacuum slot-blot manifold. The membrane was

then blocked in 3% BSA in TBST (TBS containing 0.1% Tween 20), incubated with primary antibodies followed by incubation with HRP-conjugated secondary antibodies. DPCs were visualised using the Bio-Rad ChemiDoc XRS Plus Analyzer. Sample loading was further confirmed by slot-blot detection of double stranded DNA (dsDNA) with a specific α- dsDNA antibody. For the dsDNA detections samples were digested with proteinase K, diluted in Tris-Borate-EDTA (TBE) buffer, and applied to nylon membrane (Hybond N+).

## 2.17 In vitro cleavage assay

### 2.17.1 Protein purification

For overexpression in *E.coli* cells SPRTN constructs were cloned in to either the pNIC-ZB vector containing a TEV cleavable Z-basic-his tag (full length SPRTN-WT, SPRTN-E112A, and SPRTN-Y117C). For purification of full length constructs cell pellets were thawed and resuspended in lysis buffer (100 mM HEPES pH 7.5, 500 mM NaCl, 10% glycerol, 10 mM imidazole, 1 mM Tris (2-carboxyethyl) phosphene (TCEP), 0.1% DDM, 1 mM $MgCl_2$, 1 x set III protease inhibitors (Merck). Cells were lysed by sonication and 1 U of Benzonase was added to lysates before the cell debris were pelleted by centrifugation. Lysates were applied to a Ni-sepharose IMAC gravity flow column, washed with 2 column volumes of wash buffer (50 mM HEPES pH 7.5, 500 mM NaCl, 10% glycerol, 45 mM imidazole, 1 mM TCEP), and eluted in elution buffer (50 mM HEPES pH 7.5, 500 mM NaCl, 10% glycerol, 300 mM imidazole, 1 mM TCEP). Elution fractions were applied directly to a 5ml Hitrap SP HP column (GE healthcare), washed with wash buffer (50 mM HEPES pH 7.5, 500 mM NaCl, 1 mM TCEP) and eluted with elution buffer (50 mM HEPES pH 7.5, 1M

NaCl, 1 mM TCEP). The purification tag was cleaved with the addition of 1:20 mass ratio of His-tagged TEV protease during overnight dialysis into buffer A (20 mM HEPES, pH 7.5, 500 mM NaCl, 0.5 mM TCEP). Samples were concentrated by ultrafiltration using a 30 kDa molecular weight cut off centrifugal concentrator and loaded onto size exclusion chromatography using a HiLoad 16/60 Superdex 200 column at 1 ml/min in buffer A. Protein identities were verified by LC/ESI-TOF Mass spectrometry and protein concentrations were determined by absorbance at 280nm (Nanodrop) using the calculated molecular mass and extinction coefficients.

## 2.18 Zebrafish study

Wild-type zebrafish (EK and AB strains) were kept under standardised conditions in a circulating water system (Tecniplast, Germany). Eggs were collected from natural mating's. At one to two cell stages, fertilised eggs were microinjected with a previously described SPRTN morpholino (MO) and newly synthesised capped RNAs encoding different CHK1 variants fused to GFP. Growth retardation was assessed at the 90% epiboly stage using an upright bright field microscope (Leica M125 with a Leica IC80 HD camera; Leica, Germany). Immunofluorescence staining was done as described in Stiff T *et al*[177]using a rabbit-anti-γH2Ax antibody (Genetex-GTX127342, 1:200 dilution) and imaged at a Leica M205FA microscope equipped with a DFC365FX camera. All procedures involving zebrafish embryos adhered to current European regulations for the use of animals and were approved by the local authorities of Ulm University.

# 3 Results

## 3.1 Establishing the role of SPRTN in general DNA replication

### 3.1.1 Introduction

p97 along with its cofactor SPRTN has recently emerged as a major player in TLS. SPARTAN (also known as SPRTN or DVC1 or C1orf124) is a newly characterised protein, which is conserved from C.elegans to humans. SPRTN is recruited to the sites of stalled DNA replication fork, but not to ionising radiation (IR) induced damage [54,55]. Furthermore, SPRTN depletion leads to cell death upon challenging with DNA replication stress inducing agents. In addition, SPRTN interacts and also co-localises with PCNA and pol-η in UV light induced manner. As a result, SPRTN was suggested to have function in replication coupled DNA damage response pathways but not with IR induced DSB repair pathways. Furthermore, SPRTN interacts with many proteins which have been well characterised in the TLS pathways. Bioinformatic and biochemical chracterisations of SPRTN suggest that it has various domains, which enable its diverse functions. SPRTN has a putative metalloprotease (SprT) domain, a PCNA interacting motif (PIP box), a p97 interacting domain (SHP domain), and a zinc finger ubiquitin-dependent domain (UBZ). SPRTN brings p97 to sites of stalled replication forks, and this recruitment is mediated by the SHP domain in SPRTN. Absence of the SHP domain does not affect SPRTN recruitment but affects p97 recruitment to the site of damage. The presence of UBZ and SHP domain explains SPRTN role in the UPS and the presence of a PIP box connects it to PCNA dependent TLS pathway.

Although, several reports suggest the role of SPRTN in TLS, collectively their data struggled to reach a consensus about the precise function of SPRTN in TLS. The confusion arises from the opposing observations made by the different groups about the involvement of SPRTN in the different segment of TLS. In summary, three general models emerged from the available literature regarding the mechanism

through which SPRTN governs TLS. The first model described that SPRTN is recruited to chromatin after UV light induced DNA damage and form co-localised foci with the translesion DNA pol-η and the DNA replication sliding clamp PCNA. Furthermore, once SPRTN is recruited to chromatin, it further recruits Rad6 (an E2 ligase) and Rad18 (E3 ligase) to chromatin in a feed forward loop, which are responsible for PCNA monoubiquitination and the recruitment of DNA pol-η to the stalled forks to initiate TLS[178,179]. Centore *et al.* further supported this model by showing that siRNA mediated SPRTN depleted cells have severely reduced DNA pol-η foci upon UV damage, which also correlated with Rad18 depletion. The second model, on the other hand, described a balance through which SPRTN controls the ubiquitination of PCNA by inhibiting the de-ubiquitinating enzyme USP1. Upon UV induced replication fork stalling, SPRTN's association with the Rad18-PCNA complex protects ubiquitinated PCNA from USP1. Absence of SPRTN therefore leads to de-ubiquitination of PCNA and the recombination mediated rescue of the damage replication forks. They further supported this model by showing that SPRTN depleted cells indeed have 2.5 fold increase in sister chromatid exchange compared to control cells and the expression of shRNA resistant SPRTN-WT rescued this phenotype[180]. Interestingly, they also doubted the first model described here, as they could rescue PCNA ubiquitination in SPRTN depleted cells by co-depleting USP1 and as well as restoring PCNA ubiquitination in USP1 overexpressing system by the simultaneous overexpression of SPRTN. The third model, on the contrary, suggested that SPRTN is involved in the termination of the TLS pathway. After the lesion is bypassed in a TLS polymerase dependent manner, the replicative polymerases need to resume their functions. This process require a polymerase switch from the translesion synthesis polymerase to a replicative polymerase. They suggested that SPRTN brings

p97 to the stalled forks and helps in the segregation of pol-η, which then aids the switching process[54,55]. In conclusion, it is clear that the p97-SPRTN complex plays a crucial role in TLS and also promotes error free TLS by suppressing error prone TLS. This is a process which requires SPRTN′s interaction with POLD3, which is mediated by the SprT domain of SPRTN [56,181]. Our recent manuscript in this regard suggested that the SprT domain of SPRTN is proteolytically active, which raises a very interesting notion as to whether SPRTN cleaves POLD3 to suppress error prone TLS, a question that remains to be answered.

### 3.1.2 AIM: To characterise SPRTN function in normal DNA replication

### 3.1.3 Results

#### 3.1.3.1 Identification and characterisation of SPRTN mutated patients

Our group in close collaboration with human geneticists has discovered a new human syndrome, now known as Ruijs-Aalfs (RJALS) or SPRTN syndrome. SPRTN syndrome is an autosomal recessive human disease caused by biallelic and monogenic mutations in the SPRTN gene, and is characterised by premature ageing and juvenile hepatocellular carcinoma (HCC). We have identified three patients from two unrelated families (family A and B). Subsequent exome sequencings suggested the patient from family A had a 1bp-deletion at cDNA position 721bp (c.721delA) in both alleles of SPRTN, which led to a premature stop codon (p. Lys241AsnfsX8) and expression of truncated protein (249 aa) with a missing C-terminal part. As the C-terminal part of SPRTN contains several well-characterised domains Ubiquitin Binding Zinc Finger 4 (UBZ4) domain, a PCNA interacting (PIP) box, and a VCP/p97 interacting (SHP) motif, the pathogenicity of this SPRTN truncated version can be easily explained. On the other hand, the two boys from family B had one allele similar to the Family A patient (SPRTN with C-terminal truncation, p.Lys239LysfsX7). However, the other allele of the family B patients had a single missense mutation in the putative metalloprotease SprT domain, which leads to an amino acid change in the SprT domain (Y117C)[173]. This indicated that the pathogenicity of the SPRTN-Y117C mutation is due to defective metalloprotease activity (**Fig 7**).

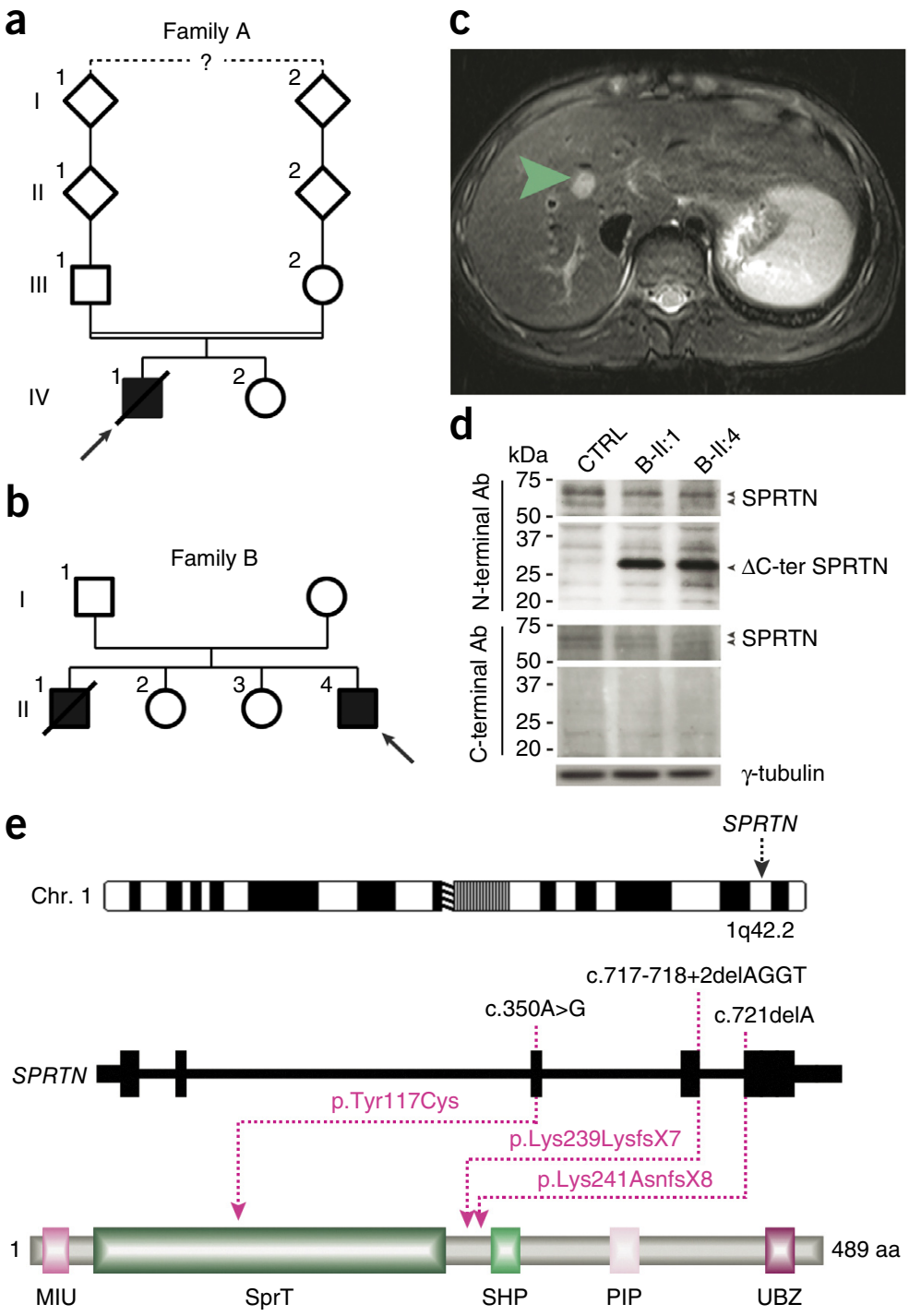



**Figure 7 Discovery of patients and identification of SPRTN mutations. a,b** The family tree of A and B. Filled and open symbols indicates affected and healthy individuals, respectively; an arrow indicates patients where whole exome sequencing were carried out, and diagonal lines denotes deceased status. The double line shows parental consanguinity, and the question mark indicates the exact degree of consanguinity is unknown. **c.** Axial view of magnetic resonance imaging of the liver of patient B-II:4. The green arrow indicates HCC. **d.** Analysis of total cell extracts of patients' LCLs with SPRTN antibodies (Ab) raised against the N- or C-terminus of the protein. **e**. Genomic localisation and protein structure of SPRTN. The genomic

structure is based on the longest ORF containing five coding exons (black rectangles). The positions of the identified mutations are shown at the both gene (top) and protein (bottom) level. The protein diagram depicts the predicted functional domains of SPRTN. aa, amino acids (Modified from Lessel et al)

### 3.1.3.2 Patient cells are hypersensitive to replication interfering drugs

SPRTN depleted cells were shown to be hypersensitive to various replication interfering drugs but not to IR. In recent years DNA replication stress was included as one of the hallmarks of cancer[182]. Interestingly, the absence of any skin anomalies (generally associated with TLS defect)[183] and haematological abnormalities (associated with defect in FA pathway) [184] followed by thorough biochemical and cell biological characterisation of SPRTN syndrome patient mutations have led us to hypothesise that SPRTN might be involved in general DNA replication. Specifically, in order to understand the function of SPRTN in vivo, we challenged SPRTN mutated patient cells with various clastogens. Indeed, patient cells treated with CPT, MMC or UV showed hypersensitivity towards these DNA damaging agents. On the contrary IR did not yield any significant difference. In addition, patient cells were marginally more sensitive towards CPT and MMC in comparison to UV (**Fig 8**). Collectively, these data suggest that patient cells are hypersensitive to those DNA damaging agents that induces DSB formation in replication stress dependent manner, but not towards aberrant DSBs caused by IR. Similar results were obtained in human cells when SPRTN protein was depleted using siRNA. In conclusion, SPRTN mutated patients and SPRTN-depleted human cells are hypersensitive to DNA replication stress inducing agents [173].

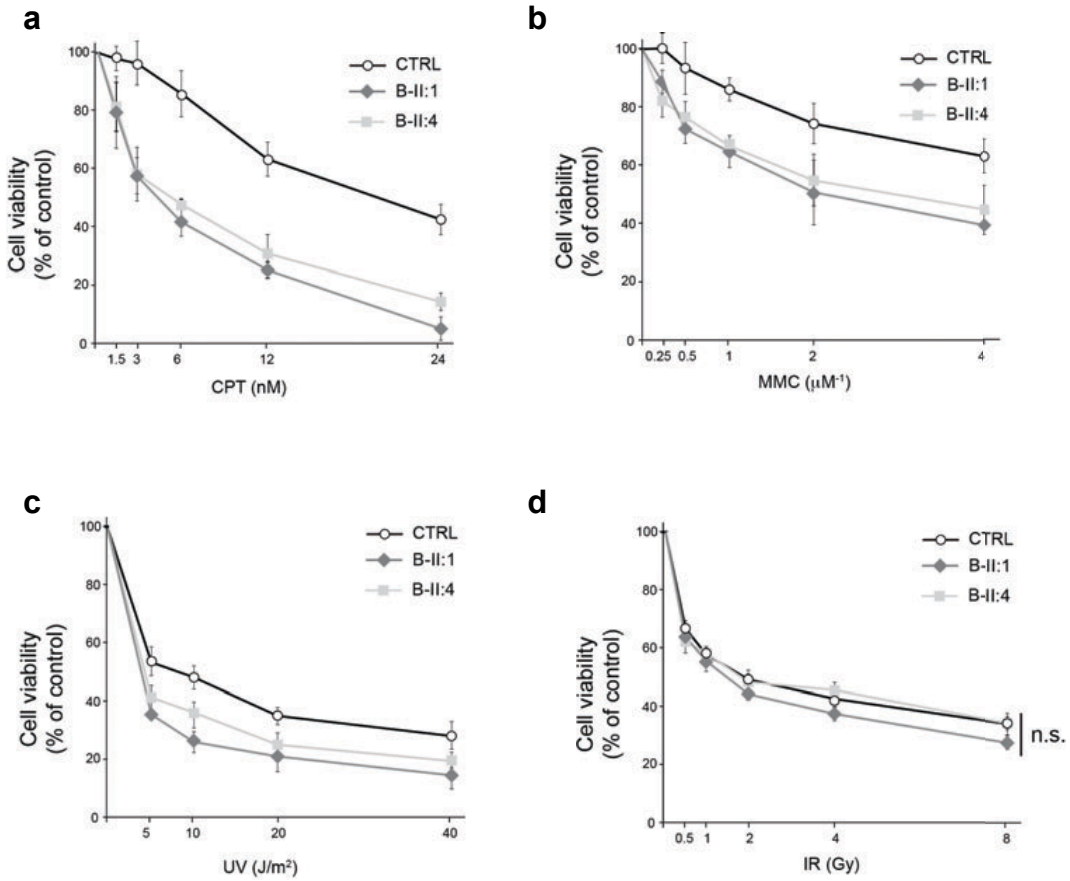



**Figure 8 Patient cells are hypersensitive to replication interfering drugs** The cell viability of control and patient LCLs after treatment with different DNA damaging agents: **a.** Camptothecin (CPT), **b.** Mitomycin C (MMC), **c.** UV-radiation, and **d.** ionising radiation (IR), using the MTT assay. The cells were treated for 48 hours with the indicated concentrations of CPT or MMC or were irradiated (UV or IR) and allowed to recover for 48 hours. n = 3. n.s. = not significant, statistical analysis were performed using an unpaired t-test via GraphPad prism software (Modified from Lessel et al)

### 3.1.3.3 Patient cells show characteristic features of DNA replication stress

53BP1 is a maker for DSBs whereas γ-H2AX has been suggested to be marker for both replication stress and DSBs[185]. In order to understand why SPRTN syndrome has genomic instability, and whether it is due to DNA replication defect, we investigated primary skin fibroblast from patient and control cells for 53BP1 and γ-H2AX foci formation. To distinguish between different cell cycle stages, we also used cyclin A as a marker for S/G2 phase and cyclin B as a marker for G2/M phase. It was recently suggested that continuous mild replication stress induced DSBs are carried to the next phase of the cell cycle, which appear as distinct, large, round shaped 53BP1 foci in G1 cells (53BP1 nuclear bodies) [186]. Thus, the presence of large 53BP1 foci in G1 phase of the cell cycle will is indicative of defective DNA replication and repair in the previous S/G2 phase. We reasoned that if SPRTN is involved in normal DNA replication, and if SPRTN patient mutations really affect DNA replication, then these cells must be struggling to replicate their genome and as an end result are prone to DSB formation. Furthermore, owing to this hypothesis, we also speculated that patient cells must show 53BP1 foci in S phase due to spontaneous DSB formation owing to defective DNA replication. Cyclin A and Cyclin B negative patient cells indeed show an elevated number of 53BP1 foci as distinct G1 nuclear bodies. Furthermore, we could also efficiently detect many smaller 53BP1 foci in Cyclin A positive cells, thus suggesting that replication stress induced spontaneous DSB formation. Additionally, Cyclin B positive patient cells showed much larger 53BP1 focus formation, thus indicating sustained DNA replication stress and an inability to repair them in a timely manner before the onset of mitosis. DNA damage in mitotic patient cells was further confirmed by the presence of γ-H2AX foci (**Fig 9 a, b**).

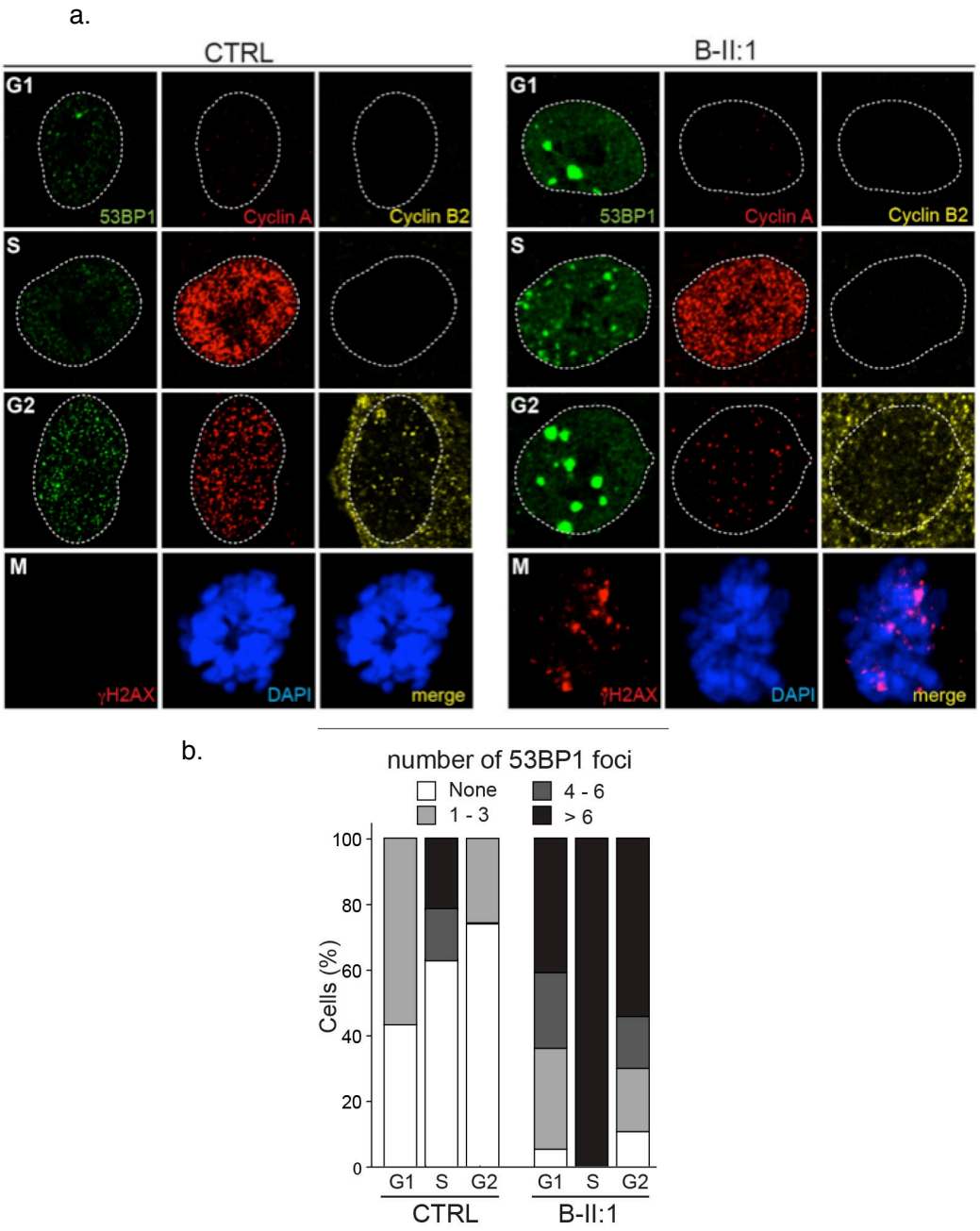



**Figure 9 Patient cells show characteristic features of DNA replication stress a.** primary skin fibroblasts were stained with S/G2 phase marker Cyclin A and G2/M marker Cyclin B2. They were further stained with a specific antibody against 53BP1 as a DNA double stranded break marker. DAPI stained mitotic cells were further stained with a γH2AX antibody as a marker for DNA damage. **b.** Quantification for **a** showing the % of cells in control (CTRL) and SPRTN mutated (B-II:1) condition having none (white), 1-3 (grey), 4-6 (dark grey) and > 6 (black) 53BP1 foci in respective G1,S and G2 phases of the cell cycle.

### 3.1.3.4 A DNA replication defect is the cause of SPRTN syndrome

In recent years, the DNA fiber assay has become the front line technique for accurately measuring DNA replication at the level of individual replication forks in human cells. The technique relies on the labelling of newly synthesised DNA by two different thymidine analogues, CldU and IdU, respectively, which is then followed by staining with specific primary and corresponding secondary antibodies. With simple permutations and combinations, the assay can be utilised for variety of measurements such as the speed of DNA replication fork progression, the number of stalled and terminated forks and newly fired origins. It can be also efficiently used for fork restart and resection experiments.

To understand the precise nature of the DNA replication problem in patient cells, we assayed DNA replication using the DNA fiber assay. To our surprise, when we compared the tract length of >300 individual forks from patient and control cells, although the difference was statistically significant between control and patient cells, the speed of DNA replication forks was not strongly affected (**Fig 10 b**). However, we did observe a 2-3 fold difference in the percentage of stalled forks and newly fired origins in patient cells in comparison to control (**Fig 10 c, d**). This observation indeed suggested that patient cells are prone to replication fork stalling, and as a result activate many more dormant origins. To better visualise the replication defect in patient cells, we challenged them with the replication interfering drug Aphidicolin (APH), which inhibits replicative DNA polymerases. We chose a very low concentration of APH (100 nM) treatment to induce mild DNA replication stress. Also to see the differences between patient and control cells more clearly, we added APH with the second nucleotide. As anticipated, even control cells struggled to replicate in the presence of a low dose of APH. However, the struggle to cope with

APH induced DNA replication stress becomes significantly more evident in patient cells. This observation clearly demonstrates a critical function of SPRTN during DNA replication, especially under mildly challenging condition (**Fig 10 e, f**). Furthermore, to prove that SPRTN mutations are indeed responsible for the DNA replication stress in SPRTN syndrome, we ectopically overexpressed GFP-SPRTN-wt or GFP-empty construct in patient LCLs. The speed of the DNA replication forks was significantly rescued by co-expression of wild type SPRTN (**Fig 10 g**). Altogether, we concluded that DNA replication stress is the main cause of SPRTN syndrome.

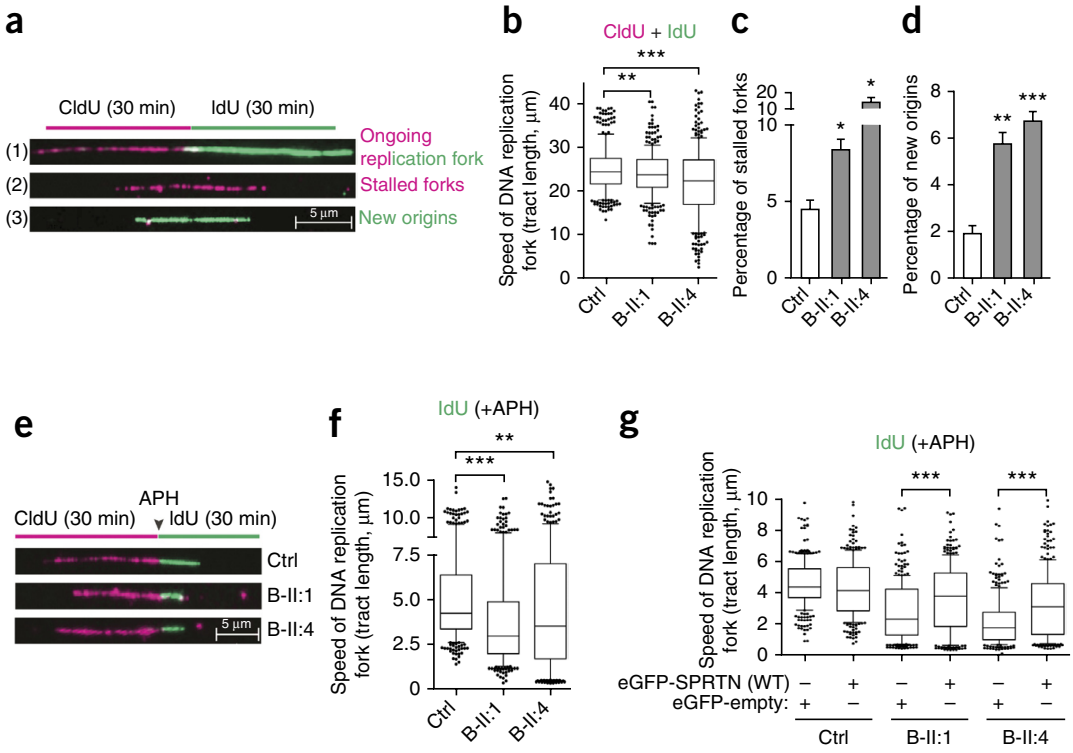



**Figure 10 A DNA replication defect is the cause of SPRTN syndrome** Continuously growing asynchronous LCL's were assayed by DNA fiber assay. **a.** Images showing different replication forks, which were used to generate data presented here and elsewhere (1) ongoing replication fork after 30 minutes of CldU (red) followed by 30 minutes of IdU (green) incubation. Under normal physiological condition due to equal incubation time CldU and IdU ratio will be 1:1. (2) Depicts a stalled fork. This fork was active during the 1st 30 minutes of incubation however was somehow stalled during IdU incubation thus did not incorporate IdU. (3) Depicts a newly fired origin. This fork was dormant during 1st 30 minutes of CldU incubation, however was activated during IdU incubation and thus did not incorporate CldU. **b**. Total tract length was measured by scoring >100 forks per condition per experiment. n = 3. **c** and **d**. >400 stalled forks and newly fired origins, respectively, were counted per condition per experiment. n = 3 **e.** representative images of DNA fibers from control and patients LCL showing the effect of APH on 2nd nucleotide incorporation. f) >100 individual tracts were scored per condition per experiment. n = 3. **g.** Effect of control or patient LCLs treated with APH followed by transient expression of either eGFP or eGFP-SPRTN(WT) vector. >100 individual tracts were scored per condition per experiment. n = 3. Data in **b, f** and **g** are shown as the median (bar) with the 25th–75th percentile range (box) and the 10th–90th percentile range (whiskers). Data in **c** and **d** are shown as the mean s.e.m. Data in **b–d, f,** and **g** were analysed with unpaired two-tailed t-test. *P < 0.0), **P < 0.001, ***P < 0.0001. (Modified from Lessel et al)

#### 3.1.3.5 Complete SPRTN depletion leads to pronounced replication defect

After observing that patient LCLs have pronounced replication fork progression defect under mildly challenging condition, we hypothesised that a complete SPRTN removal will lead to severe replication stress even under normal physiological condition. Indeed, SPRTN depletion leads to severe replication defect as shown below. Asynchronously growing U2OS cells were treated with control siRNA or two different siRNA targeting SPRTN. After 72 hours of siRNA transfection, cells were incubated with thymidine analogues and the DNA fiber assay were carried out as mentioned earlier. SPRTN-depleted cells have a severe reduction in DNA replication fork speed and an increased number of unscheduled dormant origin firing and stalled active forks (**Fig 11 a, b, c**). Furthermore, like in patient cells, SPRTN depletion leads to an increased formation of DSBs (53BP1 foci) in S-phase cells (EdU positive) (**Fig 11 d, e**). In addition, the EdU signal in SPRTN depleted cells were much weaker than in control cells, further supporting our finding that SPRTN inactivation leads to a severe DNA replication defect.

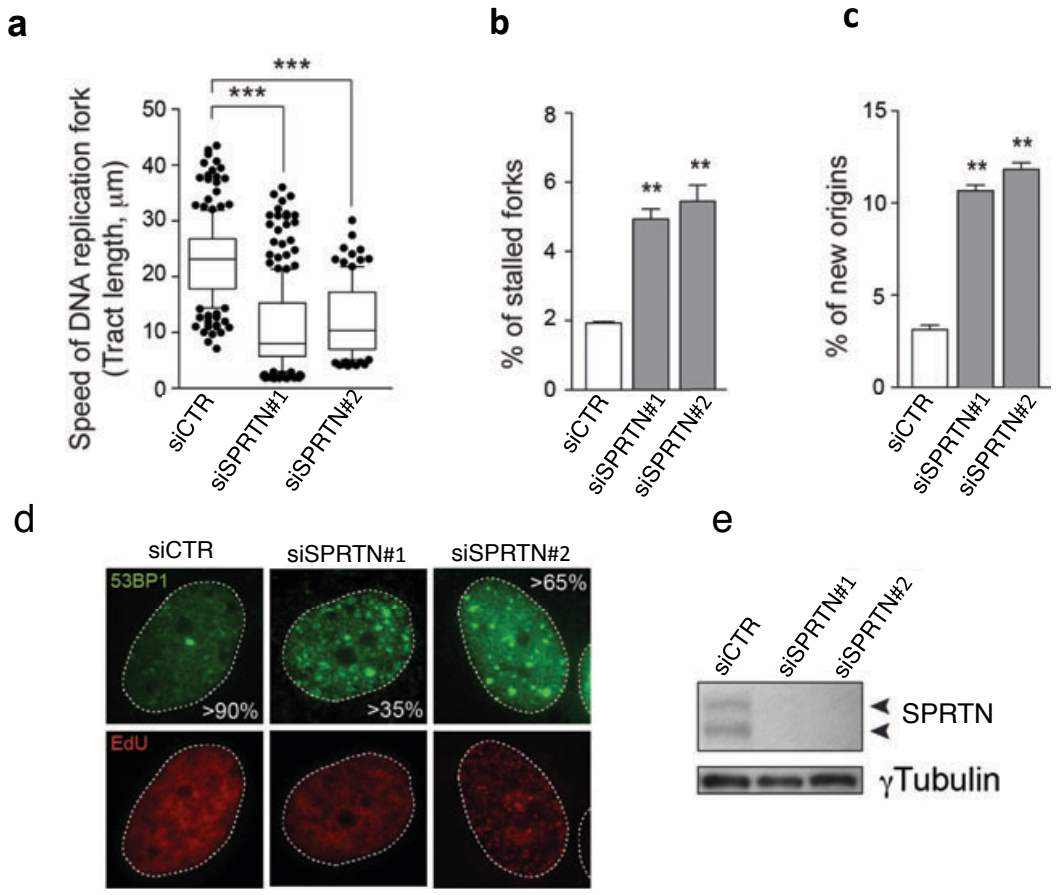



**Figure 11 Complete SPRTN depletion leads to pronounced replication defect a, b, c** U2OS cells were treated with two different siRNAs against SPRTN (siSPRTN#1 or siSPRTN#2) or control siRNA (siCTR) and DNA replication forks were analysed. The quantification is from three independent experiments using the same methodology as in the earlier figure Panels **a-d**. **b**. Representative S-phase cells (EdU-positive; cells were grown in the presence of EdU for 60 minutes before fixation) with 53BP1 (markers of DSBs) foci in control or SPRTN-depleted U2OS cells. The % of cells with the depicted phenotypes when more than 100 cells were scored per condition in three independent experiments. **e**. Efficiency of siRNA mediated SPRTN depletion. (Modified from Lessel et al)

### 3.1.3.6 Characterisation of patient mutations

To fully understand the functional consequences of the patient mutations, we generated constructs mimicking SPRTN mutations (Flag-SPRTN-ΔC-ter and Flag-SPRTN-Y117C as shown in (**Fig 12 a**). Furthermore, we transiently expressed these constructs in U2OS cells, which were depleted of endogenous SPRTN with siRNA targeting the 3' UTR (siSPRTN#1) region of SPRTN. Ectopic expression of SPRTN-WT almost completely rescued the DNA replication defect in SPRTN depleted cells. The expression of SPRTN-ΔC was also able to restore DNA replication fork speed defect, however to a much lesser extent than SPRTN-WT. This observation suggests that the C-terminal part of SPRTN has an important role in fork progression under physiological condition. The function of the missing C-terminus became more pronounced when cells were exposed to mild replication stress (APH). Interestingly, ectopic expression of SPRTN-Y117C was entirely faulty in the rescue of fork progression. This observation thus suggests a previously uncharacterised essential function of the putative metalloprotease SprT domain of SPRTN in DNA replication and genome stability. Transient co-expression of both patient variants, SPRTN-ΔC and Tyr117Cys, to mimic the situation in family B patients, leads to a significant rescue in fork speed, similar to SPRTN-ΔC expression alone (**Fig 12 b, c, d**). Collectively, characterisation of patient mutation provided valuable information about how SPRTN coordinates DNA replication fork progression. and further demonstrated that the DNA replication defect is the main cause of this syndrome.

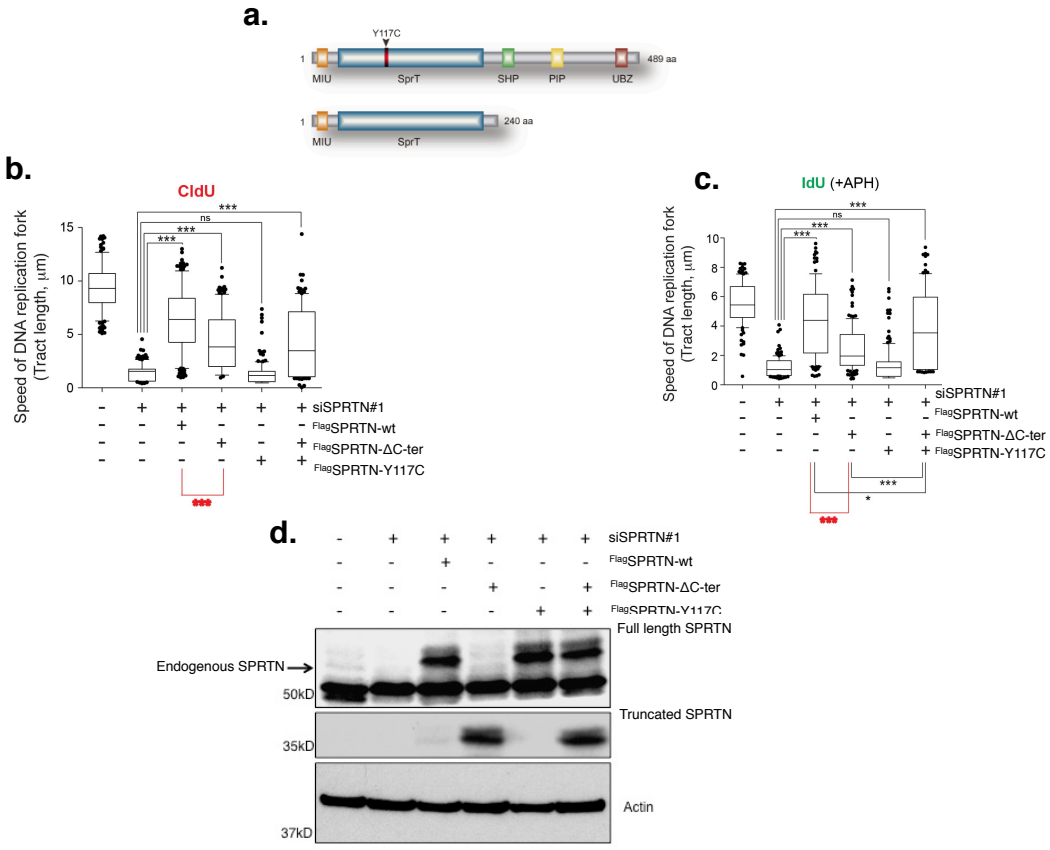



**Figure 12 Characterisation of patient mutations a.** Depiction of constructs mimicking patient mutation. **b, c** U2OS cells were labelled with CldU for 30 minutes (physiological condition, **b**) and IdU for 30 minutes in presence of APH (mild replication stress, **c**), followed by scoring of >100 individual forks per condition per experiment. n = 3. Statistical analyses were done as mentioned earlier in figure 10. **d** Western blot analysis of the same U2OS cells that were used for DNA fiber assay in **b** and **c** showing the depletion of endogenous SPRTN by 3'UTR targeting siRNA (siSPRTN#1) followed by ectopic expression of siRNA-resistant WT SPRTN, SPRTN-ΔC, Tyr117Cys or co-expression of both SPRTN-ΔC and Tyr117Cys. (Modified from Lessel et al)

### 3.1.3.7 Pol-η codepletion cannot rescue replication defect in SPRTN mutated patient LCLs or in endogenously depleted U2OS cells

It is well established from the available literature that SPRTN plays a critical role in TLS. Among the different modes of action of SPRTN in TLS, the $p97^{-SPRTN}$ complex mediated extraction of pol-η after lesion bypass (DNA polymerase switch) is suggested to be important for the resumption of the normal mode of DNA replication by replicative DNA polymerases [54,55]. Therefore it can be assumed that the hyperaccumulation of pol-η is the main cause of DNA replication stress in SPRTN inactive cells. To investigate this hypothesis, we depleted pol-η in both patient LCLs and in U2OS cells devoid of endogenous SPRTN. Interestingly, under mildly challenging condition, depletion of pol-η failed to rescue DNA replication fork speed in both control and patient LCLs(**Fig 13 a, b**). Also, we were not able to rescue the fork speed in U2OS cells after co-depletion of SPRTN and pol-η in both physiological (CldU) and mildly challenging condition (IdU+APH)) (**Fig 13 c, d**). Collectively, our data suggest that the hyperaccumulation of pol-η is not the main cause of defective DNA replication in SPRTN syndrome patient or SPRTN-depleted cells

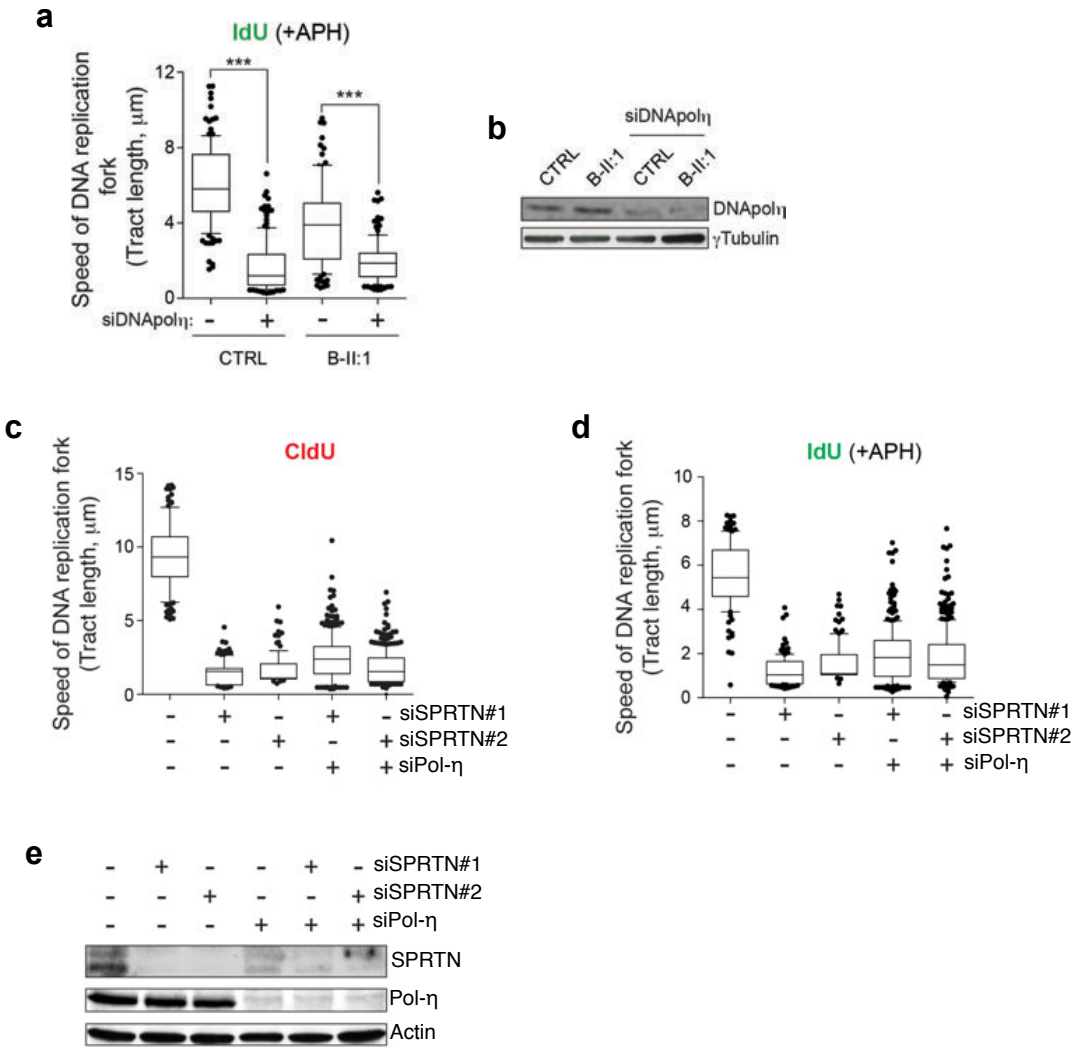



**Figure 13 Pol-η codepletion cannot rescue replication defect in SPRTN mutated patient LCLs or in endogenously depleted U2OS cells.** Analysis by DNA fiber assay of DNA replication tract length in patient LCLs or SPRTN-depleted U2OS cells +/- co-depletion of DNA polymerase-η. **a.** DNA fiber analysis of patient LCLs in the presence of APH. **b** Efficiency of siRNA mediated pol-η depletion. **c, d** Analysis of DNA replication tract length in siRNA-depleted U2OS cells under both physiological and mildly challenging condition. **e** Immunoblot showing depletion of SPRTN and pol-η. Actin was used as a loading control. (**a, c and d**) Two independent experiments with >200 fibers per condition per experiment. Measurements of DNA fibers and statistical analysis were done as mentioned earlier. (Modified from Lessel et al)

### 3.1.4 Discussion

Ageing is a natural process by which our overall physio-metabolic functions slowly deteriorates over time. It is also characterised by incomplete DNA replication followed by accumulation of DNA damage and the inability to evoke a proper repair response. As a result, ageing cells enter senescence stage (inability to proliferate). Cellular senescence is one of the main characteristics of ageing[187]. What causes an ageing cell (inability to proliferate) to become cancerous (highly proliferative) is still unknown. Paradoxically, we also do not know how an individual can suffer from both premature ageing and cancer at the same time, such as in, Werner syndrome, Bloom syndrome and Rothmund-Thomson syndrome among others. Interestingly, all of these abovementioned syndromes are monogenic in nature and studying the involved gene have provided valuable insights about ageing, the DNA damage response, genomic instability and cancer and also highlighted the importance of such studies[188]. To this end, our discovery of SPRTN syndromes demonstrates that the origin of cancer and ageing originates form the same source.

SPRTN syndrome occurs due to monogenic and biallelic mutations in the SPRTN gene. In-depth molecular analysis suggested that the DNA replication defect is the cause of premature ageing and HCC in patients suffering from biallelic mutations in SPRTN. Detailed molecular analysis of patient mutations (-ΔC and -Y117C) also helped us to understand the function of SPRTN in DNA replication. Analysis of the clinical SPRTN-ΔC mutation (the C-terminal truncation) highlighted the importance of SPRTN′s interactions with other factors such as PCNA (PIP box), p97 (SHP domain) and Ubiquitin (UBZ domain)) in a DNA replication context and the overall pathogenicity associated with the loss of these interactions, probably deriving from the associated defect in the TLS and FA pathways respectively. Interestingly, skin

anomalies and leukemia, which are commonly associated with defect in the TLS and FA pathways, respectively, are not associated with SPRTN syndrome. Interestingly, it was proposed that SPRTN, with the help of p97, extracts DNA Pol-η after UV-lesion bypass. This suggests that SPRTN inactivation leads to the hyperaccumulation of DNA Pol-η at sites of stalled/bypassed DNA replication, therefore resulting in the observed replication defect. However, we were not able to rescue the DNA replication defect in either SPRTN mutated or depleted cells by simultaneous co-depletion of DNA Pol-η. This result further supported our hypothesis that SPRTN has a much broader role in general DNA replication than solely in TLS. To this end, characterisation of a single patient mutation in the putative metalloprotease SprT domain of SPRTN (SPRTN-Y117C) suggested that the putative metalloprotease domain is essential for DNA replication.

It is still unknown why SPRTN mutations specifically cause hepatocellular carcinoma. Furthermore, external factors such as viruses, toxins, smoking and alcohol exposure were not found to play a role in the clinical status of all the three patients characterised here. It thus raises the question as to whether the chemical environment in the liver is responsible for the predisposition towards liver cancer in patients suffering from SPRTN syndromes. By the time our manuscript was in press (2014), WSS1 in yeast was shown to be proteolytically active and involved in DNA-protein crosslinks (DPC) removal. They also suggested, owing to its overall similarity to the active site (HEXXH motif) of SPRTN, that mammalian SPRTN is the yeast homologue of WSS1[49,170,172]. This finding had opened up a plethora of opportunities to investigate whether, 1) SPRTN also possess an intrinsic metalloprotease activity, 2) what are the functional consequences of patient mutations with regard to SPRTN's protease activity, 3) what are the potential substrates of SPRTN, 4) How DPC

removal is associated with unperturbed DNA replication, and last but not least, 5) knowing the hypoxic nature of the liver, alongside a massive production of highly reactive endogenous metabolic bi-products, makes it especially appealing to investigate SPRTN's role in DPC removal and its relevance in liver cancer.

## 3.2 Characterisation of the ATR-CHK1 signalling in SPRTN depleted cells

### 3.2.1 Introduction

ATR and its downstream effector kinase, CHK1 are important genes for many developmental processes and normal tissue homeostasis. Both ATR and CHK1 depletion is embryonically lethal[146,189]. ATR heterozygous mice develop normally but with an increased risk of tumor development by 18 months of age. Furthermore, conditional knockout of ATR in adult mice, leads to a plethora of premature ageing phenotypes[190]. In humans, mutation in the ATR gene is associated with Seckel syndrome characterised by severe growth retardation, microcephaly and facial and osteoskeletal abnormalities [191]. In laboratory cell culture, removal of ATR or CHK1 leads to spontaneous chromosomal breaks and cell death due to apoptosis, which has been linked to their role in replication and associated repair response. In addition, to the numerous genetic and cell biological studies, it has become evident that proper functioning of the ATR-CHK1 pathway is absolutely necessary for unperturbed replication and also during DNA damage repair[192]. Full activation of the ATR-CHK1 pathway depends on the presence of ssDNA, which occurs either due to replication stress (polymerase-helicase uncoupling) or due to the resection of DSBs, as mentioned earlier. Fully active CHK1 then stops the cell cycle by inhibiting CDKs. Mechanistically, CHK1 phosphorylates and activates Wee1 kinase, which phosphorylates CDK2 at Tyr-15,consequently inhibiting it. In addition, CHK1 phosphorylates CDC25A phosphatase, resulting in CDC25A's proteasomal degradation. CDC25A is generally associated with the removal of inhibitory phosphate groups from CDK2, therefore making it active to drive the cell cycle. Once checkpoint activation has occurred, CHK1 also physically associates with the stalled replication forks preventing their degradation and spontaneous collapse, as well as promoting DNA replication fork to restart. Collectively, CHK1 is important for

normal replication (controlling fork speed and preventing unscheduled origin firing) and for induction of both the intra S-phase and G2/M checkpoints upon DNA damage. Interestingly, CHK1 overexpression is positively correlated with a number of human malignancies such as liver, breast, colon, gastric and nasopharyngeal carcinoma[193]. These observations suggest that CHK1 promotes tumor growth. Based on these facts and the potent anti-apoptotic role of both ATR and CHK1, it was hypothesised that they might be an excellent target for anticancer therapy, either as a mono-therapy or in combination with other replication interfering drugs or ionising radiation. however, active development and clinical trials concerning ATR and CHK1 inhibitors has been severely hampered due to their off-target effects and toxicity, thus alternative strategies with novel therapeutic approaches are required to fully utilise ATR and CHK1 inhibitors as successful anticancer agents[194,195].

Mutation or complete removal of SPRTN leads to severe replication stress manifested as decreased replication fork velocity followed by increased number of stalled forks and newly fired dormant origins. Analysis of patient primary fibroblasts suggested they have severe DNA damage in every stage of the cell cycle. We also observed a severe G2/M checkpoint defect in both SPRTN syndrome patients and SPRTN knockout U2OS cells. We finally concluded that DNA damage in SPRTN syndrome and SPRTN-depleted cells is originating due to defective DNA replication and is transferring to the next phase of the cell cycle due to leaky G2/M checkpoint response. We also observed that the function of SPRTN in TLS is insignificant in a replication stress context, as we could not rescue replication defect in both patient LCLs or SPRTN knockdown U2OS cells by codepleting DNA Pol-η. At this point, it is thus important to find out the precise molecular mechanism as to why a deficiency or depletion of SPRTN leads to DNA replication stress. To this end, considering all of

the abovementioned and well documented functions of ATR and CHK1 in DNA replication and checkpoint responses and after correlating them with SPRTN patient phenotypes (premature aging, genomic instability, tumor; defective DNA replication and G2/M checkpoint), we hypothesised that SPRTN's role in DNA replication and G2/M-checkpoint is connected to the ATR-CHK1 signalling cascade.

### 3.2.2 AIM: To investigate the ATR-CHK1 signalling cascade in the context of DNA replication in SPRTN-depleted cells

### 3.2.3 Results

#### 3.2.3.1 Characterisation of the ATR-CHK1 signalling cascade in SPRTN depleted cells

Hydroxyurea (HU) affects DNA replication by inhibiting ribonucleotide reductase (RNR), which is responsible for dNTP production. HU treatment thus leads to immediate replication fork stalling and the appearance of RPA coated ssDNA leading to full activation of the ATR-CHK1 signalling pathway. We analysed DNA replication stress in HEK293 cells after siRNA mediated SPRTN depletion using HU as a positive control for DNA replication stress. As expected (**Fig 14 a**), the DNA replication fork velocity was not affected in control cells, and was severely affected in both HU treated and SPRTN depleted cells. Western blot analysis of the abovementioned samples showed basal activation of the ATR-CHK1 pathway in control and unchallenged cells, measured by phosphorylation of CHK1 at Ser345 residue (**Fig 14 b**), which suggested a basal level of CHK1 activation is essential for DNA replication fork progression. Furthermore, HU treatment led to robust activation of ATR-CHK1 pathway as shown by hyper-phosphorylation of CHK1 at Ser345, which is followed by rapid degradation of CDC25A and activation of cell cycle checkpoints. Surprisingly, SPRTN depletion by three different siRNAs promoted severe defect in DNA replication fork velocity and as a consequence activated γ-H2AX however it failed to activate the ATR-CHK1 pathway, as shown by diminished phosphorylation of CHK1 at Ser345 (**Fig 14 b**) in SPRTN depleted samples, which is strongly evident after HU treatment. Additionally, suboptimal CHK1 phosphorylation

in SPRTN-depleted cells resulted in hyper-accumulation of CDC25A, thus further indicating the sub-optimal ATR-CHK1 pathway in SPRTN depleted cells. Accumulation of CDC25A in SPRTN depleted cells further suggested that SPRTN might act as a secondary cofactor of p97(p97$^{-UFD1-NPL4-SPRTN}$) for the proteasomal degradation of CDC25A after its phosphorylation by CHK1, which require further experiment to prove[127].

It is well documented in the literature that proper activation of CHK1 by ATR requires multiple other factors such as TopBP1, Claspin[196] and BRCA1[197] along with other accessory molecules of ATR, such as ATRIP. We wondered whether the CHK1 activation problem in SPRTN-depleted cells is due to the deregulation of these accessory factors. To address this, we challenged SPRTN depleted cells with HU. To our surprise, upon HU treatment, we observed a robust activation of the ATR-CHK1 pathway, as shown by phosphorylation of CHK1 at Ser296, Ser345 and Ser317, (**Figure 14 c**). We also confirmed that replication stress induced DSB formation upon HU treatment in both control and SPRTN depleted cells, as demonstrated by robust phosphorylation of RPA, CHK2 and ATM. The presence of DNA damage in SPRTN depleted cells is further confirmed by the robust activation of γ-H2AX, which interestingly followed a similar trend to that of the ATR-CHK1 and ATM-CHK2 signalling-pathways. In summary, our data indicates that SPRTN depleted cells have a fully functional ATR-CHK1 and ATM-CHK2 pathway, however they are unable to activate these two essential pathways under basal condition even though they have severe replication defect and accompanying DSBs (as shown earlier by 53BP1 foci formation in SPRTN mutated patient LCLs (**Fig 9 a**) and SPRTN depleted U2OS cells (**Fig 11 d**)).

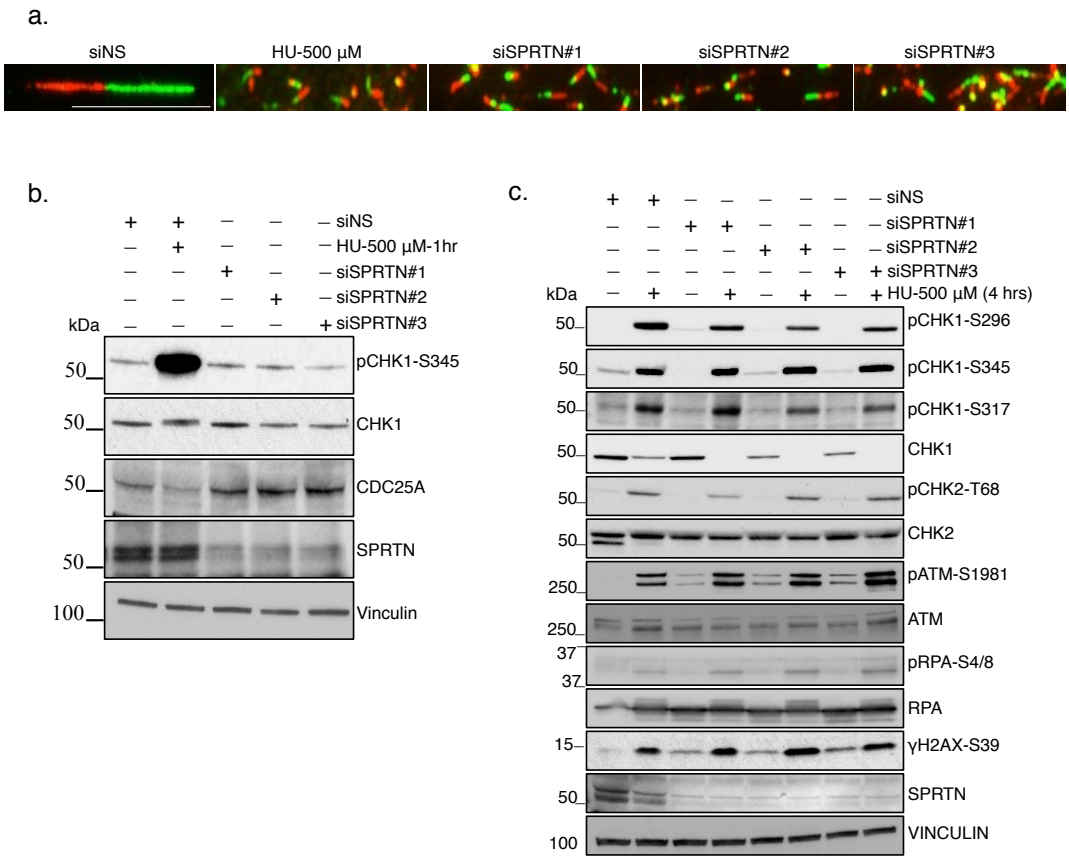



**Figure 14 Characterisation of the ATR-CHK1 signalling cascade in SPRTN depleted cells**. For all the experiments, HEK293 cells were used. The DNA fiber assays were performed by standard 30 minutes CldU incorporation, followed by 30 minutes of IdU incubation. siRNA treatment was carried out for 72 hours. Plasmid expression was carried out for 48 hours. **a.** Showing the representative images of DNA fibers in mock treated (siNS), HU treated and SPRTN depleted cells. Scale is 10 µm **b.** Western blot analysis of the same experiment as in A, showing the faulty ATR-CHK1 pathway after SPRTN depletion. Please compare pCHK1 and CDC25A between HU and SPRTN depleted condition. **c.** Western blot analysis of the DNA damage signalling cascade in control and SPRTN depleted cells with -/+ HU, showing the inability of SPRTN depleted cells to evoke the DNA damage response under basal condition

### 3.2.3.2 SPRTN forms a physical complex with DNA replication and DDR associated factors

To investigate whether SPRTN physically interacts with components of the DDR pathways, we utilised the doxycycline inducible HEK293 cell system expressing SPRTN-WT with a C-terminal SSH tag. We also induced mild replication stress by treating cells with 25 nM camptothecin (CPT) (**Fig 15 a**)[185]. We affinity isolated SPRTN interacting protein complexes with streptactin beads and looked for components of the ATR-CHK1 and ATM-CHK2 pathway. PCNA and p97 served as positive controls for the SPRTN interactome. Interestingly, mild replication stress (+CPT) leads to an increased interaction between SPRTN and proteins involved in the DDR-phosphorylation cascade such as RPA, CHK2, ATM and CHK1 to some extent. These findings suggested that SPRTN forms a physical complex with components of the DDR-phospho signalling pathways under physiological conditions and this interaction is enhanced after DNA replication stress. In addition, we have also observed that SPRTN interacts with the complete PP2A holozyme consisting of the catalytic C, scaffold A and regulatory B subunit B55α. Our pull-down experiments also suggested that SPRTN interacts with the basic components of DNA replication such as PCNA, RPA and CHK1 under physiological (unchallenged) condition, which further indicated that SPRTN is a constitutive component of the DNA replication fork. Altogether, it is evident that SPRTN forms a physical complex with CHK1 and the absence of SPRTN leads to a faulty ATR-CHK1 signalling cascade.

The essential function of CHK1 in DNA replication and the associated damage response is well characterised. ATR and ATM mediated phosphorylation of Ser345 and Ser317 of CHK1 in the DNA damage response and the G2/M checkpoint response is also well established in the literature. Furthermore, there are reports that

mutations in Ser345 (Ser345Ala) of CHK1 affects endogenous CHK1 function as conditional knockouts in the human colorectal cancer cell line DLD-1CHK1-S345 is lethal. In contrast, mutations in Ser317 (Ser317Ala) did not affect the viability or growth defect in DLD cells. In addition, Ser345Ala mutated cells are not able to evoke CHK1 phosphorylation upon HU treatment in both Ser345 and Ser317; in contrast Ser317 mutants retained the ability to evoke phosphorylation at Ser345. The authors finally concluded that phosphorylation at Ser345 of CHK1 has replication related essential function. Phosphorylation of Ser317, on the other hand, becomes important in the context of DNA damage[198]. Similar data was also obtained from mouse embryonic stem cells where the lethality of CHK1 depletion can be rescued by the WT CHK1 expression and with CHK1-Ser317Ala but not with a CHK1-Ser345Ala mutant[199]. They also showed rapid phosphorylation of these two moieties of CHK1 in unperturbed S-phase, which had been subsequently corroborated by others as basal CHK1 activity. Furthermore, massive follow up work from many different groups in this context gave rise to a general understanding that phosphorylation of CHK1 at Ser345 and Ser317 stimulates its kinase activity, which is required for efficient DNA damage response. Furthermore, the presence of basal phosphorylation at these two residues is required during unperturbed S phase progression[200–202]. Therefore, we wondered whether CHK1 signalling defects in SPRTN-depleted cells are one of the main reasons for DNA replication defects in SPRTN-defective cells.

To address this question, we ectopically over-expressed CHK1-WT or CHK1 phospho-defective mutants (CHK1Ser345Ala and CHK1Ser317Ala) in SPRTN-depleted cells and measured the speed of DNA replication forks by the DNA fiber assay. 1$^{st}$ of all, we observed profound dominant negative effects of overexpression of

phospho-defective mutants of CHK1-S345A and CHK1-S317A, suggesting the basal phosphorylation of these two residues is critical for replication fork progression during unperturbed S-phase. Furthermore, dominant negative effect of CHK1-S345A mutant upon replication fork progression is much more pronounced than that of CHK1-S317A, which is in accordance with the literature indicating replication related essential function of CHK1-S345 phosphorylation[198]. Indeed, CHK1-WT, but not CHK1-phosphodead mutants rescued DNA replication defect in SPRTN depleted cell (**Fig 15 b, c**). In addition to the abovementioned observations, we expressed either CHK1-WT or phospho-defective mutants and assessed their ability to suppress the genomic instability in SPARTAN depleted cells.(**Fig 15 d**). SPRTN depletion by two different siRNA sequences led to pronounced genomic instability, which can be rescued by ectopic expression of WT-SPRTN, again validating the monogenic function of SPRTN in preventing replication stress and DNA damage related genomic instability. Most interestingly, SPRTN depleted genomic instability can be efficiently rescued by ectopic expression of CHK1-WT but not by phosphodead CHK1Ser345Ala. Overall, our data clearly demonstrated an essential function of SPRTN in the activation of CHK1 signalling cascade under basal condition. However, it is not mechanistically clear how exactly ectopic expression of CHK1-WT rescues DNA replication defect and associated genomic instabilities in SPRTN depleted cells. It is known from literature that functionally similar checkpoint kinase CHK2 can auto-phosphorylate and activate itself in trans- and thus abrogate the need for IR induced ATM dependent phosphorylation and subsequent activation[203] when exogenously overexpressed. However similar mechanism is not known for the activation of CHK1. It is therefore tempting to speculate whether ectopic over-expression of CHK1-WT activates endogenous CHK1 and subsequently rescues DNA

replication fork defect and associated genomic instabilities in SPRTN depleted cells. Measurements of the phosphorylation status of CHK1 in SPRTN depleted cells which were additionally co-expressed either with CHK1-WT or phospho-defective mutants of CHK1 will shed light in this regard. It might be very well possible that CHK1-WT stimulates the kinase activity of endogenous CHK1 or self- stimulate itself, once it is in the vicinity of the DNA replication fork, and as a result rescues DNA replication defect in SPRTN depleted cells (please look figure 24 f).

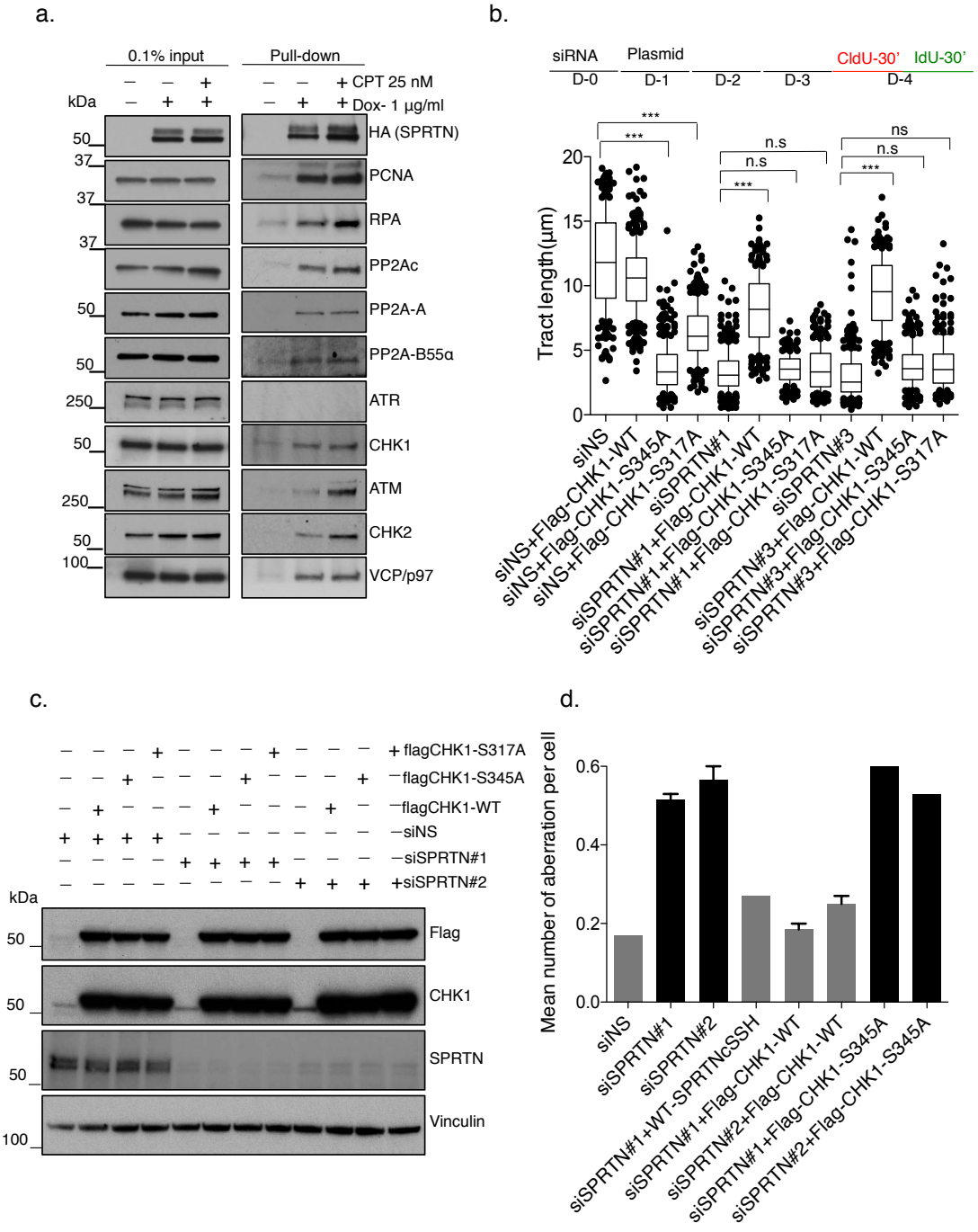



**Figure 15 SPRTN forms a physical complex with DNA replication and DDR associated factors.** For all of the experiments HEK293 cells were used. siRNA treatment and plasmid expression was carried out for 72 and 48 hours, respectively. **a**. Analysis of the SPRTN intercatome by pull-down assay. Doxycycline was used for 24 hours and -/+25 nM for 1 hour CPT as indicated. **b**. Analysis of total tract length by the DNA fiber assay. >100 individual tracts were scored per experiment per condition. Tract length was measured by ImageJ software and converted to micron scale. n=2. Data is shown as the median (bar) with the 25th–75th percentile range (box) and the 10th–90th percentile range (whiskers), P values were obtained by unpaired two-tailed t-test. *P < 0.0), **P < 0.001, ***P < 0.0001 by GraphPad Prism software. **c.** Western

blot analysis confirming the expression of CHK1 WT by both Flag and endogenous CHK1 antibodies along with SPRTN depletion. Vinculin was used as a loading control. **d**. Following siRNA treatment and plasmid expression (as indicated above), cells were treated with 0.1 mg/ml colcemid for 2 hours followed by harvesting and preparation of metaphase spread as mentioned in the materials and methods. >30 cells were scored per condition per experiments and mean values were shown with s.e.m by Graphpad Prism software

#### 3.2.3.3 NSC663284, a potent CDC25 inhibitor, rescues DNA replication fork speed in SPRTN depleted cells

Severe replication stress coupled with the inability to evoke robust activation of the ATR-CHK1 pathway resulted in the accumulation of a CHK1-downsteram target CDC25A in SPRTN depleted cells (As shown in **Fig 14 b**). These results suggested that DNA replication defect in SPRTN-depleted cells was due to the abnormal ATR-CHK1 pathway inducing high levels of CDK activity that consequently affects DNA replication fork progression. Thus, we hypothesised that a short treatment (2 hours) with a CDC25 inhibitor (CDC25 INH),NSC663284, would rescue DNA replication defect in SPRTN depleted cells [204]. Furthermore, a rescue experiment with CDC25 INH would additionally confirm that replication defect originated from the faulty ATR-CHK1 cascade in SPRTN depleted cells. Western blot analysis again suggested that faulty CHK1 activation upon SPRTN depletion by two siRNA sequences, as shown in **Figure 16 a**, followed by CDC25A accumulation. CDC25A is well known for its role in activating CDKs by removing their inhibitory phosphorylations[126]. Furthermore, CDK2 activity can be positively correlated with the phosphorylation status of one of its well-characterised substrates, for example phospho PP1 at Thr-320[205]. HU treatment, which was used as a positive control, resulted in hyperphosphorylation of CHK1 followed by rapid degradation of CDC25A, as well as resulting in the reduction of phosphorylation on pPP1-T320 in comparison to control condition (siNS). Interestingly, the absence of CHK1 phosphorylation followed by accumulation of CDC25A led to hyperactive CDK2 in SPRTN-depleted cells, as shown by hyper-phosphorylation of pPP1-T320. As expected, treatment with CDC25 INH in SPRTN depleted cells led to significant reversal of PP1 phosphorylation at T320. Once we biochemically confirmed the mode of action of the CDC25 INH in

SPRTN depleted cells, we used the same strategy for the DNA fiber assay (Biochemistry and Fiber analysis are from the same experiment). Indeed, short exposure to CDC25 INH led to a complete rescue of the DNA replication fork velocity (**Fig 16 b and c**), along with a rescue of the number of stalled forks and newly fired origins (data not shown). These results further supported our earlier observation that the DNA replication defect in SPRTN depleted cells is due to the sub-optimal ATR-CHK1 cascade.

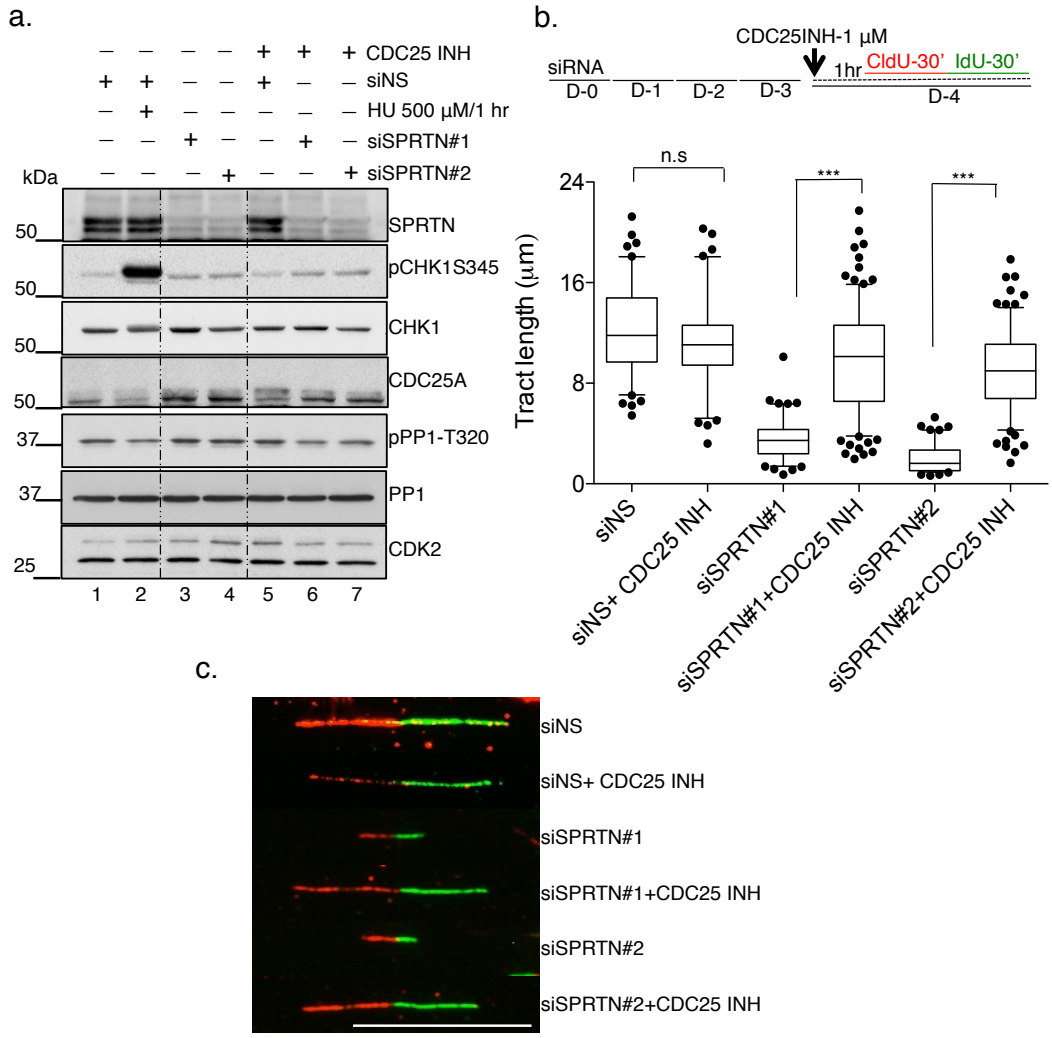



**Figure 16 NSC663284, a potent CDC25 inhibitor, rescues DNA replication fork speed in SPRTN depleted cells**. All the experiments were done in HEK293 cells **a**. Showing accumulation of CDC25A followed by hyperactive CDKs indicated by pPP1-T320 phosphorylation in SPRTN depleted cells. HU was used as a positive control. Dotted lines signify the differences between HU treated lane numbers 2 to SPRTN depleted lane 3, 4 followed by the difference between lane 3,4 to CDC25INH treated SPRTN depleted lane 6 and 7. **b.** Illustration showing the strategy of DNA fiber assay followed by the graph showing the rescue of DNA fiber tract length when SPRTN depleted cells were treated with CDC25INH. n=2. >100 individual tracts were scored per condition per experiment. Data is shown as the median (bar) with the 25th–75th percentile range (box) and the 10th–90th percentile range (whiskers), P values were obtained by unpaired two-tailed t-test. *P < 0.0), **P < 0.001, ***P < 0.0001 by GraphPad Prism software. n.s stands for non significant. **c**. Representative images of DNA fibers for B. Scale 10 µm.

#### 3.2.3.4 Roscovitine, a potent CDK inhibitor, rescues DNA replication fork speed in SPRTN depleted cells

In depth biochemical and molecular analysis of SPRTN depleted cells suggested a CHK1 defective phenotype, which resulted in the accumulation of CDC25A followed by hyperactive CDKs as measured by PP1 phosphorylation at Thr-320 (PP1 is a substrate of CDK). So far, we were able to rescue replication defects in SPRTN depleted cells by the ectopic overexpression of CHK1-WT or by short exposure to CDC25 INH. In order to rule out the involvement of any other factors in this signal transduction pathway from ATR to CDKs (ATR>CHK1>CDC25A>CDK2), we exposed SPRTN depleted cells to the CDK inhibitor roscovitine[206]. We took a similar experimental approach to the one we used for CDC25 INH. Indeed, we (**Fig 17 a**) again detected suboptimal CHK1 phosphorylation (pCHK1-Ser345) upon SPRTN depletion, which resulted in the hyper-phosphorylation of pPP1-Thr-320, a CDK substrate. Interestingly, treating cells with roscovitine, a potent CDK inhibitor, completely reversed the phosphorylation status of PP1 at Thr-320. After biochemical confirmation, we next analysed the effect of roscovitine in SPRTN depleted cells by the DNA fiber assay (Western blot and fiber assay are from same experiment). As shown in (**Fig 17 b and c**) roscovitine treatment completely rescued the DNA replication defect in SPRTN depleted cells. Altogether, our results demonstrated an essential role for SPRTN in the regulation of the ATR-CHK1-CDC25A-CDK2 axis during normal DNA replication.

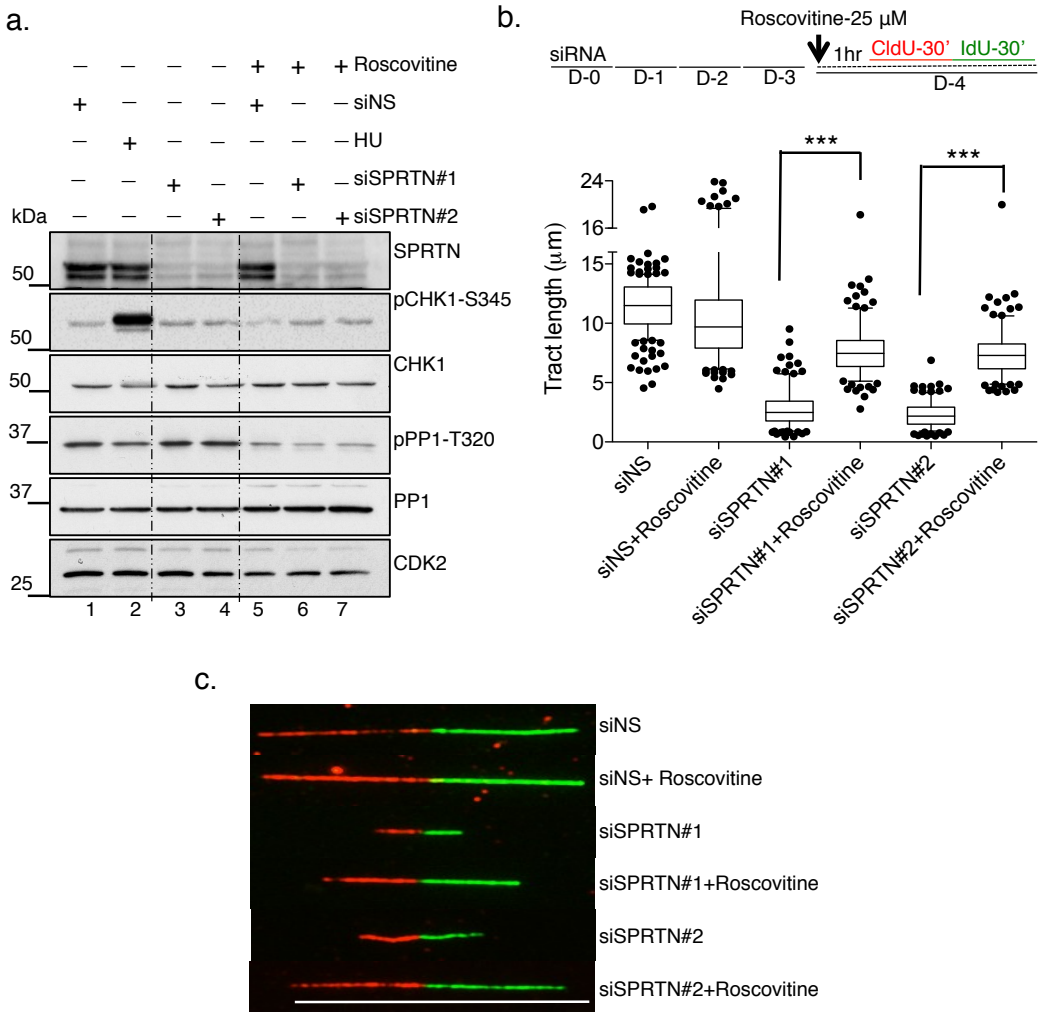



**Figure 17 Roscovitine, a potent CDK inhibitor, rescues DNA replication fork speed in SPRTN depleted cells**. All of the experiments were carried out in HEK293 cells **a**. Showing pPP1-T320 hyper-phosphorylation as a measure of hyperactive CDKs in SPRTN depleted cells. HU was used as a positive control. Dotted lines signify the differences between HU treated lane numbers 2 to SPRTN depleted lane 3, 4 followed by the difference between lane 3 and 4 to CDC25INH treated SPRTN depleted lane 6 and 7. **b.** Illustration showing the strategy of the DNA fiber assay followed by the graph showing the rescue of the DNA fiber tract length when SPRTN depleted cells were treated with roscovitine. n=2. >100 individual tracts were scored per condition per experiment. Data is shown as the median (bar) with the 25th–75th percentile range (box) and the 10th–90th percentile range (whiskers), P values were obtained by unpaired two-tailed t-test. *P < 0.0), **P < 0.001, ***P < 0.0001 by GraphPad Prism software. **c**. Showing the representative images of DNA fibers for B. Scale10 µm

#### 3.2.3.5 Sub-optimal CHK1 phosphorylation in SPRTN depleted cells is rescued by the PP2A inhibitor okadaic acid

Aforementioned data suggested a sub-optimal ATR-CHK1 response SPRTN depleted cells. Experiments with CHK1 kinase defective mutants such as S345A and S317A, also provided valuable insights about the activity of CHK1 in SPRTN depleted cells. As it is evident from the literature that CHK1 can only be activated by targeted phosphorylation of different Serine residues (S296, S317, S345) located in its C-terminal S/T-Q sites, we wondered whether the diminished CHK1 function in SPRTN cells is due to deregulation of some key phosphatases. According to the published literature, the roles of phosphatases have been well documented in the DNA damage response. For example, PP1 is shown to dephosphorylate ATM, CHK1, Histone H3, pRB, Mdm2, KAP1 and p53. Similarly, PP2A has also been shown to dephosphorylate ATM, γ-H2AX, CHK1, CHK2, DNAPK, pRB and RPA2. Furthermore, there are also reports of other phosphatases like Wip1, PP4, PP5 and PP6 that either alone or in combination with other phosphatases dephosphorylate a wide range of DDR factors[207]. It is therefore extremely important to precisely identify the specific phosphatase, which might dephosphorylate the CHK1 in SPRTN depleted cell. Interestingly, careful literature analysis also suggested that there might be many different phosphatases associated with the DDR; however, only PP1 and PP2A have been characterised, with most of the factors that either efficiently pull-down by SPRTN, or their phosphorylation status was affected in SPRTN depleted cells. Interestingly, CDK2 phosphorylates and consequently inhibits PP1 phosphatase activity. Therefore, based on the published literature and our results, due to hyperactive CDK2 in SPRTN-depleted cells we ruled out PP1 as a potential inhibitor of CHK1 phosphorylation in SPRTN-depleted cells. Furthermore, published data

suggested a tight regulation of CHK1 activity by PP2A under physiological conditions. Due to the basal activity of ATR, CHK1 is continuously phosphorylated at S345 and S317. Basal CHK1 activity is absolutely essential for replication fork progression. However, continuous stimulation by ATR will lead to hyperphosphorylation of CHK1 at S345 and S317, and by default, this will activate the cell cycle checkpoints during an unperturbed S-phase. Therefore, there has to be a mechanism which maintains CHK1 homeostasis during normal, unperturbed replication. PP2A mediated dephosphorylation of CHK1 was shown to control this process. Upon DNA damage, the balance of the PP2A-CHK1 axis is altered, CHK1 is fully activated by ssDNA-ATR and inhibits PP2A though its kinase activity [208].

Based on the fact that CHK1 inhibits PP2A, and our results that SPRTN and PP2A form a physical complex, we asked whether PP2A is hyperactive in SPRTN-depleted cells, as these cells have a defective CHK1 cascade. In order to test this hypothesis, we inhibited PP2As enzymatic activity using okadaic acid (OA). OA is a specific inhibitor of PP2A and PP1 phosphatases, but at concentration <50 nM, it was shown to be specific towards PP2A[209,210]. As expected, suboptimal CHK1 phosphorylation upon SPRTN depletion is completely rescued by treating cells with the PP2A inhibitor OA (**Fig 18 a**). Furthermore, we rescued CHK1′s phosphorylation status at all of the three well-characterised moieties such as S296, S317 and S345, thus strongly indicating that PP2A mediates the dephosphorylation of these residues under basal condition in SPRTN depleted cell. Once we obtained convincing biochemical data, we next asked whether the inhibition of PP2A could rescue the DNA replication defect in SPRTN-depleted cells. Owing to the global function of PP2A, we took a very stringent approach to answer this question. We traced nascent DNA synthesis by CldU incubation for 30 minutes. We then changed the CldU containing media and

added media containing IdU-/+OA. This approach enabled us to specifically monitor those IdU tracts that were already fired during CldU incubation and are thus marked with CldU. As anticipated, (**Fig 18 b**) treatment of cells with low dose and short pulses of OA significantly rescued the DNA replication fork velocity in SPRTN-depleted cells. Overall, these observations suggested that PP2A inhibition brings back CHK1 phosphorylation and rescues CHK1 kinase activity, which immediately rescued the DNA replication fork velocity, locally at the level of individual forks in SPRTN depleted cells. We also analysed the global effect of the OA mediated rescue of CHK1 kinase activity in terms of fork stalling (first nucleotide, CldU only) and dormant origin firing (second nucleotide, IdU only). As anticipated, treatment of cells with OA significantly rescued aberrant fork stalling and inhibited dormant origin firing in SPRTN depleted cells (**Fig 18 c, d**).

Finally, we analysed the relevance of this pathway (PP2A-CHK1) in SPRTN deficient patient LCLs. As shown earlier in **Figure 10 b**, we did not observe a marked difference in terms of replication fork speed when we compared control LCLs to patient LCLs under unchallenging condition. However, this situation changed dramatically upon exposure of patient's cells to the mild replication stress inducing agent APH. We concluded that in SPRTN syndrome patient cells, DNA replication fork progression is severely affected under mildly challenging condition. We revisited the same experiment and asked whether inhibition of PP2A will rescue DNA replication fork speed in SPRTN-mutated patient LCLs under mildly challenging condition (100 nM APH). We took the same stringent approach as mentioned earlier during the rescue of SPRTN depleted HEK293 cells by OA (30 minutes CldU followed by 60 minutes IdU+APH-/+OA and measure IdU tract length). As expected, we did not observe any difference in control LCL cells treated with APH-/+OA,

suggesting that control LCLs have fully functional endogenous CHK1. Interestingly, treating patient LCLs with APH lead to a marked decrease in tract length comparing to control LCLs. Importantly, this replication defect in SPRTN patient LCLs is completely rescued by OA (**Fig 18 e, f**). These data suggested that SPRTN deficient patient LCLs also suffer from sub-optimal CHK1 kinase activity, like SPRTN-depleted cells. Altogether, our data indicated that SPRTN inactivation severely impairs CHK1 kinase activity, and this defect is caused, at least to a certain extent, by hyperactivity of PP2A.

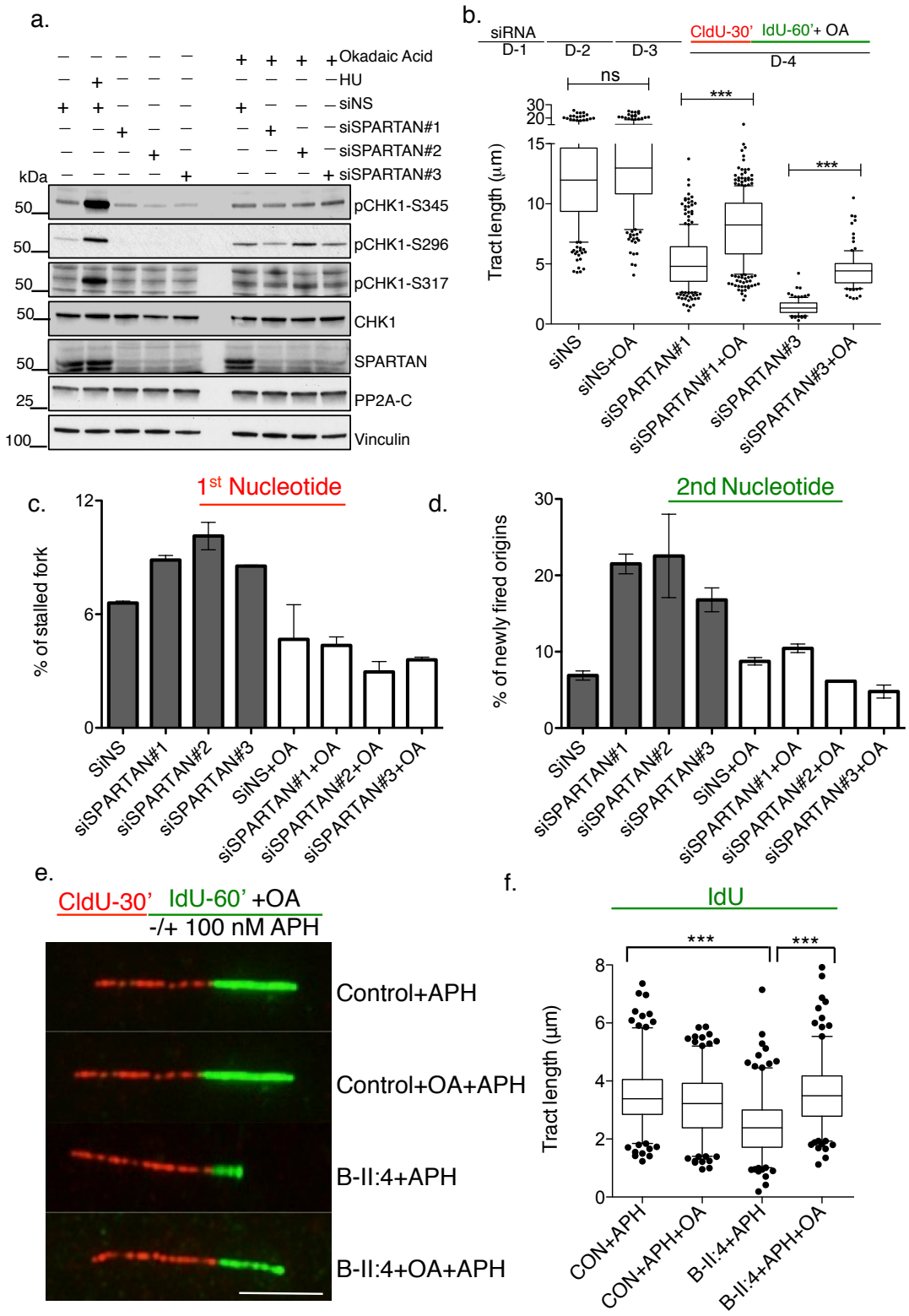



**Figure 18**. **Sub-optimal CHK1 phosphorylation in SPRTN depleted cells is rescued by the PP2A inhibitor okadaic acid.** All the experiments were carried out in HEK293 cells, unless otherwise indicated. siRNA treatment was carried out for 72 hours followed by treatment with 1 hour of 10 nM Okadaic acid (OA) or as mentioned **a.** Western blot analysis showing the rescue of phopsho CHK1 at Ser345, Ser296 and Ser317 in SPRTN depleted cells by Okadaic acid (OA) followed by total

CHK1 and PP2A-C and the efficiency of SPRTN depletion. Vinculin was used as a loading control. **b**. Showing the strategy of the DNA fiber assay followed by rescue of IdU tract length by OA in SPRTN depleted cells. **c** and **d** showing the % of stalled forks and newly fired origins. >400 CldU only (first nucleotide) or IdU only (second nucleotide) were scored per condition per experiments as mentioned and mean values were shown with s.e.m by GraphpadPrism software. n=2. **e.** Strategy of the DNA fiber assay in control and patient LCLs followed by representative images F. measurements of IdU tract length in control and patient LCLs in presence of APH-/+OA. Data in **b** and **d** are shown as the median (bar) with the 25th–75th percentile range (box) and the 10th–90th percentile range (whiskers). P values were obtained by unpaired two-tailed t-test. ***P < 0.0001.n.s is non significant. Statistical analysis was done by GraphpadPrism software. >100 individual tracts were scored per condition per experiment. n=2.

### 3.2.3.6 PP2A regulatory subunit B55α links PP2A to CHK1

PP2A is a major Ser/Thr phosphatases, which has been shown to be involved in many diverse cellular processes. The PP2A holozyme is composed of a 36 kDa catalytic C subunit (PP2A-C), a 65 kDa scaffolding A subunit (PP2A-A) and a regulatory B subunit (PP2A-B). The core of the enzyme is made up of PP2A-A and PP2A-C (PP2A-A/C) followed by association of one of the many regulatory B subunits to form the complete holozyme. It is the regulatory B subunit that is responsible for substrate recognition followed by binding to the PP2A-A/C complex to form complete holozyme, which ultimately leads to dephosphorylation of the specific substrates. The diversity of PP2A function is regulated by various B subunits, which are divided into four major classes B/PR55, B'/PR61, B''/PR72 and B'''/PR93/PR110. Additionally, each of them further exists in at least 4 different isoforms thus altogether in different combinations represents 1% of total cellular proteins, much like p97 and its diverse sets of cofactors, which incidentally also represents 1% of the total cellular proteins [211].

As shown earlier, DNA replication defect in both SPRTN depleted and SPRTN deficient patient LCLs were rescued by OA. To directly prove that PP2A and moreover its specific sub-complex is involved in the regulation of CHK1 activity and thus DNA replication fork progression, we aimed to identify the specific PP2A sub-complex involved in this regulation. To this end, we analysed mass-spectrometry data of the p97 proteome performed in our lab, and identified PP2A regulatory B subunit B55α as one of the top hits. Therefore we asked whether SPRTN form a physical complex with PP2A and its regulatory subunit B55α. Previously SPRTN pull-down demonstrated that the PP2A holozyme is composed of the scaffolding A, Catalytic C and the regulatory B55-α subunit, which form a physical complex with SPRTN

(Figure D). Additionally, the role of PP2A and B55α in S phase progression was demonstrated in Xenopus egg extracts. Early Xenopus laevis embryos grow rapidly, and their cell cycle consists of M-phase and S-phase (interphase). This situation changes dramatically at the onset of midblastula transition, owing to the higher nuclear to cytoplasmic ratio. From this point onwards the cell cycle more resembles a somatic one, as it incorporates the respective Gap phases such as G1 and G2. This is achieved by limiting the availability of PP2A and B55α, which leads to reduction in the number of total origin activation, therefore increases the length of the S phase. This report thus directly implicates the PP2A regulatory subunit B55α in S phase progression[212]. Based on the abovementioned facts, we decided to co-deplete B55α in SPRTN depleted cells to determine whether it is responsible for CHK1 dephosphorylation. Indeed, Western blot analysis suggested that co-depletion of B55-α in SPRTN depleted cells convincingly rescues CHK1-S345 phosphorylation(**Figure 19 a**). In agreement with our previous findings, co-depletion of B55-α in SPRTN-depleted cells rescued several defective phenotypes, such as DNA replication velocity and the restart of stalled replication forks (**Fig 19 b, c and d**). In conclusion B55α codepletion rescued the CHK1 kinase defect in SPRTN depleted cells. Finally, we asked whether co-depletion of B55a in SPRTN-depleted cells rescues genomic instability, measured by the number of chromosomal aberrations per metaphase cell. As anticipated, SPRTN depletion caused a 2-3 fold increases in chromosomal aberrations, which is completely rescued by co-depletion of B55a. (**Fig 19 e, f**). Altogether, our data demonstrated that the hyperactive PP2A-B55α complex is responsible for suboptimal CHK1 phosphorylation in SPRTN depleted cells that leads to DNA replication defects and ultimately genomic instability.

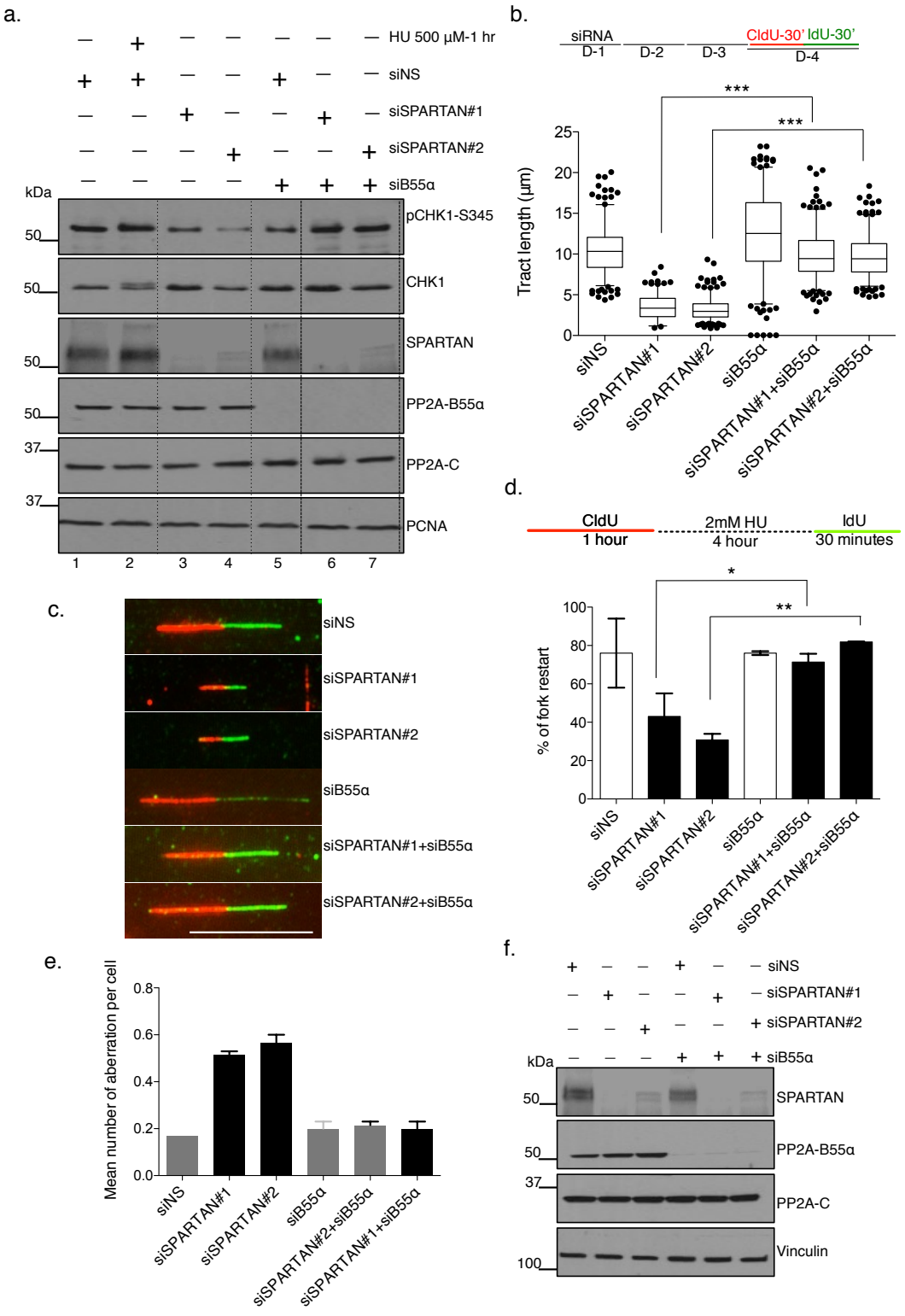



**Figure 19 PP2A regulatory subunit B55α links PP2A to CHK1**. All experiments were carried out in HEK293 cells. siRNA treatment were carried out for 72 hours. **a.** Western blot analysis showing pCHK1 rescue at Ser345 in SPRTN depleted cells by co-depletion of PP2A regulatory subunit B55α. Dotted lines and lane numbers at the bottom of the blots were used to point out the differences in phosphorylation status of CHK1 in SPRTN depleted and co-depleted condition. Efficiency of SPRTN and B55-

α depletion also shown followed by total PP2A-C. PCNA was shown as a loading control. **b.** Showing the strategy for DNA fiber assay followed by measurements of total DNA tract lengths. Data in B is shown as the median (bar) with the 25th–75th percentile range (box) and the 10th–90th percentile range (whiskers). >100 tracts were scored per condition per experiments. n=2. **c.** Representative images of DNA fibers as shown in **d.** Strategy of fork restart experiments followed by the rescue in the ability of SPRTN depleted cells to restart stalled forks when additionally co-depleted with B55-α. >400 forks were counted per condition per experiment for their ability to incorporate IdU after HU removal. Data shown as the s.e.m. n=2 **e.** Suppression of genomic instability in SPRTN depleted cells when additionally co-depleted with B55-α.>30 cells were scored per condition per experiments and mean values were shown with s.e.m. n=2 **f.** Efficiency of SPRTN and B55-α depletion for genomic instability experiments as shown in **e**, followed by total PP2A-C. Vinculin was shown as a loading control. P values were obtained in **b** and **d** by unpaired two-tailed t-test. *P < 0.01, **P < 0.001, ***P < 0.0001. Statistical analysis was done by GraphpadPrism software.

### 3.2.3.7 Ectopic expression of CHK1-WT enables SPRTN depleted cells to efficiently restart stalled replication forks

It is obvious from the aforementioned results that SPRTN inactivation leads to severe DNA replication stress due to defective ATR-CHK1 signalling cascade. Among the various important functions of CHK1 in S-phase, one is being able to stabilise stalled replication forks. It is one of the key mechanisms through which CHK1 prevents DSB formation during fork stalling. Numerous lines of evidence suggests that replication fork stalling leads to the appearance of ssDNA structures, which leads to full activation of CHK1[213]. Fully activated CHK1 then protects the replisome components at the stalled forks such as MCM2, PCNA, DNA polymerase-α and ε by preventing their chromatin release[214]. In the meantime, activated CHK1 inhibits CDKs through inactivation of CDC25 phosphatases to stops cell cycle progression. Moreover inhibition of CDKs also prevents global dormant origin firing. CHK1 also protects from Mus81/Eme1 endonuclease mediated aberrant processing of stalled forks, which would otherwise lead to DSB formation[215]. Kinase active CHK1 also actively facilitates the restart of the stalled forks, which requires the assistance of Bloom (BLM)[139] and Werner helicases (WRN)[216]. These well-characterised functions of CHK1 have prompted us to hypothesise whether SPRTN depleted cells have a defect in DNA replication fork protection after prolonged stalling.

To precisely answer this question, we analysed the ability of SPRTN depleted cells to restart stalled replication forks by the DNA fiber assay. Specifically, SPRTN-depleted cells were pulse labeled with the first nucleotide (CldU) for 1 hour and then the progression of DNA replication fork was stalled for 4 hours by 2mM HU treatment. After HU induced forced fork stalling, the replication fork restart was measured by adding second nucleotide (IdU) for 30 minutes in normal medium as shown in Figure

20 **a**. Continuous incorporation of the second nucleotide (IdU), after HU induce forced stalling would indicate that the DNA replication fork was intact during HU-treatment. Control cells (siNS) were able to efficiently restart most stalled forks (~80%), however SPRTN depleted cells showed severe defect in restart of the stalled forks (~35-40%). Most interestingly, ectopic over expression of CHK1-WT completely restored the fork restart defect in SPRTN depleted cells (**Fig 20 b and c**). These observations further demonstrated the CHK1 problem in SPRTN depleted cells.

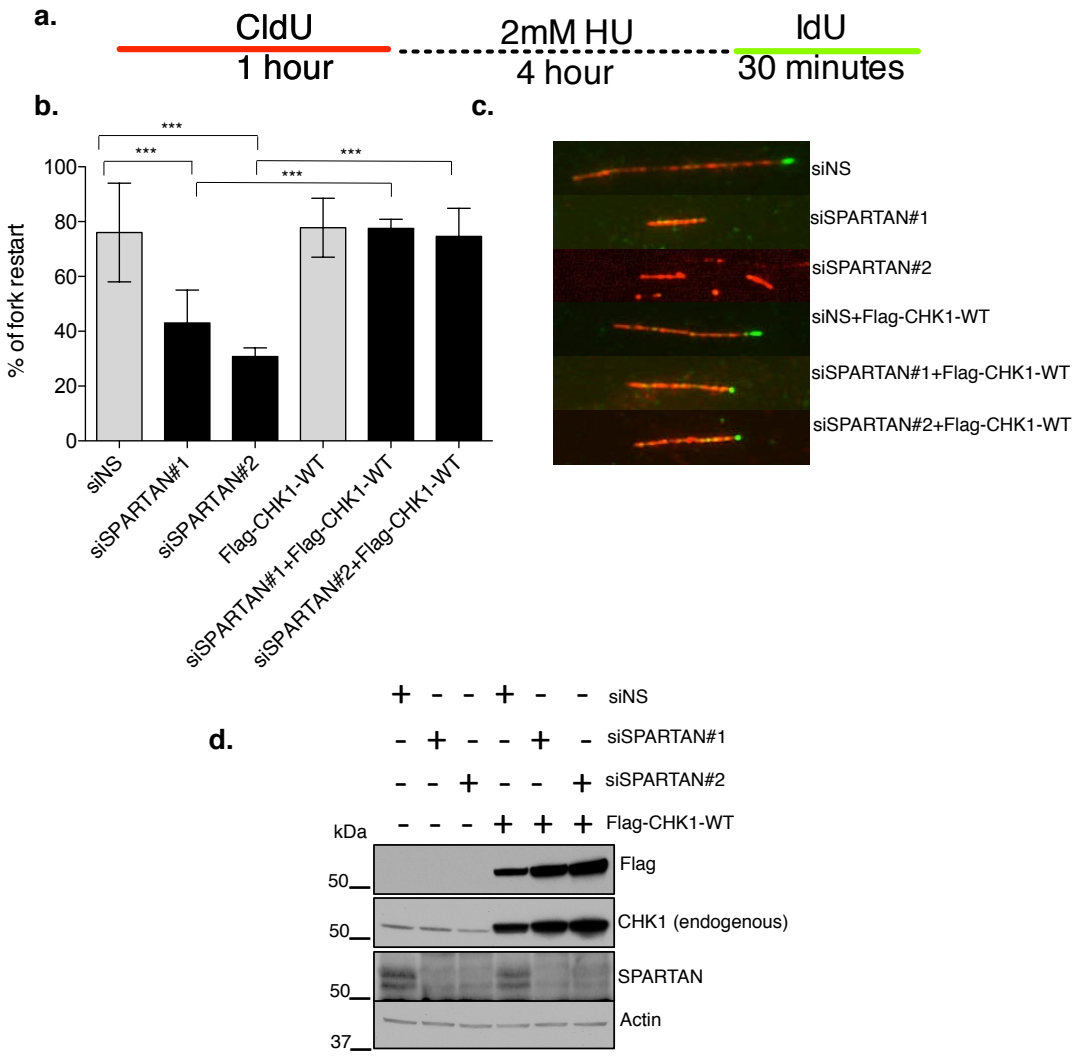



**Figure 20 Ectopic expression of CHK1-WT enables SPRTN depleted cells to efficiently restart stalled replication forks**. All of the experiments were carried out in HEK293 cells. siRNA treatment was carried out for 72 hours. Plasmid expression was carried out for 48 hour. **a.** Strategy of the DNA fiber assay for fork restart experiments. **b**. >400 forks were counted per condition per experiment for their ability to incorporate IdU after HU removal. Data shown as the s.e.m. Data were analysed with unpaired two-tailed t-test. *P < 0.01, **P < 0.001, ***P < 0.0001. n = 2. **c.** DNA fibers showing representative images for fork restart. **d.** Western blot analysis for B and C, showing CHK1 expression and SPRTN depletion. Vinculin was shown as a loading control.

#### 3.2.3.8 CHK1 protects stalled replication forks from MRE11 dependent resection

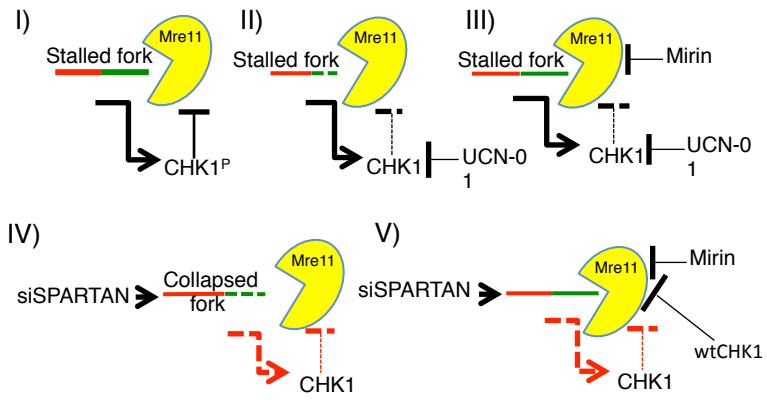
Next, we wanted to understand how stalled forks in SPRTN-defective cells collapse and converts to DSBs. The inability of SPRTN-depleted cells to protect stalled replication forks after prolonged stalling suggested that stalled forks are recognised by nucleases and subsequently degraded by them. It is known that CHK1 protects stalled replication forks from MUS81/EME1 endonuclease mediated degradation and subsequent DSB formation[215]. However, it is also evident from the literature that stalled replication forks need to be processed by MRE11 to create ssDNA, which then would apparently become substrates for MUS81/EME1 to form DSBs[217]. Furthermore, BRCA2 mediated RAD51 loading was demonstrated to be one of the main cascades for the protection of stalled DNA replication forks from nucleolytic attack[142]. The BRCA2-Rad51 cascade is under strict control of CHK1. CHK1 promotes RAD51 loading and foci formation upon DNA damage[144], through inhibition of CDK, which negatively regulates BRCA2 mediated RAD51 loading[143]. In summary, it can be safely interpreted that replication stress (fork stalling) mediated activation of CHK1 promotes RAD51 loading to the stalled replication forks. Furthermore, loading of RAD51 then counterbalances MRE11 mediated degradation of the stalled forks[141]. Based on the abovementioned facts, we hypothesised that the absence of functional CHK1 in SPRTN-inactivated cells, would lead to the MRE11 dependent processing of these stalled forks to form ssDNA structures, which will then apparently become substrates for MUS81/EME1, resulting in DSB formation.

We wondered whether this mechanism is responsible for replication stress induced DSB formation in SPRTN depleted cells. Measurements of nascent DNA tract length (**Figure 21 B**) after one hour of IdU incubation -/+ HU or HU + Mirin (MRE11

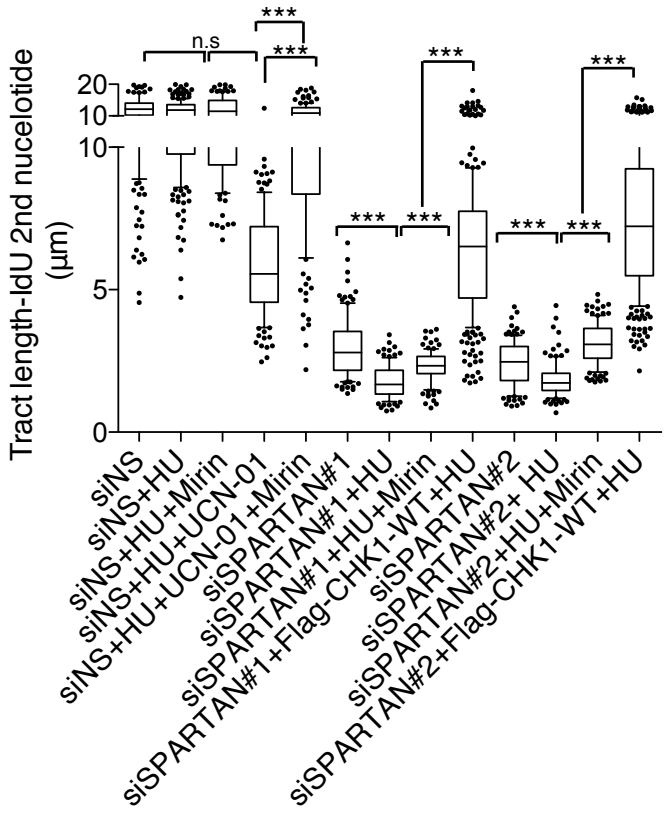
inhibitor) did not yield any difference in control cells. It suggested that HU induced stalled forks in control cells have fully functional CHK1, which prevented fork degradation and inhibition of MRE11 have no effect in such condition. However, chemical inhibition of CHK1, by the potent CHK1 inhibitor UCN-01, in the presence of HU, led to hyper-resection of nascent DNA. Interestingly, MRE11 inhibition (HU+UCN-01+mirin) by mirin completely reversed this fork degradation (**Fig 21 a, b**). This experiment directly suggested that CHK1 kinase activity negatively regulates MRE11 nuclease activity at the stalled replication forks, which protects nascent DNA from MRE11 mediated degradation. Absence of this protective mechanism would otherwise lead to fork collapse and DSB formation. Indeed, we observed hyper-resection of stalled forks in SPRTN-depleted cells (+HU), further confirming the CHK1 defect. Most importantly, excessive fork resection in SPRTN-depleted cells is significantly suppressed after inhibition of MRE11 nuclease activity (siSPRTN + HU + Mirin), and completely recovered after ectopic expression of CHK1-WT (**Figure 21 b**).

In conclusion, our data provides the first direct evidence about how CHK1 prevents MRE11 mediated degradation of stalled replication forks and the relevance of SPRTN in this mechanism.

**a.**


I)
Stalled fork
Mre11
CHK1P
II)
Stalled fork
Mre11
CHK1
UCN-01
III)
Stalled fork
Mre11
Mirin
CHK1
UCN-01
IV)
siSPARTAN
Collapsed fork
Mre11
CHK1
V)
siSPARTAN
Mre11
Mirin
wtCHK1
CHK1

**b.**


Tract length-IdU 2nd nucelotide (µm)
20
10
10
5
0
n.s
***
siNS
siNS+HU
siNS+HU+Mirin
siNS+HU+UCN-01
siNS+HU+UCN-01+Mirin
siSPARTAN#1
siSPARTAN#1+HU
siSPARTAN#1+HU+Mirin
siSPARTAN#1+Flag-CHK1-WT+HU
siSPARTAN#2
siSPARTAN#2+ HU
siSPARTAN#2+HU+Mirin
siSPARTAN#2+Flag-CHK1-WT+HU

**c.**

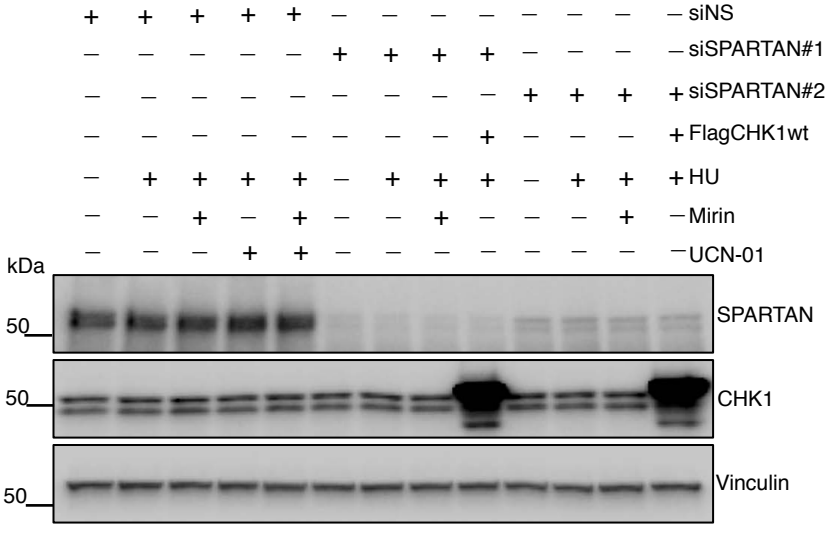

siNS
siSPARTAN#1
siSPARTAN#2
FlagCHK1wt
HU
Mirin
UCN-01
kDa
50
SPARTAN
CHK1
Vinculin

**Figure 21 CHK1 protects stalled replication forks from MRE11 dependent resection**. All experiments were carried out in HEK293 cells. siRNA treatment and Plasmid expression was carried out for 72 and 48 hours, respectively. Nascent DNA was first incubated with CldU for 30 minutes followed by 60 minutes of IdU incubation. Following this, the reaction is either terminated (siNS, siSPRTN) by ice cold PBS or treated with 2mM HU for 4 hours in the presence or absence of UCN-01 and Mirin, either alone or in combination, as indicated. **a.** Explanation of the experiment at **b**. **i)** Fork stalling leads to immediate activation of CHK1 which protects stalled forks from MRE11 mediated degradation **ii**) under this condition if CHK1 is inhibited by UCN-01, MRE11 degrades stalled fork (dotted IdU line) **iii)** presence of MRE11 inhibitor, Mirin prevents fork degradation by MRE11 **iv)** in SPRTN depleted cells HU induced replication blocks leads to collapsed replication forks due to the absence of robust CHK1 activity (shown by dotted CHK1 activation and response), which leads to MRE11 mediated fork degradation (dotted IdU line) **v**) under the same condition, either ectopic expression of CHK1-WT or MRE11 inhibitor Mirin rescue this phenotype. **b.** >50 individual tracts were scored per condition per experiment. Data is shown as the median (bar) with the 25th–75th percentile range (box) and the 10th–90th percentile range (whiskers). Mean differences in micron value were obtained by analysing column statistics in GraphPad Prism software, which was converted to kb value (1 μm= 2.6 kb). P values were obtained by unpaired two-tailed t-test. ***P < 0.0001. n=2 **c.** Western blot analysis showing SPRTN depletion and Flag CHK1-WT expression. Vinculin was used as a loading control

### 3.2.4 Discussion

The function of the ATR-CHK1 signaling pathway in replication stress response and the G2/M checkpoint is well established. Mechanistically, the presence of long stretches of ssDNA, either due to replication stress (helicase-polymerase uncoupling) or as a result of resection of DSBs, leads to full activation of the ATR-CHK1 pathway. The activity of CHK1 is measured by the hyper-phosphorylation status of different Serine residues, such as Ser345, Ser317 and Ser296, at its C-terminal S/T-Q motif. Once fully activated, CHK1 stops cell cycle progression by inhibiting CDKs through phosphorylation of WEE1 kinase and CDC25 phosphatases. Cell cycle arrest allows CHK1 critical time to activate various well-characterised replication stress response pathways. CHK1 achieves this by abolishing the inhibition of dormant origin firing though inhibition of CDKs, as well as by restarting stalled replication forks by protecting replisome components at stalled forks. CHK1 also prevents spontaneous collapsing of stalled forks by negatively regulating the function of EME1/MUS81.

So far, we have observed that SPRTN deficiency leads to severe replication defects, which we analysed using the DNA fiber assay. We have also demonstrated that, due to faulty DNA replication, SPRTN depleted cells accumulate severe DNA damage, which was visualised by 53BP1 (marker of DSB) and γ-H2AX foci formation throughout the cell cycle. These findings have led us to study the DNA damage induced G2/M checkpoint response in SPRTN deficient cells. We found that SPRTN defective cells (patient and siRNA-depleted) have severe G2/M checkpoint defects, especially after CPT treatment. Collectively, all of these phenotypes in SPRTN deficient cells indicate a faulty ATR-CHK1 pathway. We demonstrate here that SPRTN depletion alone could not evoke robust ATR-CHK1 response under basal

condition, which we measured by the phosphorylation status of CHK1 at Ser296, Ser317 and Ser345. Interestingly, our data also highlighted the absence of robust ATM-CHK2 signalling pathway in SPRTN depleted cells, which we measured by the phosphorylation status of RPA, CHK2 and ATM. The presence of severe replication stress and DSBs, accompanied by diminished ATR-CHK1 and ATM-CHK2 pathway in SPRTN depleted cells led us to test whether these two cascades are entirely defective after treating the cells with HU. Intriguingly, HU treatment led to robust activation of the both ATR-CHK1 and ATM-CHK2 pathways in SPRTN-depleted cells. This indicates that SPRTN is not needed for the proper activation of the ATR-CHK1 or ATM-CHK2 signaling cascades when cells are treated with a strong genotoxic agents like HU, but is required for the activation of these cascades during normal DNA synthesis. Based on these observations, we concluded that SPTRN depleted cells have fully functional ATR-CHK1 and ATM-CHK2 pathways but they are unable to fully activate these two pathways under basal condition and these two essential pathways are somehow masked in SPRTN depleted cells. Altogether, our results suggest that the DNA replication defect is the primary phenotype of SPRTN syndrome, and is most probably due to the inability of SPRTN-depleted cells to properly activate the CHK1 signalling pathway during unperturbed DNA synthesis. Furthermore, the essential function of ATR and CHK1 in normal (unperturbed) DNA replication is further supported by the early embryonic lethality of ATR[146] and CHK1[189] knockout mice, the phenotype also observed in SPRTN knockout mice[218]. In contrary, ATM knockout mice are viable[219]. Altogether this has prompted us to correlate SPRTN defects more towards the ATR-CHK1 pathway rather than the ATM signaling pathway. Indeed, ectopic expression of CHK1-WT, but not CHK1-phospho-mutants, in SPRTN depleted cells restores the DNA replication defect and reduces

genomic instability, which demonstrated a strong functional link between SPRTN and CHK1.

We further demonstrated that due to sub-optimal CHK1 response in SPRTN-depleted cells, these cells hyper accumulate CDC25A, which resulted in hyperactive CDK2 (measured by the phosphorylation status of pPP1 at Tth320). Precise mechanism behind hyper-accumulation of CDC25A in SPRTN-depleted cells is not clear. However, due to the involvement of the p97 system in the proteasomal degradation of CDC25A after ionising radiation[127], we would like to speculate that SPRTN acts as a second tier of cofactors for such processes, which require further investigation. Interestingly, the inhibition of CDC25 phosphatases or CDKs rescues the DNA replication defect (velocity, fork stalling and dormant origins). Our findings thus recapitulate a very well characterised function of CHK1 through CDC25A to CDK2, to elicit cell cycle arrest and further demonstrating the relevance of SPRTN in this signal transduction pathway.

As mentioned earlier, one of the major functions of CHK1 in S phase is to protect the integrity of stalled replication forks. It does so by preserving the replisome components and by counterbalancing EME1/MUS81 mediated cleavage of stalled forks. As a result, CHK1 promotes fork restart and prevent DSB formation. We indeed demonstrated that HU induced stalled forks are not able to restart in SPRTN depleted cells, but can be efficiently restarted by ectopic expression CHK1-WT. Furthermore, CDK2 mediated BRCA2 phosphorylation and abolishment of RAD51 recruitment is well characterised in the literature. Additionally, RAD51 dependent nascent fork protection by counterbalancing MRE11 is also well established. We also found evidence from the literature that CHK1 physically interacts with RAD51 and promotes its foci formation upon DNA damage. Based on these facts, we concluded

that replication stress induced CHK1 activation leads to CDK2 inhibition, which stimulates BRCA2-RAD51 interaction, followed by RAD51 dependent nascent strand protection, therefore counterbalancing MRE11 mediated resection. Thus, the absence of robust CHK1 phosphorylation, followed by hyperactive CDK2 in SPRTN depleted cells, has led us to hypothesise that stalled DNA replication forks in SPRTN depleted cells are prone to MRE11 mediated resection. Indeed, we have demonstrated that degradation of DNA replication fork in SPRTN depleted cells is rescued either by treatment of cells with the MRE11 inhibitor, mirin, or by the ectopic expression of CHK1-WT.

Owing to the report that PP2A counterbalances CHK1 during unperturbed DNA replication followed by our observation that CHK1 activity is severely diminished in SPRTN depleted cells, we hypothesised it might be due to PP2A phosphatase. Indeed, transient inhibition of PP2A's enzyme activity by OA efficiently restored CHK1 phosphorylation status, which subsequently rescued DNA replication fork velocity and suppressed aberrant fork stalling and dormant origin firing in SPRTN depleted cells. These data further suggest that SPRTN deficient patient cells suffer from CHK1 defects, as we could rescue replication defect using OA. Co-depletion of B55α additionally suppressed the genomic instability by rescuing DNA replication and fork restart defects in SPRTN depleted cells, which, we could demonstrate is due to the rescue of CHK1 kinase activity (CHK1Ser345 phosphorylation).

Mechanistically, it still remains to be understood despite having fully functional ATR-CHK1 pathway why SPRTN depleted cells could not utilise this pathway. Therefore, in the next chapter we aim to understand, 1) Why SPRTN defective cells cannot activate the ATR-CHK1 pathway during normal DNA replication, 2) Whether

the putative SPRTN enzymatic activity is functionally related to CHK1 activation, and 3) Whether CHK1 is a substrate of SPRTN.

## 3.3 SPRTN proteolytically removes CHK1 from chromatin

### 3.3.1 Introduction

DNA-protein crosslinks (DPCs) are highly cytotoxic DNA lesions. DPCs occur endogenously due to metabolic bi-products, like formaldehyde, or enzymatically when some DNA metabolic enzymes form a transient crosslink with DNA due to the nature of their enzymatic activity like topoisomerases or glycosylases. DPCs are also induced by exogenous factors such as UV-light, IR or chemicals presents in automobile exhausts or in various dermatological ointments. DPCs are bulky DNA lesions that represent a physical barrier to DNA replication and the transcription machinery[157]. Interestingly, our understanding of DPC repair is limited and we are not aware of any specialised DPC repair pathway. It is accepted that NER, HR and proteasomal degradation are involved in DPC removal and repair[172]. However, the NER pathway is only able to remove DPCs of a limited size, maximum of 11-15 kDa in size[220]. On the contrary, the HR pathway needs DSB formation, and if not properly orchestrated it can be mutagenic and cytotoxic. Also, the proteasome mainly processes ubiquitinated substrates, and it was shown that formaldehyde induced DPCs are not polyubiquitinated in vivo, thus severely limiting proteasome function in this context[221]. Interestingly, the DNA-dependent metalloprotease WSS1 (Weak Suppressor of Sumo 1) was recently shown to proteolytically remove DPCs in yeast [169,170]. However, whether specialised mechanism for DPC removal and repair exists in metazoans in not yet known. We have just discovered that SPRTN is a novel DNA-dependent metalloprotease for the removal of DPCs in metazoans[222]. Collectively, our data suggested that SPRTN travels with the replication fork and proteolytically removes DPCs which blocks replication fork progression. We also found that RJALS patient cells, due to a mutation in the protease domain of SPRTN, have much a higher total endogenous DPC load. Also, similar to SPRTN-depleted cells, RJALS cells are

hypersensitivity to various DPC-promoting agents such as formaldehyde, methylglyoxal, camptothecin and etoposide. Mass spectrometry analysis of DPCs in SPRTN-depleted cells led to the identification of specific SPRTN substrates, some of which we have validated both *in vivo* and *in vitro*. To this end, we have observed SPRTN proteolytically cleaves TopoI, TopoIIα, Histone H2A, H2B and H3. Altogether, our results suggested that inactivation of SPRTN leads to the accumulation of DPCs in proliferating cells and we hypothesise that this is the basis of RJALS syndromes.

Based on our previous results we hypothesised that the defect in the CHK1 signalling cascade in SPRTN-depleted cells might be due to the covalent attachment of CHK1 to chromatin. Indeed, we could demonstrate that CHK1 is covalently attached to chromatin in SPRTN-depleted cells and SPRTN proteolytically removes CHK1 from chromatin.

### 3.3.2 AIM: To characterise SPRTN function in proteolytic CHK1 activation

### 3.3.3 Results

#### 3.3.3.1 Formaldehyde induced replication fork slowing, similar to SPRTN depletion, failed to evoke CHK1 phosphorylation

Our group has just demonstrated that SPRTN proteolytically removes DPCs from DNA, and that inactivation of SPRTN leads to an accumulation of endogenous DPCs. My data in this regard suggested that SPRTN depletion leads to faulty CHK1 activation. Thus it is important to understand whether there is any relationship between aberrant DPCs and CHK1 activation and whether SPRTN controls this regulatory mechanism. To understand this, we treated HEK293 cells with different genotoxic agents (**Fig 22 a**). Treatment with HU (500-μM) led to robust CHK1 phosphorylation at both Ser296 and Ser345, suggesting that the classical ATR-CHK1 pathway is activated. Absence of hyperphosphorylation of Thr68 of CHK2 and Ser1981 of ATM suggested no DSB formation under this condition, which is also in accordance with the published literature. Low doses of APH (300 nM) and CPT (100 nM) led to moderate activation of the ATR-CHK1 pathway but did not activate the ATM-CHK2 pathway. Interestingly, treatment with CPT (1 μM) led to robust activation of both ATR-CHK1 and ATM-CHK2 pathway, suggesting DSB induced ssDNA formation, which is also in accordance with the published literature[112]. Formaldehyde (FA) treatment, on the contrary, led to dose dependent activation of ATR-CHK1 and ATM-CHK2 pathways[118,223]. Interestingly, at lower concentrations of FA (50 μM and 100 μM), γ-H2AX was activated but the ATR-CHK1 and ATM-CHK2 pathways were not. This is a trend that we observed upon SPRTN depletion. Therefore, we hypothesised whether low doses of FA behave similarly to SPRTN

depletion. To test our hypothesis, we treated cells with 50 μM FA (2nd Nucleotide) and used HU as a positive control for replication stress induced ATR-CHK1 pathway activation. Additionally, we used high doses of CPT as a positive control for ATM-CHK2 cascades activation, for corresponding Western blots experiments, to categorically demonstrate that FA treatment does not led to ATM-CHK2 activation due to DSB formation. To our surprise, we observed severe replication fork slowing in FA treated cells as measured by decrease in replication fork velocity but with sub-optimal CHK1 phosphorylation. This finding exactly mimics SPRTN depleted condition (**Fig 22 b & c**). Altogether, our data demonstrated that DPCs induced by low doses of FA treatment or SPRTN depletion severely decreases replication fork speed but failed to properly activate the ATR-CHK1 pathway, the main signalling cascade that protects DNA replication forks upon DNA damage.

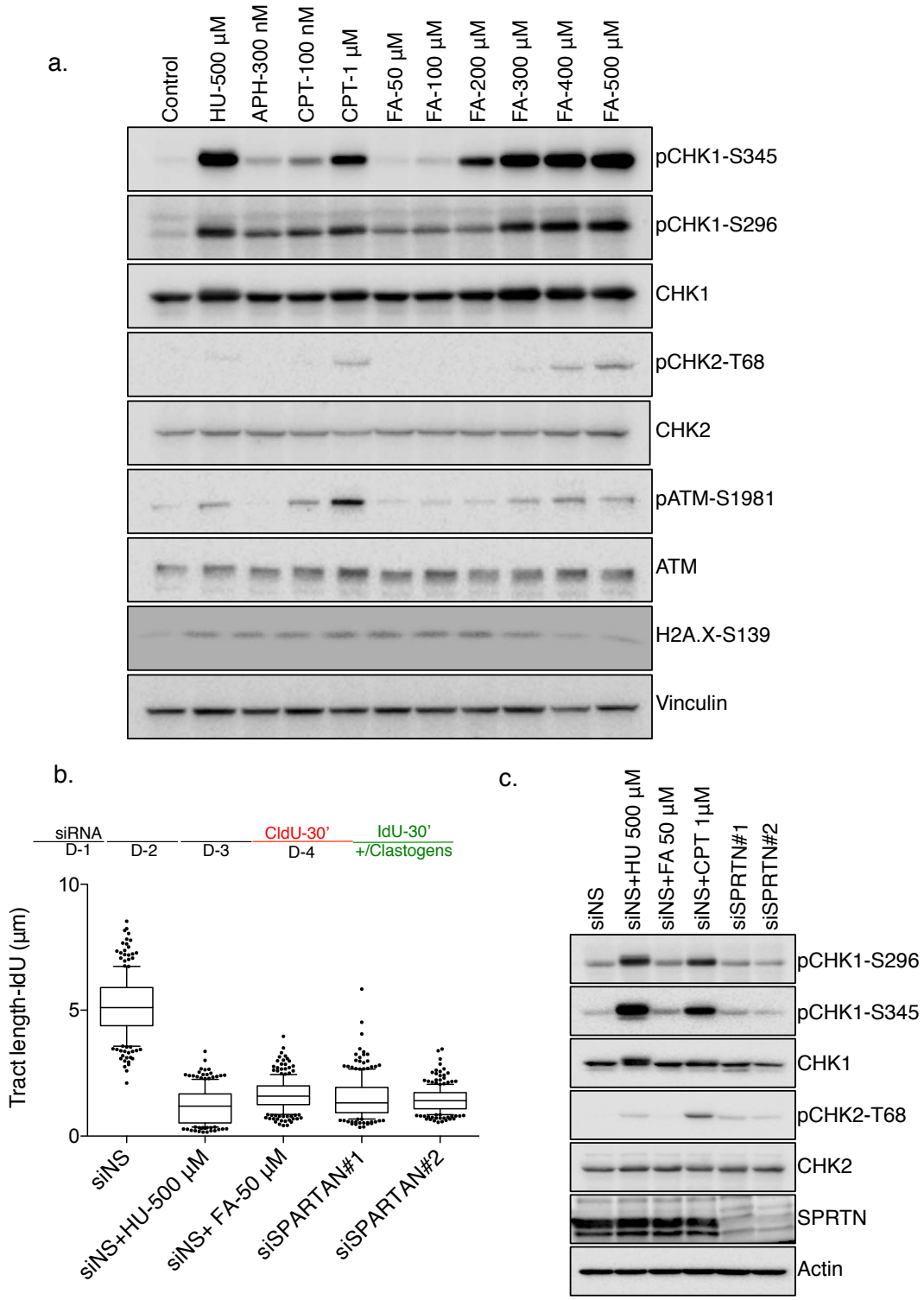



**Figure 22 Formaldehyde induced replication fork slowing, similar to SPRTN depletion, failed to evoke CHK1 phosphorylation** Experiments were performed in HEK293 cells. **a.** Western blots showing the effect of different clastogens on ATR-CHK1 and ATM-CHK2 signalling cascade.γH2AX was used as a marker for DNA damage. Vinculin was used as a loading control. Drug treatment was carried out for 1

hour. **b.** Schematics of DNA fiber assay followed by measurements of IdU tracts. Data was analysed as mentioned previously. n=2 >100 individual tracts were scored per condition per experiments. **c.** Western blots showing the efficiency of SPRTN depletion and effect of HU and FA in ATR-CHK1 and ATM-CHK2 pathway. CPT was used as an additional control to create DSB to better read the differences between different signalling cascades. Actin was used as a loading control.

### 3.3.3.2 Bulky DPCs bocks helicase-polymerase uncoupling

Formaldehyde is a well-characterised DNA-protein crosslinker. To this end, we demonstrated in our recent manuscript that SPRTN inactivation leads to hyperaccumulation of aberrant endogenous DPC. Analysis of DNA replication and its associated signalling cascade suggested that both formaldehyde treatment and SPRTN depletion leads to replication stress induced DNA damage, as measured by severe defect in replication fork velocity followed by activation of γ-H2AX. Intriguingly, both SPRTN depletion and FA treatment failed to activate CHK1. Therefore it is important to find out the precise molecular mechanism, which prevented CHK1 activation upon DPCs formation. As mentioned in the introduction, replication stress induced ssDNA formation remains one of the key mechanisms that leads to CHK1 activation[111]. Furthermore, replicative polymerases are prone to stalling due to structural disadvantages in their active pocket in accommodating DNA lesions or distorted DNA. CMG helicases, on the contrary, have a much larger ring shaped structure and are capable of overcoming most of these polymerase-stalling DNA lesions, which are ultimately responsible for ssDNA formation and consequent CHK1 activation[118]. We asked whether DPCs block polymerase-helicase uncoupling. To answer this, we have used the most specific technique, which enables the detection of ssDNA under non-denaturing condition. Thymidine analogue, BrdU, was incorporated into the cells for two cell doublings (48 hours). The bromine atom of a BrdU molecule remains hidden under the phosphodiester bond of double helix DNA and is not accessible to antibody epitopes under native condition[224]. Thus the detection of a BrdU signal under native condition would demonstrate the presence of ssDNA, arising either from replication stress (polymerase-helicase uncoupling) or DSB induced end resection (3' overhang). Indeed, analysis of ssDNA (**Fig 23 a, b**)

under native (non-denaturing) condition in control cells indicated the presence of basal replication stress as we observed that fewer than <3% of S-phase cells have more than15 ssDNA foci, which is also in accordance with the published literature (BrdU being an halogenated nucleotide is prone to oxidation which cause damage). Interestingly, HU induced dNTP starvation led to a robust detection of ssDNA foci suggesting severe replication stress, which is also in accordance with the phosphorylation of CHK1 under this condition (as shown in previous figure). Please recall that this is due to polymerase-helicase uncoupling, as we did not observe ATM-CHK2 pathway activation under this condition, thus suggesting the absence of DSBs and subsequent end resection. Treatment of cells with CPT (100 nM) led to moderate detection of ssDNA foci, explaining the low level of replication stress, which is also in accordance with the moderate phosphorylation of CHK1 under this condition. As mentioned earlier, CPT treatment led to covalent trapping of TopoI-ccs to the DNA and detection of ssDNA under this condition suggested that CMG helicases can easily bypass TopoI–ccs (DPCs) but replicative polymerases cannot, which resulted in ssDNA formation and subsequent CHK1 activation. This situation changed dramatically when we challenged cells with CPT(1μM), as it led to a robust detection of ssDNA foci. Furthermore, activation of the ATM-CHK2 and ATR-CHK1 pathways under this condition indicated DSBs formation. Thus 1μM CPT induced ssDNA foci indicated resection of DSBs followed by the appearances of ssDNA[112]. To our surprise, FA treatment or SPRTN depletion failed to induce ssDNA foci, which conclusively explained why these cells suffered from suboptimal CHK1 phosphorylation. Our data thus clearly demonstrated that aberrant bulky DPCs (due to FA treatment or SPRTN depletion) cannot be bypassed by CMG helicases, which

prevents helicase mediated unwinding of dsDNA, which further results in the absence of ssDNA and thus inactivation of the ATR-CHK1 pathway under these conditions.

To further show that SPRTN depleted cells have fully functional end-resection pathways, we challenged these cells with HU and CPT (**Fig 23 c**) and indeed found that HU and CPT treatment leads to a robust detection of ssDNA foci. Interestingly, we have shown in the previous result chapter that challenging SPRTN depleted cells with additional genotoxic agents successfully activated both the ATR-CHK1 and the ATM-CHK2 pathways. Therefore, the immunofluorescence data (ssDNA foci) presented here additionally supports our biochemical data in this regard.

Furthermore, we previously observed that PP2A-B55α depletion in SPRTN-depleted cells rescued replication fork velocity, fork restart, dormant origin firing, aberrant fork stalling and genomic instabilities in SPRTN depleted cells (**Fig 19 a-f**). We demonstrated that this is due to the recovery of CHK1 phosphorylation and subsequently its activation. Thus it becomes important to understand whether B55α codepletion also led to the rescue of ssDNA formation in SPRTN-depleted cells. Interestingly, B55α depletion in SPRTN-depleted cells did not increase ssDNA foci formation (**Fig 23 d**) thus suggesting B55α co-depletion neither cause replication stress (polymerase-helicase uncoupling) nor DSB mediated end resection.

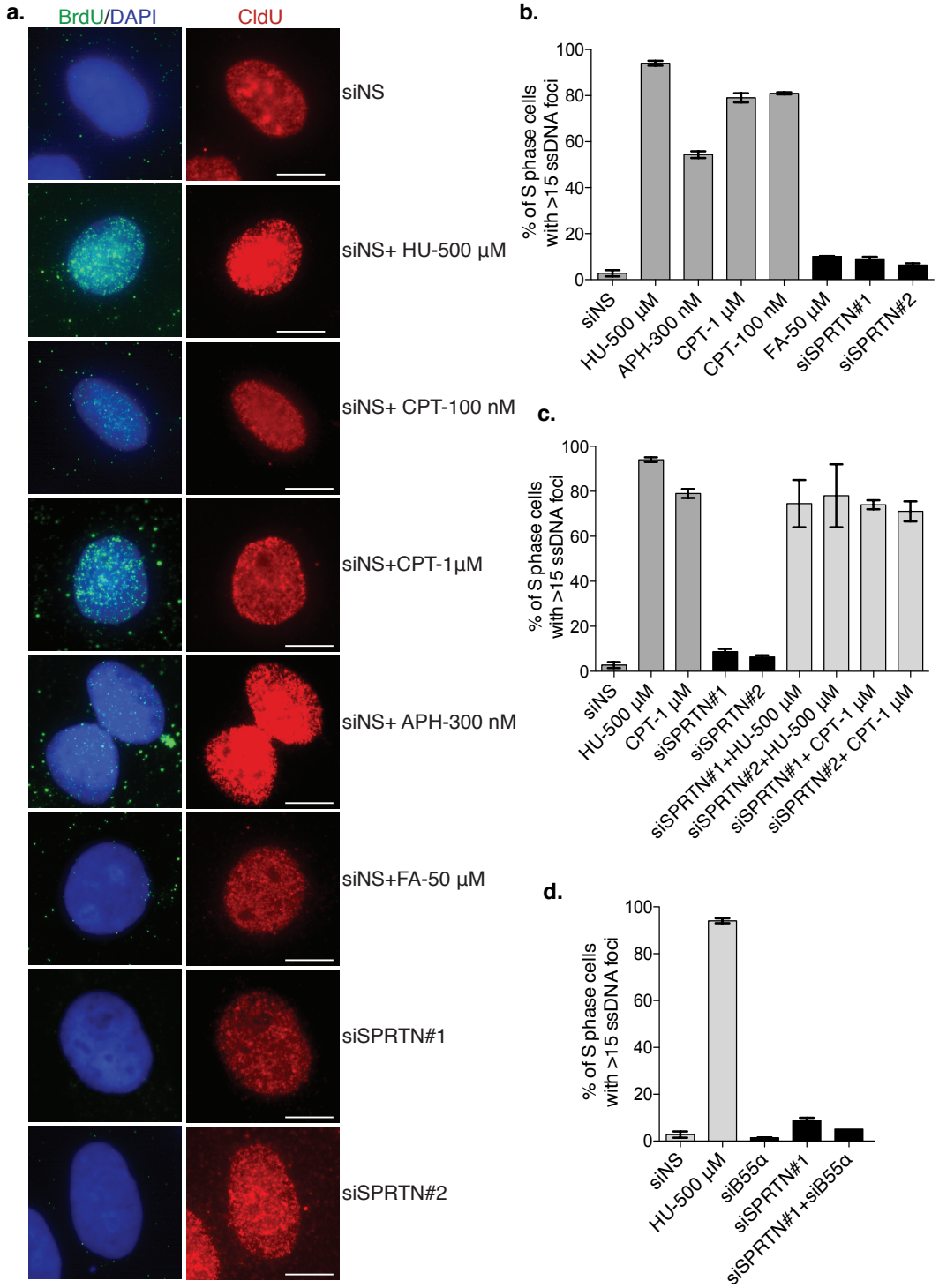



**Figure 23 Bulky DPCs bock helicase-polymerase uncoupling** All experiments were performed in HeLa cells. Drug treatment was carried out for 1 hour and experiments were immediately terminated by ice-cold PBS except for 1µM CPT, which was allowed to recover for 1 hour in normal mediated after CPT removal **a**. Representative images of ssDNA foci as merged images of DAPI (nucleus) and BrdU (ssDNA foci). CldU indicates replicating cells. Scale bar 10 µM **b**. Analysis of ssDNA foci for **a**. **c**. analysis of ssDNA foci in control and SPRTN depleted cell -/+ HU & CPT. **d.**

analysis of ssDNA foci in control and SPRTN depleted and B55α codepleted condition. HU was used as a positive control. n=3. >100 individual S-phase cells were scored per condition per experiments and mean values were shown with s.e.m by Graphpad Prism software. n=3

#### 3.3.3.3 SPRTN is a constitutive member of the DNA replication fork

Pronounced DNA replication defect coupled with sub-optimal CHK1 response in SPRTN-depleted cells indicate that SPRTN is functionally linked with DNA replication and CHK1 activation. Published literature suggested that CHK1 travels with replication fork and upon fork stalling, is phosphorylated, activated and subsequently released. Additionally, isolation of proteins from nascent DNA (iPOND) and subsequent proteome analysis showed that SPRTN is present at the fork although this observation was not biochemically validated[225]. We wondered whether SPRTN is indeed a constitutive member of DNA replication machinery, to answer this, we mildly overexpressed SPRTN-SSH and affinity isolated the SPRTN interacting proteome using streptactin beads and searched for components of the DNA replication apparatus in this complex. Indeed, we observed a robust presence of PCNA, MCM2, MCM6 (MCM complexes) and Polymerase-δ, which strongly suggested that SPRTN form a physical complex with the components of the DNA replication machinery (**Fig 24 a**). To directly demonstrate that SPRTN is physically present at the replication fork, we performed iPOND experiment and pulled-down protein complexes from the newly synthesised nascent DNA as well as from chased matured DNA samples. As anticipated, SPRTN was detected on nascent DNA, along with Polymerase-δ, PCNA and MCM3. Furthermore, SPRTN also moved with the fork as we did not detect any of the abovementioned replication factors on matured DNA (**Fig 24 b**). Previously, we demonstrated a severe defect in polymerase-helicase uncoupling in SPRTN depleted cells, which also positively correlated with FA treatment and altogether suggested a DPC induced replication block. We thus hypothesised that due to DPCs mediated replication block, replication forks in SPRTN depleted cells will not progress and will allow us to detect replisome components upon chasing the

replication forks (Matured DNA), which would be undetectable in corresponding control cells. Indeed, pulse-chase experiments with WT HeLa cells strongly demonstrated that MCM3, PCNA and CHK1 move along with the fork, as they are no longer detected on matured DNA samples in WT HeLa cells (**Fig 24 c**). In contrast, we could efficiently detect MCM3, PCNA and CHK1 on 10 minutes chased matured DNA samples from haploinsufficient SPRTN (Δ-SPRTN) HeLa cells. Our iPOND data thus clearly demonstrated that DNA replication fork progression is severely blocked in Δ-SPRTN cells, most probably due to the accumulation of bulky DPCs which prevents DNA polymerase/helicase uncoupling and consequently inhibits ssDNA formation and proper CHK1 activation.

We have previously demonstrated that either SPRTN or CHK1 over-expression can rescue replication defect in SPRTN depleted cells. To investigate whether SPRTN or CHK1 are required for DNA replication fork progression in the presence of DPCs-inducing agents we ectopically over-expressed either SPRTN-WT or CHK1-WT, followed by treatment with FA, and measured replication fork velocity by the DNA fiber assay (**Fig 24 e & f**). As anticipated, control cells showed pronounced defects in replication fork velocity upon FA treatment, which can be efficiently rescued by overexpression of either SPRTN-WT or CHK1-WT. Altogether, our data demonstrated that SPRTN moves along with the forks and facilitates the fork progression in the presence of DPCs.

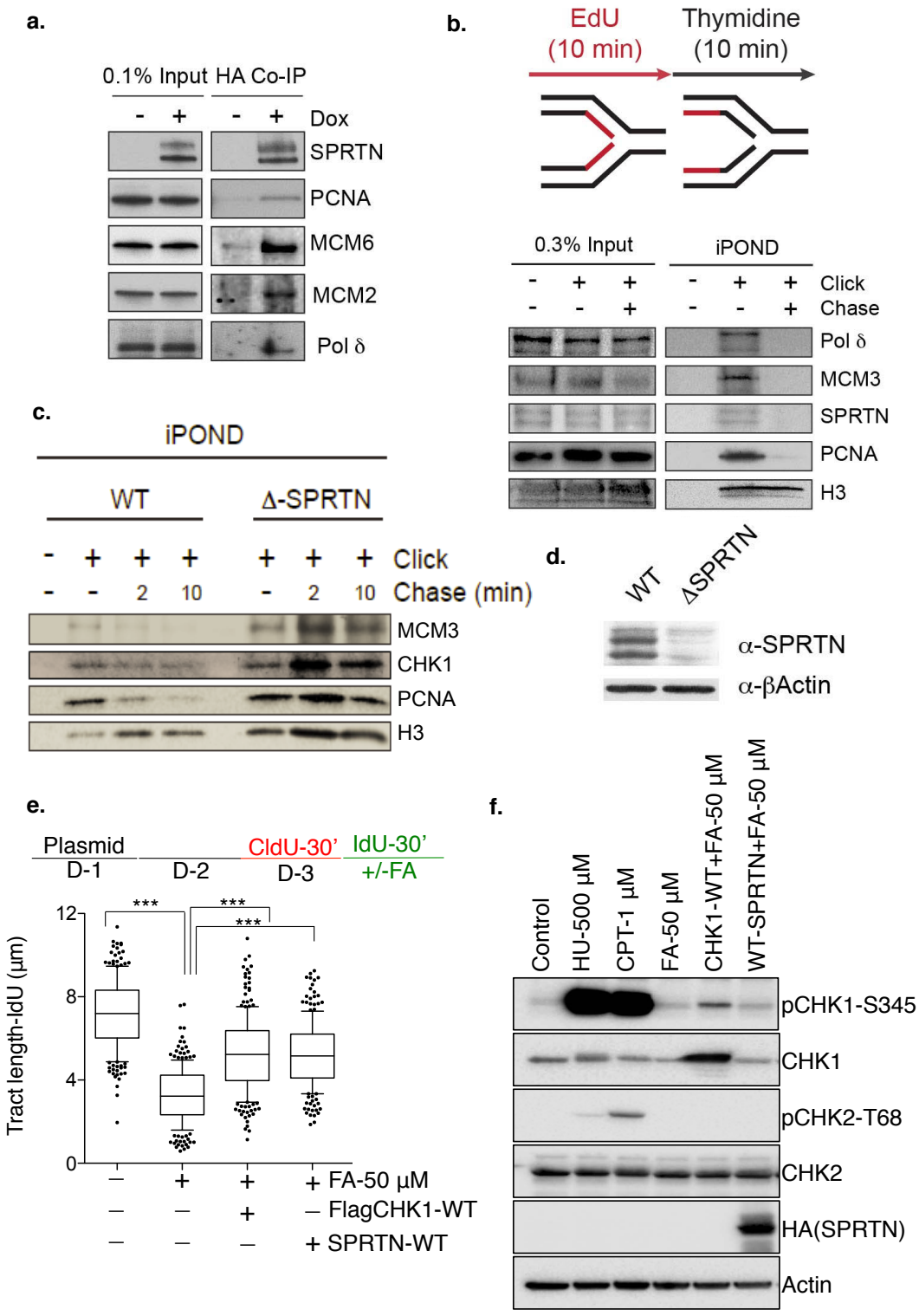



**Figure 24 SPRTN is a constitutive member of the DNA replication fork** Co-IP **a.**, the DNA fiber assay **e.** and corresponding Western blots **f.** were performed in HEK293 cells. iPOND **b.** & **c.** and corresponding Western blots **d**. were performed in HeLa cells. **a**. SPRTN forms a complex with the main components of the replisome. Co-immunoprecipitation (Co-IP) of SPRTN-WT-cSSH was performed upon Doxycyclin (1mg/ml for 48 hours) (Dox) induction in Flip/In HEK293 cells using

StrepTactin beads in presence of high salt and detergents (150 mM NaCl 1% Triton X-100 ) to remove all unspecific binding proteins from SPRTN-complexes in vivo. **b.** SPRTN moves with the replisome. Schematic of the iPOND approach (isolation of Proteins On Nascent DNA). HEK293 cells were treated with EdU for 10 minutes to label nascent DNA, and then chased with thymidine (10 minutes) where indicated (mature DNA). Click - used as a negative control. **c.** Δ-SPRTN HeLa cells exhibit increased retention of replisome proteins on mature DNA (thymidine chase for 2 min or 10 min). iPOND was performed as in **b. d.** Western blot showing SPRTN depletion in Δ-SPRTN CRISPR/Cas9 HeLa cells. **e**. SPRTN and CHK1 promotes DNA replication fork progression in the presence of DPC-inducing agents (50 μM FA). HU was used as a positive control. Fork progression was monitored by DNA fiber assay in HEK293 cells transfected with SPRTNWT-cSSH or FlagCHK1-WT.Schematics are shown in upper panel. >100 DNA fibers were analysed per experiment per condition (n = 3). **f.** Western blot analysis showing SPRTN and CHK1 expression for **e.** CPT was used to create DSB and to show that ectopic expression of SPRTN and CHK1 does not cause DSB formation. Actin was used as a loading control. Image **b,c,d** contributed by John Fielden.

### 3.3.3.4 SPRTN proteolytically removes DPCs

Our data thus far suggested a strong similarity between FA treatment and SPRTN depletion, as both led to pronounced DNA replication fork progression defect but strangely failed to evoke a CHK1 response. To this end, analysis of ssDNA foci followed by iPOND experiments suggested this is due to bulky DPCs mediated helicase stalling. Thus, it became important to demonstrate that FA treatment or SPRTN depletion leads to accumulation of endogenous DPCs and that SPRTN is a DPCs specific protease. To investigate the role of SPRTN in DPC repair, we isolated total genomic DNA from HeLa cells and analysed the amount of DPCs using RADAR (Rapid Approach to DNA Adducts Recovery) coupled to SDS-PAGE/Silver staining [176]. The isolation of DNA under stringent denaturing conditions allowed us to exclusively detect proteins that are cross-linked to DNA (DPCs). Indeed, short FA treatment led to the hyper accumulation of DPCs (**Fig 25 a)**. Quantitative analysis of total DPCs by silver staining in Δ-SPRTN HeLa cells showed a 3-4 fold increase in total DPCs. To investigate if the putative protease domain in SPRTN plays a role in DPC removal, we ectopically expressed SPRTN wild-type (SPRTN-WT) or E112A (SPRTN-E112A), a variant containing a glutamic acid to alanine substitution in a predicted protease active center (HEXXH, H; histidine, E; glutamic acid, X; any amino acid), in Δ-SPRTN HeLa cells. Overexpression of SPRTN-WT, but not SPRTN-E112A, completely rescued basal DPCs accumulation (compare lanes 3 and 4 **Fig 25 b**). This data suggested that SPRTN is a protease for the removal of endogenously formed DPCs. To specifically show that SPRTN cleaves its substrate, we performed *in vitro* cleavage activity assays using purified SPRTN-WT protein. SPRTN-WT cleaved histones H3 in a DNA-dependent manner but catalytically inactive SPRTN-E112A did not cleave histone H3. The Patient mutation SPRTN-

Y117C was severely affected with respect to histone H3 cleavage (~ 8% active), whereas SPRTN-ΔC (C-terminal truncation, patient mutation) retained similar activity to SPRTN-WT (**Fig 25 c**).

We next asked whether CHK1 is proteolysed by SPRTN. To address this question, we incubated purified CHK1 with SPRTN-WT or SPRTN-E112A in the presence of ds-DNA. We found that SPRTN-WT, but not the protease dead variant (E112A), cleaved CHK1 leaving at least three cleavage products of the following sizes: 26, 31 and 36 kDa. Western blot analysis with an anti-Flag antibody showed all three cleavage products were N-terminal as Flag tag was located on the N-terminus of immuno-purified Chk1. (**Fig 25 d**). Altogether our data firmly demonstrated that SPRTN is a novel DPC specific protease and it enzymatically cleaves CHK1.

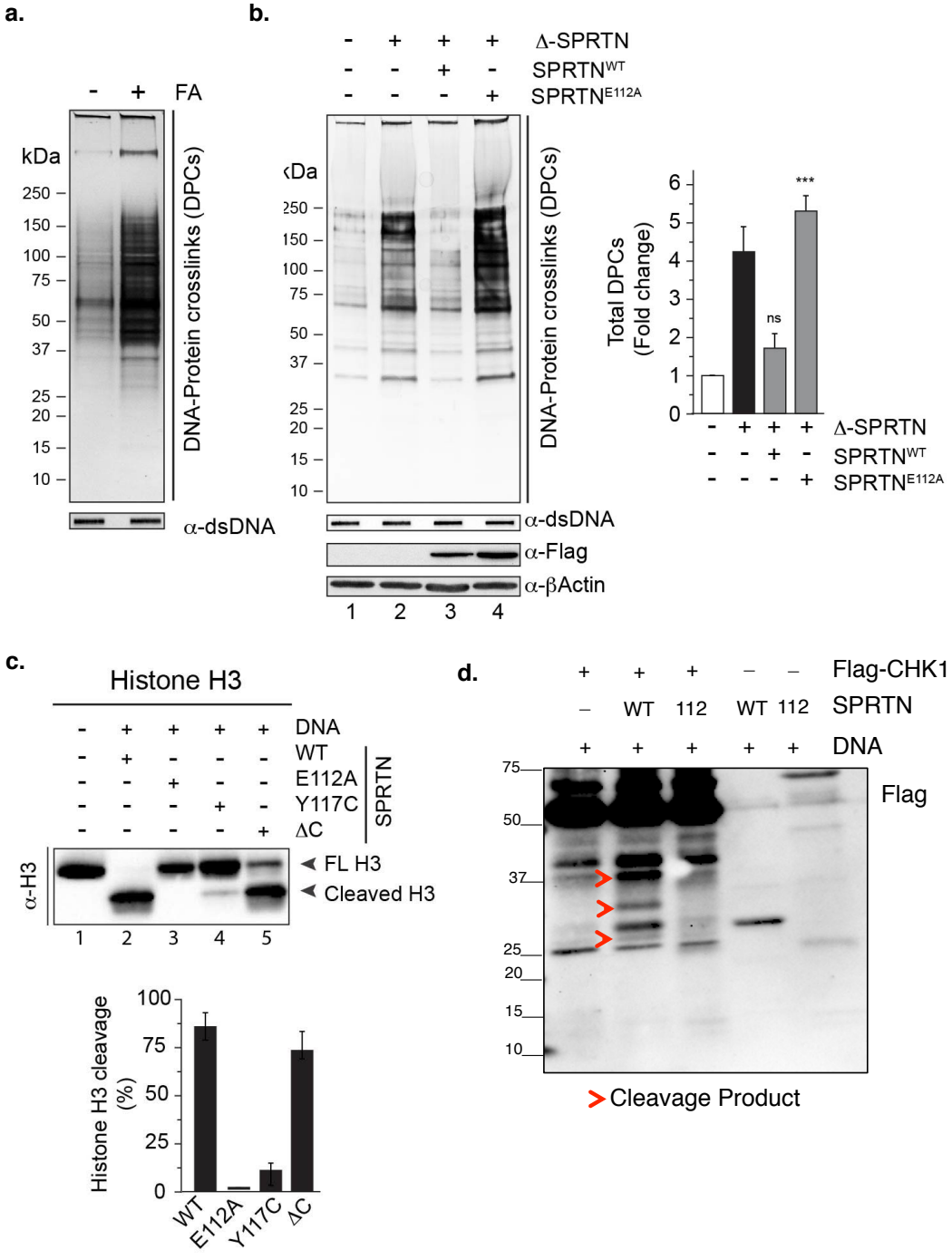



**Figure 25 SPRTN proteolytically removes DPCs a.** DPC accumulation in HeLa cells after FA treatment (2.5mM, 30min). **b.** Ectopic expression of SPRTN WT but not E112A rescues DPC accumulation, and quantification (n = 3). **c & d.** Histone H3 and CHK1 are substrates of the SPRTN protease. Enzymatic reactions were performed with purified SPRTN proteins (as indicated), histone H3 and CHK1 in the presence of dsDNA (37℃/8 hours). Proteolytic activity was monitored by Western blot using H3 and CHK1 antibody, as indicated. Quantification of cleavage activity is expressed as a percentage of total histone H3 in the reaction (n = 3). Image a, b is contributed by Bruno Vaz. Image c & d contributed by Marta Popovic.

### 3.3.3.5 SPRTN facilitates chromatin release of CHK1

To show that SPRTN removes crosslinked proteins in replication dependent manner and that CHK1 is indeed crosslinked to DNA in SPRTN depleted cells, we again analysed DPCs by RADAR as mentioned previously. We arrested HeLa WT and Δ-SPRTN cells by double thymidine block at the G1/S boundary and harvested them at 0, 4 and 8 hours after their release into S-phase (**Fig 26 a**). The propidium iodide (PI) profile indeed demonstrated that the cells were arrested at G1/S boundary and progressed through S-phase over indicated time points once they were released into normal media (**Fig 26 b**). Total DPCs analysis by silver staining suggested that endogenous DPCs accumulated in G1/S arrested WT and Δ-SPRTN cells. However, WT cells were able to remove endogenous DPCs in replication dependent manner when they progressed through S-phase. Interestingly, Δ-SPRTN cells progressed through S-phase similar to control cells but failed to remove endogenous DPCs, indicating the function of SPRTN in DPCs removal in a replication dependent manner. We next looked for specific DPCs and found that CHK1, along with PP2A-B55α is increasingly crosslinked to DNA in haploinsufficient Δ-SPRTN cells as they progressed through S-phase, clearly demonstrating the inability of Δ-SPRTN cells to process CHK1 and PP2A-B55α (**Fig 26 c**). To demonstrate that SPRTN′s protease activity is involved in processing of its substrates, we affinity isolated SPRTN interacting protein complexes from SPRTN-WT and protease defective SPRTN-Y117C cells (**Fig 26 c**). We found that SPRTN readily interacted with PCNA, ORC2, MCM3, Polymerase-δ, p97, PP2A-B55α, PP2A-C and CHK1. However, analysis of the SPRTN-Y117C interactome demonstrated that some components of the SPRTN complex are heavily enriched, such as CHK1, PP2A-B55α, Polymerase-δ and ORC2,

suggesting that protease inactive SPRTN traps these components and prevent their proteolysis.

In order to demonstrate the dynamic behavior of CHK1 during replication stress, we treated cells with FA, HU, as well as also depleted endogenous SPRTN and studied CHK1 presence in different sub-cellular locations (**Fig 26 d**). Treating cells with HU led to the immediate release of CHK1, as shown by pCHK1-S345 in nuclear soluble (N.Sol) fraction. FA treatment, on the contrary, failed to evoke such a response and as a result CHK1 was retained in the chromatin (CHR) fraction. Interestingly, chromatin retention of CHK1 is further enhanced in SPRTN depleted cells. Our data thus suggest that SPRTN proteolytically removes CHK1 from chromatin and facilitates its activation.

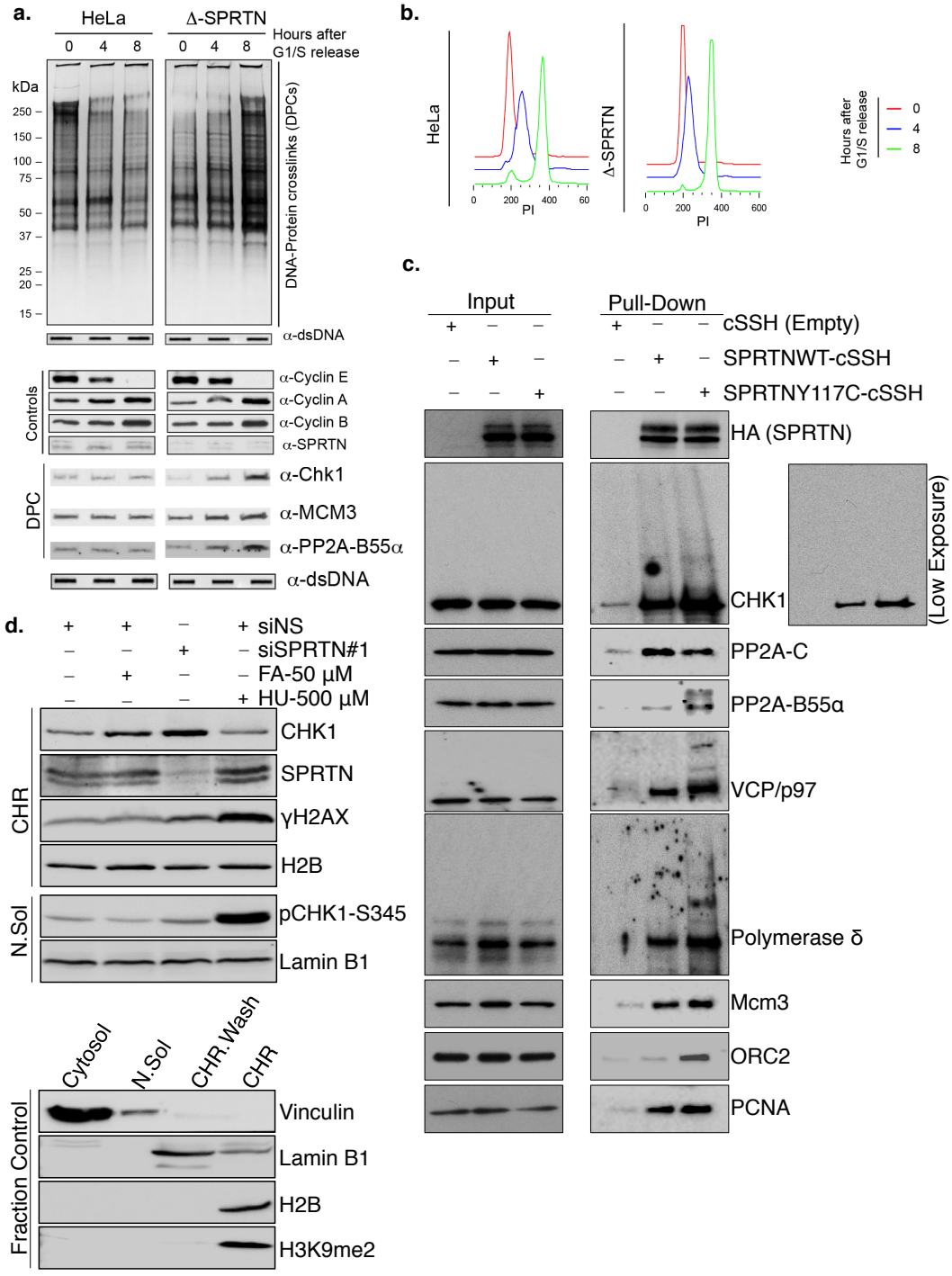



**Figure 26 SPRTN facilitates chromatin release of CHK1 a.** HeLa WT or Δ-SPRTN cells were double thymidine blocked (as mentioned in the materials and methods section) released and harvested as mentioned. Total DPCs were analysed by silver staining after Benzonase digestion. dsDNA was obtained by slot blot analysis showing the equal amount of starting materials after Proteinase-K digestion for total DPCs upper panel. Proteins extract showing Controls for cell cycle markers. Specific DPCs were detected by indicated antibodies after Benzonase digestion. n=3 **b.** showing the FACS profile of cell cycle stages by PI staining. n=3. **c.** Co-immunoprecipitation (Co-IP) of SPRTN-WT-cSSH and protease defective SPRTNY117C-cSSH was performed upon Doxycycline (1mg/ml for 48 hours) (Dox)

induction in Flip/In HEK293 cells using StrepTactin beads in presence of high salt and detergents (150 mM NaCl 1% Triton X-100 ) to remove all unspecific binding proteins from SPRTN-complexes in vivo followed by Western blot analysis of specific antibodies as indicated **d.** Cell fractionation assay by Western blots in HEK293 cells. Drug treatment was carried out for 1 hour. siRNA treatment were carried out for 72 hours. CHR stands for Chromatin and N.Sol is Nuclear Soluble. Fractionation controls showing different markers in different cellular compartments. Image **a, b** contributed by Bruno Vaz, **d** contributed by Ignacio Torrecilla.

### 3.3.3.6 SPRTN mediated CHK1 activation is evolutionarily conserved

We previously demonstrated that morpholino-mediated down-regulation of the SPRTN ortholog in zebrafish (LOC101886162*)* led to a substantial increase in the number of γ-H2AX foci, which indicated an evolutionary conserved role for SPRTN in the DNA damage response [173]. Furthermore, higher doses of SPRTN morpholino (MO) injection led to early mortality or delayed development in zebrafish embryos. This phenotype was partially rescued by co-injection of WT human SPRTN mRNA but not by equimolar amounts of mRNA from C-terminal truncation or protease domain mutated (Y117C) SPRTN. We wondered whether SPRTN mediated CHK1 activation is the fundamental reason for the SPRTN defective developmental delay and mortality in zebrafish embryos, and whether the expression of CHK1-WT would rescue this phenotype. To answer this question, we microinjected fertilized eggs with a previously described SPRTN MO and newly synthesized capped RNAs encoding different CHK1 variants (CHK1Ser345Ala, CHK1Ser317Ala and CHK1-WT) fused to GFP. Growth retardation was assessed at the 90% epiboly stage. We found significant rescue of the retarded phenotype and the number of γH2AX foci upon co-expression of CHK1-WT with SPRTN morpholino. Interestingly, co-expression of CHK1S345A or CHK1S317A did not rescue either retarded phenotype or the presence of γH2AX foci (**Fig 27 a, b, c, d**). Our data thus clearly demonstrated that a defect induced by SPRTN inactivation can be rescued by CHK1, and that the SPRTN-CHK1 cascade is an evolutionarily conserved mechanism.

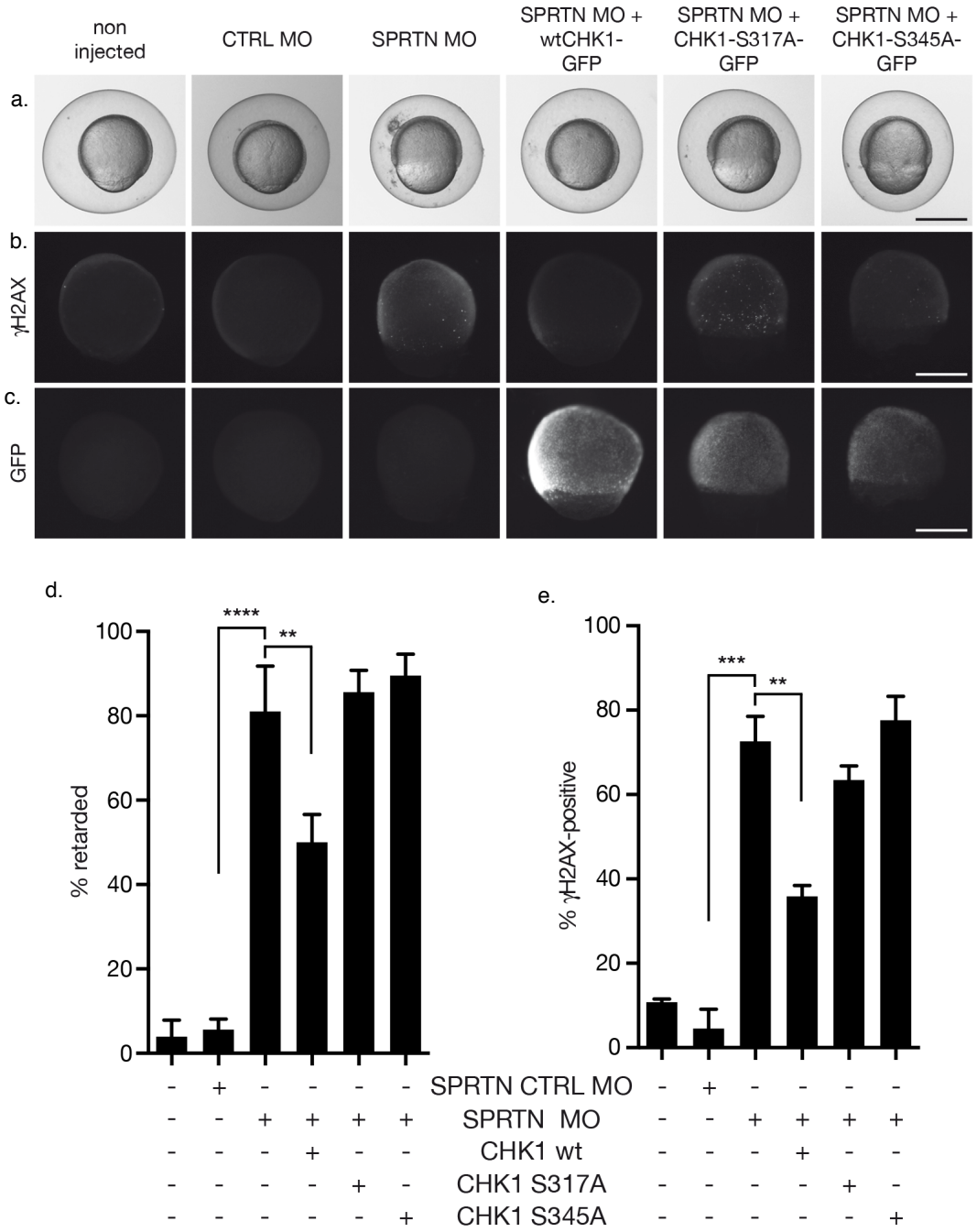



**Figure 27 SPRTN mediated CHK1 activation is evolutionary conserved** Overexpression of CH1-WT rescues delayed development and accumulation of γH2AX foci in SPRTN morphant zebrafish embryos. **a.** SPRTN morphant zebrafish embryos (SPRTN MO) showed a delay in development at 9 hours-post-fertilization (hpf) as compared to non injected controls or embryos injected with a SPRTN control morpholino (CTRL MO). Co-injection of GFP-fused RNA encoding wild type Chk1 rescued this delay, while mutated Chk1 (S317A or S345A) did not. **b.** SPRTN KD causes accumulation of □H2AX foci, which is only rescued by simultaneous overexpression of wild type but not mutated Chk1. **c.** Control for injection of GFP-

fused RNA encoding different versions of Chk1. **d.** Summary of four independent experiments regarding delay of development. Number of embryos analysed in total: non injected=78; CTRL MO=73; SPRTN MO=81; SPRTN MO+wtChk1=70; SPRTN MO+Chk1-S317A=85; SPRTN MO+Chk1-S345A=81. One-way ANOVA was applied as statistical test. $p<0.0001$ (SPRTN CTRL MO vs SPRTN MO); $p<0.05$ (SPRTN MO vs SPRTN MO+wtChk1). **e.** Quantification of γH2AX focus formation after KD of SPRTN. Only GFP-positive embryos were taken into account, when Chk1 RNAs were injected. n=2 independent experiments. Number of embryos analysed in total: non injected=36; CTRL MO=29; SPRTN MO=38; SPRTN MO+wtChk1=31; SPRTN MO+Chk1-S317A=36; SPRTN MO+Chk1-S345A=31. One-way ANOVA was applied as statistical test. $p<0.001$ (SPRTN CTRL MO vs SPRTN MO); $p<0.01$ (SPRTN MO vs SPRTN MO+wtChk1). The idea for this experiment, cloning of constructs, plasmid isolation and experiment design was based on data presented in this thesis. The Actual experiment followed by data analysis and final figures were assembled by our collaborators Melanie Philipp and Martin Burkhalter.

### 3.3.4 Discussion

DNA-protein crosslinks are highly toxic DNA adducts that can occur both endogenously and exogenously. Little is known about how cells cope with these toxic DPCs and whether there exists a specific DPC repair pathway. Recent studies in yeast demonstrated the presence of a specific protease, WSS1, that removes toxic DPC adducts[169,170]. Our discovery of SPARTAN syndrome (RJALS), followed by the characterisation of the putative metalloprotease domain of SPRTN, suggests that the SprT domain is essential for genome stability and protection from accelerated ageing and liver cancer[49,173]. Bioinformatic analysis of yeast WSS1 and human SPRTN suggest that both proteins have a similar metalloprotease active center motif (HEXXH). Thus SPRTN was hypothesised to be the homologue of yeast WSS1[170,172]. WSS1 was recently demonstrated to be proteolytically active and involved in DPC repair in yeast. However, the laboratory of Ivan Dikic was unable to rescue the sensitivity of WSS1-null yeast to DPC-inducing agents by overexpression of human SPRTN[226]. This result suggests that SPRTN is not a functional homolog of WSS1. Although, both proteins are DNA-dependent metalloproteases and have been shown to process DPCs, however, their cellular functions are different. SPRTN processes all DPCs in human proliferative cells and SPRTN is coupled to the DNA replication machinery. In contrary, WSS1 does not process general DPCs in yeast cells; the involvement of WSS1 dysfunction (WSS1-deleted strain) in the removal of specific DPCs, like Top-cc, is only observed upon the inactivation of Tdp1, another enzyme involved in the enzymatic processing of Top1-cc. Moreover, SPRTN-depleted human cells are hypersensitive to FA but WSS1-null yeast cells are not[170]. As our understanding of DPC repair remains limited, the signaling pathways associated with DPC repair also remain largely unknown. Data presented here establishes the crucial

requirement for the CHK1 pathway and its tight association with DPC removal in a SPRTN dependent manner.

We observed that, due to the elevated level of DPCs, as seen in the case of SPRTN depleted cells, or when cells are exposed to DPC-inducing agents, such as FA, and despite severe DNA replication defect, cells are not able to activate the ATR-CHK1 pathway. This was demonstrated both biochemically (WB showing sub-optimal CHK1 phosphorylation in SPRTN-depleted cells) and by immunofluorescent labelling (no ssDNA foci in SPRTN-depleted cells). We further demonstrated that the accumulation of bulky DPCs blocks polymerase-helicase uncoupling and ssDNA formation in both SPRTN depleted and FA treated cells. We therefore concluded that the absence of ssDNA formation is one of the main reasons why the ATR-CHK1 cascade is not activated in SPRTN-depleted or FA-treated cells. We additionally found that CHK1 is crosslinked to DNA in SPRTN-depleted or FA-treated cells; crosslinked CHK1 is unable to be released from chromatin and properly activated. As our results also demonstrated that CHK1 and SPRTN are constitutive members of the DNA replication fork, and CHK1, along with other replisome components is retained at the fork in the haploinsufficient Δ-SPRTN cells. Altogether, we propose a model where SPRTN protease activity removes DPCs in front of the DNA replication fork and also proteolytically activates CHK1 and once activated, CHK1 controls unperturbed DNA replication fork progression.

In addition to this proposed model, we also demonstrated that SPRTN-depleted cells have an increased amount of PP2A-B55α crosslinked to DNA. As PP2A-B55α mediates CHK1 regulation, the increased chromatin concentration of PP2A-B55α counteracts optimal CHK1 activation under unperturbed conditions. Indeed, co-depletion of B55α or treatment of SPRTN-depleted cells with OA rescues optimal

(physiological) CHK1 phosphorylation and suppresses DNA replication stress phenotypes, as measured by the DNA fiber assay. Along this line, the treatment of SPRTN syndrome patient cells with OA rescues DNA replication fork velocity. Thus, the inactivation of PP2A-B55α abolished its phosphatase mediated negative regulation of CHK1, which ultimately rescued CHK1 kinase activity and its function in S phase. However, it still remains to be understood whether B55α co-depletion in SPRTN-defective cells rescues endogenous DPCs. Altogether, the results presented here suggest that SPRTN regulates the optimal and physiological activation of CHK1 during normal DNA synthesis. This regulation is essential to prevent the DNA replication stress and genomic instability that prevents premature ageing and cancer. However, it seems that SPRTN regulates physiological CHK1 activity at multiple levels: (i) SPRTN is essential for DPC removal in front of the DNA replication fork and thus the formation of ssDNA, which remains the major platform for CHK1 activation (ii) CHK1 is also crosslinked to DNA, and has to be proteolytically released by SPRTN for its optimal activation and (iii) and the third, PP2A-B55α dependent de-phosphorylation and inactivation of CHK1 and the role of SPRTN in this PP2A-CHK1 axis, which allows for the proper activation of CHK1. Further work is needed to completely delineate the exact role of how SPRTN regulates CHK1 during normal DNA synthesis.

## 3.4 Characterisation of FAF1, a bonafide p97 cofactor, in DNA replication

### 3.4.1 Introduction

DNA replication is a tightly regulated process in eukaryotes and it occurs only once per cell cycle. Mechanistically, this is achieved by licensing all the potential origins during late G1 followed by rapid degradation of the replication licensing factor CDT1 at the onset of S phase. After licensing of all the potential origins, CDT1 is rapidly degraded by the ubiquitin proteasome system (UPS). The ubiquitination of CDT1 is mediated by two independent but redundant Cullin-based E3-Ub ligases, $CUL4^{-DDB1-CDT2}$ and $SCF^{-Skp2}$ in humans. While $CUL4^{-DDB1CDT2}$ mediated degradation of CDT1 only occurs in S phase and is an evolutionarily conserved pathway, the $SCF^{-Skp2}$ mediated CDT1 degradation pathway is functional throughout the cell cycle and is not conserved in yeast, invertebrates or other vertebrates [69–72]. Beside its degradation, CDT1 is additionally regulated by binding of Geminin, which prevents CDT-1 interaction with MCM complex and also inhibits its binding to DNA[227,228].

p97 plays essential role in chromatin-associated degradation processes involving DNA replication and DNA damage response. Although the precise mechanism how p97 regulates DNA replication was not previously known. Recent work from two independent laboratories demonstrated that p97-dependent CDT-1 chromatin extraction and its subsequent proteasomal degradation is essential for DNA replication. p97 together with its core cofactors Ufd1-Npl4, binds to ubiquitinated CDT-1 and physically removes it from chromatin. Collectively, their work suggested that $p97^{-Ufd1-Npl4}$ mediated degradation of ubiquitinated CDT1 is an evolutionarily conserved pathway from worms to humans, and inactivation leads to chromatin retention of CDT1[73,74]. As retention of CDT1 leads to massive re-replication and genomic instability[229,230], the abovementioned reports suggested an essential function

for p97 in the proper regulation of replication initiation and thus the maintenance of genomic stability.

In collaboration with the laboratory of Thorsten Hoppe, we have recently identified UBXN-3/FAF1 as an additional second tier adaptor required for $p97^{-Ufdd1-Npl4}$ binding to CDT1, thus providing further specificity and also complexity to the p97 system in the regulation of DNA replication initiation[174]. FAS-associated factor 1 or FAF1 is an evolutionarily conserved protein and have been implicated in both p97 dependent and independent processes. It is a member of tumor necrosis factor (TNF) superfamily. It has FAS-interacting domain (FID), a death effector domain interacting domain (DEDID) on its N-terminus and multiple ubiquitin-related domains on its C-terminus with the UBX domain being the primary site for its interaction with p97[231]. FAF1 was initially shown to promote FAS-induced apoptosis by binding to the FAS receptor, but FAF1 expression was later shown to negatively regulate NFκB activity [232].

To specifically understand the substrate and cofactor requirements of p97, which governs its function in DNA replication and cell cycle progression, the Hoppe group conducted a large scale screening using RNA interference approach in C.elegans. Their screening identified UBXN-3 (ubiquitin regulatory X (UBX) domain-containing protein in nematodes) as an important factor along with CDC-48 (p97) that is required for DNA replication. To further understand UBXN-3′s role in DNA replication and associated genomic instability, they challenged UBXN-3 (which are also additionally depleted with CDC-48) depleted cells with replication inhibitor HU. Depletion of UBXN-3 alone affected the viability of the embryos, which was further aggravated after HU treatment, thus suggesting UBXN-3 in association with CDC-48, has a major role in replication stress response. They further confirmed the exclusive role of UBXN-3 in CDC-48 dependent DNA replication by showing that depletion of

other members of the UBX-family like UBXN-1, UBXN-2, UBXN-4 or UBXN-6 has no effect on DNA replication. The authors thus concluded that UBXN-3 functionally interacted with the CDC-48$^{-UFD-1/NPL-4}$ complex during embryogenesis and has a major role in DNA replication stress response. Their data also indicated cofactor specificity in this regard. They further observed RAD-51 foci formation in UBXN-3-CDC-48 co-depleted cells and concluded it was due to collapsed replication forks. Their earlier data in this regard suggested that the CDC-48$^{-UFD-1/NPL-4}$ complex had profound role in the removal of replication licensing factors CDT-1, CDC-45 and GINS from chromatin[74]. Furthermore, abrogation of the CDC-48$^{-UFD-1/NPL-4}$ complex led to retention of these replication factors on mitotic chromatin, which they concluded was due to the impairment of CDC-48$^{-UFD-1/NPL-4}$ segregase function on chromatin. Upon observing a strong genetic interaction with UBXN-3 and CDC-48$^{-UFD-1/NPL-4}$ complex, they revisited this issue and asked whether UBXN-3 acts as a second tier cofactor for CDC-48$^{-UFD-1/NPL-4}$ complex dependent extraction of CDT-1 and GINS from chromatin. Indeed, they observed a strong retention of CDT1, CDC-45 and SLD-5, a subunit of GINS complex, on mitotic chromatin in UBXN-3-CDC-48 co-depleted cells. Hoppe group further confirmed the direct interaction between UBXN-3 and CDC-48 by performing immunoprecipitation studies where they also detected CDT-1. To this end, their data suggested that UBXN-3 binds ubiquitinated CDT-1, and collectively they summarised that CDC-48$^{-UBXN-3}$ removes ubiquitinated CDT-1 and other replication factors from chromatin which is important to preserve genomic integrity[174].

Hoppe group collaborated with us to answer whether the UBXN-3 human ortholog FAF1 has the same phenotype that they observed in *C.elegans*.

### 3.4.2 AIM: To characterise the role of FAF in DNA replication

### 3.4.3 Results

#### 3.4.3.1 FAF1 depletion in U2OS cells causes severe replication stress

As mentioned earlier, worms depleted of UBXN-3 (FAF1) in a CDC-48 depleted background leads to cell cycle delay and collapsed replication forks. Thus it is important to clarify whether FAF1 depletion has the same collective phenotype in mammalian cells and whether FAF1′s role in DNA replication is evolutionary conserved. We asked whether depletion of FAF1 leads to a similar replication defect in mammalian cells. To answer this question, we depleted FAF1 by four different siRNA sequences in human osteosarcoma cell lines (U2OS) and performed DNA fiber analysis. Indeed, we observed a very strong replication defect upon FAF1 depletion in U2OS cells (**Fig 28 b and c**). We also observed a significantly higher number of stalled forks (**Fig 28 d**) and newly fired origins (**Fig 28 e**). Collectively, our observations clearly demonstrated that FAF1 depletion in U2OS cells leads to pronounced replication stress.

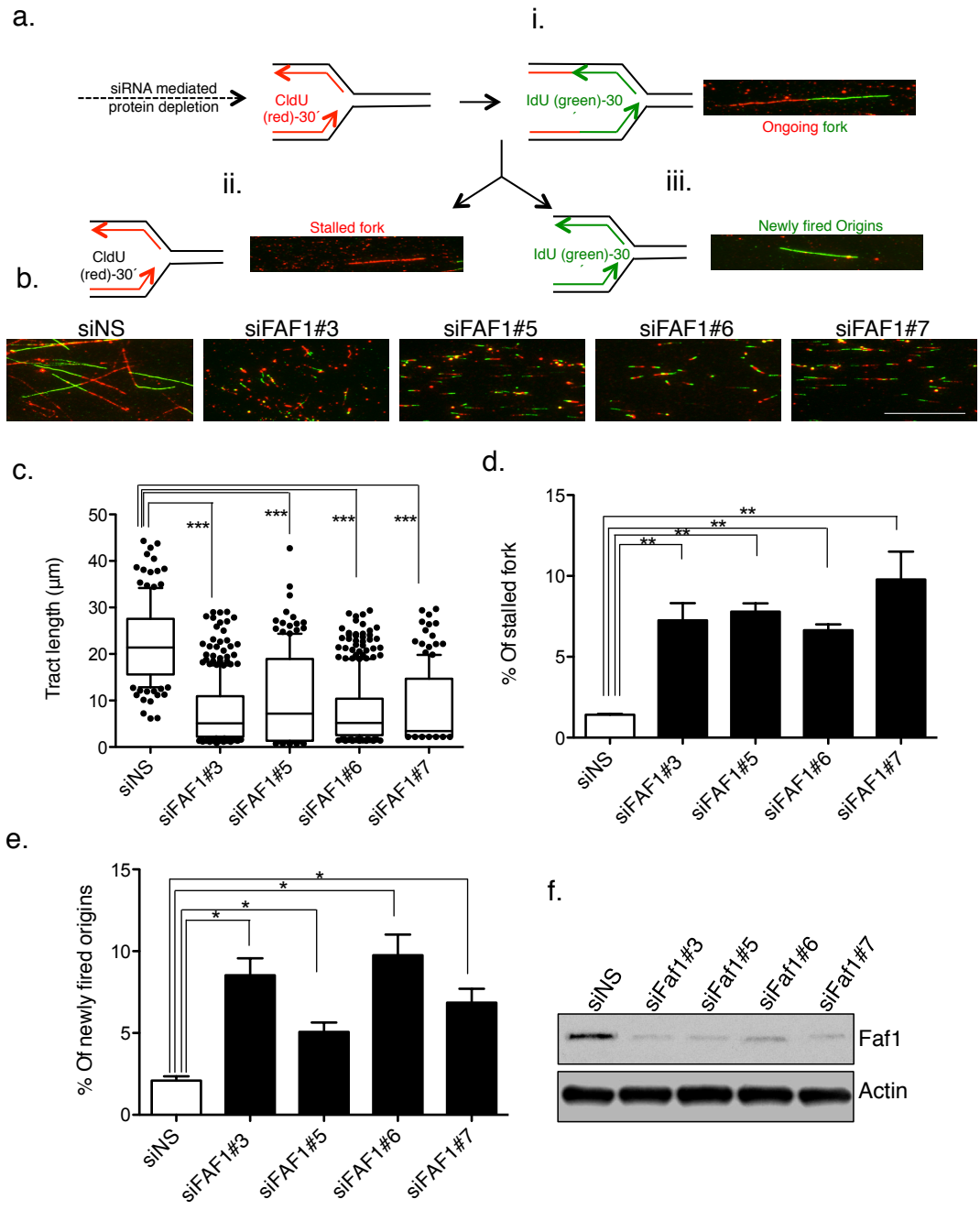



**Figure 28 FAF1 depletion in U2OS cells causes severe replication stress.** a. Schematics of the strategy of DNA fiber assay.i. Ongoing fork ii. stalled fork iii. newly fired origin. b. Representative images of DNA fiber results as indicated c. Measurements of total DNA tract lengths in control and FAF1 depleted cells. >100 individual tracts were scored per experiment per condition. Tract length was measured by ImageJ software and converted to micron scale. n=3. Data is shown as the median (bar) with the 25th–75th percentile range (box) and the 10th–90th percentile range (whiskers), P values were obtained by unpaired two-tailed t-test. *P < 0.0), **P < 0.001, ***P < 0.0001 by GraphPad Prism software. d. and e. analysis of stalled forks and newly fired origins, respectively. >400 forks were scored per condition per experiments and mean values were shown with s.e.m by GraphpadPrism software. f.

Western blot analysis showing the efficiency of FAF1 depletion. Actin was used as a loading control.

#### 3.4.3.2 Co-depletion of CDT1 rescues DNA replication stress in FAF1 depleted cells

We next asked whether the replication defect upon FAF1 depletion is due to the accumulation of CDT1 in U2OS cells. We co-depleted CDT1 in FAF1 depleted cells and analysed DNA replication fork progression in U2OS cells. Depletion of CDT1 alone caused severe replication stress, as measured by a decrease in replication fork velocity, accompanied by a significant increase in the number of stalled forks and dormant origins firing. This is consistent with the idea that depletion of essential replication factors leads to pronounced replication stress. To our surprise, we observed almost complete rescue in replication fork velocity, followed by suppression of number of stalled forks and newly fired origins in cells, which were co-depleted with both FAF1 and CDT1 (**Fig 29 a-e**). Our data strongly suggested that FAF1 dependent CDT1 turnover is important for proper DNA replication fork progression. Interestingly, it was recently reported that p97 regulates termination of the DNA replication forks. p97 binds and extracts ubiquitinated MCM7 from chromatin using its ATPase activity. The inactivation of p97 in this regard leads to hyperaccumulation of the MCM2-7 complex on chromatin and a severe defect in termination of DNA replication. However, the authors did not report any involvement of the core p97 cofactors such as UFD-1 or NPL-4 or any second tier cofactors in the regulation of DNA replication fork termination. Thus it becomes important to rule out that the replication defect upon FAF1 depletion is not due to the failure of replication fork termination followed by faulty disassembly and retention of the MCM2-7 complex on chromatin, and its global effect on DNA replication fork progression that we have observed so far. Technically, this is very challenging to perform in mammalian cells and even in synchronised cells, as origin firing is random and occurs throughout the S

phase. Interestingly, the DNA fiber assay can be utilised for such purposes by counting the number of second label termination events, which shows the termination of two neighboring forks from opposite direction (Fig 29 **f)** Indeed, depletion of FAF1, due to severe replication defects, resulted in the failure to terminate most of the ongoing replication forks. However, co-depletion of CDT1, under such conditions, enables those FAF1 depleted cells to complete DNA replication, as measured by total number of terminated events. Our data thus strongly demonstrates that the $p97^{-FAF1}$ dependent extraction of CDT1 is critical for DNA replication fork progression.

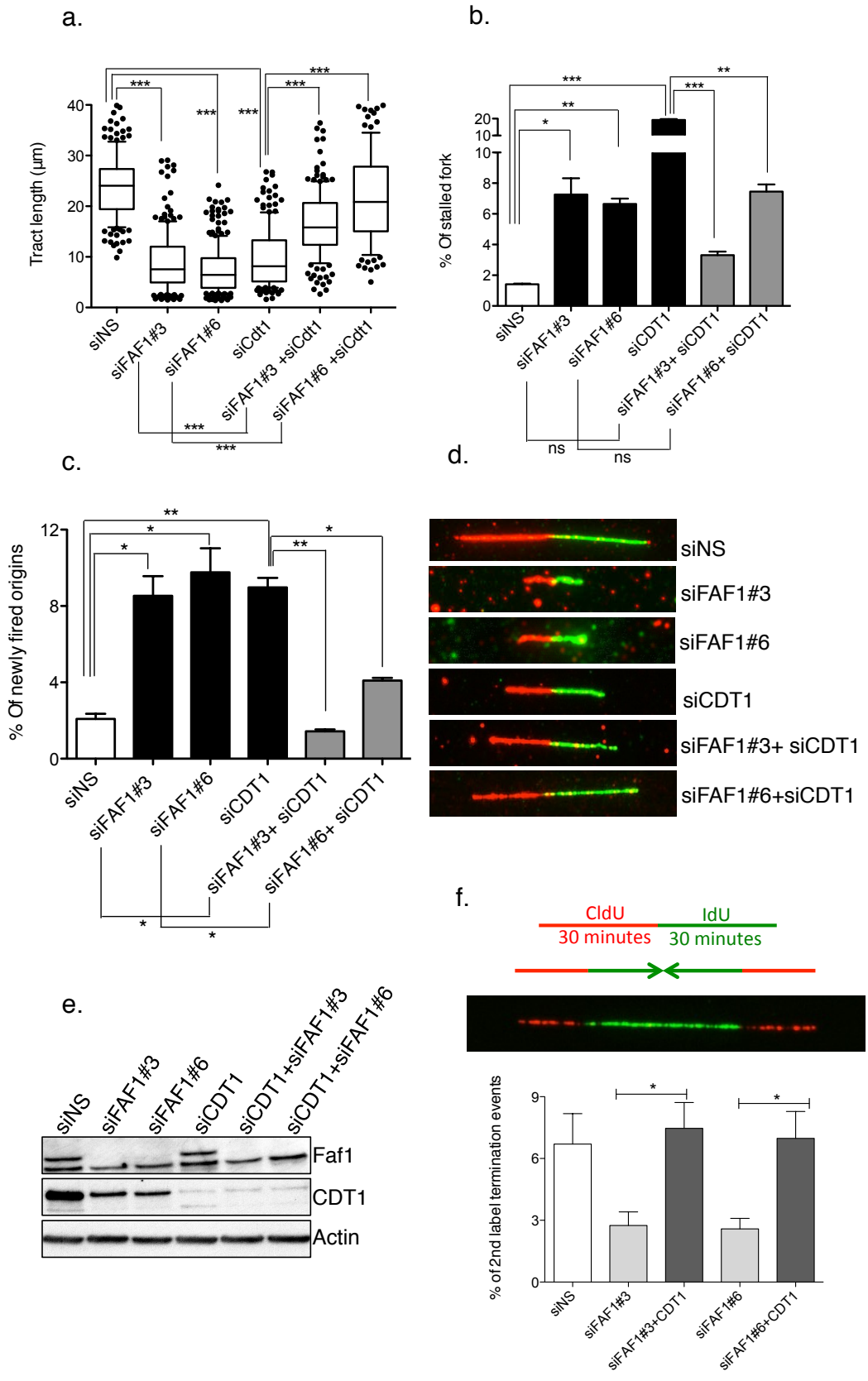



**Figure 29 Codepletion of CDT1 rescues DNA replication stress in FAF1 depleted cells. a.** Analysis of total DNA tract length. >100 forks were scored per experiment per condition. n=3. Data analyses were done as mentioned previously. **b.** and **c.**

analysis of stalled and newly fired origins, respectively. >400 forks were scored per experiment per condition. Data analyses were done as mentioned previously. **d.** Representative images for **a. e.** Western blot showing the efficiency of CDT1 and FAF1 depletion. Actin was used as a loading control. **f.** Graphical illustration showing the second label (IdU-Green) termination followed by representative image of a terminated fork. >400 forks were scored per experiment per condition and mean values were shown with s.e.m by Graphpad Prism software. n=3.

### 3.4.3.3 FAF1 depletion causes severe DNA replication stress in HEK293 cells

We next asked whether the FAF1 induced replication defect and its rescue by CDT1 co-depletion is also conserved in among other human cell lines. Therefore, we tested two additional cell lines, namely HEK293 and T24. We first focused on HEK293. We performed the same rescue experiment in HEK293 cells as in U2OS cell and analysed DNA replication by the DNA fiber assay. Interestingly, we observed pronounced overall differences, in term of replication fork velocity under basal condition between U2OS and HEK293 cells. The average tract length in control U2OS cells were ~ 20 μm, but we found much shorter ~12 μm average tract length in HEK293 cells under the same experimental condition. This finding was consistent in our all experiments, thus suggesting it is not a technical error. Furthermore, the biological aspect of these differences between U2OS and HEK293 cell lines became clear when we measured the total number of newly fired origins and stalled forks in HEK293 cells and found that they have a much higher number of dormant origin firing and stalled forks under basal condition compared to U2OS cells. These observations suggested that due to their embryonic lineage, HEK293 cells activate a much higher number of origins to complete replication, which affects the overall fork speed. Nevertheless, depletion of FAF1 by two independent siRNA sequences led to severe replication stress, which can be efficiently rescued by co-depletion of CDT1 (**Fig 30 a, b and c**). Under co-depleted condition, we could also suppress the total number of stalled forks but not dormant origin firing (**Fig 30 d, e**), suggesting that there are significant biological differences between U2OS and HEK293 cells. However, irrespective of that, FAF1 function is conserved.

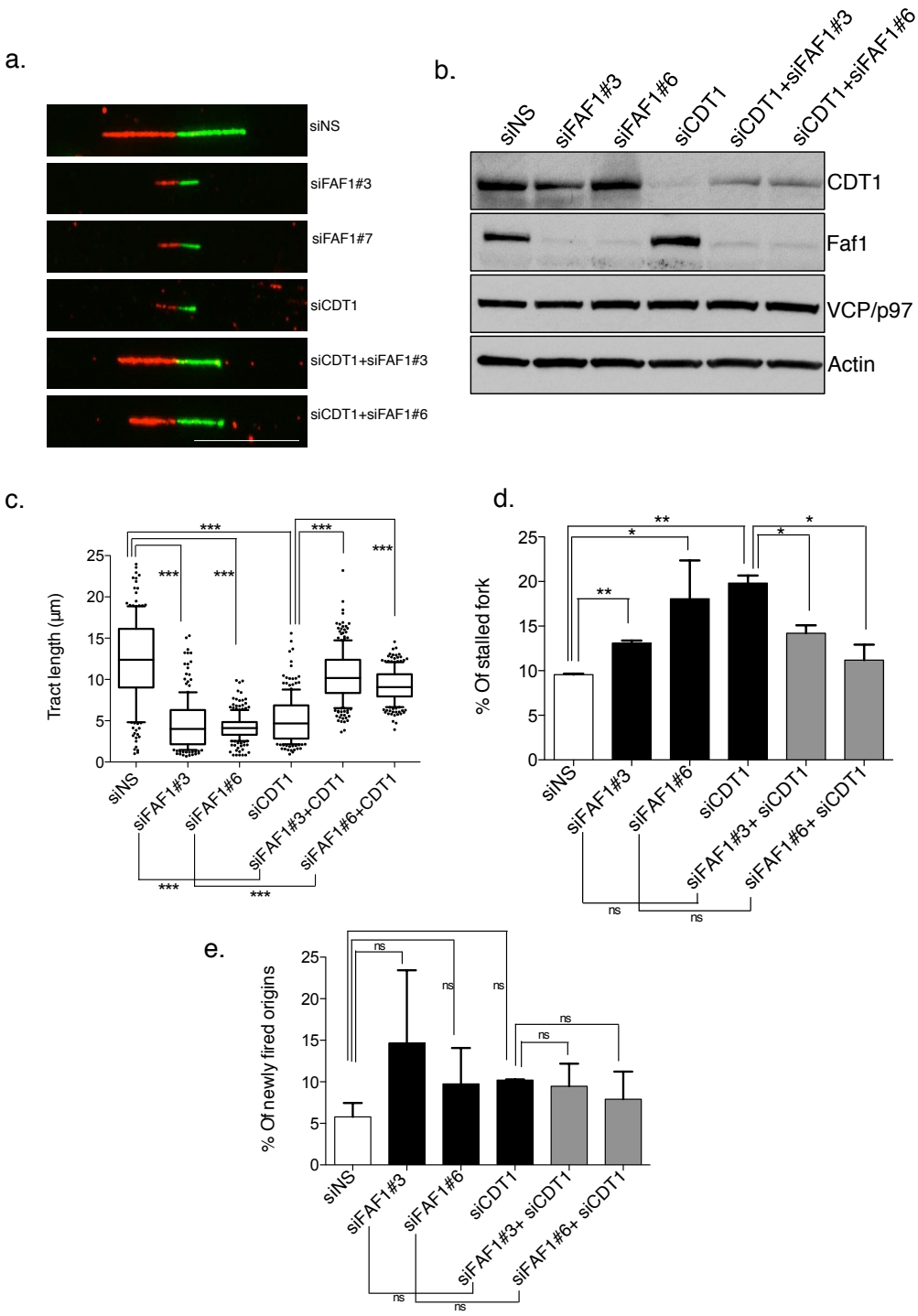



**Figure 30 FAF1 depletion causes severe DNA replication stress in HEK293 cells** **a**. and **c**. representative images and analysis of total DNA tract length. >100 forks were scored per experiment per condition. Data analyses were performed as mentioned previously. **b.** Showing CDT1 and FAF1 depletion. Expression of p97 remain stable under these conditions. Actin was used as a loading control. **d** and **e** analysis of stalled forks and newly fired origins. >400 forks were scored per

experiment per condition and mean values were shown with s.e.m by GraphpadPrism software. n=3.

### 3.4.3.4 FAF1 depletion causes severe DNA replication defect in T24 cells

It is evident from U2OS and HEK293 cells that FAF1 depletion cause severe replication stress. Therefore we asked whether it is the inherited DNA damage due to defective DNA replication in the previous cell cycle, which is affecting DNA replication, as these cells were continuously cycling during RNAi treatment. One way to answer this would be to synchronise cells at G1/S boundary by thymidine block and deplete FAF1 followed by the measurement of DNA replication by the DNA fiber assay upon their release into S phase. However it is known that thymidine block causes DNA damage and activates ATR and ATM dependent pathways in time dependent manner [233]. Therefore we chose an unbiased approach to answer this question by utilising the human urinary bladder carcinoma cell line, T24. Once confluent, due to contact inhibition, T24 cells become quiescent[234]. We seeded T24 cells in such way that they become confluent next day, once confluent we either mock treated or treated them with FAF1 siRNA. After 48 hours of siRNA treatment, we trypsinised them and seeded them at a low density and after 12 hours performed the DNA fiber assay to catch mid-S phase (time points chosen on the basis of propidium iodide (PI) profile by FACS analysis, data not shown). Indeed, FAF1 depletion led to severe replication defect similar to thoese we observed so far with U2OS and HEK293 cells (**Fig 31 a-c**), thus confirming FAF1 is an essential factor for DNA replication fork progression.

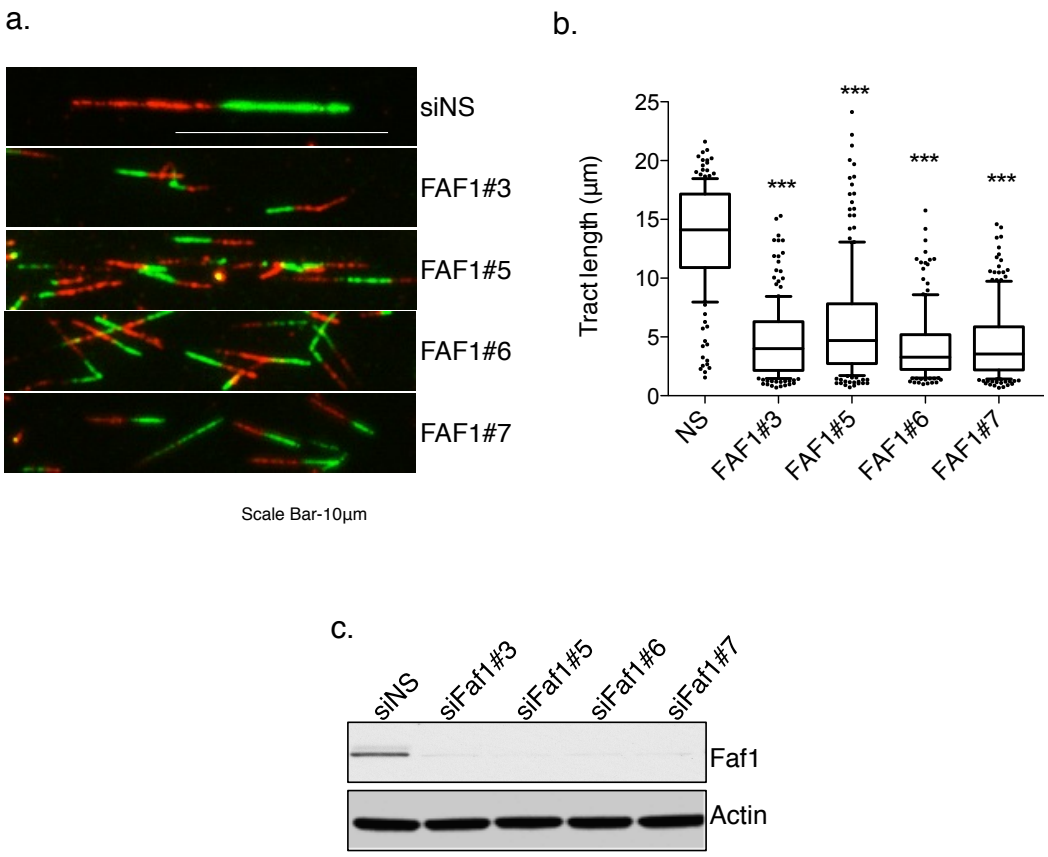



**Figure 31 FAF1 depletion causes severe replication defect in T24 cells.** Bladder cancer T24 cells were seeded in such way that they become fully confluent next day. Being contact inhibited they will be arrested when confluent. The following day siRNA treatment was carried out and after 48 hours cells were trypsinised and seeded at a low density. Nucleotide incorporation were carried out at 12 hours after low density seeding to catch mid S phase. **a.** Representative images of DNA replication forks in conditions mentioned **b.** Analysis of total DNA tract length. >100 individual forks were scored per condition per experiment. Data analyses were performed as mentioned earlier. **c.** Western blot showing the efficiency of FAF1 depletion. Actin was used as a loading control.

### 3.4.3.5 Depletion of FAF1 activates the DNA damage signalling cascade

So far, we have observed that FAF1 depletion leads to severe replication defect in three different human cell lines. Thus it become important to study whether severe DNA replication stress in FAF1 depleted human cell lines leads to activation of the ATR-CHK1 and ATM-CHK2 signalling pathway. Indeed, depletion of FAF1 by two different siRNA sequences led to robust activation of ATR-CHK1 pathway as shown by phosphorylation of ATR-Ser428 and pCHK1-Ser345 (**Fig 32 a**). Furthermore, severe DNA replication stress-induced prolonged fork stalling leads to collapsed replication forks, which results in the activation of the ATM-CHK2 signalling pathway as demonstrated by phosphorylation of ATM-Ser1981 and pCHK2-Thr68. FAF1 depleted cells also showed robust activation of phosphorylated H2AX at Ser 139. In conclusion, inactivation of FAF1 leads to severe DNA replication stress and collapsed DNA replication forks.

### 3.4.3.6 $p97^{-FAF1}$ regulates CDT1 turnover

Furthermore, to show that FAF1 physically interact with CDT1, we ectopically expressed HA-FAF1 in HEK293 cells stably expressing the p97-E587Q substrate trapping mutant. As shown in **Fig 32 b**, FAF1 co-purified together with CDT1 and p97. To further demonstrate that FAF1 is responsible for CDT1 turnover, we depleted FAF1 and then treated these cells with cyclohexamide (CHX) for the indicated times. Intriguingly, FAF1 depletion led to the hyper-accumulation of CDT1, thus again demonstrating that the $p97^{-FAF1}$ complex determines CDT1 turnover in proteasome dependent manner (**Fig 32 c**). Finally, we could rescue FAF1 depleted replication

defect by ectopic expression of siRNA resistant HA-FAF1-WT, which validated all our previous observation and ruled out any off target effect of siFAF1 (**Fig 32 d**).

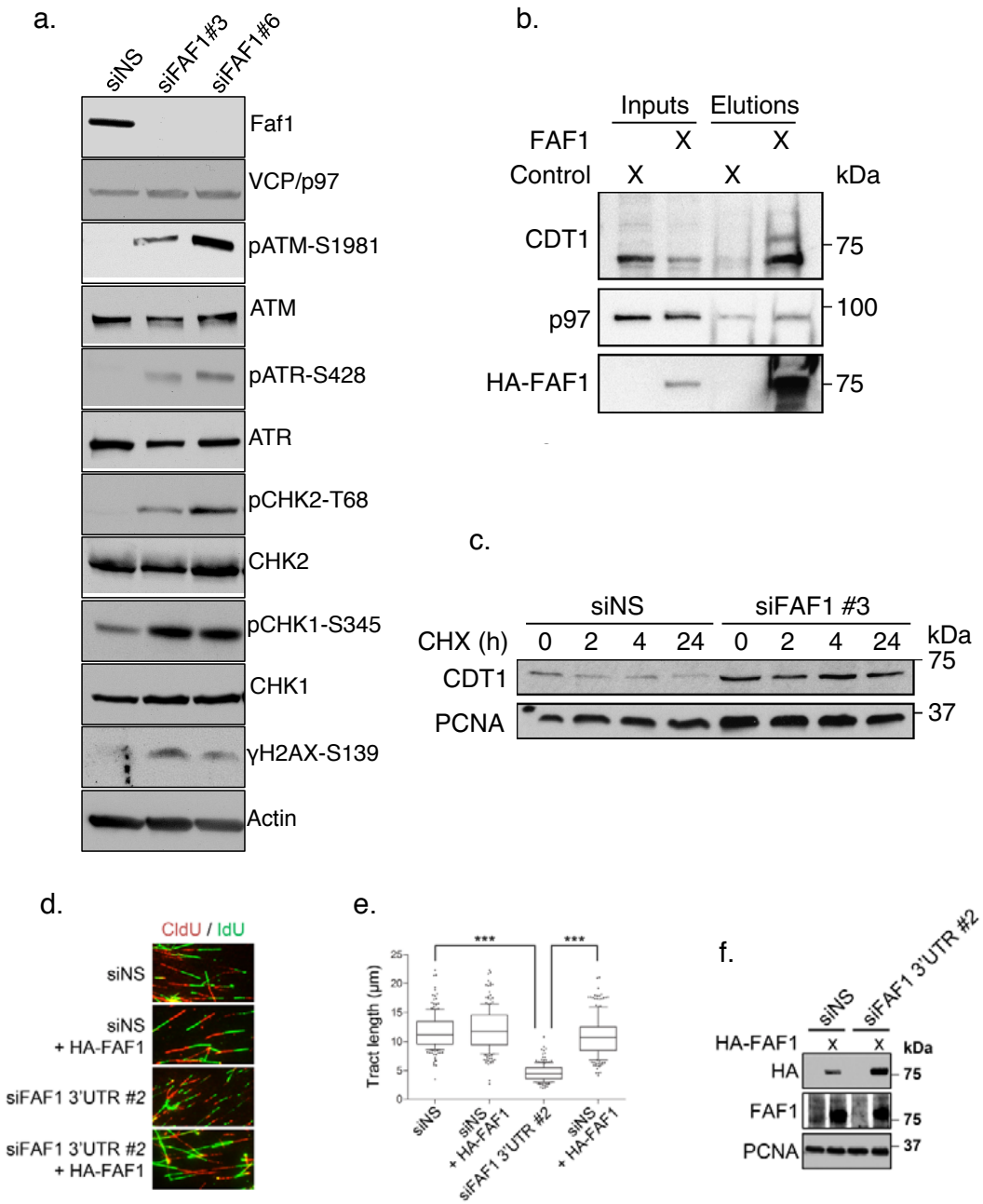



**Figure 32 Depletion of FAF1 activates the DNA damage signalling cascade.** p97-FAF1 complex regulates CDT1 turnover **a.** Western blot analysis of DNA damage signalling cascade in control and FAF1 depleted HEK293 cells under basal condition. **b.** Western blot analysis of control HA and HA-FAF1 co-IPs. The experiment was done in p97-E587Q cells, which can bind to its substrates but cannot process them due to its defective ATPase activity. **c.** HEK293 cells were either mock depleted (siNS) or depleted with siFAF1. CDT-1 and PCNA levels were monitored at indicated time points after 50 μg/ml CHX treatment by Western blot analysis. **d.** Representative images of DNA fibers in HEK293 cells after thindicated siRNA transfection in combination without/with expression of siRNA-resistant HA-FAF1. **e.** Analysis of DNA fibers. >100 forks were scored per experiment per condition. Data analyses

were performed as mentioned previously. **f.** Western blots showing the expression of HA-FAF1 and its resistance towards siRNA mediated depletion.

### 3.4.4 Discussion

In collaboration with the Hoppe laboratory, we have characterised the role of UBXN-3/FAF1 in DNA replication. FAF1 is a bonafide cofactor of p97 and has a well-characterised role in the NFκB signaling pathway. FAF1 expression was found to be downregulated in many different cancers, and was speculated to be associated with high NFκB activity and the overall aggressiveness of these cancers. To this end, we demonstrated a novel function of FAF1 by showing its direct involvement in CDT-1 degradation, and thus in DNA replication. It is well known that prolonged disturbance of the DNA replication machinery leads to DNA replication stress and consequently genomic instability[132]. DNA replication stress is one of the main causes of sporadic but also hereditary cancers. Thus the FAF1 down-regulation observed in some cancers could be directly linked with its function in DNA replication. Our data suggests that FAF1 depletion causes severe DNA replication defects in several human cell lines. Data obtained from *C. elegans* suggests that UBXN-3 (FAF1) depletion causes the chromatin retention of CDT1, CDC45 and GINS. Owing to the prior knowledge that the $p97^{-UFD\text{-}1/NPL\text{-}4}$ complex is responsible for CDT1 degradation, we asked whether FAF1 is a second tier cofactor of the p97 system required for CDT1 degradation.

Indeed, we rescued the FAF1 induced replication defect by co-depletion of the replication licensing factor CDT1. Furthermore, our data suggests that the $p97^{-FAF1}$ complex is responsible for CDT1 degradation. Additionally, owing to the report that p97 is responsible for the chromatin extraction of MCM7 upon replication termination, and due to the fact that CDT1 binding to the pre-RC leads to MCM2-7 binding to chromatin, we asked whether replication defects in FAF1 depleted cells are due to a defect in the termination of the DNA replication fork. If so, one would expect

an increased number of termination events. In contrast, our data suggests that FAF1 depleted cells have less termination events than control cells. This data alternatively argues that FAF1 is responsible for CDT-1 degradation and the regulation of origin firing and thus involved in replication initiation rather than DNA replication fork termination.

According to the literature, it is well known that the association of CDT1 with the pre-RC leads to further loading of MCM complexes[235]. Additionally, it is also known that a vast excess of MCM complexes (5-20 fold) are loaded onto the chromatin at the beginning of S-phase, which was suggested to be required for the restart of stalled forks upon replication stress[236]. If the two neighboring forks, approaching each other from opposite directions, stall, then the pre-licensed and dormant origin located between two stalled forks is activated, in order to complete DNA replication. However, it is not mechanistically clear how this excess of MCM molecules is evicted from the chromatin during unperturbed DNA replication. From our data, it is obvious that FAF1 depletion leads to hyperaccumulation of CDT1 on chromatin. This might suggest that an excess of CDT1 in FAF1 depleted cells leads to a vast chromatin retention of MCM complexes, which might negatively affect the progression of the DNA replication fork. Thus the depletion of CDT1 might reduce the number of chromatin bound MCM complexes which hinders unperturbed DNA replication fork progression. This could be a reason as to why depletion of CDT-1 in FAF1-depleted cells rescues the DNA replication fork progression. However, this hypothesis should be experimentally tested.

In summary, our experiments clearly demonstrate that FAF1 has a direct role on DNA replication fork progression and that depletion of FAF1 leads to severe DNA replication stress, which efficiently activates the DNA damage response pathways.

However, additional experiments are required to precisely demonstrate FAF1-CDT1 connection in the context of DNA replication..

# 4 General Discussion

VCP/p97 is an ubiquitin-dependent AAA ATPase, which has recently emerged as a central player in the ubiquitin proteasome system (UPS). p97 binds various and mostly ubiquitinated substrates and then converts its own ATPase activity (ATP hydrolysis) into mechanical force to remodel substrates from different cellular locations and protein macro-complexes. Thus, p97 serves as a ubiquitin-dependent unfoldase or segregase. In the majority of cases, the substrates processed by p97 are subsequently delivered to the proteasome for their final degradation, or are recycled by the help of deubiquitinating enzymes. Apart from the role of p97 in protein homeostasis, p97 is also involved in the regulation of distinct biological pathways. The diversity of p97's functions is orchestrated by a variety of p97-interacting proteins that serve as p97 cofactors (also known as adaptors). Recent evidence suggests that p97 governs diverse cellular functions with the help of 3 main, and mutually exclusive, core cofactors, namely the Ufd1-Npl4 heterodimer, p47 and UBXD1[49,50,237,238]. In addition to these three main cofactors, there are at least an additional 30 cofactors, which form different sub-complexes with p97 and its main cofactors. However, we are not yet aware of how many different p97 sub-complexes exist in the cell. p97 knockdown is lethal in both unicellular and multicellular organisms, thus indicating the essential role of p97 in cellular homeostasis[239]. Interestingly, p97 overexpression correlates with a number of human malignancies with high metastatic rate and poor survival[240,240–243]. Furthermore, potent anti-apoptotic function of p97 has been argued to be the driving force for cancer cell survival[244]. Indeed, recent work from several laboratories has demonstrates that p97-inhibitors have a potent anti-cancer effect. Although the exact mechanism of why p97-inhibitors kill cancer cells is not clear. There is a body of evidence that inhibition of p97 leads to an increased accumulation of proteins in the cell due to the inhibition

of endoplasmic reticulum-associated degradation, where p97 plays an essential role[41–45]. The pathological accumulation of proteins in the cells upon p97 inhibition leads to proteotoxic crisis. Thus, cancer cells are hypersensitive to p97 inhibition, as cancer cells are, in general, loaded with an excess of proteins due to an increased number of chromosomes in comparison to healthy cells[237]. However, given the essential nature of p97 for both healthy and cancer cell survival, it can be assumed that general p97 inhibitors will be toxic to both healthy and cancer cells. Thus, a detailed understanding of p97 sub-complexes in diverse cellular processes might reveal a specific p97 cofactor whose inhibition will lead to inactivation of a specific cellular process that is regulated by p97. In this way, we will be able to directly target the p97 sub-complex, on which, cancer cells depend upon, e.g. DNA replication only or DSB repair after radiotherapy. My DPhil work was focused on the identification of those p97 cofactors that are involved in the DNA replication. As DNA replication stress is one of the hallmarks of cancer, we believe that targeting p97 cofactors specifically involved in DNA replication might lead to cancer cell hypersensitivity, and especially in those cancers where the pool of chromatin bound proteins is heavily enriched. In this thesis I have characterised two bonafide p97 cofactors, SPRTN and FAF1, as essential components of DNA replication.

SPRTN is a newly characterised gene. Several groups have demonstrated the role of SPRTN in translesion DNA synthesis (TLS). However, the exact function of SPRTN in TLS remained controversial due to conflicting data obtained by different research groups. Our discovery of Ruijs-Aalfs or SPRTN syndrome demonstrates that monogenic and biallelic mutations in SPRTN lead to premature ageing and early onset hepatocellular carcinoma (HCC) in humans. Interestingly, SPRTN syndrome patients did not show any sensitivity to UV-light, although two brothers from family

B were born and lived in Australia (a country associated with the strong sunlight). Thus, our discovery of SPRTN syndrome suggests the essential role of SPRTN in maintaining genome stability, which is most probably not linked to TLS. Characterisation of the family A patient further supported this statement. This patient had mutations in both alleles that caused a premature stop codon and expressed a C-terminally truncated SPRTN protein (SPRTN-ΔC). SPRTN-ΔC is missing both its UBZ-domain and PIP box, two regions of SPRTN that were shown to be essential for TLS. As the family A patient was also not sensitive to UV-light, we concluded that SPRTN's role in TLS is not the main function of SPRTN that is responsible for genome stability. Most importantly, we found that a single mutation at Tyrosine 117 to Cysteine in the putative metalloprotease SprT domain of SPRTN is pathogenic. This mutation was identified in both family B patients (SPRTN-Y117C/SPRTN-ΔC). This finding strongly suggests that the metalloprotease activity is essential for protection against premature ageing and liver cancer. Our further characterisation of SPRTN-WT protein and patient variants (SPRTN-Y117C and SPRTN-ΔC) revealed that SPRTN is a DNA-dependent metalloprotease and is a constitutive component of DNA replication machinery. SPRTN physically associates with the main components of the DNA replication machinery and is physically present at DNA replication forks, as demonstrated by our iPOND experiments. Moreover, we demonstrated that SPRTN is essential for the DNA replication fork progression, and especially when the DNA replication fork is challenged with DNA damaging agents, such as FA, CPT or UV, that induce DNA-protein crosslinks. Interestingly, the DNA replication fork is able to progress with a slightly decreased in the fork velocity in SPRTN-depleted cells which ectopically express SPRTN-ΔC. However, the progression of the DNA replication fork is completely blocked in the cells that express SPRTN with a single mutation in

SprT-domain (Y117C). Altogether, these data strongly suggested that SPRTN is a metalloprotease, and that SPRTN metalloprotease activity is essential for DNA replication fork progression. Indeed, our laboratory has just demonstrated that SPRTN is a DNA-dependent metalloprotease for the removal of DNA-protein crosslinks in front of the DNA replication fork. The biochemical characterisation of SPRTN's metalloprotease activity was not a part of my DPhil work, however, I have included and also discussed several key experiments, which demonstrated SPRTN's metalloprotease activity in this thesis.

The main part of this thesis is focused on the regulation of the CHK1 signaling cascade by SPRTN. The regulation of CHK1 activity by SPRTN metalloprotease activity was a hypothesis driven project, as SPRTN syndrome patients suffer from both DNA replication stress and a G2/M-checkpoint defect. As CHK1 is one of the main regulators of DNA replication and G2/M-checkpoint, we asked whether a defect in SPRTN metalloprotease activity affects CHK1 activity and the associated signaling cascade.

Analysis of the DNA damage signalling cascade in SPRTN defective cells indeed suggested a faulty ATR-CHK1 pathway. To this end, we are able to demonstrate that SPRTN form a physical complex with CHK1, and that SPRTN depletion in several human cell lines induces severe DNA replication stress, giving rise to extremely short DNA fibers, increased numbers of stalled replication forks, newly fired origins and an increased number of 53BP1 foci formation in S phase cells. To this end, we found that DNA replication stress in SPRTN depleted cells mirrors DNA replication stress in cells treated with HU. However, HU induced replication stress leads to strong activation of the ATR-CHK1 signaling cascade, which was completely absent in SPRTN depleted cells. Moreover, when we challenged SPRTN depleted cells with

HU, we also observed a strong induction of the ATR-CHK1 signaling cascade, followed by the activation of the ATM-CHK2 signaling pathway. Thus, our results suggest that SPRTN is not essential for CHK1 activation, which is mediated by the formation of collapsed DNA replication forks (DSB-formation and the activation of ATM-CHK2 signalling cascade). However, SPRTN function become essential to activate CHK1 during normal DNA synthesis, when the DNA replication fork approaches various endogenously induced obstacles. Moreover, we demonstrated that overexpression of CHK1-WT, but not its phospho-defective mutants, is able to rescue faulty DNA replication in SPRTN depleted cells. Our results further demonstrate that the defect in CHK1 activation in SPRTN depleted cells is multifactorial: (i) due to retention of CHK1 on chromatin, and (ii) due to the inability of SPRTN depleted cells to form ssDNA when the DNA replication fork is stalled. It is well known that the formation of ssDNA is a prerequisite for the activation of the CHK1 signaling cascade. It is also known that after its activation, CHK1, as a signalling molecule, has to be released from chromatin. Also, there is strong evidence that the phosphorylation status of CHK1 is regulated by the phosphatase PP2A. To this end, we observed that treatment with FA, a strong DPC-inducing agent, caused a similar phenotypes to SPRTN depletion. This has led us to the hypothesis that SPRTN-inactivation leads to an increased formation of DPCs that consequently block DNA replication fork progression, and at the same time inhibit ssDNA formation. By biochemical isolation of DPCs, we proved this hypothesis and demonstrated that both CHK1 and PP2A-B55α indeed are covalently linked to DNA, and that the overexpression of SPRTN-WT enzymatically removes CHK1 from chromatin. We also demonstrated that SPRTN-WT, but not SPRTN-enzymatic dead variant, cleaves CHK1 *in vitro*. Finally, the restoration of Zebrafish developmental defects in SPRTN-depleted embryos after

CHK1 overexpression strongly supports our biochemical and cell biological data obtained from mammalian cell systems. In summary, we have discovered a new human syndrome that is caused by a defect in SPRTN protease activity, which consequently leads to the hyperaccumulation of DPCs. We also demonstrated that SPRTN is a core enzyme in DNA replication-coupled DNA-protein crosslink repair. One of the main crosslinks that interferes with the proper orchestration of DNA replication and G2/M-checkpoint is CHK1. To this end, our data suggests that SPRTN proteolytically removes CHK1 from chromatin. Altogether, we would like to speculate the following model explaining the complexity of the DPCs induced DNA replication stress and the relevance of SPRTN dependent non-canonical CHK1 activation in this regard to preserve genomic integrity.

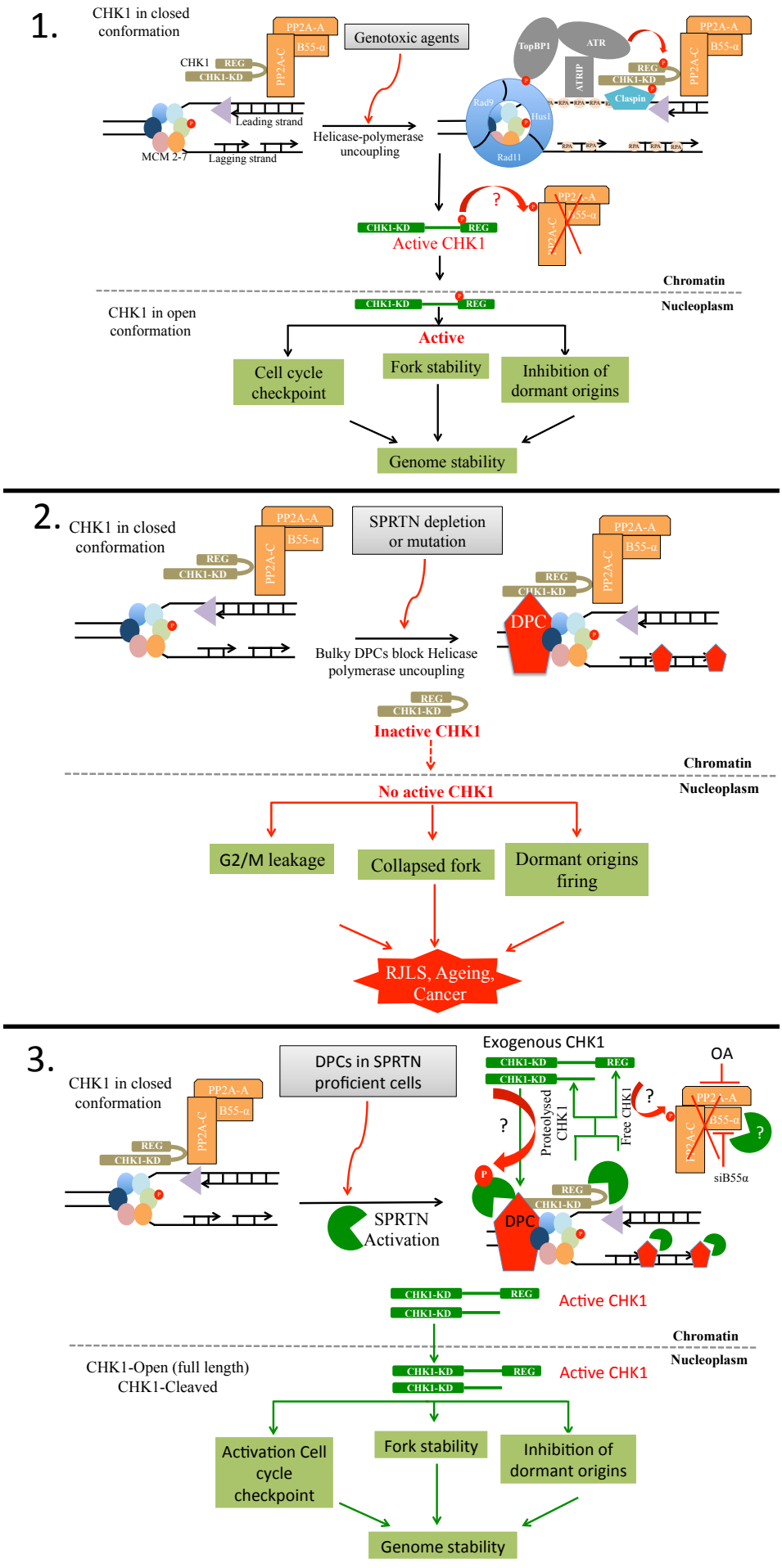

1.
CHK1 in closed conformation
PP2A-A
B55-α
PP2A-C
CHK1
REG
CHK1-KD
Genotoxic agents
Leading strand
MCM 2-7
Lagging strand
Helicase-polymerase uncoupling
TopBP1
ATR
ATRIP
Claspin
Rad9
Hus1
Rad11
RPA
?
Active CHK1
Chromatin
Nucleoplasm
CHK1 in open conformation
Active
Cell cycle checkpoint
Fork stability
Inhibition of dormant origins
Genome stability
2.
CHK1 in closed conformation
SPRTN depletion or mutation
DPC
Bulky DPCs block Helicase polymerase uncoupling
Inactive CHK1
No active CHK1
G2/M leakage
Collapsed fork
Dormant origins firing
RJLS, Ageing, Cancer
3.
CHK1 in closed conformation
DPCs in SPRTN proficient cells
SPRTN Activation
Exogenous CHK1
Proteolysed CHK1
Free CHK1
OA
siB55α
Active CHK1
CHK1-Open (full length)
CHK1-Cleaved
Activation Cell cycle checkpoint
Fork stability
Inhibition of dormant origins
Genome stability

**Figure 33 1.** General mechanism for CHK1 activation **2.** Model explaining why CHK1 cannot be fully activated in SPARTAN deficient cells **3.** Our proposed model of SPRTN dependent non-canonical CHK1 activation

According to published literature, during unperturbed DNA replication CHK1 is maintained in a closed conformation and low activity state due to negative regulation of the N-terminal kinase domain by the C-terminal regulatory domain involving an intra-molecular interaction[245201]. Recent literature also suggested that CHK1 has a C-terminal putative PPI motif which is known to interact with PP2C family of phosphatases[246]. As it is known that during unperturbed S-phase, CHK1 activity is also negatively regulated by PP2A and owing to our finding that SPRTN strongly co-immunoprecipitate with CHK1, PP2A-A (scaffold), PP2A-C (catalytic) and B55α (regulatory), we would like to speculate that complete PP2A holozyme (consist of PP2A-A, C and B55α) also keep CHK1 in a low activity state[208]. This situation changes dramatically when replication fork approaches various obstacles and as a result replication fork stalls. Due to the structural advantages of the ring shaped CMG helicases, it keeps unwinding double stranded DNA and thus creating long stretches of single stranded DNA (ssDNA), which gets immediately coated with RPA. ssDNA-RPA stimulates ATRIP and ATR recruitment to the chromatin. The ATR-ATRIP complex then phosphorylate CHK1 at S345 and stimulate its kinase activity. ATR mediated CHK1 activation also depends on two adaptor protein TopBP1 and Claspin. TopBP1 is recruited to ssDNA-RPA via PCNA like RAD9-RAD1-HUS1 (9-1-1 complex) checkpoint clamp. Claspin, on the contrary, travels with the fork and is an active component of replisome. Upon fork stalling, Claspin is phosphorylated by ATR, which binds to CHK1 and further stimulate ATR mediated CHK1 phosphorylation[121]. Phosphorylation of CHK1 by ATR at S345 induces major

conformational change at the C-terminal regulatory domain (Claspin was also suggested to be involved in this process) and therefore relieves CHK1 from a low activity closed conformation to a hyperactive open conformation[245]. This leads to the release of CHK1 from chromatin. The kinase active CHK1 might also phosphorylates and inactivates PP2A catalytic subunit. Once in the nucleoplasm, kinase active CHK1 then phosphorylates its substrates and induces downstream signaling cascades and as a result activates cell cycle checkpoint, inhibits dormant origin firing and also physically associates with the stalled replication forks. This is the general mechanism how the ATR-CHK1 pathway maintains genomic integrity **(Figure 33 Model 1)**.

Treatment of cells with low doses of formaldehyde (FA) or SPRTN deficiency leads to a pronounced replication stress as measured by the DNA fiber assay in this thesis. Biochemical analysis suggested that either FA treatment or SPRTN deficiency failed to robustly activate CHK1, which we duly confirmed due to the absence of ssDNA. This along with multiple other evidence presented in this thesis suggest that due to the formation of aberrant bulky DPCs, SPRTN deficient cells despite having functional ATR-CHK1 signaling cascade failed to activate this essential signaling pathway. As a consequence, CHK1 in SPRTN deficient cells remains in closed conformation and CHK1 activity is further attenuated by the association of the PP2A complex. Absence of kinase active CHK1 in the nucleoplasm resulted in G2/M checkpoint leakage followed by aberrant dormant origin firing and collapsed replication fork, which ultimately resulted in RJLS, ageing and cancer **(Figure 33 Model 2**).

In depth biochemical analysis also suggested that both FA treatment and SPRTN inactivation led to retention of CHK1 on chromatin. We also found that CHK1 and PP2A regulatory subunit B55α is crosslinked to DNA in SPRTN deficient cells. Further analysis also suggested that either FA exposure or SPRTN inactivation led to

massive accumulation of bulky DPCs in the DNA. *In vitro* analysis suggested SPRTN cleaves CHK1 leaving at least 3 N-terminal fragments with intact kinase domain. Additionally, we found strong evidence that both SPRTN and CHK1 promotes DNA replication fork progression in the presence of DPC inducing agents. Furthermore, either ectopic expression of CHK1-WT or treating cells with okadaic acid (OA) or siRNA mediated knockdown of the regulatory subunit of PP2Acomplex namely B55α resulted in the rescue of DNA replication defect and associated genomic instabilities in SPRTN deficient cells. Our data thus indicate a model where SPRTN is involved in the non-canonical CHK1 activation, when CHK1 cannot be activated by the ssDNA-ATR axis especially in the context of DPCs formation. The model is such that upon detection of DPCs, SPRTN is immediately activated[247]. Activated SPRTN then proteolytically removes DPCs in front of the DNA replication fork[222]. Bulky DPCs also abolish replication dependent (polymerase-helicase uncoupling) ssDNA formation (the ultimate structural requirement for the ATR-CHK1 pathway activation) due to the blocking of the CMG helicases. Therefore CHK1 continues to be maintained in a low activity state. However DPCs induced stalled replication forks are vulnerable to collapsing and DSB formation and to aid cells from this potentially lethal replication catastrophe, SPRTN proteolytically releases CHK1 from chromatin. Kinase active truncated CHK1 then stops cell cycle progression, inhibit dormant origin firing and stabilise stalled replication forks. SPRTN mediated proteolytic cleavage of CHK1 also liberate CHK1 from PP2A mediated negative regulation. Additionally, SPRTN might cleave B55α and abolish the assembly of PP2A complex, thus further promoting CHK1 activation. **(Figure 33 Model 3)**

Owing to our observations that either ectopic expression of CHK1-WT or co-depletion of B55α rescued DNA replication defect in SPRTN deficient cells and our

data in this regard suggested that this is due to the rescue of CHK1's kinase activity, we would like to speculate a CHK1 dependent SPRTN activation system involving a feed-forward loop. The reason for this hypothesis is due to the fact that DNA replication defect in SPRTN deficient cells are due to DPCs formation and except SPRTN none of the proteins which rescued DNA replication defect in SPRTN deficient cells is a protease. So these rescue events in SPRTN deficient cells must involve a protease. As we are not aware of any other proteases like SPRTN which is involved in aberrant DPC removal, we would like to speculate that the rescuing of the kinase activity of CHK1, either by CHK1-WT or by OA or by co-depletion of B55α ultimately resulted in a CHK1 dependent phosphorylation and activation of the remaining SPRTN molecules (siRNA mediated SPRTN depletion is never 100% and we anticipate 10-20% of the functional SPRTN protein in siSPRTN cells) in siSPRTN cells, which as a result rescued DPCs, DNA replication defect and ultimately genomic instability.

In order to understand this mechanism, we plan to identify any CHK1 dependent phosphorylation events on SPRTN. To further prove the biological significance of these unique phosphorylation events on SPRTN by CHK1, we will mutate these residues and study its relevance *in vivo*.

**The role of FAF1 in DNA replication**

Identification and characterisation of another bonafide p97 cofactor, FAF1, in DNA replication highlights the complexity of the p97 system in DNA replication. Although the role of FAF1 has been well characterised in the apoptotic pathway, here we identified an important function of FAF1 in CDT1 turnover. Our data suggests a general model where the p97-$^{Npl4\text{-}Ufd1\text{-}FAF1}$ complex binds to ubiquitinated CDT1 after replication initiation and is responsible for CDT1 degradation. We have also

demonstrated that FAF1 depletion causes severe DNA replication stress and co-depletion of CDT1 rescues this phenotype. Mechanistically, it is not yet clear how CDT1 co-depletion rescues DNA replication defect in FAF1 depleted cells. However, increased chromatin retention of CDT1 in FAF1-depleted cells could result in increased loading of MCM complexes onto chromatin, which might consequently cause an increase in dormant origin firing and indirectly affect replication fork velocity. In contrary to SPRTN-depleted cells, FAF1-depleted cells have a functionally intact CHK1 signaling cascade.

Despite similar DNA replication stress signatures in FAF1- and SPRTN-depleted cells, these two p97 cofactors have markedly different molecular mechanisms by which they orchestrate DNA replication. Whilst SPRTN proteolytically cleaves substrates, which are covalently attached to DNA (DPCs) and thus allows unperturbed DNA replication fork progression when it meets protein "roadblocks", FAF1, in contrast, binds ubiquitinated substrates such as CDT-1 and with the help of p97's ATPase activity, delivers them to the proteasome for their final degradation. Our data so far suggests that there are two different modes of p97-dependent proteolysis at sites of DNA replication: (i) SPRTN dependent proteolysis, and (ii) proteasome dependent proteolysis. Collectively, our study of two p97 cofactors in DNA replication, with two disti molecular mechanisms, provides valuable insights into the p97 system in the maintenance of genomic integrity. Thus, we conclude that p97 has a strategic role in different aspects of DNA replication, which are essential for genome stability.

Factors involved in DNA replication, especially those with enzymatic activities, are potential druggable targets for cancer therapy. The best example is the recently approved PARP inhibitor Olaparib (Lynparza). Thus, my thesis emphasises a great

potential of the p97 system and its cofactors as druggable targets for cancer therapy, but also potential biomarkers for early diagnosis. For example, biallelic and monogenic mutations in SPRTN could be used as a marker for early-onset hepatocellular carcinoma.

# 5 References


1. Simpson, M. V. The release of labeled amino acids from the proteins of rat liver slices. *J Biol Chem* **201,** 143–154 (1953).
2. Varshavsky, A. The early history of the ubiquitin field. *Protein Sci.* **15,** 647–54 (2006).
3. Baumeister, W. *et al.* Varshavsky's contributions. *Science (New York, N.Y.)* **306,** 1290–1292 (2004).
4. Deshaies, R. J. Proteotoxic crisis, the ubiquitin-proteasome system, and cancer therapy. *BMC Biol.* **12,** 94 (2014).
5. Pickart, C. M. & Eddins, M. J. Ubiquitin: structures, functions, mechanisms. *Biochim. Biophys. Acta* **1695,** 55–72 (2004).
6. Komander, D. & Rape, M. The Ubiquitin Code. *Annu. Rev. Biochem.* **81,** 203–229 (2012).
7. Bassermann, F., Eichner, R. & Pagano, M. The ubiquitin proteasome system - implications for cell cycle control and the targeted treatment of cancer. *Biochim. Biophys. Acta* **1843,** 150–62 (2014).
8. Sadowski, M. & Sarcevic, B. Mechanisms of mono- and poly-ubiquitination: Ubiquitination specificity depends on compatibility between the E2 catalytic core and amino acid residues proximal to the lysine. *Cell Div.* **5,** 19 (2010).
9. Meyer, H.-J. & Rape, M. Enhanced protein degradation by branched ubiquitin chains. *Cell* **157,** 910–921 (2014).
10. Lu, Y., Wang, W. & Kirschner, M. W. Specificity of the anaphase-promoting complex: a single-molecule study. *Science* **348,** 1248737 (2015).
11. MacGurn, J. A., Hsu, P.-C. & Emr, S. D. Ubiquitin and membrane protein

turnover: from cradle to grave. *Annu. Rev. Biochem.* **81,** 231–259 (2012).

12. Deshaies, R. J. & Joazeiro, C. A. P. RING domain E3 ubiquitin ligases. *Annu. Rev. Biochem.* **78,** 399–434 (2009).
13. Ye, Y. & Rape, M. Building ubiquitin chains: E2 enzymes at work. *Nat. Rev. Mol. Cell Biol.* **10,** 755–764 (2009).
14. Rotin, D. & Kumar, S. Physiological functions of the HECT family of ubiquitin ligases. *Nat Rev Mol Cell Biol* **10,** 398–409 (2009).
15. Deshaies, R. J. & Joazeiro, C. A. RING domain E3 ubiquitin ligases. *Annu Rev Biochem* **78,** 399–434 (2009).
16. Dikic, I., Wakatsuki, S. & Walters, K. J. Ubiquitin-binding domains - from structures to functions. *Nat. Rev. Mol. Cell Biol.* **10,** 659–671 (2009).
17. Clague, M. J. *et al.* Cellular functions of the DUBs. *J. Cell Sci.* **125,** 277–86 (2012).
18. Turcu Francisca E. Reyes, Ventii Karen H., W. K. D. NIH Public Access. *Annu Rev Biochem* 363–397 (2010). doi:10.1146/annurev.biochem.78.082307.091526.Regulation
19. Livneh, I., Cohen-kaplan, V., Cohen-rosenzweig, C., Avni, N. & Ciechanover, A. The life cycle of the 26S proteasome : from birth , through regulation and function , and onto its death. *Cell Res.* **In Press,** 869–885 (2016).
20. Gallastegui, N. & Groll, M. The 26S proteasome: assembly and function of a destructive machine. *Trends Biochem. Sci.* **35,** 634–642 (2010).
21. Lee, M. J., Lee, B.-H., Hanna, J., King, R. W. & Finley, D. Trimming of ubiquitin chains by proteasome-associated deubiquitinating enzymes. *Mol. Cell. Proteomics* **10,** R110.003871 (2011).
22. Marshall, R. S., Li, F., Gemperline, D. C., Book, A. J. & Vierstra, R. D.

Autophagic Degradation of the 26S Proteasome Is Mediated by the Dual ATG8/Ubiquitin Receptor RPN10 in Arabidopsis. *Mol. Cell* **58,** 1053–1066 (2015).

23. Waite, K. A., De-La Mota-Peynado, A., Vontz, G. & Roelofs, J. Starvation Induces Proteasome Autophagy with Different Pathways for Core and Regulatory Particles. *J. Biol. Chem.* **291,** 3239–3253 (2016).
24. Kevei, E. & Hoppe, T. Ubiquitin sets the timer: impacts on aging and longevity. *Nat. Struct. Mol. Biol.* **21,** 290–292 (2014).
25. Vilchez, D., Saez, I. & Dillin, A. The role of protein clearance mechanisms in organismal ageing and age-related diseases. *Nat. Commun.* **5,** 5659 (2014).
26. Hoeller, D. & Dikic, I. Targeting the ubiquitin system in cancer therapy. *Nature* **458,** 438–44 (2009).
27. Weathington, N. M. & Mallampalli, R. K. Emerging therapies targeting the ubiquitin proteasome system in cancer. *J. Clin. Invest.* **124,** 6–12 (2014).
28. Ramadan, K. & Meerang, M. Degradation-linked ubiquitin signal and proteasome are integral components of DNA double strand break repair: New perspectives for anti-cancer therapy. *FEBS Lett.* **585,** 2868–2875 (2011).
29. Vassilev, L. T. MDM2 inhibitors for cancer therapy. *Trends Mol. Med.* **13,** 23–31 (2007).
30. Millard, M., Pathania, D., Grande, F., Xu, S. & Neamati, N. Small-molecule inhibitors of p53-MDM2 interaction: the 2006-2010 update. *Curr. Pharm. Des.* **17,** 536–559 (2011).
31. Feng, F. Y. *et al.* MDM2 Inhibition Sensitizes Prostate Cancer Cells to Androgen Ablation and Radiotherapy in a p53-Dependent Manner. *Neoplasia* **18,** 213–222 (2016).

32. Issaeva, N. *et al.* Small molecule RITA binds to p53, blocks p53-HDM-2 interaction and activates p53 function in tumors. *Nat. Med.* **10,** 1321–1328 (2004).

33. Bernal, F. *et al.* NIH Public Access. **18,** 411–422 (2011).

34. Nag, S., Qin, J., Srivenugopal, K. S., Wang, M. & Zhang, R. The MDM2-p53 pathway revisited. *J. Biomed. Res.* **27,** 254–71 (2013).

35. Li, Q. & Lozano, G. Molecular pathways: Targeting Mdm2 and Mdm4 in cancer therapy. *Clin. Cancer Res.* **19,** 34–41 (2013).

36. Srinivasula, S. M. & Ashwell, J. D. IAPs: what's in a name? *Mol. Cell* **30,** 123–135 (2008).

37. Vaux, D. L. & Silke, J. IAPs, RINGs and ubiquitylation. *Nat. Rev. Mol. Cell Biol.* **6,** 287–297 (2005).

38. Liang, Q. *et al.* A selective USP1-UAF1 inhibitor links deubiquitination to DNA damage responses. *Nat. Chem. Biol.* **10,** 298–304 (2014).

39. Lecona, E. *et al.* USP7 is a SUMO deubiquitinase essential for DNA replication. *Nat. Struct. Mol. Biol.* **23,** 270–7 (2016).

40. Zhang, D., Zaugg, K., Mak, T. W. & Elledge, S. J. A role for the deubiquitinating enzyme USP28 in control of the DNA-damage response. *Cell* **126,** 529–542 (2006).

41. Alverez, C. *et al.* Allosteric Indole Amide Inhibitors of p97: Identification of a Novel Probe of the Ubiquitin Pathway. *ACS Med. Chem. Lett.* **7,** 182–187 (2016).

42. Zhou, H.-J. *et al.* Discovery of a First-in-Class, Potent, Selective, and Orally Bioavailable Inhibitor of the p97 AAA ATPase (CB-5083). *J. Med. Chem.* **58,** 9480–9497 (2015).

43. Anderson, D. J. *et al.* Targeting the AAA ATPase p97 as an Approach to Treat Cancer through Disruption of Protein Homeostasis. *Cancer Cell* **28,** 653–665 (2015).

44. Chou, T.-F. & Deshaies, R. J. Development of p97 AAA ATPase inhibitors. *Autophagy* **7,** 1091–1092 (2011).

45. Chapman, E., Maksim, N., de la Cruz, F. & La Clair, J. J. Inhibitors of the AAA+ chaperone p97. *Molecules* **20,** 3027–3049 (2015).

46. Nie, M. & Boddy, M. N. Cooperativity of the SUMO and Ubiquitin Pathways in Genome Stability. *Biomolecules* **6,** 14 (2016).

47. Song, C., Wang, Q. & Li, C. C. H. ATPase activity of p97-valosin-containing protein (VCP): D2 mediates the major enzyme activity, and D1 contributes to the heat-induced activity. *J. Biol. Chem.* **278,** 3648–3655 (2003).

48. Vaz, B., Halder, S. & Ramadan, K. Role of p97/VCP (Cdc48) in genome stability. *Front. Genet.* **4,** 60 (2013).

49. Ramadan, K., Halder, S., Wiseman, K. & Vaz, B. Strategic role of the ubiquitin-dependent segregase p97 (VCP or Cdc48) in DNA replication. *Chromosoma* 1–16 (2016). doi:10.1007/s00412-016-0587-4

50. Meyer, H., Bug, M. & Bremer, S. Emerging functions of the VCP/p97 AAA-ATPase in the ubiquitin system. *Nat. Cell Biol.* **14,** 117–23 (2012).

51. Yamanaka, K., Sasagawa, Y. & Ogura, T. Recent advances in p97/VCP/Cdc48 cellular functions. *Biochimica et Biophysica Acta - Molecular Cell Research* **1823,** 130–137 (2012).

52. Alexandru, G. *et al.* UBXD7 binds multiple ubiquitin ligases and implicates p97 in HIF1alpha turnover. *Cell* **134,** 804–816 (2008).

53. Verma, R., Oania, R., Fang, R., Smith, G. T. & Deshaies, R. J. Cdc48/p97

mediates UV-dependent turnover of RNA Pol II. *Mol. Cell* **41,** 82–92 (2011).

54. Davis, E. J. *et al.* DVC1 (C1orf124) recruits the p97 protein segregase to sites of DNA damage. *Nat. Struct. Mol. Biol.* **19,** 1093–1100 (2012).

55. Mosbech, A. *et al.* DVC1 (C1orf124) is a DNA damage-targeting p97 adaptor that promotes ubiquitin-dependent responses to replication blocks. *Nat. Struct. Mol. Biol.* **19,** 1084–1092 (2012).

56. Kim, M. S. *et al.* Regulation of error-prone translesion synthesis by Spartan/C1orf124. *Nucleic Acids Res.* **41,** 1661–1668 (2013).

57. Ghosal, G., Leung, J. W. C., Nair, B. C., Fong, K. W. & Chen, J. Proliferating Cell Nuclear Antigen (PCNA)-binding protein C1orf124 is a regulator of translesion synthesis. *J. Biol. Chem.* **287,** 34225–34233 (2012).

58. Tresse, E. *et al.* VCP/p97 is essential for maturation of ubiquitin-containing autophagosomes and this function is impaired by mutations that cause IBMPFD. *Autophagy* **6,** 217–227 (2010).

59. Ramanathan, H. N. & Ye, Y. The p97 ATPase associates with EEA1 to regulate the size of early endosomes. *Cell Res.* **22,** 346–359 (2012).

60. Malumbres, M. & Barbacid, M. Cell cycle, CDKs and cancer: a changing paradigm. *Nat. Rev. Cancer* **9,** 153–166 (2009).

61. Satyanarayana, A. & Kaldis, P. Mammalian cell-cycle regulation: several Cdks, numerous cyclins and diverse compensatory mechanisms. *Oncogene* **28,** 2925–2939 (2009).

62. Schafer, K. A. The cell cycle: a review. *Vet. Pathol.* **35,** 461–478 (1998).

63. Fu, X., Ng, C., Feng, D. & Liang, C. Cdc48p is required for the cell cycle commitment point at Start via degradation of the G1-CDK inhibitor Far1p. *J. Cell Biol.* **163,** 21–26 (2003).

64. Mouysset, J. *et al.* Cell cycle progression requires the CDC-48UFD-1/NPL-4 complex for efficient DNA replication. *Proc. Natl. Acad. Sci. U. S. A.* **105,** 12879–12884 (2008).

65. Ramadan, K. *et al.* Cdc48/p97 promotes reformation of the nucleus by extracting the kinase Aurora B from chromatin. *Nature* **450,** 1258–1262 (2007).

66. Dobrynin, G. *et al.* Cdc48/p97-Ufd1-Npl4 antagonizes Aurora B during chromosome segregation in HeLa cells. *J. Cell Sci.* **124,** 1571–1580 (2011).

67. Remus, D. *et al.* Concerted loading of Mcm2-7 double hexamers around DNA during DNA replication origin licensing. *Cell* **139,** 719–730 (2009).

68. Gambus, A. *et al.* GINS maintains association of Cdc45 with MCM in replisome progression complexes at eukaryotic DNA replication forks. *Nat. Cell Biol.* **8,** 358–366 (2006).

69. Hu, J., McCall, C. M., Ohta, T. & Xiong, Y. Targeted ubiquitination of CDT1 by the DDB1-CUL4A-ROC1 ligase in response to DNA damage. *Nat. Cell Biol.* **6,** 1003–1009 (2004).

70. Kondo, T. *et al.* Rapid degradation of Cdt1 upon UV-induced DNA damage is mediated by SCFSkp2 complex. *J. Biol. Chem.* **279,** 27315–27319 (2004).

71. Nishitani, H. *et al.* Two E3 ubiquitin ligases, SCF-Skp2 and DDB1-Cul4, target human Cdt1 for proteolysis. *EMBO J.* **25,** 1126–1136 (2006).

72. Zhong, W., Feng, H., Santiago, F. E. & Kipreos, E. T. CUL-4 ubiquitin ligase maintains genome stability by restraining DNA-replication licensing. *Nature* **423,** 885–889 (2003).

73. Raman, M., Havens, C. G., Walter, J. C. & Harper, J. W. A Genome-wide Screen Identifies p97 as an Essential Regulator of DNA Damage-Dependent

CDT1 Destruction. *Mol. Cell* **44,** 72–84 (2011).

74. Franz, A. *et al.* CDC-48/p97 Coordinates CDT-1 Degradation with GINS Chromatin Dissociation to Ensure Faithful DNA Replication. *Mol. Cell* **44,** 85–96 (2011).

75. Moyer, S. E., Lewis, P. W. & Botchan, M. R. Isolation of the Cdc45/Mcm2-7/GINS (CMG) complex, a candidate for the eukaryotic DNA replication fork helicase. *Proc. Natl. Acad. Sci. U. S. A.* **103,** 10236–10241 (2006).

76. Waga, S. & Stillman, B. The DNA replication fork in eukaryotic cells. *Annu. Rev. Biochem.* **67,** 721–751 (1998).

77. Kanke, M., Kodama, Y., Takahashi, T. S., Nakagawa, T. & Masukata, H. Mcm10 plays an essential role in origin DNA unwinding after loading of the CMG components. *EMBO J.* **3168,** 2182–2194 (2012).

78. Pursell, Z. F., Isoz, I., Lundström, E.-B., Johansson, E. & Kunkel, T. A. Yeast DNA polymerase epsilon participates in leading-strand DNA replication. *Science (80-. ).* **317,** 127–30 (2007).

79. Aze, A., Zhou, J. C., Costa, A. & Costanzo, V. DNA replication and homologous recombination factors: Acting together to maintain genome stability. *Chromosoma* **122,** 401–413 (2013).

80. Moreno, S. P. & Gambus, A. Regulation of Unperturbed DNA Replication by Ubiquitylation. *Genes (Basel).* **6,** 451–468 (2015).

81. Maric, M., Maculins, T., De Piccoli, G. & Labib, K. Cdc48 and a ubiquitin ligase drive disassembly of the CMG helicase at the end of DNA replication. *Science* **346,** 1253596 (2014).

82. Moreno, S. P., Bailey, R., Campion, N., Herron, S. & Gambus, A. Polyubiquitylation drives replisome disassembly at the termination of DNA

replication. *Science* **346,** 477–481 (2014).

83. Sasagawa, Y., Higashitani, A., Urano, T., Ogura, T. & Yamanaka, K. CDC-48/p97 is required for proper meiotic chromosome segregation via controlling AIR-2/Aurora B kinase localization in Caenorhabditis elegans. *J. Struct. Biol.* **179,** 104–111 (2012).

84. Cheng, Y.-L. & Chen, R.-H. The AAA-ATPase Cdc48 and cofactor Shp1 promote chromosome bi-orientation by balancing Aurora B activity. *J. Cell Sci.* **123,** 2025–2034 (2010).

85. Cao, K. & Zheng, Y. The Cdc48/p97-Ufd1-Npl4 complex: its potential role in coordinating cellular morphogenesis during the M-G1 transition. *Cell Cycle* **3,** 422–424 (2004).

86. Cao, K., Nakajima, R., Meyer, H. H. & Zheng, Y. The AAA-ATPase Cdc48/p97 regulates spindle disassembly at the end of mitosis. *Cell* **115,** 355–367 (2003).

87. Hoeijmakers, J. H. J. DNA damage, aging, and cancer. *N. Engl. J. Med.* **361,** 1475–85 (2009).

88. Ciccia, A. & Elledge, S. J. The DNA Damage Response: Making It Safe to Play with Knives. *Mol. Cell* **40,** 179–204 (2010).

89. Bonner, W. M. *et al.* GammaH2AX and cancer. *Nat. Rev. Cancer* **8,** 957–67 (2008).

90. Antoccia, A., Kobayashi, J., Tauchi, H., Matsuura, S. & Komatsu, K. Nijmegen breakage syndrome and functions of the responsible protein, NBS1. *Genome Dyn.* **1,** 191–205 (2006).

91. Goldberg, M. *et al.* MDC1 is required for the intra-S-phase DNA damage checkpoint. *Nature* **421,** 952–956 (2003).

92. Lukas, C. *et al.* Mdc1 couples DNA double-strand break recognition by Nbs1 with its H2AX-dependent chromatin retention. *EMBO J.* **23,** 2674–2683 (2004).

93. Fernandez-Capetillo, O., Lee, A., Nussenzweig, M. & Nussenzweig, A. H2AX: the histone guardian of the genome. *DNA Repair (Amst).* **3,** 959–967 (2004).

94. Lukas, J., Lukas, C. & Bartek, J. More than just a focus: The chromatin response to DNA damage and its role in genome integrity maintenance. *Nat. Cell Biol.* **13,** 1161–9 (2011).

95. Neal, J. A. & Meek, K. Choosing the right path: Does DNA-PK help make the decision? *Mutation Research - Fundamental and Molecular Mechanisms of Mutagenesis* **711,** 73–86 (2011).

96. Shibata, A. & Jeggo, P. A. DNA double-strand break repair in a cellular context. *Clin. Oncol. (R. Coll. Radiol).* **26,** 243–249 (2014).

97. Orthwein, A. *et al.* A mechanism for the suppression of homologous recombination in G1 cells. *Nature* **528,** 422–426 (2015).

98. Zimmermann, M. & de Lange, T. 53BP1: pro choice in DNA repair. *Trends Cell Biol.* **24,** 108–117 (2014).

99. Chapman, J. R. *et al.* RIF1 is essential for 53BP1-dependent nonhomologous end joining and suppression of DNA double-strand break resection. *Mol. Cell* **49,** 858–871 (2013).

100. Di Virgilio, M. *et al.* Rif1 prevents resection of DNA breaks and promotes immunoglobulin class switching. *Science* **339,** 711–715 (2013).

101. Bunting, S. F. *et al.* 53BP1 inhibits homologous recombination in Brca1-deficient cells by blocking resection of DNA breaks. *Cell* **141,** 243–254 (2010).

102. Ochs, F. *et al.* 53BP1 fosters fidelity of homology-directed DNA repair. *Nat.*

*Struct. Mol. Biol.* **23,** 714–721 (2016).

103. Aparicio, T. & Gautier, J. BRCA1-CtIP interaction in the repair of DNA double-strand breaks. *Mol. Cell. Oncol.* **3,** e1169343 (2016).

104. Sartori, A. A. *et al.* Human CtIP promotes DNA end resection. *Nature* **450,** 509–514 (2007).

105. Broderick, R. *et al.* EXD2 promotes homologous recombination by facilitating DNA end resection. *Nat. Cell Biol.* **18,** 271–280 (2016).

106. Li, X. & Heyer, W. D. Homologous recombination in DNA repair and DNA damage tolerance. *Cell Res.* **18,** 99–113 (2008).

107. Meerang, M. *et al.* The ubiquitin-selective segregase VCP/p97 orchestrates the response to DNA double-strand breaks. *Nat. Cell Biol.* **13,** 1376–1382 (2011).

108. Acs, K. *et al.* The AAA-ATPase VCP/p97 promotes 53BP1 recruitment by removing L3MBTL1 from DNA double-strand breaks. *Nat. Struct. Mol. Biol.* **18,** 1345–1350 (2011).

109. Mallette, F. A. *et al.* RNF8- and RNF168-dependent degradation of KDM4A/JMJD2A triggers 53BP1 recruitment to DNA damage sites. *EMBO J.* **31,** 1865–1878 (2012).

110. Jossen, R. & Bermejo, R. The DNA damage checkpoint response to replication stress: A Game of Forks. *Front. Genet.* **4,** 26 (2013).

111. Byun, T. S., Pacek, M., Yee, M., Walter, J. C. & Cimprich, K. A. Functional uncoupling of MCM helicase and DNA polymerase activities activates the ATR-dependent checkpoint. *Genes Dev.* **19,** 1040–1052 (2005).

112. Zellweger, R. *et al.* Rad51-mediated replication fork reversal is a global response to genotoxic treatments in human cells. *J. Cell Biol.* **208,** 563–579 (2015).

113. Brewster, A. S. *et al.* Crystal structure of a near-full-length archaeal MCM: Functional insights for an AAA+ hexameric helicase. *Proc. Natl. Acad. Sci.* **105,** 20191–20196 (2008).

114. Pape, T. *et al.* Hexameric ring structure of the full-length archaeal MCM protein complex. *EMBO Rep.* **4,** 1079–1083 (2003).

115. Bruck, I. & Kaplan, D. L. Cdc45 protein-single-stranded DNA interaction is important for stalling the helicase during replication stress. *J. Biol. Chem.* **288,** 7550–7563 (2013).

116. Smith, J., Mun Tho, L., Xu, N. & A. Gillespie, D. The ATM-Chk2 and ATR-Chk1 pathways in DNA damage signaling and cancer. *Adv. Cancer Res.* **108,** 73–112 (2010).

117. Sokka, M., Parkkinen, S., Pospiech, H. & Syvaoja, J. E. Function of TopBP1 in genome stability. *Subcell. Biochem.* **50,** 119–141 (2010).

118. Wong, V. C.-L., Cash, H. L., Morse, J. L., Lu, S. & Zhitkovich, A. S-phase sensing of DNA-protein crosslinks triggers TopBP1-independent ATR activation and p53-mediated cell death by formaldehyde. *Cell Cycle* **11,** 2526–2537 (2012).

119. Kumagai, A. & Dunphy, W. G. Claspin, a novel protein required for the activation of Chk1 during a DNA replication checkpoint response in Xenopus egg extracts. *Mol. Cell* **6,** 839–849 (2000).

120. Chini, C. C. S. & Chen, J. Human claspin is required for replication checkpoint control. *J. Biol. Chem.* **278,** 30057–30062 (2003).

121. Sorensen, C. S., Syljuasen, R. G., Lukas, J. & Bartek, J. ATR, Claspin and the Rad9-Rad1-Hus1 complex regulate Chk1 and Cdc25A in the absence of DNA damage. *Cell Cycle* **3,** 941–945 (2004).

122. Chou, D. M. & Elledge, S. J. Tipin and Timeless form a mutually protective complex required for genotoxic stress resistance and checkpoint function. *Proc. Natl. Acad. Sci. U. S. A.* **103,** 18143–18147 (2006).

123. Yoshizawa-Sugata, N. & Masai, H. Human Tim/Timeless-interacting protein, Tipin, is required for efficient progression of S phase and DNA replication checkpoint. *J. Biol. Chem.* **282,** 2729–2740 (2007).

124. Min, W. *et al.* Poly(ADP-ribose) binding to Chk1 at stalled replication forks is required for S-phase checkpoint activation. *Nat. Commun.* **4,** 2993 (2013).

125. Smits, V. A. J., Reaper, P. M. & Jackson, S. P. Rapid PIKK-dependent release of Chk1 from chromatin promotes the DNA-damage checkpoint response. *Curr. Biol.* **16,** 150–159 (2006).

126. Donzelli, M. & Draetta, G. F. Regulating mammalian checkpoints through Cdc25 inactivation. *EMBO Rep.* **4,** 671–7 (2003).

127. Riemer, A. *et al.* The p97-Ufd1-Npl4 ATPase complex ensures robustness of the G2/M checkpoint by facilitating CDC25A degradation. *Cell Cycle* **13,** 919–927 (2014).

128. Bartek, J. & Lukas, J. Chk1 and Chk2 kinases in checkpoint control and cancer. 421–429 (2003).

129. Falck, J., Mailand, N., Syljuåsen, R. G., Bartek, J. & Lukas, J. The ATM-Chk2-Cdc25A checkpoint pathway guards against radioresistant DNA synthesis. *Nature* **410,** 842–847 (2001).

130. Blow, J. J., Ge, X. Q., Jackson, D. A. & Dd, D. Europe PMC Funders Group How dormant origins promote complete genome replication. **36,** 405–414 (2012).

131. Mcintosh, D. *et al.* and the Response to Replicative Stresses. 1–10 (2012).

132. Gaillard, H., Garcia-Muse, T. & Aguilera, A. Replication stress and cancer. *Nat Rev Cancer* **15,** 276–289 (2015).

133. Hills, S. A. & Diffley, J. F. X. DNA replication and oncogene-induced replicative stress. *Curr. Biol.* **24,** R435-44 (2014).

134. Macheret, M. & Halazonetis, T. D. DNA replication stress as a hallmark of cancer. *Annu. Rev. Pathol.* **10,** 425–48 (2015).

135. Lopes, M. *et al.* The DNA replication checkpoint response stabilizes stalled replication forks. *Nature* **412,** 557–561 (2001).

136. Cobb, J. A., Bjergbaek, L., Shimada, K., Frei, C. & Gasser, S. M. DNA polymerase stabilization at stalled replication forks requires Mec1 and the RecQ helicase Sgs1. *EMBO J.* **22,** 4325–4336 (2003).

137. Meister, P. *et al.* Temporal separation of replication and recombination requires the intra-S checkpoint. *J. Cell Biol.* **168,** 537–544 (2005).

138. Kai, M., Boddy, M. N., Russell, P. & Wang, T. S.-F. Replication checkpoint kinase Cds1 regulates Mus81 to preserve genome integrity during replication stress. *Genes Dev.* **19,** 919–932 (2005).

139. Kaur, S. *et al.* Chk1-dependent constitutive phosphorylation of BLM helicase at serine 646 decreases after DNA damage. *Mol. Cancer Res.* **8,** 1234–1247 (2010).

140. Pirzio, L. M., Pichierri, P., Bignami, M. & Franchitto, A. Werner syndrome helicase activity is essential in maintaining fragile site stability. *J. Cell Biol.* **180,** 305–314 (2008).

141. Hashimoto, Y., Chaudhuri, A. R., Lopes, M. & Costanzo, V. Rad51 protects nascent DNA from Mre11-dependent degradation and promotes continuous DNA synthesis. *Nat. Struct. Mol. Biol.* **17,** 1305–1311 (2010).

142. Schlacher, K. *et al.* Double-strand break repair-independent role for BRCA2 in blocking stalled replication fork degradation by MRE11. *Cell* **145,** 529–542 (2011).

143. Esashi, F. *et al.* CDK-dependent phosphorylation of BRCA2 as a regulatory mechanism for recombinational repair. *Nature* **434,** 598–604 (2005).

144. Sorensen, C. S. *et al.* The cell-cycle checkpoint kinase Chk1 is required for mammalian homologous recombination repair. *Nat. Cell Biol.* **7,** 195–201 (2005).

145. Hilton, B. A. *et al.* ATR Plays a Direct Antiapoptotic Role at Mitochondria, which Is Regulated by Prolyl Isomerase Pin1. *Mol. Cell* **60,** 35–46 (2015).

146. Brown, E. J. & Baltimore, D. ATR disruption leads to chromosomal fragmentation and early embryonic lethality. *Genes Dev.* **14,** 397–402 (2000).

147. Myers, K., Gagou, M. E., Zuazua-Villar, P., Rodriguez, R. & Meuth, M. ATR and Chk1 suppress a caspase-3-dependent apoptotic response following DNA replication stress. *PLoS Genet.* **5,** (2009).

148. Mirkin, E. V & Mirkin, S. M. Replication fork stalling at natural impediments. *Microbiol. Mol. Biol. Rev.* **71,** 13–35 (2007).

149. Daigaku, Y., Davies, A. A. & Ulrich, H. D. Ubiquitin-dependent DNA damage bypass is separable from genome replication. *Nature* **465,** 951–955 (2010).

150. Hicks, J. K. *et al.* Differential roles for DNA polymerases eta, zeta, and REV1 in lesion bypass of intrastrand versus interstrand DNA cross-links. *Mol. Cell. Biol.* **30,** 1217–30 (2010).

151. Waters, L. S. *et al.* Eukaryotic translesion polymerases and their roles and regulation in DNA damage tolerance. *Microbiol. Mol. Biol. Rev.* **73,** 134–154 (2009).

152. Ceccaldi, R., Sarangi, P. & D'Andrea, A. D. The Fanconi anaemia pathway: new players and new functions. *Nat. Rev. Mol. Cell Biol.* **17,** 337–349 (2016).

153. Jones, M. J. K. & Huang, T. T. The Fanconi anemia pathway in replication stress and DNA crosslink repair. *Cellular and Molecular Life Sciences* **69,** 3963–3974 (2012).

154. Stone, M. P. *et al.* Interstrand DNA cross-links induced by alpha,beta-unsaturated aldehydes derived from lipid peroxidation and environmental sources. *Acc. Chem. Res.* **41,** 793–804 (2008).

155. Hodson, C. & Walden, H. Towards a molecular understanding of the fanconi anemia core complex. *Anemia* **2012,** (2012).

156. Gibbs-Seymour, I. *et al.* Ubiquitin-SUMO circuitry controls activated fanconi anemia ID complex dosage in response to DNA damage. *Mol. Cell* **57,** 150–164 (2015).

157. Barker, S., Weinfeld, M. & Murray, D. DNA-protein crosslinks: Their induction, repair, and biological consequences. *Mutation Research - Reviews in Mutation Research* **589,** 111–135 (2005).

158. Pommier, Y., Sun, Y., Huang, S.-Y. N. & Nitiss, J. L. Roles of eukaryotic topoisomerases in transcription, replication and genomic stability. *Nat. Rev. Mol. Cell Biol.* (2016). doi:10.1038/nrm.2016.111

159. Pommier, Y., Leo, E., Zhang, H. & Marchand, C. DNA topoisomerases and their poisoning by anticancer and antibacterial drugs. *Chem. Biol.* **17,** 421–433 (2010).

160. Pommier, Y. Topoisomerase I inhibitors: camptothecins and beyond. *Nat. Rev. Cancer* **6,** 789–802 (2006).

161. Gmeiner, W. H., Yu, S., Pon, R. T., Pourquier, P. & Pommier, Y. Structural

basis for topoisomerase I inhibition by nucleoside analogs. *Nucleosides. Nucleotides Nucleic Acids* **22,** 653–658 (2003).

162. Pommier, Y., Tanizawa, A. & Kohn, K. W. Mechanisms of topoisomerase I inhibition by anticancer drugs. *Adv. Pharmacol.* **29B,** 73–92 (1994).

163. Pommier, Y. DNA topoisomerase I and II in cancer chemotherapy: update and perspectives. *Cancer Chemother. Pharmacol.* **32,** 103–108 (1993).

164. Pommier, Y. *et al.* Tyrosyl-DNA-phosphodiesterases (TDP1 and TDP2). *DNA Repair (Amst).* **19,** 114–129 (2014).

165. Cortes Ledesma, F., El Khamisy, S. F., Zuma, M. C., Osborn, K. & Caldecott, K. W. A human 5'-tyrosyl DNA phosphodiesterase that repairs topoisomerase-mediated DNA damage. *Nature* **461,** 674–678 (2009).

166. Takashima, H. *et al.* Mutation of TDP1, encoding a topoisomerase I-dependent DNA damage repair enzyme, in spinocerebellar ataxia with axonal neuropathy. *Nat. Genet.* **32,** 267–272 (2002).

167. Pouliot, J. J., Yao, K. C., Robertson, C. A. & Nash, H. A. Yeast gene for a Tyr-DNA phosphodiesterase that repairs topoisomerase I complexes. *Science* **286,** 552–555 (1999).

168. Interthal, H; Champoux, J. Effects of DNA and protein size on substrate clevage by human tyrosyl-DNA phosphodiseterase 1 (TDP1). *Biochem. J.* **436,** 559–566 (2011).

169. Balakirev, M. Y. *et al.* Wss1 metalloprotease partners with Cdc48/Doa1 in processing genotoxic SUMO conjugates. *Elife* **4,** (2015).

170. Stingele, J., Schwarz, M. S., Bloemeke, N., Wolf, P. G. & Jentsch, S. A DNA-dependent protease involved in DNA-protein crosslink repair. *Cell* **158,** 327–338 (2014).

171. Duxin, J. P., Dewar, J. M., Yardimci, H. & Walter, J. C. Repair of a DNA-protein crosslink by replication-coupled proteolysis. *Cell* **159,** 346–357 (2014).

172. Stingele, J., Habermann, B. & Jentsch, S. DNA-protein crosslink repair: proteases as DNA repair enzymes. *Trends Biochem. Sci.* **40,** 67–71 (2015).

173. Lessel, D. *et al.* Mutations in SPRTN cause early onset hepatocellular carcinoma, genomic instability and progeroid features. *Nat. Genet.* **46,** 1239–1244 (2014).

174. Franz, A. *et al.* Chromatin-associated degradation is defined by UBXN-3/FAF1 to safeguard DNA replication fork progression. *Nat. Commun.* **7,** 10612 (2016).

175. Sirbu, B. M. *et al.* Analysis of protein dynamics at active, stalled, and collapsed replication forks. *Genes Dev.* **25,** 1320–1327 (2011).

176. Kiianitsa, K. & Maizels, N. A rapid and sensitive assay for DNA-protein covalent complexes in living cells. *Nucleic Acids Res.* **41,** e104 (2013).

177. Stiff, T., Casar Tena, T., O'Driscoll, M., Jeggo, P. A. & Philipp, M. ATR promotes cilia signalling: links to developmental impacts. *Hum. Mol. Genet.* **25,** 1574–1587 (2016).

178. Machida, Y., Kim, M. S. & Machida, Y. J. Spartan/C1orf124 is important to prevent UV-induced mutagenesis. *Cell Cycle* **11,** 3395–3402 (2012).

179. Centore, R. C., Yazinski, S. A., Tse, A. & Zou, L. Spartan/C1orf124, a reader of PCNA ubiquitylation and a regulator of UV-induced DNA damage response. *Mol. Cell* **46,** 625–635 (2012).

180. Juhasz, S. *et al.* Characterization of human Spartan/C1orf124, an ubiquitin-PCNA interacting regulator of DNA damage tolerance. *Nucleic Acids Res.* **40,** 10795–10808 (2012).

181. Ghosal, G., Leung, J. W.-C., Nair, B. C., Fong, K.-W. & Chen, J. Proliferating

cell nuclear antigen (PCNA)-binding protein C1orf124 is a regulator of translesion synthesis. *J. Biol. Chem.* **287,** 34225–34233 (2012).

182. Macheret, M. & Halazonetis, T. D. DNA replication stress as a hallmark of cancer. *Annu. Rev. Pathol.* **10,** 425–448 (2015).

183. Masutani, C. *et al.* The XPV (xeroderma pigmentosum variant) gene encodes human DNA polymerase eta. *Nature* **399,** 700–704 (1999).

184. Geiselhart, A., Lier, A., Walter, D. & Milsom, M. D. Disrupted signaling through the fanconi anemia pathway leads to dysfunctional hematopoietic stem cell biology: Underlying mechanisms and potential therapeutic strategies. *Anemia* **2012,** (2012).

185. Ray Chaudhuri, A. *et al.* Topoisomerase I poisoning results in PARP-mediated replication fork reversal. *Nat. Struct. Mol. Biol.* **19,** 417–423 (2012).

186. Lukas, C. *et al.* 53BP1 nuclear bodies form around DNA lesions generated by mitotic transmission of chromosomes under replication stress. *Nat. Cell Biol.* **13,** 243–253 (2011).

187. López-Otín, C., Blasco, M. A., Partridge, L., Serrano, M. & Kroemer, G. The hallmarks of aging. TL - 153. *Cell* **153 VN-,** 1194–1217 (2013).

188. Burtner, C. R. & Kennedy, B. K. Progeria syndromes and ageing: what is the connection? *Nat. Rev. Mol. Cell Biol.* **11,** 567–578 (2010).

189. Liu, Q. *et al.* Chk1 is an essential kinase that is regulated by Atr and required for the G2/M DNA damage checkpoint. *Genes Dev.* **14,** 1448–1459 (2000).

190. Ruzankina, Y. *et al.* Deletion of ATR gene in adult mice leads to stem cell loss. **1,** 113–126 (2007).

191. O'Driscoll, M., Ruiz-Perez, V. L., Woods, C. G., Jeggo, P. A. & Goodship, J. A. A splicing mutation affecting expression of ataxia-telangiectasia and Rad3-

related protein (ATR) results in Seckel syndrome. *Nat. Genet.* **33,** 497–501 (2003).

192. Murga, M. *et al.* A mouse model of ATR-Seckel shows embryonic replicative stress and accelerated aging. *Nat. Genet.* **41,** 891–8 (2009).

193. Zhang, Y. & Hunter, T. Roles of Chk1 in cell biology and cancer therapy. *Int. J. Cancer* **134,** 1013–1023 (2014).

194. Sakurikar, N. & Eastman, A. Will targeting Chk1 have a role in the future of cancer therapy? *J. Clin. Oncol.* **33,** 1075–1077 (2015).

195. Manic, G., Obrist, F., Sistigu, A. & Vitale, I. Trial Watch: Targeting ATM-CHK2 and ATR-CHK1 pathways for anticancer therapy. *Mol. Cell. Oncol.* **2,** e1012976 (2015).

196. Liu, S. *et al.* Claspin operates downstream of TopBP1 to direct ATR signaling towards Chk1 activation. *Mol. Cell. Biol.* **26,** 6056–6064 (2006).

197. Draga, M. *et al.* BRCA1 Is Required for Maintenance of Phospho-Chk1 and G2/M Arrest during DNA Cross-Link Repair in DT40 Cells. *Mol. Cell. Biol.* **35,** 3829–3840 (2015).

198. Wilsker, D., Petermann, E., Helleday, T. & Bunz, F. Essential function of Chk1 can be uncoupled from DNA damage checkpoint and replication control. *Proc. Natl. Acad. Sci. U. S. A.* **105,** 20752–7 (2008).

199. Niida, H., Katsuno, Y., Banerjee, B., Hande, M. P. & Nakanishi, M. Specific role of Chk1 phosphorylations in cell survival and checkpoint activation. *Mol. Cell. Biol.* **27,** 2572–2581 (2007).

200. Petermann, E. & Caldecott, K. W. Evidence that the ATR/Chk1 pathway maintains normal replication fork progression during unperturbed S phase. *Cell Cycle* **5,** 2203–2209 (2006).

201. Tapia-Alveal, C., Calonge, T. M. & O'Connell, M. J. Regulation of chk1. *Cell Div.* **4,** 1–7 (2009).

202. Platel, M. *et al.* Tight Chk1 levels control replication cluster activation in Xenopus. *PLoS One* **10,** 1–27 (2015).

203. Cai, Z., Chehab, N. H. & Pavletich, N. P. Structure and Activation Mechanism of the CHK2 DNA Damage Checkpoint Kinase. *Mol. Cell* **35,** 818–829 (2009).

204. Pu, L., Amoscato, A. A., Bier, M. E. & Lazo, J. S. Dual G1 and G2 phase inhibition by a novel, selective Cdc25 inhibitor 7-chloro-6-(2-morpholin-4-ylethylamino)-quinoline-5,8-dione. *J. Biol. Chem.* **277,** 46877–46885 (2002).

205. Kwon, Y. G., Lee, S. Y., Choi, Y., Greengard, P. & Nairn, A. C. Cell cycle-dependent phosphorylation of mammalian protein phosphatase 1 by cdc2 kinase. *Proc Natl Acad Sci U S A* **94,** 2168–2173 (1997).

206. Petermann, E., Woodcock, M. & Helleday, T. Chk1 promotes replication fork progression by controlling replication initiation. *Proc. Natl. Acad. Sci. U. S. A.* **107,** 16090–16095 (2010).

207. Shimada, M. & Nakanishi, M. Response to DNA damage: why do we need to focus on protein phosphatases? *Front. Oncol.* **3,** 8 (2013).

208. Leung-Pineda, V., Ryan, C. E. & Piwnica-Worms, H. Phosphorylation of Chk1 by ATR is antagonized by a Chk1-regulated protein phosphatase 2A circuit. *Mol. Cell. Biol.* **26,** 7529–38 (2006).

209. Chowdhury, D. *et al.* gamma-H2AX dephosphorylation by protein phosphatase 2A facilitates DNA double-strand break repair. *Mol. Cell* **20,** 801–809 (2005).

210. Takai, A. *et al.* Inhibition of specific binding of okadaic acid to protein phosphatase 2A by microcystin-LR, calyculin-A and tautomycin: method of analysis of interactions of tight-binding ligands with target protein. *Biochem. J.*

**306 ( Pt 3,** 657–65 (1995).

211. Lin, G. G. & Scott, J. G. NIH Public Access. **100,** 130–134 (2012).

212. Murphy, C. M. & Michael, W. M. Control of DNA replication by the nucleus/cytoplasm ratio in xenopus. *J. Biol. Chem.* **288,** 29382–29393 (2013).

213. Cimprich, K. A. & Cortez, D. ATR: an essential regulator of genome integrity. *Nat. Rev. Mol. Cell Biol.* **9,** 616–27 (2008).

214. Paulsen, R. D. & Cimprich, K. A. The ATR pathway: Fine-tuning the fork. *DNA Repair (Amst).* **6,** 953–966 (2007).

215. Forment, J. V., Blasius, M., Guerini, I. & Jackson, S. P. Structure-specific DNA endonuclease mus81/eme1 generates DNA damage caused by chk1 inactivation. *PLoS One* **6,** (2011).

216. Petermann, E. & Helleday, T. Pathways of mammalian replication fork restart. *Nat. Rev. Mol. Cell Biol.* **11,** 683–7 (2010).

217. Thompson, R., Montano, R. & Eastman, A. The mre11 nuclease is critical for the sensitivity of cells to chk1 inhibition. *PLoS One* **7,** (2012).

218. Maskey, R. S. *et al.* Spartan deficiency causes genomic instability and progeroid phenotypes. *Nat. Commun.* **5,** 5744 (2014).

219. Xu, Y., Ashley, T. & Brainerd, E. E. Targeted disruption of A T M leads to growth retardation , chromosomal tragmentation during meiosis , immun e defects , and thymic lymphoma. *Genes Dev.* 2411–2422 (1996). doi:10.1101/gad.10.19.2411

220. Ide, H., Nakano, T., Shoulkamy, M. I. & Salem, A. M. H. Formation , Repair , and Biological Effects of DNA – Protein Cross-Link Damage.

221. Nakano, T. *et al.* Homologous recombination but not nucleotide excision repair plays a pivotal role in tolerance of DNA-protein cross-links in mammalian

cells. *J. Biol. Chem.* **284,** 27065–27076 (2009).

222. Vaz, B. *et al.* Metalloprotease SPRTN/DVC1 Orchestrates Replication-Coupled DNA-Protein Crosslink Repair. *Mol. Cell* **64,** 704–719 (2016).

223. Ortega-Atienza, S., Wong, V. C., DeLoughery, Z., Luczak, M. W. & Zhitkovich, A. ATM and KAT5 safeguard replicating chromatin against formaldehyde damage. *Nucleic Acids Res.* **44,** 198–209 (2016).

224. Haaf, T. *et al.* Sequestration of mammalian Rad51- recombination protein into micronuclei. *J. Cell Biol.* **144,** 11–20 (1999).

225. Dungrawala, H. *et al.* The Replication Checkpoint Prevents Two Types of Fork Collapse without Regulating Replisome Stability. *Mol. Cell* **59,** 998–1010 (2015).

226. Lopez-Mosqueda, J. *et al.* SPRTN is a mammalian DNA-binding metalloprotease that resolves DNA-protein crosslinks. *Elife* **5,** (2016).

227. Yanagi, K. I., Mizuno, T., You, Z. & Hanaoka, F. Mouse geminin inhibits not only Cdt1-MCM6 interactions but also a novel intrinsic Cdt1 DNA binding activity. *J. Biol. Chem.* **277,** 40871–40880 (2002).

228. Kaitna, S. & Kaitna, S. Letters To Nature. *Nature* **430,** 913–917 (2004).

229. Kim, Y. & Kipreos, E. T. Cdt1 degradation to prevent DNA re-replication: conserved and non-conserved pathways. *Cell Div.* **2,** 18 (2007).

230. Tatsumi, Y. *et al.* Deregulation of Cdt1 induces chromosomal damage without rereplication and leads to chromosomal instability. *J. Cell Sci.* **119,** 3128–40 (2006).

231. Menges, C. W., Altomare, D. A. & Testa, J. R. FAS-associated factor 1 (FAF1): Diverse functions and implications for oncogenesis. *Cell Cycle* **8,** 2528–2534 (2009).

232. Park, M.-Y., Jang, H. D., Lee, S. Y., Lee, K.-J. & Kim, E. Fas-associated factor-1 inhibits nuclear factor-kappaB (NF-kappaB) activity by interfering with nuclear translocation of the RelA (p65) subunit of NF-kappaB. *J. Biol. Chem.* **279,** 2544–2549 (2004).

233. Bolderson, E., Scorah, J., Helleday, T., Smythe, C. & Meuth, M. ATM is required for the cellular response to thymidine induced replication fork stress. *Hum. Mol. Genet.* **13,** 2937–2945 (2004).

234. Jin, Y. *et al.* Cell cycle-dependent colocalization of BARD1 and BRCA1 proteins in discrete nuclear domains. *Proc Natl Acad Sci U S A* **94,** 12075–12080 (1997).

235. Frigola, J., Remus, D., Mehanna, A. & Diffley, J. F. X. ATPase-dependent quality control of DNA replication origin licensing. *Nature* **495,** 339–43 (2013).

236. Aparicio, T., Megías, D. & Méndez, J. Visualization of the MCM DNA helicase at replication factories before the onset of DNA synthesis. *Chromosoma* **121,** 499–507 (2012).

237. Vekaria, P. H., Home, T., Weir, S., Schoenen, F. J. & Rao, R. Targeting p97 to Disrupt Protein Homeostasis in Cancer. *Front. Oncol.* **6,** 181 (2016).

238. Ramadan, K., Halder, S., Wiseman, K. & Vaz, B. Strategic role of the ubiquitin-dependent segregase p97 (VCP or Cdc48) in DNA replication. *Chromosoma* (2016). doi:10.1007/s00412-016-0587-4

239. Müller, J. M. M., Deinhardt, K., Rosewell, I., Warren, G. & Shima, D. T. Targeted deletion of p97 (VCP/CDC48) in mouse results in early embryonic lethality. *Biochem. Biophys. Res. Commun.* **354,** 459–465 (2007).

240. Tsujimoto, Y. *et al.* Elevated expression of valosin-containing protein (p97) is

associated with poor prognosis of prostate cancer. *Clin. Cancer Res.* **10,** 3007–3012 (2004).

241. Yamamoto, S. *et al.* Expression level of valosin-containing protein (p97) is associated with prognosis of esophageal carcinoma. *Clin. Cancer Res.* **10,** 5558–5565 (2004).

242. Yamamoto, S. *et al.* Expression level of valosin-containing protein is strongly associated with progression and prognosis of gastric carcinoma. *J. Clin. Oncol.* **21,** 2537–2544 (2003).

243. Yamamoto, S. *et al.* Elevated expression of valosin-containing protein (p97) in hepatocellular carcinoma is correlated with increased incidence of tumor recurrence. *J. Clin. Oncol.* **21,** 447–452 (2003).

244. Valle, C. W. *et al.* Critical role of VCP/p97 in the pathogenesis and progression of non-small cell lung carcinoma. *PLoS One* **6,** 1–12 (2011).

245. Katsuragi, Y. & Sagata, N. Regulation of Chk1 kinase by autoinhibition and ATR-mediated phosphorylation. *Mol. Biol. Cell* **15,** 1680–9 (2004).

246. Smits, V. A. J. & Gillespie, D. A. DNA damage control: regulation and functions of checkpoint kinase 1. *FEBS J.* **282,** 3681–92 (2015).

247. Stingele, J. *et al.* Mechanism and Regulation of DNA-Protein Crosslink Repair by the DNA-Dependent Metalloprotease SPRTN. *Mol. Cell* **64,** 688–703 (2016).

# 6 Appendix

Publications originated during this thesis

1) Metalloprotease SPRTN/DVC1 Orchestrates Replication-Coupled DNA-Protein Crosslink Repair**,** Bruno Vaz, Marta Popovic, Joseph Newman, John Fielden, Hazel Aitkenhead, **Swagata Halder**, Abhay Narayan Singh, Iolanda Vendrell, Roman Fischer , Ignacio Torrecilla, Neele Drobnitzky, Raimundo Freire, David Amor, Paul Lockhart, Benedikt Kessler, Opher Gileadi and Kristijan Ramadan **Mol Cell (Accepted)** (attached)

2) A ruthenium(II) polypyridyl intercalator stalls DNA replication forks and radiosensitizes human cancer cells. Martin R. Gill1, Siti Norain Harun, **Swagata Halder**, Ramon A. Boghozian1, Norazizah Shafee, Kristijan Ramadan, Haslina . Ahmad and Katherine A. Vallis, **Scientific Report** 2016 Aug 25;6:31973

3) Strategic role of the ubiquitin-dependent segregase p97 (VCP or Cdc48) in DNA replication**.** Ramadan K, **Halder S**, Wiseman K, Vaz B. **Chromosoma.** 2016 Apr 18

4) Chromatin-associated degradation is defined by UBXN-3/FAF1 to safeguard DNA replication fork progression.Franz A, Pirson PA, Pilger D, **Halder S**, Achuthankutty D, Kashkar H, Ramadan K, Hoppe T.**Nat Commun**. 2016 Feb (attached)

5) Targeting BRCA1 and BRCA2 Deficiencies with G-Quadruplex-Interacting Compounds.Zimmer J, Tacconi EM, Folio C, Badie S, Porru M, Klare K, Tumiati M, Markkanen E, **Halder S**, Ryan A, Jackson SP, Ramadan K, Kuznetsov SG, Biroccio A, Sale JE, Tarsounas M.**Mol Cell**. 2016 Feb 4;61(3):449-60.

6) Mutations in SPRTN cause early onset hepatocellular carcinoma, genomic instability and progeroid features.Lessel D, Vaz B, **Halder S**, Lockhart PJ, Marinovic-Terzic I, Lopez-Mosqueda J, Philipp M, Sim JC, Smith KR, Oehler J, Cabrera E, Freire R, Pope K, Nahid A, Norris F, Leventer RJ, Delatycki MB, Barbi G, von Ameln S, Högel J, Degoricija M, Fertig R, Burkhalter MD, Hofmann K, Thiele H, Altmüller J, Nürnberg G, Nürnberg P, Bahlo M, Martin GM, Aalfs CM, Oshima J, Terzic J, Amor DJ, Dikic I, Ramadan K, Kubisch C.**Nat Genet**. 2014 Nov;46(11):1239-44 **(Co-First Author)** (attached)

7**)** Role of p97/VCP (Cdc48) in genome stability**.**Vaz B, **Halder S**, Ramadan K.**Front Genet**. 2013 Apr 30;4:60**.**

# NATURE PUBLISHING GROUP LICENSE TERMS AND CONDITIONS

Jun 07, 2017

This Agreement between Dr. Swagata Halder ("You") and Nature Publishing Group ("Nature Publishing Group") consists of your license details and the terms and conditions provided by Nature Publishing Group and Copyright Clearance Center.

| | |
|---|---|
| License Number | 4123710859954 |
| License date | Jun 07, 2017 |
| Licensed Content Publisher | Nature Publishing Group |
| Licensed Content Publication | Nature Cell Biology |
| Licensed Content Title | Emerging functions of the VCP/p97 AAA-ATPase in the ubiquitin system |
| Licensed Content Author | Hemmo Meyer, Monika Bug, Sebastian Bremer |
| Licensed Content Date | Feb 2, 2012 |
| Licensed Content Volume | 14 |
| Licensed Content Issue | 2 |
| Type of Use | reuse in a dissertation / thesis |
| Requestor type | academic/educational |
| Format | print and electronic |
| Portion | figures/tables/illustrations |
| Number of figures/tables/illustrations | 1 |
| High-res required | no |
| Figures | Figure 2 Overview of p97 structure, domain organisation and its cofactors |
| Author of this NPG article | no |
| Your reference number | |
| Title of your thesis / dissertation | The role of p97 cofactors SPRTN and FAF1 in DNA replication |
| Expected completion date | Jun 2017 |
| Estimated size (number of pages) | 235 |
| Requestor Location | Dr. Swagata Halder<br>Linacare College<br>St.Cross Road<br><br>Oxford, Oxfordshire OX1 3JA<br>United Kingdom<br>Attn: Dr. Swagata Halder |
| Billing Type | Invoice |
| Billing Address | Dr. Swagata Halder |

Linacare College
St.Cross Road

Oxford, United Kingdom OX1 3JA
Attn:

Total 0.00 GBP

Terms and Conditions

## Terms and Conditions for Permissions

Nature Publishing Group hereby grants you a non-exclusive license to reproduce this material for this purpose, and for no other use,subject to the conditions below:

1. NPG warrants that it has, to the best of its knowledge, the rights to license reuse of this material. However, you should ensure that the material you are requesting is original to Nature Publishing Group and does not carry the copyright of another entity (as credited in the published version). If the credit line on any part of the material you have requested indicates that it was reprinted or adapted by NPG with permission from another source, then you should also seek permission from that source to reuse the material.

2. Permission granted free of charge for material in print is also usually granted for any electronic version of that work, provided that the material is incidental to the work as a whole and that the electronic version is essentially equivalent to, or substitutes for, the print version.Where print permission has been granted for a fee, separate permission must be obtained for any additional, electronic re-use (unless, as in the case of a full paper, this has already been accounted for during your initial request in the calculation of a print run).NB: In all cases, web-based use of full-text articles must be authorized separately through the 'Use on a Web Site' option when requesting permission.

3. Permission granted for a first edition does not apply to second and subsequent editions and for editions in other languages (except for signatories to the STM Permissions Guidelines, or where the first edition permission was granted for free).

4. Nature Publishing Group's permission must be acknowledged next to the figure, table or abstract in print. In electronic form, this acknowledgement must be visible at the same time as the figure/table/abstract, and must be hyperlinked to the journal's homepage.

5. The credit line should read:
   Reprinted by permission from Macmillan Publishers Ltd: [JOURNAL NAME] (reference citation), copyright (year of publication)
   For AOP papers, the credit line should read:
   Reprinted by permission from Macmillan Publishers Ltd: [JOURNAL NAME], advance online publication, day month year (doi: 10.1038/sj.[JOURNAL ACRONYM].XXXXX)

   **Note: For republication from the *British Journal of Cancer,* the following credit lines apply.**
   Reprinted by permission from Macmillan Publishers Ltd on behalf of Cancer Research UK: [JOURNAL NAME] (reference citation), copyright (year of publication)For AOP papers, the credit line should read:
   Reprinted by permission from Macmillan Publishers Ltd on behalf of Cancer Research UK: [JOURNAL NAME], advance online publication, day month year (doi: 10.1038/sj.[JOURNAL ACRONYM].XXXXX)

6. Adaptations of single figures do not require NPG approval. However, the adaptation should be credited as follows:

   Adapted by permission from Macmillan Publishers Ltd: [JOURNAL NAME] (reference citation), copyright (year of publication)

**Note: For adaptation from the *British Journal of Cancer*, the following credit line applies.**
Adapted by permission from Macmillan Publishers Ltd on behalf of Cancer Research UK: [JOURNAL NAME] (reference citation), copyright (year of publication)

7. Translations of 401 words up to a whole article require NPG approval. Please visit http://www.macmillanmedicalcommunications.com for more information.Translations of up to a 400 words do not require NPG approval. The translation should be credited as follows:

   Translated by permission from Macmillan Publishers Ltd: [JOURNAL NAME] (reference citation), copyright (year of publication).

   **Note: For translation from the *British Journal of Cancer*, the following credit line applies.**
   Translated by permission from Macmillan Publishers Ltd on behalf of Cancer Research UK: [JOURNAL NAME] (reference citation), copyright (year of publication)

We are certain that all parties will benefit from this agreement and wish you the best in the use of this material. Thank you.
Special Terms:
v1.1

**Questions? customercare@copyright.com or +1-855-239-3415 (toll free in the US) or +1-978-646-2777.**

Copyright Clearance Center RightsLink®

Home | Account Info | Help

nature publishing group

| | |
|---|---|
| **Title:** | Genome maintenance mechanisms for preventing cancer |
| **Author:** | Jan H. J. Hoeijmakers |
| **Publication:** | Nature |
| **Publisher:** | Nature Publishing Group |
| **Date:** | May 17, 2001 |

Copyright © 2001, Rights Managed by Nature Publishing Group

Logged in as:
Swagata Halder
LOGOUT

## Order Completed

Thank you for your order.

This Agreement between Dr. Swagata Halder ("You") and Nature Publishing Group ("Nature Publishing Group") consists of your license details and the terms and conditions provided by Nature Publishing Group and Copyright Clearance Center.

Your confirmation email will contain your order number for future reference.

Printable details.

| | |
|---|---|
| License Number | 4123711164719 |
| License date | Jun 07, 2017 |
| Licensed Content Publisher | Nature Publishing Group |
| Licensed Content Publication | Nature |
| Licensed Content Title | Genome maintenance mechanisms for preventing cancer |
| Licensed Content Author | Jan H. J. Hoeijmakers |
| Licensed Content Date | May 17, 2001 |
| Licensed Content Volume | 411 |
| Licensed Content Issue | 6835 |
| Type of Use | reuse in a dissertation / thesis |
| Requestor type | academic/educational |
| Format | print and electronic |
| Portion | figures/tables/illustrations |
| Number of figures/tables/illustrations | 1 |
| Figures | Figure 4 Overview of the different DNA repair pathways inside the cell |
| Author of this NPG article | no |
| Your reference number | |
| Title of your thesis / dissertation | The role of p97 cofactors SPRTN and FAF1 in DNA replication |
| Expected completion date | Jun 2017 |
| Estimated size (number of pages) | 235 |
| Requestor Location | Dr. Swagata Halder<br>Linacare College<br>St.Cross Road<br><br>Oxford, Oxfordshire OX1 3JA<br>United Kingdom<br>Attn: Dr. Swagata Halder |
| Billing Type | Invoice |

| | |
|---|---|
| Billing address | Dr. Swagata Halder<br>Linacare College<br>St.Cross Road<br><br>Oxford, United Kingdom OX1 3JA<br>Attn: |
| Total | 0.00 GBP |

ORDER MORE CLOSE WINDOW

Copyright © 2017 Copyright Clearance Center, Inc. All Rights Reserved. Privacy statement. Terms and Conditions.
Comments? We would like to hear from you. E-mail us at customercare@copyright.com